

Theoretical feedbacks between Neoproterozoic glaciations and eukaryotic evolution

Richard Anthony Boyle

School of Environmental Sciences

Thesis submitted to the University of East Anglia for the degree of

Doctor of Philosophy, May 2008.



(The copy of the thesis has been supplied on the condition that anyone who consults it is understood to recognise that its copyright rests with the author and that no quotation from the thesis, nor any information derived therefrom, may be published without the author's prior, written consent. The thesis is approximately 60,000 words in length.)

Acknowledgements

I am very grateful to my supervisors, Tim Lenton and Andy Watson, for providing me with three and a half years of patient encouragement, useful input and interesting debate. Despite being crazily busy with teaching and other research commitments, Andy always remained enthusiastic, encouraging and constructively skeptical. Tim struck a perfect balance between pragmatically keeping me on a path that would lead to useful results, and entertaining my (more) speculative ideas and desire to learn more mathematics than was strictly necessary for the project. Although as a student I tend to develop working patterns that can be inefficient and counter-productive, I can honestly say that I could not have had better supervision. That this is the case is to the immense credit of Tim and Andy, both as academics and as people. I thank the UEA School of Environmental Sciences for funding. I thank the various researchers with whom I have been lucky enough to have discussions, both verbally and via email, including Hywel Williams, Jo Ridley, Matthew Herron, Richard Michod, the referees of my second paper, Noam Bergman, Mark Williamson, Andy Ridgwell, Jamie Wood, James Dyke and David Schwartzman, for a great deal of helpful input. I thank my examiners Nick Butterfield and Julian Andrews. I am very grateful to Naomi Vaughan for all sorts of things. I wish to express a great deal of gratitude to Julia Leggett, not least for providing a homeless Phd student with food and shelter, and tolerating my nocturnal working hours and immature sexist jokes. Speaking of immaturity, I thank various fellow grads bar reprobates, in particular Andy Hind, Liz Farmer, the Graham Mills/Dave Stewart drinking show, and, of course, Paul Rankin. Without them, the whole thesis would probably have been done in much less time with a far less severe hangover. I thank all of my long-suffering flatmates and office-mates for tolerating my untidiness, particularly Claire Powell and Sally Lavender for not evicting me after my washing up went mouldy. Thanks to all my friends from Oxford for remaining supportive during my more self-destructive moments - in particular Hal Stockley, Al Catto, Tony Goh, Ant Hucklesby and Tom Handley. I thank my sister Helen, for putting up with lots of emails expressing my frustration with C, Matlab, Fortran, and my general uselessness, and Glenda, for lots of encouragement. But most of all, I thank one person for years of support (including recent financial parasitism), without whom academic qualifications would be irrelevant, as I simply would not be around. My father.

“Just as cold arose out of the abode of mist, and all terrible things, so also all that looked to the realm of fire became hot and glowing. But seeming emptiness was as mild as windless air, and when the breath of heat met the rime, so that it melted and dripped, life was quickened from the yeast drops by the power of that which sent the heat, and became a man’s form.”

Norse creation myth, 1st century B.C. or earlier.

“Life remains unalterable in its essential traits throughout all geological times, and changes only in forms. All the vital films (plankton, bottom and soil) and all the vital concentrations (littoral, sargassic and fresh water) have always existed. Their mutual relationships and the quantity of matter contained within them have changed from time to time, but these modifications could not have been large, because the energy input from the sun has been constant, or nearly so, throughout geological time, and because the distribution of energy in these vital films can only have been determined by living matter - the fundamental part, the only variable part, of the thermodynamic field of the biosphere.”

Vladimir Vernadsky, 1926.

“If you have a simple idea, state it simply.”

William D. Hamilton, 1996.

Abstract

1) Physiological consequences of transitions in the level of selection explain the existence of Neoproterozoic lichen symbioses. Between-individual differentiation within groups causes physiological buffering, giving altruists higher fitness than cheaters in variable environments. Altruists increase from rarity given $\alpha \cdot |V - V_{opt}| > C$ (cost C , deleterious abiotic variation $|V - V_{opt}|$, buffering α). Reciprocal feedback between a genotype frequency $\frac{G}{G+P}$ and an abiotic state $\frac{|V-V_{opt}|}{|V-V_{opt}|+|V_{abiotic}-V_{opt}|}$ may be equivalent to kin selection, i.e. $\frac{b}{C} > \frac{1}{r}$, $\frac{\alpha|V-V_{opt}|}{C} > \frac{1}{\frac{G}{G+P} \cdot \frac{|V-V_{opt}|}{|V-V_{opt}|+|V_{abiotic}-V_{opt}|}} \in \frac{b}{C} > \frac{1}{r}$.

2) At contemporary degassing rate, biotic silicate weathering enhancement 10 – 20 times greater than present would have been required for a biologically-triggered snowball Earth. However, biotic enhancement could have compensated for declining abiotic silicate weathering rate at low temperatures - sufficiently to accentuate a tectonically-driven glaciation.

3) Marine carbonate speciation causes a slushball ocean to become a net CO_2 source at large reservoir sizes, making glacial duration shorter than a hard snowball by a factor of the atmospheric CO_2 degassing fraction. Equilibrated oceans require a carbonate weathering:burial ratio $W_{carb} : B_{carb} > 1$ for deglaciation by $CO_{2(g)}$ increase.

4) If adequate biotic silicate weathering enhancement rapidly occurs after deglaciation, subsequent reglaciation will occur within 3 – 5Myrs. The contrast with the ~ 50 Ma separating Neoproterozoic events invokes the elapse of a coevolutionary “succession time”, before which biotically-triggered reglaciation is improbable. Low post-glacial silicate weathering is consistent with *Si*-depleted cap carbonates. Phanerozoic reduction in glacial susceptibility resulted from physiological evolution of biotic weathering and/or calcification.

5) Emergence of terminal cellular differentiation in Ediacara/Metazoa required an environmental context E , provided by Neoproterozoic glaciations, in which the high fitness cost C was adaptive (versus relatedness r , benefit b) $\frac{d}{dt}(rb - C) = \frac{\partial}{\partial E}(rb - C)\frac{\partial E}{\partial t}$. Restriction of the biosphere to refugia experiencing extreme, repeated founder effects raised kin selection for altruism. Between-group isolation limited cheat migration, accentuating group viability selection for altruism. Both processes occurred globally, over multi-million year timescales; explaining subsequent proliferation of Ediacaran macrobiota.

Contents

Chapter 1: The Neoproterozoic Earth.....6

Chapter 2: Theoretical justification for
hypothesizing the presence of

Neoproterozoic terrestrial lichens.....52

Chapter 3: A biological trigger for snowball Earth?.....76

Chapter 4: Atmosphere-ocean CO_2 equilibration and glacial
duration.....116

Chapter 5: Changes in susceptibility to global-scale glaciation
over Earth history.....148

Chapter 6: Neoproterozoic glaciations and the
evolution of altruism.....180

Chapter 7: Conclusions.....202

Chapter 1: The Neoproterozoic Earth

Summary

An ice albedo instability probably exists in Earth's climate, but the severity of its effects and the temperature boundary conditions of its occurrence are not precisely known. The synchronicity of a significant number of (apparent) low paleolatitude tillites with disturbances in Carbon cycle isotopic composition and depositional dynamics, make it very difficult to interpret Neoproterozoic climate in terms of a Phanerozoic model. Banded Iron formations are probably a localised phenomenon, but Sulphur isotopes also support ocean anoxia, and Boron isotopes arguably support at least one interval of ocean acidification. Oxygen isotopes imply low marine temperatures over time intervals consistent with that implied by putative glacial deposits. Though subject to poorly constrained influx rate estimates, Iridium accumulation is consistent with extensive surface ice cover, and probably does not originate from a volcanic or hydrogenous source. Strontium isotopes imply a largely steady increase in terrestrial bulk weathering that is apparently uninterrupted by glacial events on a global scale, but does exhibit localised fluctuation roughly synchronous with tillite deposition. Slushball solutions easily explain the persistence of biotic refugia, but lack a rigorous, consistent explanation for dynamic stability of low-latitude, non-equatorial ice sheets. A high-tilt Earth would invoke a rapid reversal to the present axial dipole for which there is no known mechanism, and extreme 6 month seasonality inconsistent with apparent long periods of geochemical stasis. Both low latitude, high altitude glaciation and rapid true polar wander are feasible explanations for some of the paleomagnetic evidence - but neither idea is a comprehensive scenario incorporating tangible links to the Carbon cycle. Therefore, global-scale glaciation, severe enough to cause massive redeposition of inorganic Carbon and/or massive reallocation between inorganic and organic Carbon pools, remains the strongest Neoproterozoic climate scenario through its ability to integrate many separate lines of evidence into a coherent picture. Thick sea ice (i.e. "hard snowball") solutions probably require too much CO_2 build up to be recoverable, but thin ice solutions may not allow sufficient solar heating of the underlying water to keep the ice thin. Extrapolation from contemporary ice-shelf environments and Arctic biomes suggests that the catastrophic impact of severe global scale glaciation on eukaryotes has been over-emphasised. Even hard snowball solutions permit refugia in land-locked, thin ice-covered seas, meltwater lakes, tropical diurnal ponds, and perhaps in geothermally-heated subterranean niches. The fossil record does not suggest a decimation of the biosphere at the time of snowball Earth events, but does suggest a qualitative increase in evolutionary tempo in their aftermath, comprising a morphological diversification of unicellular eukaryotes and the sudden Ediacaran radiation of macroscopic form that probably included the immediate ancestors of the Metazoa.

Introduction

The idea of a completely frozen planet Earth is probably theological in origin (Leeming & Leeming, 1994), demonstrating the emotive appeal of such “end member” phenomena (e.g. Corsetti et al, 2004). But evidence for low-latitude Proterozoic glaciation has continued to stand up to criticism since the nineteenth century (Agassiz, 1842, Mawson, 1949, Harland & Bidgood, 1959, Roberts, 1971), and has more recently been strongly linked with extreme disturbances in geochemical cycling of Carbon and other elements (Kirschvink, 1992, Hoffman et al, 1998, Hoffman & Schragg, 2002, Rothman et al, 2003). This chapter introduces the snowball Earth problem in the context of the processes that control planetary temperature over geologic time, and outlines the remaining unanswered questions concerning Neoproterozoic glaciations and their interaction with the biosphere.

Theoretical background

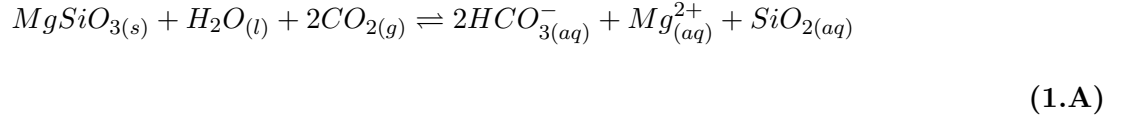
The ice albedo instability

Ice-covered surfaces reflect a significantly higher fraction of received radiation than surfaces lacking ice cover (Around 0.9 for fresh snow compared with between 0.1 and 0.4 for forested surfaces, (Rees, 1990)), causing them to experience less warming for a given radiation forcing (e.g. Lian & Cess, 1977). Over time, this means that changes in ice-cover accentuate themselves, imposing a positive feedback on climate (Budyko, 1969). This positive feedback probably leads to a bistability - two different, stable values in the dependent variable for the same level of forcing (Figure 1.1). For a given level of insolation, there exists (in theory) a maximum ice-covered fraction that, if exceeded, will lead to global glaciation via a runaway ice-albedo feedback of increasing strength (North et al, 1981, Caldeira & Kasting, 1992, Pierrehumbert, 2002, 2005). The importance of this mechanism over geologic time depends upon the contribution of surface albedo to total planetary albedo, a parameter that is uncertain (e.g. McGuffie & Henderson-Sellers, 1997) and may have been overestimated previously (Lian & Cess, 1977), but most likely increases dramatically as the ice-covered state is approached (Pierrehumbert, 2005). The latitudinal position of ice-cover, the planetary temperature, level of hydrologic activity and strength of atmospheric heat diffusion that correspond to the onset of the ice-albedo instability, are all highly contentious (Caldeira & Kasting, 1992, Ikeda & Tajika, 1999, Hyde et al, 2000, Baum & Crowley, 2003, Pierrehumbert, 2005). As a result, so is the question of whether this instability was ever realised during the planet’s history. Demonstration of a runaway sea ice instability may be impaired by the inclusion of a variable depth mixed layer (as opposed to a more strictly stratified “slab”) ocean (Chandler & Sohl, 2000), or by global climate models that fully resolve other ocean dynamics (Poulsen et al, 2001, 2002, 2003). The very existence of the ice-albedo instability (at least in terms of a limiting case

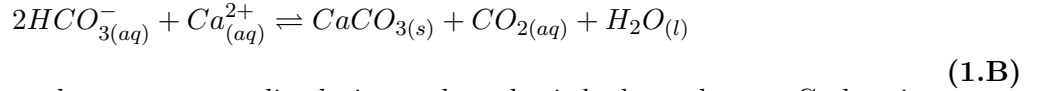
runaway feedback) has consequently been questioned (e.g. Ridgwell 2004). But open water, low-latitude ice cover solutions are probably negated by sea-ice dynamics (Lewis et al, 2007) unless untestable and somewhat ad-hoc assumptions about atmosphere and ocean heat transport are made (Pollard & Kasting, 2005). A consistent explanation is lacking as to why low-latitude global ice cover can be sustained in a “slushball” solution, without a runaway ice-albedo feedback to a hard snowball occurring.

The “faint young sun” problem and the Urey reaction

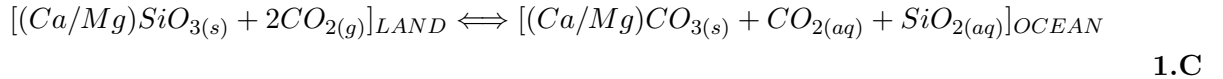
The Sun was significantly less bright in the distant past, but evidence suggests that liquid water has nevertheless been continuously present on the planet’s surface - implying that planetary temperature was not correspondingly low (Sagen & Mullen, 1972, Lowe, 1980). A suggested resolution to this apparent contradiction, known as the “faint young sun” problem, was proposed by Walker, Hayes & Kasting (1981). Weathering of (predominantly magnesium) silicate rocks on land withdraws $CO_{2(g)}$ from the atmosphere, causing a flux of Carbonic acids and aqueous silica to the ocean - via run off through the water table. (Note that throughout the thesis, chemical reactions are indexed with a letter, equations are indexed with a number):



This dissolved marine CO_2 subsequently forms precipitates of Calcium Ca and Magnesium Mg carbonates (predominantly the former):



Where marine carbonates escape dissolution and are buried, the carbonate Carbon is isolated from the atmosphere-ocean system, until it is returned to the atmosphere many millions of years later by tectonic outgassing (e.g. Ronov, 1976). The net consequence of reactions 1.A and 1.B is the conversion of a terrestrial silicate rock to a marine carbonate rock, the stoichiometry of which gives rise to a net removal of 1 mole of CO_2 from the system. The cumulative stoichiometry of these two sets of reactions (using (Ca/Mg) to denote either one of the cations) is referred to as the “Urey reaction”:



Walker, Hayes, and Kasting were the first to notice that, because the silicate weathering reactions summarised in (1.A) depend on temperature and atmospheric $CO_{2(g)}$, but also decrease temperature and atmospheric $CO_{2(g)}$ via marine reactions summarised in (1.B), the magnitude of the terrestrial silicate weathering flux gives rise to an important negative

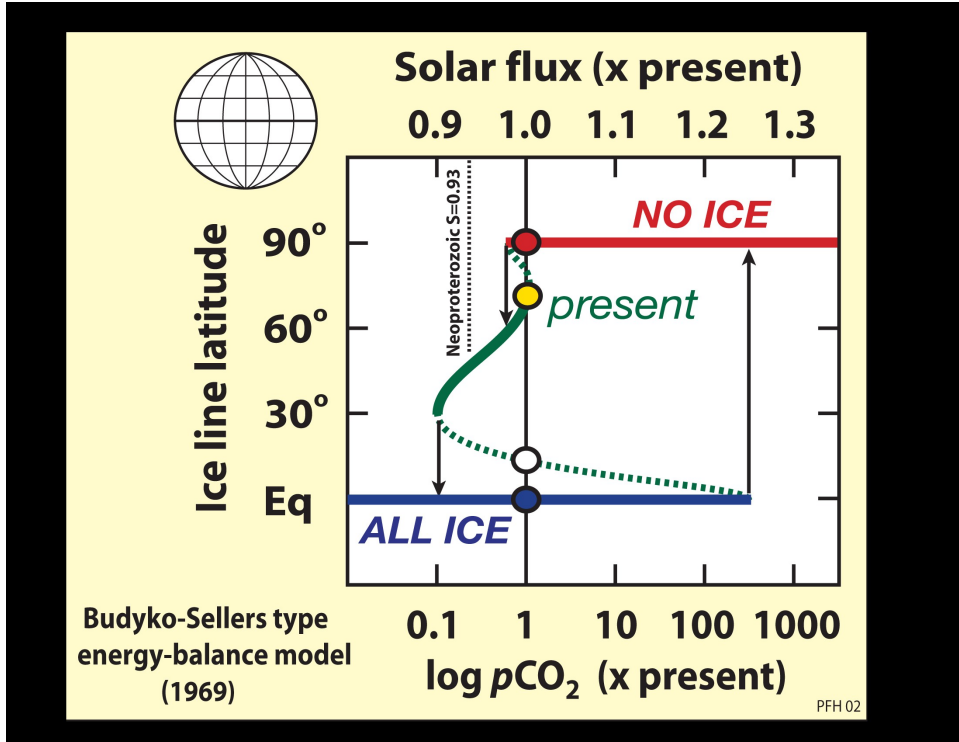


Figure 1.1 - The spectral properties of ice-covered surfaces give rise to a bistability in the “Earth system”. Figure shows Energy balance model results from Budyko (1969). Y-axis shows the latitude of the lower limit of the ice line, X-axis the external temperature forcing, which can be altered by varying Solar luminosity (top) or varying greenhouse gas forcing (bottom). Note that the ice-covered “hard snowball” (lower blue dot) and ice-free (upper red dot) can correspond to the same external temperature forcing. Which solution is realised depends upon the state that the system starts in - an example of hysteresis (memory of previous state) in the system. A contentious issue is whether and how a third, small ice-cover “slushball” solution (yellow dot) may be possible. Large ice cover (lower white dot) is unstable due to its high albedo, and jumps instantaneously (over geologic time) to complete ice cover (blue). But lower values of ice-cover may be stable at high enough temperature forcings. The left hand point where the hyperbola changes from a dashed to a solid line represents a change from a hard snowball to a steady state slushball solution (Pollard & Kasting, 2005). To achieve this by melting a hard snowball probably requires extremely high external temperature forcing (lower right hand dashed curve) (Pierrehumbert, 2005). Consequently if an external forcing (i.e. CO_2 build up through degassing) can melt a hard snowball, the jump to the ice-free state (upward pointing arrow) will be instantaneous. If the occurrence of the ice-free state causes a second forcing (such as silicate weathering) that will lower the temperature (i.e. move the system left along the upper line toward the downward arrow), then there exists a theoretical potential for sustained oscillation between ice-covered and ice-free states - a “limit cycle” in the terminology of dynamical systems theory (e.g. Saltzman, 2002). Image courtesy of P.F. Hoffman (<http://www.snowballearth.org>).

feedback that may control planetary temperature over geologic time - resolving the faint young sun through a higher steady-state greenhouse CO_2 forcing (Walker et al, 1981). Quantifying what (if any) enhancement of silicate weathering occurs through the activity of the biosphere is arguably the most important unanswered question (Berner et al, 1998, Schwartzman, 1999) in resolving whether regulation around habitable temperatures is driven by the presence of life (Lovelock, 1979).

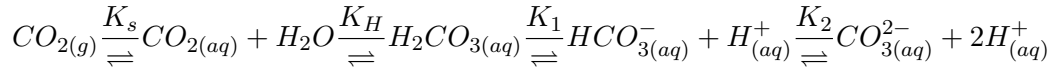
Ocean Carbon Chemistry

Most of the CO_2 on the surface of the Earth is in the oceans (e.g. Libes, 1992). Ocean chemical speciation determines the atmospheric fraction of the total ocean-atmosphere CO_2 reservoir, $\Sigma_{OA}CO_2$, therefore has climatic implications through the atmospheric $CO_{2(g)}$ partial pressure. Dissolved $CO_{2(aq)}$ molecules, the only species directly continuous with the atmosphere, make up a negligible fraction of total marine CO_2 :

$$\Sigma_{OA}CO_2 = CO_{2(g)} + CO_{2(aq)} + HCO_{3(aq)}^- + CO_{3(aq)}^{2-} \simeq CO_{2(g)} + HCO_{3(aq)}^- + CO_{3(aq)}^{2-}$$

1.D

The reason for this relative partitioning lies in the thermodynamics of equilibration between Carbonic acid anions, which result in dissolved CO_2 being dominated by the bicarbonate anion $HCO_{3(aq)}^-$. Equilibration of marine CO_2 can be summarised:



1.E

Where K_s is the solubility of CO_2 in seawater, K_H the rate constant for hydration of dissolved CO_2 , and K_1, K_2 equilibrium constants for (respectively) the partitioning of Carbonic acid $H_2CO_{3(aq)}$ into bicarbonate $HCO_{3(aq)}^-$ and carbonate $CO_{3(aq)}^{2-}$ anions. The values of these equilibrium constants are sensitive to temperature, salinity and ocean alkalinity, therefore so is atmospheric $CO_{2(g)}$, therefore so is climate. For example, acidification of the deep ocean by bacterial heterotrophic respiration can solubilise $CaCO_{3(s)}$ before it is buried, liberating aqueous calcium cations. These cations act as a trapping agent for bicarbonate anions, shifting the equilibrium towards their formation and consequently promoting movement of CO_2 from the ocean to the atmosphere (Archer and Maier-Raimer, 1994).

The oceans also contain 95% of the water and 99% of the surface Earth's heat, making their dynamics critical for explaining major climatic changes. Equilibration of the three carbonate ions in a theoretical sealed, steady state ocean would yield a higher atmospheric CO_2 than observed (e.g. Saltzman, 2001). This is reconciled in view of three principal fluxes responsible for reducing the CO_2 content of the system:

1) Solubility pump - Cold water has higher retention capacity for CO_2 because more energy input is required to shift a CO_2 molecule to the gas phase (e.g. Libes, 1992). Hence transport of surface waters from warm low latitudes to cool high latitudes results in net CO_2 uptake by water, that then redistributes the CO_2 as it is deep-convected (e.g. the contemporary North Atlantic).

2) Biological pump - This refers to a fraction of Carbon in the photic zone that is reduced photosynthetically and sinks into the ocean interior, after which a fraction of it may escape remineralisation and be buried.

3) Calcite pump- Sinking of $CaCO_{3(s)}$ (and $MgCO_{3(s)}$) from inorganic formation and biotic calcification removes $CO_{3(aq)}^{2-}$ from the water column, and if the carbonates escape remineralisation the process removes CO_2 from the atmosphere-ocean system as a whole. $Ca/MgCO_{3(s)}$ burial must also balance cation input from silicate weathering for steady state CO_2 and alkalinity.

The phenomena

The Neoproterozoic geological record contains a number of independent geochemical features that are difficult to reconcile with a climate of the Phanerozoic archetype. Arguably the most coherent, integrative interpretation of the pattern is the snowball Earth hypothesis (Kirschvink, 1992, Hoffman et al, 1998) of global scale glaciation coupled with extreme Carbon cycle disturbance, although a series of alternatives have been proposed. This section reviews the evidence that led to the various hypotheses.

Glacial deposits with primary equatorial remnant magnetism

The Earth contains a magnetic dipole at an angle of around 11 degrees from its axis of rotation (e.g. Hollenbach & Herndon, 2001). When a charged particle moves through a magnetic field it feels a force perpendicular to both the motion of the particle and the field itself. When this process occurs due to the interaction between an external magnetic field and the orbital motions of the valence electrons of certain elements, these orbits acquire an orientation parallel to the magnetic field (e.g. Griffiths, 1998). A permanent magnet is an element that will retain this electronic orbital orientation (acquire a “remnant magnetism”) after the removal of the external magnetic field, unless it is heated above an element-specific “Curie temperature”. The remnant magnetism in Iron, relative to the dipole between the Earth’s North and South poles, indicates the latitude at which a sediment was deposited. If the remnant magnetism is parallel to the folding of the rock stratum, it can be assumed that it is primary - i.e. it reflects the rock’s latitude at the time of deposition. If the remnant magnetism is uncorrelated with the rock’s folding it is referred to as secondary,

and the implicit paleolatitude reflects the position of the rock at a point after its deposition and subsequent heating above Curie temperature (Figure 1.2).

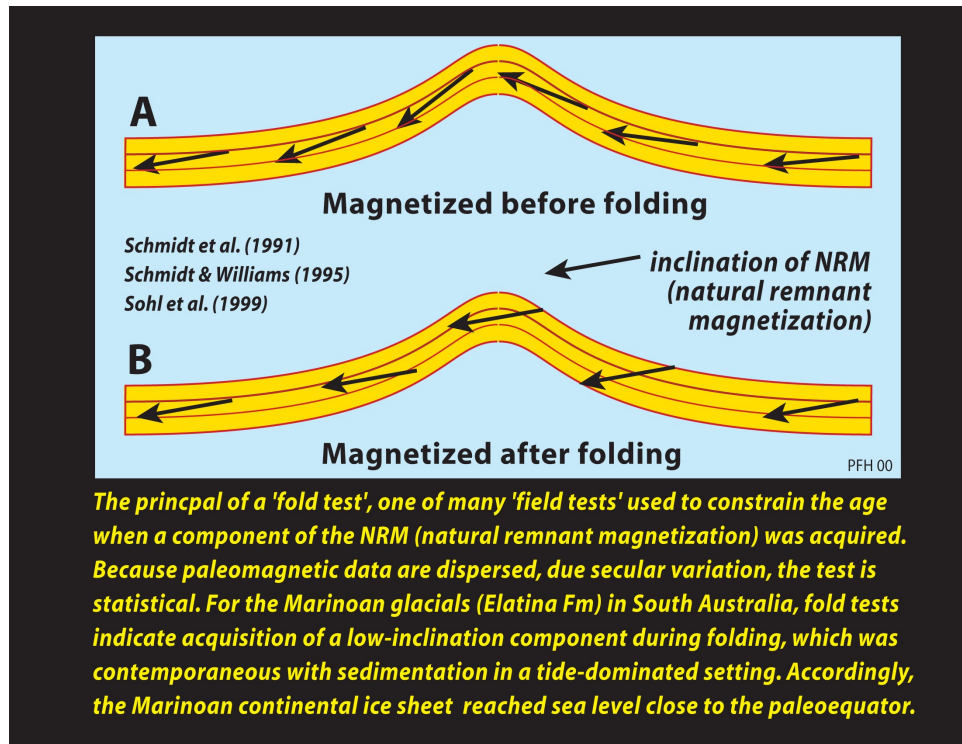


Figure 1.2 - The relationship between the plane of stratum folding and the plane of magnetic alignment can be used to determine whether the remnant magnetism of a sediment was acquired before or after it was deposited. Image courtesy of P.F. Hoffman (<http://www.snowballearth.org>).

Diamictites are sedimentary rocks composed of an unsorted, fine-grained heterogenous matrix, of which tillites are a sub-group specifically glacial in origin. A tillite is a rock formed by compaction and burial of a heterogenous collection of sediments, deposited directly by glacial action. Neoproterozoic sediments contain tillites with implicit low latitude remnant magnetism in significantly greater abundance than would be expected from a uniform distribution over the Earth's surface (Evans, 2000, Halverson, 2006). Although the error bar on paleolatitude is large, this low latitude glaciation result has consistently withstood criticism from alternative hypotheses (Spencer, 1971, Hambrey & Harland, 1981, Sohl et al, 1999, Hurtgen, 2005, Halverson, 2006, Fairchild & Kennedy, 2007). Diagnosis of a glacial origin for a sediment is contentious; many original "late Neoproterozoic glacial strata" (hereafter LNGD, (Hoffman & Schragg 2002)) have subsequently been reinterpreted as debris flow (Schermerhorn, 1974), asteroid impact events (Rampino, 1994, Williams, 1998), the flow and deposition of unsorted sediment (Eyles & Eyles, 1992, Eyles & Januszczak, 2004), and by weathering and mudflow in tectonic environments (Waythomas & Wallace, 2002). (The acronym LNGD is used hereafter, but the requirement for caution as to the reliability of

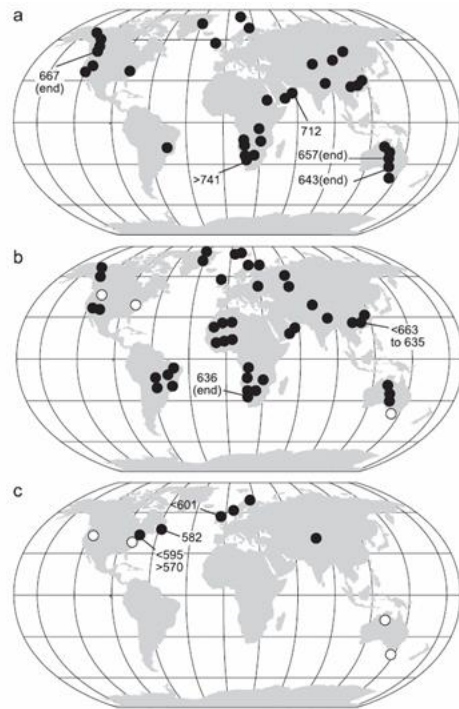


Figure 1.3 - The Global distribution of late Neoproterozoic glacial strata (LNGD) into three distinct intervals: “Sturtian” (Upper, 740 – 660Ma), “Marinoan” (Middle, < 660 – 635Ma), and (more contentiously) “Gaskiers” ~ 580Ma. Although stratigraphic constraints are loose, the sheer number and global synchronicity of LNGD weakens the suggestion that they lack a consistent, global-scale, paleoclimatic interpretation or are the result of systematic misdiagnosis in the field. Open circles show deposits whose diagnosis as glacial is uncertain. Figure from Fairchild & Kennedy, (2007).

the “glacial” part of the interpretation is noted). Glacial diamictites are characterised by stark vertical striation and complexity, implicitly due to fluctuating hydrology and sedimentation at ice fronts, as well as limited vertical thickness due to rapid sediment dumping (Eyles & Eyles, 1992). Critics argue that most Neoproterozoic diamictites are submarine “debrites” recording the flow then deposition of unsorted sediment in shallow water - a process that may happen at any latitude, without a unique paleoclimatic interpretation (Eyles & Januszczak, 2004). But the global scale, temporal synchronicity and sheer number of LNGD strengthens the converse viewpoint - that the deposits reflect a significant, global, climatic phenomenon (Figure 1.3).

It is worth noting that contemporary equatorial glaciers occur above about 4800 metres elevation (Haeberli et al, 1989), and mid latitude icebergs can potentially move up to 30 degrees equatorward before melting (Crowell, 1983). If Neoproterozoic glaciers behaved similarly, this represents a potential source of glacial dropstones with genuine low latitude remnant magnetism that is not indicative of global scale glaciation. The problem with this interpretation is that there needs to be an extremely large number of such deposits and they need to be correlated with extreme Carbon cycle disturbances. Assertions of a tectonic mass-flow origin for Neoproterozoic diamictites are both disputed on a case by case basis (Prave, 1999) and weakened by the stratigraphic discontinuities that provide evidence of glaciation that is distinct from stratum morphology (Sohl et al, 1999, Allen & Hoffman, 2005). Evans (2000) surveys around 80 putative glacial deposits, concluding that despite poor chronostratigraphic resolution, at least a small subset of the data can genuinely be interpreted as low-latitude glacial strata (Evans, 2000, Hoffman & Schragg, 2002, Halverson, 2006).

The precise age of most LNGD is poorly constrained. There may be up to three discrete glacial formations, but they always represent only a small percentage of the total thickness of Neoproterozoic sediments (Hambrey & Harland, 1981, Fairchild & Kennedy, 2007). The glacial deposits can be grouped into three broad time intervals, of descending order of geographical abundance (Evans, 2000). LNGD from between 740 and 720 Ma can be found on all continents, those from 620 – 600 Ma on most continents, and those from 580 – 570Ma only on the Avalonia-Cadomia subcontinent, possibly followed by a (highly contested) set of intercontinental glacial deposits from around 545Ma (Evans, 2000). In general, the idea of the global scale of the 580 events is becoming increasingly contested, and its recognition as a true snowball Earth may eventually turn out to be invalid (Fairchild & Kennedy, 2007). Lead zircon dating has been shown to be more reliable than previously used techniques such as *Rb – Sr* dating (Fairchild & Kennedy, 2007). Uranium *U* undergoes radioactive decay to lead *Pb*, according to $^{238}\text{U} \rightarrow ^{206}\text{Pb}$ and $^{235}\text{U} \rightarrow ^{207}\text{Pb}$. Both these Uranium isotopes are found in the mineral zircon $\text{ZrSiO}_{4(s)}$, but the mineral formation process strongly rejects lead, allowing the assumption that all *Pb* present in a sample derives solely

from radioactive decay, hence a dating (within the assumptions of negligible *Pb* leakage and the sample not having been heated above $\sim 900^{\circ}\text{C}$) (Parrish & Noble, 2003). Lead Zircon dating broadly supports the timing of the three major glacial intervals - Sturtian ($\sim 740 - 647\text{Ma}$), Marinoan ($\sim 660 - 635\text{Ma}$) and Gaskiers ($\sim 580\text{Ma}$) (Evans, 2000, Brasier et al, 2000, Dempster et al, 2002, Rumble et al, 2002, Hoffman & Schrag, 2002, Fairchild & Kennedy, 2007).

The geographical positions of geomagnetic North and South poles, with respect to the Earth's axial poles appear to have undergone periodic interchange during Earth history. The periodicity of these reversals varies significantly, but during Phanerozoic time appears to have been of an order of hundreds of thousands to millions of years (e.g. Okada & Niitsuma, 1989). Some LNGD show evidence of up to 6 geomagnetic reversal events (Preiss et al, 1987, Young & Gostin, 1990, Sohl et al 1999), and can be (subjectively) interpreted as indicating glacial duration of 3 – 30Ma (Sohl et al, 1999, Hoffman & Schrag, 2002). Platinum group elements (PGEs) such as Iridium are more abundant in extra-terrestrial material than in the Earth's crust (Wasson, 1985) - implying that high concentrations of PGEs indicate either increased exposure to the influx of extra-terrestrial matter, or reduced activity of the tectonic and weather systems that dilute this influx today. One scenario corresponding to the latter circumstance is accumulation of PGEs on the top of an ice layer during a snowball state. Anomalously high *Ir* accumulation has been observed at the LNGD-carbonate boundary of three sites (Bodieselitsch, 2005). When divided by (highly uncertain) estimates of contemporary extra-terrestrial influx rate (Kite & Wasson, 1986), these anomalies imply glacial duration between 40^{+20}Myrs and 12^{+4}Myrs (Bodieselitsch, 2005), compared to $\sim 3\text{Myrs}$ assuming a higher influx rate (Schmidt et al, 1997, Bodieselitsch, 2005). In theory, terrestrial sources for the *Ir* anomaly were ruled out by Bodieselitsch et al - for example no evidence of hydrogenous “nodule” precipitation of *Ir* with *Ni*, *Co* or *Mn* was seen, and the lack of *Al*, *Th* or *K* argued against a volcanic source (Bodieselitsch, 2005, supp. mat.). But the assumptions of uniform rate of carbonate deposition and that of a static ice sheet have been questioned, and the case made for PGE accumulation in a disturbed hydrogenous deposition regime (Fairchild & Kennedy, 2007). Nonetheless, the apparent PGE accumulation remains at least consistent with global-scale ice cover.

The hydrological regime represented by LNGD is ambiguous. Many diamictites show evidence of glacial scouring of the underlying rock, suggesting that glaciers were moving and/or changing in size (Rice & Hofmann, 2000, Hoffman & Schrag, 2002). Sedimentary rocks indicate repeated cycles of some tidal action within shallow equatorial water (Young & Gostin, 1990), but are undisturbed by wave action, consistent with waves being damped by globally abundant sea ice and a constrained hydrological cycle (Hoffman, 1999). But evidence of this sort for hydrologic activity amongst LNGD strata is proximal, therefore

potentially consistent with mutually exclusive models of Neoproterozoic climate (below).

Extensive “cap” carbonates

The upper layer of most LNGD is covered with carbonate platforms, often rich in the mineral dolomite $CaMg(CO_3)_{2(s)}$, usually < 5 metres but sometimes up to tens of metres thick (Spencer & Spencer, 1972, Williams, 1979, Deynoux, 1980, Fairchild, 1993, Brookfield, 1994, Kennedy, 1996, Hoffman et al, 1998). These capping carbonates generally overly glacial facies in an uninterrupted pattern - implying a causal, rather than just temporal, connection between the two phenomena (Fairchild & Kennedy, 2007). This connection has sometimes been called into question, but only one stereotypical cap carbonate deposit has been observed in the absence of an obvious candidate glacial deposit (Corsetti et al, 2004), compared with the near ubiquitous evidence for an active association between the two phenomena (Williams, 1979, Kennedy et al, 1998, Hoffman & Schrag, 2002, Shields, 2005). Detecting the likely duration of cap carbonate deposition is problematic - a critical question being whether the sediments record steady-state carbonate dynamics or reallocation of a non-steady state Carbon pool, presumably from the biosphere. Long term (~ 5 Myr) tectonic subsidence is required to create the accommodation space (difference between eustatic sea level and sea level including sediments and water mass) needed to protect instantaneously deposited carbonates from the erosion driven by gravitational equilibrium between the lithosphere and the asthenosphere and permit their accumulation and persistence (Hoffman & Schrag, 2002, Halverson et al, 2002). Some authors have argued that this was achieved by a near lack of sedimentation over this timescale (i.e. the cessation of terrestrial weathering during a global-scale glaciation), and that carbonate precipitation filled this accommodation space rapidly in the glacial aftermath, over timescales of hundreds to tens of thousands of years (Grotzinger & Knoll, 1995, Hoffman et al, 1998, Kennedy et al, 2001, Hoffman & Schrag, 2002). More recently, it has been argued that the whole idea of sudden deposition of carbonates, in a context that is relatively protected from erosion, is made obsolete by the idea that cap carbonates record a multi-million year sedimentation pattern, rather than a sudden post-glacial event. Diagnostic morphological features such as “tepee” (Aitken, 1991, Allen & Hoffman, 2005), “fan” (James et al, 2001) and tube-like (Cloud et al, 1974, Corsetti & Grotzinger, 2005) structures have been interpreted as diagnostic of rapid deposition in a “highly oscillatory flow regime” (Hoffman & Schrag, 2002), in contexts including deep water (Kennedy, 1996), supratidal spray zones (Deynoux & Trompette, 1976) and marine shallow shelf environments (James et al, 2001, Ridgwell et al, 2003). But the proposal of rapid deposition is weakened significantly by the observation of paleomagnetic reversals and excursions in carbonates (Trindade et al, 2003), as well as interfingering between carbonates and silicates, which imply a timescale of the order of 1Myrs for deposition to occur (Dyson & von der Borch, 1994). A more recent consensus on cap carbonate deposition, less consistent with earlier models of rapid formation, proposes

“cap carbonates as a shelfal record of condensation of background carbonate sedimentation in the absence of siliclastic deposition” (Fairchild & Kennedy, 2007), rather than a high resolution record of marine chemistry. The temporal constraints of the dating of cap carbonate deposition relative to the LNGD have been proposed to be too weak to support the claim that cap carbonates “immediately” overlie the putative glacial deposits, and attributed to deposition of clastic carbonate in rift basins during supercontinental disintegration, or to extreme changes in marine production (Eyles & Januszczak, 2004). But more uniformitarian explanations fail to account for why (for example) clastic deposition associated with continental breakup should be so heavily biased towards carbonates, or give rise to such a distinct geomorphology. Opponents of the snowball Earth hypothesis nevertheless accept the need to explain the global scale and (at least apparent) synchronicity in cap carbonate deposition (Kennedy et al, 1998, Prave, 1999).

Extreme Carbon isotope $\delta^{13}C$ excursions

The ratio between the two main isotopes of Carbon, $^{13}C/^{12}C$ in rock samples is inferred to closely parallel changes in productivity - ultimately as a result of a kinetic bias in favour of ^{12}C by Ribulose-1,5-biphosphate Carboxylase Oxygenase (“Rubisco”), the enzyme responsible for the Carbon fixation “dark” reactions of photosynthesis (Mook, 1986). The inference is that an inorganic carbonate enriched in ^{13}C was deposited in a context of high photosynthetic productivity. By convention, the $^{13}C/^{12}C$ isotope ratio is expressed in terms of its deviation $\delta^{13}C$ from a standard, the “Pee Dee Belemite” $^{13}C/^{12}C_{PDB} = 0.112372$ (Craig, 1957), measured in parts per thousand (‰).

$$\delta^{13}C_{sample} = \left(\frac{(^{13}C/^{12}C)_{sample}}{(^{13}C/^{12}C)_{PDB}} - 1 \right) \cdot 1000 \tag{1.1}$$

The Neoproterozoic Carbon isotopic record (Figure 1.4) exhibits fluctuations qualitatively greater than those seen over Phanerozoic time, and the largest of these fluctuations occurs either side of LNGD (Knoll & Walter, 1992, Kaufman & Knoll, 1995, Jacobsen & Kaufman, 1999, Hayes et al, 1999, Hoffman et al, 1998, Walter et al, 2000, Rothman et al, 2003). A systematic, reproducible trend across unrelated basins suggests that the pattern records a global change in seawater chemistry (Knoll et al, 2006, Fairchild & Kennedy, 2007). The cap carbonate formations are nearly without exception $\delta^{13}C$ depleted, (i.e. relatively ^{12}C rich), as is carbonate in other diamictites associated with LNGD (Crossing & Gostin, 1994, Kennedy et al, 2001, Hoffman & Schrag, 2002, Fairchild & Kennedy, 2007). The systematic trend within separate cap carbonates - starting at about $\delta^{13}C = 0 \text{ ‰}$, then declining to as low as $\delta^{13}C = -6 \text{ ‰}$ - strengthens the idea that they reflect a global-scale record of seawater chemistry (Jacobsen & Kaufman, 1999, Fairchild & Kennedy, 2007). An original feature of the description of cap carbonates within the snowball Earth

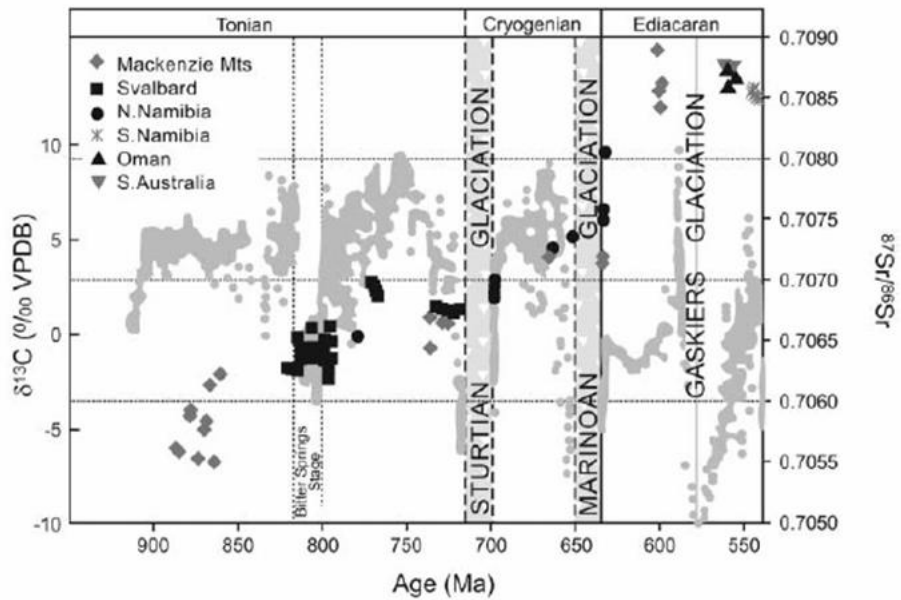


Figure 1.4 - The Neoproterozoic Carbon $\delta^{13}C$ and Strontium $^{87}Sr/^{86}Sr$ isotopic records of marine Carbonates (Data from Halverson et al, 2007). Carbon isotopic data $\delta^{13}C$, left Y-axis shown with faint symbols, Strontium isotopic data $^{87}Sr/^{86}Sr$ (right Y-axis) with bold symbols (depending on the region shown in the legend) - both in parts per thousand (‰). Age of deposit (Ma) shown on X-axis, timing of glaciations indicated with an arbitrary duration interval. Carbon isotopic data showing pre-glacial increase (which is probably polygenetic) and post-glacial decline in $\delta^{13}C$, can be contrasted with the roughly linear progressive increase in the Strontium $^{87}Sr/^{86}Sr$ ratio. (Figure credit Fairchild & Kennedy, 2007).

hypothesis was the observed pre-glacial increases in isotopic enrichment $\delta^{13}C > 5 \text{ ‰}$, consistent with elevated productivity before the glacial event (Hoffman et al, 1998, Jacobsen & Kaufman, 1999 Hoffman & Schrag, 2002). However, with increasing amounts of data, the observation of any unique, globally reproducible $\delta^{13}C$ pattern has of late been called into question (Fairchild & Kennedy, 2007). Isotopic excursion does not uniquely coincide with cap carbonates and may continue after their deposition has ceased - presenting the realistic possibility that the two phenomena are decoupled (Kennedy et al, 2001, Jiang et al, 2003).

Incompletely oxidised Iron-rich rocks

Iron predominantly occurs in Earth’s atmospheres and oceans in two forms - the trivalent, “ferric” Fe^{3+} form, which is insoluble in water, and the divalent “ferrous” Fe^{2+} form. In contemporary oxic marine environments, Fe^{2+} is oxidised to Fe^{3+} then precipitated as $Fe(III)$ oxides (e.g. Stanley, 1999). This relationship between the phase of Fe and the oxidation status of the oceans is used to explain the relative abundance of “Banded Iron formations” during different eras of Earth’s history. A banded iron formation (BIF) is a sedimentary rock in which layers of iron oxides are interspersed with the silicate mineral chert (predominantly made of interlocking quartz SiO_2 crystals). Some of the iron in BIFs is incompletely oxidised - e.g. in magnetite $Fe_3O_{4(s)}$, which contains one Fe^{2+} ion. The extensive deposition of incompletely oxidised Iron-rich rocks at the base of the Earth’s oceans has three prerequisites:

- 1) Anoxic conditions permissive for accumulation of $Fe_{(aq)}^{2+}$ (Holland, 1984).
- 2) A restriction on the supply of hydrogen sulphide H_2S (Drever, 1974, Holland, 1984, Hoffman & Schrag, 2002). This mimises the removal of ferrous Iron through bacterial Sulphide metabolism:



(1.F)

Under oxic conditions the pyrite FeS_2 produced by this reaction can be recycled by a series of reactions involving a Manganese intermediate and the formation of sulphate SO_4^{2-} , but in anoxic conditions a pyrite $FeS_{2(s)}$ burial flux may give rise to a net loss of Iron from the system. A ratio $H_2S : Fe^{2+} < 2$ ensures that not all available Fe is lost in this way (Amend et al, 2004). The restricted supply of Sulphur implicit in this condition has been interpreted as consistent with (and perhaps contingent upon) limited runoff from terrestrial weathering - and therefore with extremely low temperatures and/or extensive terrestrial ice cover (Canfield & Raiswell, 1999). I.e., banded Iron formations may depend more on the absence of an $SO_{4(aq)}^{2-}$ influx from weathering than the absence of oxygen in the atmosphere.

3) The presence of a local oxidant - probably required to cause the precipitation of an Iron oxide precursor (Hoffman & Schrag, 2002).

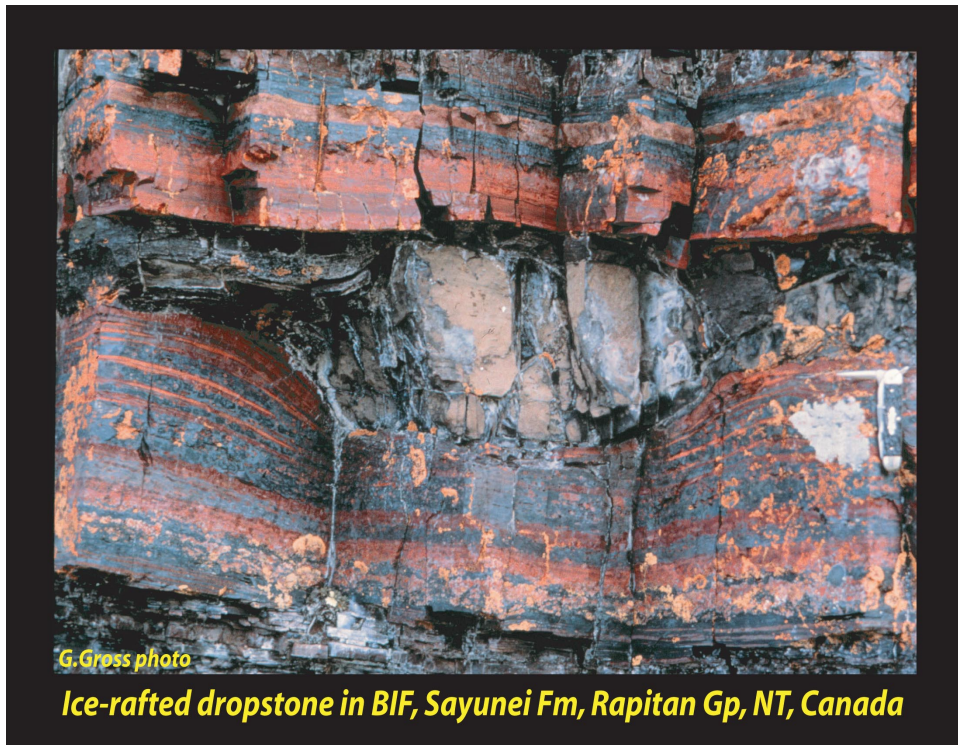


Figure 1.5 - The (restricted, localised) reappearance of incompletely oxidised iron-rich rocks during the Neoproterozoic occurs uniquely within and immediately above LNGD. Above, large rock fragments proposed to be glacial “dropstones” (i.e. dropped by floating ice) are contained within a banded Iron section. (Figure credit P.F. Hoffman www.snowballearth.org).

Most banded Iron formations date from between 3.2 and 1.85 Billion years before present, spanning the Paleoproterozoic “great” oxidation of the atmosphere at $\sim 2.4 - 2.0\text{Ga}$ (Holland, 2002). After approximately 2.0Ga they are increasingly replaced by “red beds” (mostly haematite $Fe_2O_{3(s)}$, rich in fully oxidised Fe^{3+}). A unique exception to the large-scale disappearance of BIFs after the great oxidation occurs during the Neoproterozoic, in which a limited number of incompletely-oxidised iron rich deposits are found - solely within and/or above LNGD (Young, 1976, Yeo, 1981, Trompette et al, 1998, Lottermoser & Ashley, 2000, Hoffman & Schrag, 2002). This was attributed to a detailed scenario involving deep ocean anoxia within the snowball Earth hypothesis (below). But in a similar way to the proposed pre-glacial $\delta^{13}C$ increase, more cautious authors have highlighted how there may be no consistent global-scale pattern in Iron deposits - and that BIFs may simply be localised and of multiple causal origin (Fairchild & Kennedy, 2007). In this light it is notable that iron formations associated with Neoproterozoic LNGD only occur at rift margins - particularly exposed to the deposition by mass flows of rocks formed elsewhere (Eyles, 1993, Eyles

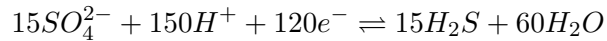
& Januszczak, 2004).

Sulphur isotopes and marine oxidation

Despite the rarity of Neoproterozoic BIFs, there is other evidence for the hypothesized deep ocean anoxia that they have been used to support. The two main isotopes of Sulphur S , ^{34}S and ^{32}S , collectively accounting for about 99% of the Earth's crustal reservoir, differ in their fractionation properties and are therefore of use in describing the element's geochemical cycling (Charlson et al, 2000). The deviation $\delta^{34}S$ from a standard $(\frac{^{34}S}{^{32}S})_{standard} = 0.450045$ (Jensen & Nakai, 1962) that the ratio of the two elements exhibits within a given sample $(\frac{^{34}S}{^{32}S})_{sample}$, is of use in determining the redox status of the S reservoir when that sample was deposited:

$$\delta^{34}S = \left(\frac{(\frac{^{34}S}{^{32}S})_{sample}}{(\frac{^{34}S}{^{32}S})_{standard}} - 1 \right) \cdot 1000 \tag{1.2}$$

Fractionation of ^{34}S is ultimately biotic in origin. The biochemistry of bacterial sulphate reduction (reaction 1.G, Rafai et al, 1998) kinetically favours the lighter isotope ^{32}S , which consequently becomes enriched within the hydrogen sulphide H_2S product.



1.G

Contemporary anoxic ocean sediments exhibit a much lower $\delta^{34}S$ than the open ocean (i.e. are relatively ^{32}S enriched, implying more prolific bacterial SO_4^{2-} reduction) - therefore a low $\delta^{34}S$ in pyritic marine strata can be interpreted as indicating anoxic conditions (Holser et al, 1988). The $\delta^{34}S$ of Neoproterozoic pyrite formation averages becomes increasingly negative compared to the averages of Sulphate formations, consistent with a near complete reduction of the marine SO_4^{2-} reservoir (Walter et al, 2000, Hurtgen et al 2002, 2004, 2005, Gorjan et al, 2003, Canfield, 2004). Large, short-term variations in $\delta^{34}S$ have been related to extremely low SO_4^{2-} concentrations in comparison to modern values, hence implicitly to low pyritic weathering fluxes and/or low atmospheric Oxygen (Pavlov et al, 2003). Conversely however, the observed low average values of $\delta^{34}S$ have been argued to still be consistent with sufficient Sulphate SO_4^{2-} to generate an anoxic, sulphidic deep ocean (Canfield, 1998). The disappearance of BIFs may thus be driven largely by high Mesoproterozoic sulphate influx and pyrite $FeS_{2(s)}$ burial, and less strongly entwined with the O_2 level in the oceans (Canfield, 1998, Fairchild & Kennedy, 2007). Though dismissive of their global-scale significance, this would explain the apparent absence of BIFs during the Cretaceous ocean anoxic events, assuming a greater SO_4^{2-} flux from terrestrial weathering

(e.g. Jenkyns, 1980). Finally, the extremely large Neoproterozoic *differences* between $\delta^{34}S$ values of Sulphate SO_4^{2-} and sulphide H_2S sediments $\delta^{34}S > 46 \text{ ‰}$ may imply secondary reoxidation of the Sulphide, then further reduction - i.e. localised bacterial sulphate reduction in an ocean that was nevertheless predominantly oxic (Canfield & Teske, 1996, Anbar & Knoll, 2002). The variation within, and resolution of, the $\delta^{34}S$ data, not to mention the subjectivity surrounding its global-scale implications, is a large source of uncertainty that, if resolved, may allow conclusive determination of Proterozoic ocean redox status, ocean-atmosphere continuity and terrestrial weathering magnitude (Fairchild & Kennedy, 2007).

Geochemistry of other isotopes

(a) Strontium

The relative abundance of the two main isotopes of Strontium $^{87}Sr/^{86}Sr$ varies in different parts of the Earth's crust, and can consequently be used to infer the relative magnitude of different geochemical fluxes (e.g. Peterman, 1970). The concentration of Sr in mid-ocean ridge (MOR) basalts is sufficiently greater than that of seawater that the isotopic composition of water ($^{87}Sr/^{86}Sr \simeq 0.7090$) flowing through MORs approaches that of the rock $0.702 \leq ^{87}Sr/^{86}Sr \leq 0.703$ (Holland, 1984). Notwithstanding large variations between different drainage basins, the average $^{87}Sr/^{86}Sr$ of terrestrial weathering runoff is around $^{87}Sr/^{86}Sr = 0.712$, therefore higher values of $^{87}Sr/^{86}Sr$ in marine carbonates imply seawater in equilibrium with greater weathering fluxes (Holland, 1984). Measurements of $^{87}Sr/^{86}Sr$ in Precambrian deposits are sparse and somewhat unreliable, due to the high mobility of the element (Derry et al, 1992). Furthermore, extrapolation of Phanerozoic $^{87}Sr/^{86}Sr$ values to the Precambrian may not be reasonable, with ancient carbonates declining to about $^{87}Sr/^{86}Sr = 0.700$ (Veizer & Compston, 1974). Despite these caveats, it is apparent that Neoproterozoic marine $^{87}Sr/^{86}Sr$ signatures exhibit a steady increase throughout the era (Sheilds & Veizer, 2002, Halverson et al, 2007), which has been interpreted (Fairchild & Kennedy, 2007) as explicable by a progressive increase in the magnitude of terrestrial silicate weathering (Figure 1.6). However, the steady increase observed in $^{87}Sr/^{86}Sr$ is seemingly unconnected with the precise timing of LNGD deposition, and the continuity of the increase is contrary to the expectation of intervals during which the ocean was isolated from the atmosphere and dominated by hydrothermal activity. Nevertheless, some brief fluctuation (not visible in Figure 1.6) occurs in localised deposits between 740 and 600Ma (Jacobsen & Kaufman, 1999, Kennedy et al, 2001). The relatively long marine residence time of $Sr \sim 0.7\text{Myrs}$ (de Villiers, 1999) may, in any case, be too long to accurately resolve most short term weathering changes relevant to glaciation, and the pattern of increasing silicate weathering runoff is roughly consistent with the snowball Earth hypothesis. Some attempts to normalise for hydrothermal influences on $^{87}Sr/^{86}Sr$ have detected a tangible, weathering-specific signal roughly associated with the

timing of putative glacial events (Sheilds, 2007).

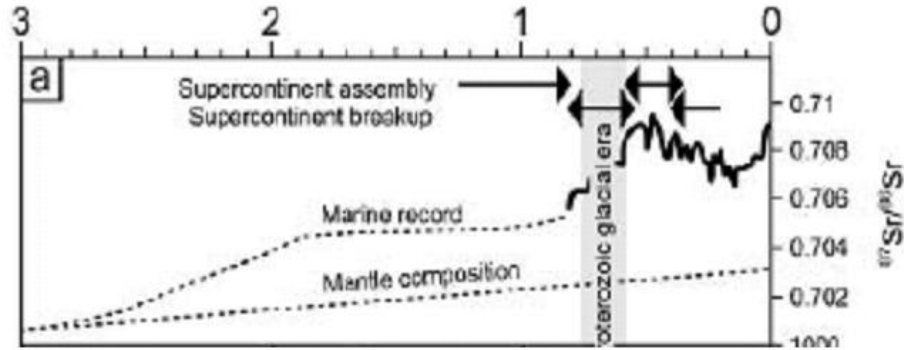


Figure 1.6 - Simplified summary of the $^{87}\text{Sr}/^{86}\text{Sr}$ signature of marine carbonates (Y-axis) over Earth system history (Sheilds & Veizer, 2002, Halverson et al, 2007), compared to the timing of geochemically significant events. X-axis (note scale at top of figure) shows time in billions of years before present, shaded block shows the timing of the Neoproterozoic glacial era. Lower dashed line shows $^{87}\text{Sr}/^{86}\text{Sr}$ of igneous rocks assumed to be representative of the mantle, upper dashed line the $^{87}\text{Sr}/^{86}\text{Sr}$ of marine carbonates assumed representative of seawater. Note the slight accentuation of the rate of increase in marine $^{87}\text{Sr}/^{86}\text{Sr}$ from about 850Ma, up to and including the Neoproterozoic glacial interval. Figure credit Fairchild & Kennedy, 2007.

(b) Oxygen

The temperature related fractionation properties of the ^{18}O isotope make it useful for making paleoclimatic inferences. Isotopically heavier water H_2^{18}O requires greater energy input to attain boiling or melting point, hence will freeze more readily and evaporate less readily (e.g Horita, 1994). The deviation exhibited by a rock sample is compared to a standard $(^{18}\text{O}/^{16}\text{O})_{\text{standard}} = 2005.2$ (e.g. Fricke & O'Neill, 1999):

$$\delta^{18}\text{O} = \left(\frac{(^{18}\text{O}/^{16}\text{O})_{\text{sample}}}{(^{18}\text{O}/^{16}\text{O})_{\text{standard}}} - 1 \right) \cdot 1000$$

(1.3)

After biases attributable to the latitude of the rock have been scaled out, higher $\delta^{18}O$ implies greater evaporation from the body of water in equilibrium with the sediment; hence higher global temperatures (Fricke & O’Neill, 1999). Extremely low $\delta^{18}O$ is observed in Neoproterozoic strata (Rumble et al, 2002, Zheng et al, 2004). But this pattern is subject to extreme stratigraphic variability (Wu et al, 2004) and $\delta^{18}O$ is highly susceptible to post-depositional modification in comparison to other isotopic signature systems (Fairchild & Kennedy, 2007). Finally, sudden high $\delta^{18}O$ characteristic of proposed post-glacial extreme greenhouse events are conspicuous in their absence.

(c) Boron

The relative abundance of the two naturally occurring and stable isotopes of Boron, ^{11}B and ^{10}B can be compared to a standard $(^{11}B/^{10}B)_{standard} = 4.0529$ (Aggarwal & Palmer, 1995) using a methodology analogous to other isotopes.

$$\delta^{11}B = \left(\frac{(^{11}B/^{10}B)_{sample}}{(^{11}B/^{10}B)_{standard}} - 1 \right) \cdot 1000 \tag{1.4}$$

Borate $B(OH)_4^-$ and Boric acid $B(OH)_3$ may substitute for (respectively) $\frac{1}{2}CO_3^{2-}$ and $CaCO_3$ during marine carbonate deposition, meaning that the $\delta^{11}B$ of a sample is considered representative of the ocean at the time of deposition (Pagani et al, 2005). Boric acid $B(OH)_3$ is relatively enriched in ^{11}B compared to Borate $B(OH)_4^-$ as a result of differing vibrational energy within the trigonal and tetrahedral species between the two isotopes (Urey, 1947, Kakihana, 1977). Partitioning between the two Boron species is a major determinant of ocean alkalinity (e.g. Millero, 1995) and $\delta^{11}B$ is therefore assumed positively correlated with ocean pH via $B(OH)_{3(aq)} + OH_{(aq)}^- \rightleftharpoons B(OH)_4^-$ (Pagani et al, 2005). A negative $\delta^{11}B$ excursion has been documented for marine carbonates formed at around 600Ma, and interpreted as consistent with marine acidification after the second proposed glacial event (Kaseman et al, 2005). Further measurements with better temporal constraints and overlaps with the other proposed glacial intervals are required in order to assess the plausibility of this interpretation.

The Neoproterozoic biosphere

Background: Multi-level selection and biological patterning Any biological pattern as stark as that observed in the Neoproterozoic must be explained in an evolutionary context that can predict the types of form that will, and will not, maximise fitness. The label “fitness” is used to describe both the survival and fecundity of a genotype. Neither an organism that produces huge numbers of offspring, then dies along with all of these offspring, nor one that ensures its own survival but does not reproduce, will increase from rarity within a population. This tension between fecundity in the short term and survival

in the long term is critical to many evolutionary trade-offs. Natural selection frequently operates hierarchically on large groups of replicators (like multicellular organisms) that are composed of smaller individual replicators (like cells). Many traits have an evolutionary impact on both the bearer and on individuals with which the bearer interacts - such traits are referred to as “social”. Often, the trait value that maximises the fitness of the bearer is different to the trait value that has the greatest positive impact on surrounding individuals - such as when genes for unrestricted cell growth lead to tumours in animals and plants. This leads to a tension between conflicting selection pressures at the individual and at the trait group levels. A trait that increases the fitness of the individuals with which the bearer interacts is termed co-operative, and a co-operative trait that imposes a fitness penalty on the bearer is termed altruistic (e.g. Lehmann & Keller, 2006) - though of course no sentience or underlying purpose is implied. If an individual interacts with an altruist, it experiences a benefit, if it interacts with a non-altruist (“cheater”) individual, it may experience decreased fitness, depending upon its own genotype. Whether or not altruistic traits are adaptive depends on the nature of the relationship between the focal “actor” individual bearing the trait, and the “recipient” individual experiencing the trait’s results. There are a number of scenarios that can give rise to co-operation, all involving some constraint on the ratio $\frac{b}{c}$, of fitness benefit to recipient b , and fitness cost to altruist c . Each scenario involves some measure of the probability that an altruistic strategy will encounter and/or cause benefit to, a copy of itself. Different circumstances that can give rise to evolutionarily stable co-operation are (from Nowak, 2006):

(a) Kin selection $\frac{b}{c} > \frac{1}{r}$ (Hamilton, 1964, 1972). This process describes the effect on the fitness of an altruistic gene of the probability that the recipient of altruism also carries a copy of that gene. This probability is termed relatedness r , but is defined specifically with respect to the focal locus and measures the probability of a correlation in trait values - which is not necessarily identical to correlation in descent. The conditions under which kin selection is relevant to a given trait depend on the balance between kin selection and kin competition, and consequently on the demographics - other more complex forms of Hamilton’s rule have been derived to incorporate the influence of population viscosity under spatially continuous conditions (e.g. Van Baalen & Rand, 1998), as well as varying ploidy and sex ratios (Hamilton, 1972).

(b) Group selection (e.g. Sober & Sloan-Wilson, 1998). This is a means of expressing the way in which natural selection operates hierarchically on group replicators (such as social groups) that are themselves composed of smaller individual replicators (such as individual organisms). In circumstances where trait values that increase the short term fitness of the smaller replicators simultaneously decrease the long term fitness of the larger replicators of which they are a part, then evolution of co-operation requires $\frac{b}{c} > 1 + \frac{n}{m}$, where n is the maximum number of individuals per group, and m is the number of groups in the higher

level population (Traulsen & Nowak 2006). This condition arises from the assumption that a group of altruists will either split more frequently (“group fecundity selection”) or have a higher probability of survival (“group viability selection”) than will a group of cheaters. It is arguable that in nature the probability of two individuals sharing a gene is reasonably approximated by $r \simeq \frac{m}{m+n}$ - i.e. that kin selection is an explicit genetic description of one type of group selection (Frank, 1998, Nowak, 2006).

(c) Reciprocity (Trivers, 1971). If an altruistic act by an individual increases the probability of that individual being the recipient of altruism, the trait may proliferate. Direct reciprocity requires $\frac{b}{c} > \frac{1}{w}$, with w , the probability of a repeated social interaction between the same two individuals, necessary to scale the mutual benefit from an interaction between two altruists by the probability that this interaction will happen again (Trivers, 1971, Axelrod & Hamilton, 1981). Reciprocity may also occur in other contexts, including spatial networks $\frac{b}{c} > k$ where k is the average number of neighbours per individual (Nowak & May, 1992).

Fossils

Eukaryotic cells walls contain steroid alcohols to increase membrane fluidity, whereas most prokaryotes use the related hopanoid compounds for the same function (e.g. Madigan & Martinko, 2005). Consequently, sterol derivatives have been used to invoke the presence of eukaryotes as far back in Earth history as the late Archean (Brocks et al, 1999) - a suggestion recently called into question in the light of sterol production by cyanobacteria (Volkman, 2005) and several other bacterial species (Cavalier-Smith, 2006). Nevertheless, eukaryotic body fossils are identified by diagnostic cell division patterns by at least the early Mesoproterozoic (Hofmann, 1990, Javaux et al, 2003, Knoll et al, 2006, Butterfield 2004, 2005, 2007). The Mesoproterozoic 1600 – 1000Ma documents the divergence of major Eukaryotic clades, including algae specimens from 1200 Ma (Butterfield, 2000) and 1000Ma (Butterfield, 2004), probable fungi at 1430Ma (Butterfield, 2005), and various unassigned “problematica”, exhibiting cellular colonies at 1000Ma (Knoll et al, 2006), possible morphologically-distinct life history phases by at least 1000Ma (Butterfield, 2005, Knoll et al, 2006), and a middle Neoproterozoic specimen with up to six distinct cell types (Butterfield et al, 1994). Despite these rare examples of eukaryotic differentiation, the overarching pattern within the Mesoproterozoic biosphere is minimal diversity and relative evolutionary stasis in both eukaryotic and prokaryotic morphological evolution (Butterfield, 2007, Gaidos et al, 2007). The starkest absence is that of macroscopic animals - of which there are none whatsoever prior to the late Neoproterozoic.

The Ediacaran period (620 – 543Ma, (Knoll et al, 2004)) exhibits a change from a predominantly low diversity microscopic biosphere, to a biosphere containing macroscopic,

morphologically diverse organisms and biogeographical partitioning (Butterfield, 2007), and the increased evolutionary tempo is most pronounced in animal evolution (Knoll & Carroll, 1999, Gaidos et al, 2007). The precambrian record of animal life records three successive 15 – 20Myr intervals of diversification (Figure 1.7) that created the context for the Cambrian “explosion” (Gaidos et al, 2007):

(1) Morphological diversification including epithelial differentiation within Metazoan stem group organisms by 580Ma, and possibly by as early as 635Ma.

(2) Bilateral symmetry and mobility by 560Ma.

(3) Biomineralisation and predation by 545Ma.

An equivalent increase was observed in the rate of evolution of organic-walled eukaryotic microfossils (of problematic, probably polyphyletic, taxonomic affinity) during the Ediacaran. Microfossil morphospecies richness increased dramatically from roughly 600Ma (Knoll, 1994, Knoll et al, 2006, Figure 1.8), at which point species longevity declined suddenly from the previous 100Myr to 15 – 50Myr (Knoll, 1994, Grey et al, 2003). The fact that this increase in the evolutionary rate of microfossils coincides with the macroscopic Ediacaran radiation invokes a common ecological cause.

Molecular clocks

The first fossil specimens of a given taxon record the latest possible date of the group’s origin (Jaanusson, 1976), making it reasonable to look for genetic constraints to corroborate the fossil record. But molecular clock techniques require a known rate of sequence change to be sufficiently conserved over the timespan of interest - a requirement rarely met with any confidence. “Maximum Likelihood” Molecular clocks, that are weighted to incorporate (assumed) sequence-specific rate heterogeneity, place the divergence of the Eumetazoan clade significantly earlier than does the fossil record (Douzery et al, 2004, Hedges et al, 2001, 2004a, 2004b). Some of these estimates of a deep root far exceed the error margin expected within the molecular clock method (by, for example intra-species diversification in specific sequences prior to the actual speciation event). E.g. deep roots in Eukaryotic phyla, including a Porifera-Eumetazoa split as early as 1351Ma have been used to argue for the existence of precursors to the Metazoa as a cryptic fauna (Hedges et al, 2004b). But these results required a dramatic relaxation of the calibration times relating sequences to the fossil record - by treating the fossil appearance of a taxon as a minimum bound, and are therefore highly circular (Gaidos et al, 2007). “Minimum Evolution” molecular clocks in which character distribution is simply discretized, and distances between taxa calculated according to a Poisson distribution, place the divergence of the Eumetazoa between

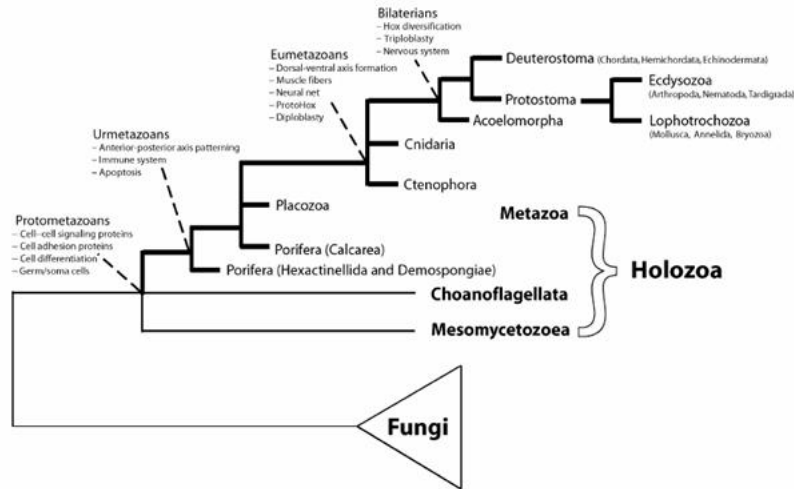


Figure 1.7 - Possible phylogenetic tree of the extant Metazoa and their closest relatives, noting the character sets thought to be sufficient for various grades of animal organisation. The timing, and in cases position, of the nodes of this tree are not conclusively established (Gaidos et al, 2007). The “Protometazoans” contain both contemporary Eumetazoa and their closest unicellular relatives. The “Urmetazoans” contains the hypothetical universal common ancestor of all animals (the Urmetazoan), and is assumed a stem group* to extant Eumetazoa. The date of the basal node of the Protometazoans is unknown, but is likely at some point during the Mesoproterozoic. The Urmetazoan basal node divergence event likely occurred during the Ediacaran, by 580Ma or earlier. Note that caspase-based apoptosis is a synapomorphy for the Urmetazoans, and the paraphyly of the Porifera is tentative, but has some empirical support (Peterson & Butterfield, 2005) (Figure credit Gaidos et al, 2007). It is important to note that there is significant uncertainty in the tree topology derived from this and equivalent studies (e.g. Roger & Hug, 2006).

**(In phylogenetics, a monophyletic group is a collection of species sharing a common ancestor - in contrast with a polyphyletic group sharing a character set, but lacking a common ancestor with that character set. A paraphyletic group shares a common ancestor, but does not contain all the descendents of that common ancestor. A crown group is a monophyletic group containing the last common ancestor of its members, and can be contrasted with a basal stem group. A stem group is more closely related to a particular crown group than is any other group, but does not contain all the descendents of its common ancestor. A stem group is thus a paraphyletic group. A synapomorphy is a character state shared by two or more taxa that originated in the most recent shared common ancestor of these taxa (e.g. Ridley, 2004). For example, above the Protometazoans are a stem group with respect to the crown group Urmetazoans, which in turn are a stem group with respect to the crown group Eumetazoa. Synapomorphies for the Urmetazoans are Anterior-posterior patterning, an immune system and caspase-based Apoptosis).*

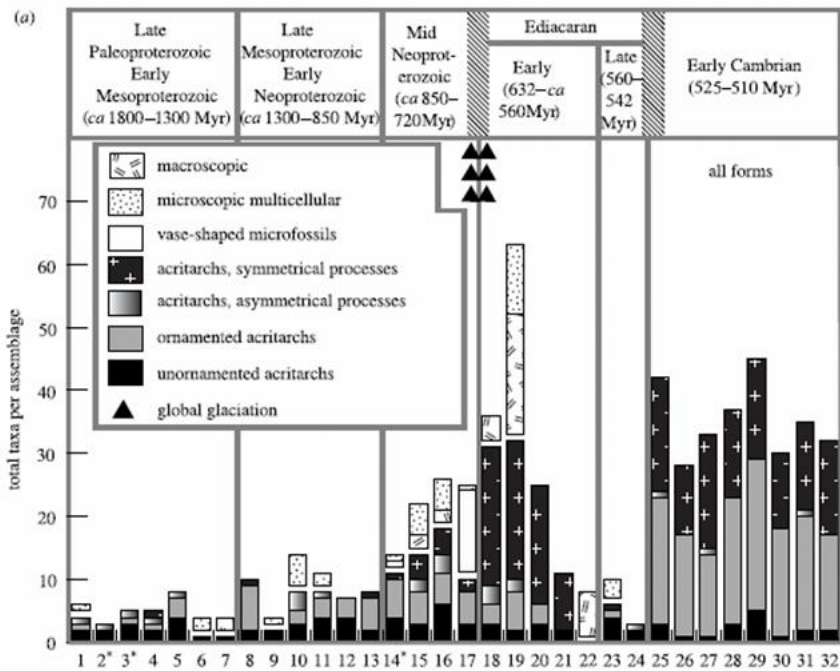


Figure 1.8 - Changes in Morphospecies richness per assemblage (Y-axis) over precambrian and early Cambrian time (X-axis, top). The numbers on the lower X-axis are labels for individual assemblages, corresponding approximately to the time scale on the upper X-axis. Each vertical bar is divided according to the fraction of each morphospecies type contained in the assemblage. Note the stark increase in the number macroscopic species after the 630Ma glaciation event. (Figure and results from Knoll et al, 2006).

634 and 604 Ma, consistent with fossil evidence for Ediacaran diversification (Peterson & Butterfield, 2005). Equivalently, complete relaxation of the molecular clock assumption, and its replacement with conditional probability models incorporating prior rate change, places divergences of Eumetazoan clades in positions roughly supported by the fossil record (Aris-Brosou & Yang, 2003, Douzery et al, 2005). These differences in conclusions and sensitivity to calibration techniques and initial assumptions serve to illustrate how molecular clocks are best viewed as a tool for determining which statistical model of evolutionary rate best fits the paleontological data, when fossils already imply a specific tree topology reasonably clearly. Molecular clocks do not provide a compelling argument for deep, cryptic Precambrian animal divergence, but nor do they rule out the possibility (Gaidos et al, 2007). In this vein, it is important to note the distinction between the construction of phylogenetic trees per se, and resolving the dates of the various nodes using molecular clock methods. Uncertainties in the tree separating major eukaryotic clades means that molecular clocks used to date divergence times within this tree can produce widely different results, depending upon initial assumptions about tree topology (Roger & Hug, 2006). Arguably therefore, molecular clocks can only be justifiably used to make the temporal resolution of a tree more precise, after an unambiguous topology has already been established within the fossil record.

Models of Neoproterozoic climate

The Neoproterozoic era combines the temperature and habitability extremes (e.g. Kopp et al, 2005, Cockell & Raven, 2007) and dramatic biological innovation (Lenton et al, 2004, Kump, 2007) that occurred during earlier parts of the Precambrian with a transition to the Phanerozoic archetype that appears to exhibit temperature fluctuation over a much less dramatic scale (e.g. Stanley, 1999, Schwartzman, 1999). As a result, scenarios depicting Neoproterozoic climate must be both extreme enough to explain the low latitude tillites and Carbon cycle fluctuations, but coherent enough to explain how the Phanerozoic archetype originated.

The snowball Earth hypothesis

In theory, an unusual concentration of landmasses at or near the equator should dramatically increase CO_2 drawdown by silicate weathering (Walker et al, 1981), potentially leading to a limiting-case, global scale glaciation. Subsequent to this, extensive ice cover should shut off most of the silicate weathering flux, permitting sufficient build up of the greenhouse gas to eventually melt the ice. This is the core of the original snowball Earth hypothesis (Kirschvink, 1992a). Kirschvink presented three testable predictions of his proposed scenario; (a) Global synchronicity of glacial deposits, (b) Independent but equivalent indicators of dramatic climate transit and (c) Deep ocean anoxia.

The basic snowball Earth model proposed by Kirschvink requires only the existence of a run away ice albedo mechanism and the impact of surface ice cover on silicate weathering, both of which are relatively uncontroversial (Lian & Cess, 1977, Walker et al, 1981). The snowball Earth hypothesis was later framed in terms of energy balance climate models and coupled more explicitly to expectations of Carbon cycle dynamics (Caldeira & Kasting, 1992, Ikeda & Tajika, 1999, Hoffman et al, 1998, Hoffman & Schrag 2002). For example, the mean surface temperature of the ice-covered state was constrained to -50°C , and the timescale of CO_2 build up to 3 – 30Myrs. The fluctuating Carbon isotope record was interpreted as indicating a global shut down in productivity (Hoffman et al, 1998), a claim later questioned (Kennedy et al, 2001a), reinterpreted in terms of unpredictable fractionation associated with a non-steady state Carbon cycle (Higgins & Schrag, 2003), then contradicted outright by evidence (Jiang et al, 2003) for the proposed (Kennedy et al, 2001b) methane release during deglaciation. But confusion has arisen about the severity of the global-scale glaciation that was originally proposed in the snowball Earth hypothesis, and about the specific evidence with which the idea is (or is not) intricately tied. The snowball Earth hypothesis has become associated with extreme “hard” snowball cases due to its appeal to a limiting case albedo/ice-cover scenario, but Kirschvink originally proposed small tracts of open water tracking the most intense insolation (Kirschvink, 1992) - and therefore (implicitly) assumed relatively thin sea ice cover. Similarly, the withdrawal of the proposed unique association between Carbon isotope fluctuations and productivity (Hoffman & Schrag, 2002), and the recent appreciation of the relative rarity of banded iron formations (Fairchild & Kennedy, 2007) has (in the polarized context of the debate) become inappropriately confused with a fundamental weakening of Kirschvink’s original idea in its simplest form.

Global Synchronicity

A globally-reproducible pattern indicative of glaciation was suggested earlier than the contemporary snowball Earth hypothesis (Harland & Rudwick, 1964), but the temporal constraints on the *Pb*-Zircon dating techniques used are poor enough for the claim of “global synchronicity” to remain heavily debated - the Sturtian glaciation has been argued to be diachronous in this regard (Fairchild & Kennedy, 2007). Additional glaciation incidences are feasible if not probable in the Paleoproterozoic (Kopp et al, 2005), and evidence for fluctuating hydrology suggests that glaciation events were not of uniform severity over time (Fairchild & Kennedy, 2007). Nevertheless, the three time intervals during which LNGD appear to have been deposited remain roughly distinct (albeit with increasing potential overlap between the first two) - Sturtian ($\sim 740 - 647\text{Ma}$), Marinoan ($\sim 660 - 635\text{Ma}$) and Gaskiers ($\sim 580\text{Ma}$) - dating constraints on LNGD deposition certainly do not imply an entirely protracted series of glacial events spread evenly over the Neoproterozoic. Furthermore, the bias towards low paleolatitude remnant magnetism contrasts to that expected

from a geographically uniform distribution of deposits (Evans, 2000, Fairchild & Kennedy, 2007). Genuine, low latitude glaciation appears to have occurred, on a global scale, in two, possibly three distinct time intervals, from which temporal constraints of independent LNGDs are highly correlated, if not unequivocally synchronous.

Independent indicators of dramatic climate transit

Carbon cycle deposition events on the scale of the cap carbonates are without precedent in the Phanerozoic, as are the observed $\delta^{13}C$ depletions and fluctuations. These trends can only be fitted together with the observed O , S and B isotope data through a scenario involving extremely cold climate, using the integrative perspective originally proposed within the snowball Earth hypothesis (Harland & Rudwick, 1964, Kirschvink, 1992). In the development of the snowball Earth hypothesis by Hoffman et al (1998), cap carbonate deposition was proposed to have occurred rapidly, as a result of ocean (carbonic) acidification during the extreme greenhouse resulting from CO_2 accumulated during the glacial interval. Isolation between ocean and atmosphere was assumed necessary to allow build up of sufficient atmospheric CO_2 to melt the ice. Rapid warming occurred through the reverse ice-albedo feedback, giving rise to a massive CO_2 greenhouse once the albedo switched to the ice free state, because the level of CO_2 required to maintain habitability under low albedo/ice cover would be much less than that required to drive the high albedo/ice cover system out of the stable glaciated state (Hoffman & Schrag, 2002). The ocean would become highly acidified as it became exposed to the massive atmospheric CO_2 level that had accumulated. The increased marine CO_2 led to the cap carbonates precipitating rapidly, over a time span potentially as brief as hundreds of years, in conjunction with charge balance due to the cation influx from terrestrial weathering - which would also be expected to exhibit a spike under conditions of an extreme greenhouse. The extreme ^{12}C enrichment of the cap carbonates is attributed to the decimation of marine production expected during ocean acidification (Hoffman & Schrag, 2002). It is important to note that although some of the details of this scenario are now disputed and are arguably better explained by alternative models, the Neoproterozoic Carbon cycle unequivocally exhibits globally synchronous, dramatic changes that are without Phanerozoic equivalent. The cap carbonates were probably deposited over a much longer timespan (Trindade et al, 2003, Fairchild & Kennedy, 2007), so do not require exceptional rates of deposition. But they do require exceptional magnitudes of deposition, biased heavily and specifically towards carbonates. The very existence of cap carbonates, distinctive morphology and $\delta^{13}C$ signature, has (to date) only been coherently explained by reallocation between reactive organic and inorganic Carbon pools (Rothman et al, 2003). The climatic transit implicit in cap carbonates may not necessarily be rapid, but it is certainly dramatic in comparison with the Phanerozoic archetype. Equivalently, the $\delta^{11}B$ evidence for ocean acidification corresponds to the expectation of atmosphere-ocean separation during the glacial interval (Kaseman et al, 2005). Furthermore, evidence

for extreme wind and wave conditions in the glacial aftermath (Allen & Hoffman, 2005), as well as geochemical signatures of sudden, localised increases in chemical weathering (Rieu et al 2007) argue for a climate switching between extremes.

Deep ocean anoxia The interpretation of banded Iron formations is subject to clauses concerning their low abundance and possible origin away from the site of deposition (Fairchild & Kennedy, 2007), yet the reasonable possibility remains that the BIFs, and the $\delta^{34}S$ data could genuinely record an anoxic ocean in conjunction with low-latitude glaciation, exactly as Kirschvink (1992a) proposed. Iron-rich rock formation supposedly resulted from upwelling of anoxic Fe^{2+} -rich water at the end of the glacial events. This idea has been criticised because the Iron-rich deposits are not generally stratigraphically distinct from LNGD, but continuous with or below them (Williams & Schmidt, 2000). However, sporadic deposition of Iron within sea ice, after its oxidation upon exposure to (rare) gaps continuous with the atmosphere, has been proposed to reconcile this (McKay, 2000). Alternatively, iron deposition may have been literally instantaneous upon melting of the glacial events, and stratigraphic heterogeneity may result simply from erosion biases (Hoffman & Schrag, 2002). Nonetheless, the rarity of marine Fe deposits after the great oxidation (Berner, 1999) strongly suggests a relationship with the oxygen content of the ocean-atmosphere system, either directly or via the oxidation state of the Sulphur reservoir. What is reasonably uncontested is the original assertion (Kirschvink, 1992a) that the ocean needs to be anoxic in order to accumulate large quantities of dissolved Iron, and that deep ocean anoxia is an inevitable consequence of long term atmosphere-ocean separation. The Sulphur isotope $\delta^{34}S$ excursions are consistent with the proposed severity and timing of the anoxic episodes (Hurtgen et al, 2004, 2005), just as the requirement for relatively low H_2S availability is consistent with restricted weathering - during, for example, an interval of extensive terrestrial ice cover. The presence of BIFs may be too rare to warrant global paleoclimatic interpretation (Fairchild & Kennedy, 2007), and the Sulphur isotope data may result from localised anoxia and/or secondary reoxidation artefacts (Anbar & Knoll, 2002). But they could just as reasonably be the evidence for deep ocean anoxia originally proposed.

In this thesis, the phrase “snowball Earth hypothesis” will be used in a more loose sense than most of the literature in that it need not agree precisely to the geological and Carbon cycle interpretations of Hoffman et al, but merely to (a) The occurrence of an equilibrium (as opposed to a dynamic steady state) solution in the ice albedo feedback with extremely high global ice cover level (Whatever the implications of this for sea ice thickness and/or tracts of open water), (b) The cessation of the CO_2 weathering buffer (of Walker et al, 1981) as a result of low temperatures and/or extensive ice cover and (c) Sufficient isolation between the ocean and the atmosphere to permit the build up of abnormally high levels of CO_2 , such that the ice-cover/albedo system leaves the equilibrium, high ice-cover state.

Although the cap carbonates were probably not deposited as rapidly as first suggested, the original predictions of the snowball Earth hypothesis remain resistant to criticism and consistent with the data, and the integrative capacity of the idea is unique.

Slushball Earth

Climate models of various levels of complexity and spatial resolution can produce solutions in which global scale ice cover occurs and may progress into the tropics, but large stretches of open ocean persist (Hyde et al, 2000, Baum & Crowley, 2001, Pollard & Kasting, 2005). This reflects a resistance to the catastrophist thinking that the snowball Earth hypothesis has become associated with, and (arguably) a starting assumption that it is self-evident that significant open water did remain - because multicellular eukaryotes clearly did survive (as they are present today), and this would have been impossible with an ice-covered ocean. These “slushball” scenarios are characterised by (a) An agreement with the snowball Earth hypothesis in the acceptance that the evidence for low latitude, global-scale glaciation is persuasive, and that the temporal constraints suggests some level of synchronicity and (b) a departure from it via the emphasis on strong hydrological activity, and a wider range of glacial severity between different locations, sometimes including a lateral gradation from glacial deposits to open marine sediments (Eyles & Eyles, 1983, Fairchild & Kennedy, 2007). Slushball Earth as a explanatory model suffers from two significant problems. Firstly, its failure to produce a consistent mechanistic explanation for the progression of ice cover being halted before the ice-albedo feedback drives the system to complete equatorial ice cover. This is reflected in the somewhat ad-hoc nature of the hydrological and heat diffusion parameterisations necessary to maintain open water despite tropical sea ice - including a dependence on cloud formation (Pierrehumbert, 2005), the absence of substantial tropical evaporation, and/or the maintenance of sea ice free from bubbles or dust (Pollard & Kasting, 2005), and perhaps even the complete absence of the dynamics of sea ice formation (Lewis et al, 2007). No zero dimensional demonstration of a stable slushball steady-state has been achieved - probably reflecting the fact that the stability of such a scenario genuinely depends on the intricacies of heat diffusion and hydrological dynamics. At best, this is unsatisfying because such an important aspect of the problem does not leave clear geological signatures. At worst, it raises the possibility that such a steady state does not exist. The second, more practical difficulty with slushball solutions is their ambiguity, and the resultant lack of distinct, testable predictions stemming from them (Fairchild & Kennedy, 2007). Slushball Earth is defined only crudely - as global scale glaciation less severe than invoked by the snowball Earth hypothesis, without an explicit mechanism to permit the dynamically stable tropical but sub-equatorial ice cover that this implies.

Zipper rift Earth

Low latitude, high altitude glaciation, or the “Zipper rift” hypothesis, is distinct from the other proposed explanations for Neoproterozoic climate, in that it suggests minimal or no qualitative differences between the Neoproterozoic and Phanerozoic tectonic and geomagnetic regimes (Eyles and Januszcak, 2004). The zipper rift model proposes that LNGD resulted from two major pulses of continental splitting and tectonic uplift - the latter giving rise to an abundance of high altitude, low latitude plateaus, on some of which glaciers formed. Zipper rift proposes an active hydrologic cycle and mild, localised glacial regimes analagous to those at present - the only “unusual” feature being high altitude equatorial land masses resulting from extreme subsidence rates. Many supposed glacial tillites are reinterpreted as being the result of debris flows in regions of tectonic activity. The Iron deposits and other evidence for ocean anoxia are suggested to be too rare and erratic to be attributed to a single climatic phenomenon, rather they are suggested to reflect anoxia in shallow inland seas. The pattern “LNGD, with/without iron deposits, overlain by thick cap carbonate rocks” is suggested to be rare and localised, and neither global nor synchronous as the supporters of the snowball Earth hypothesis claim. Consistent with the idea of parity with the Phanerozoic, cycles in the abundance of geochemically mobile soil cations (relative to elements whose soil concentration remains largely unaltered during chemical weathering), are interpreted as suggesting cyclical bursts of weathering and aridity, corresponding to the interglacial and glacial intervals, that are more consistent with a model of contemporary ice ages than global climatic phenomena (Rieu et al, 2007). This would imply an active hydrologic cycle, requiring at least some open water, within the supposed glacial interval. Though entirely theoretically reasonable as an explanation for the LNGD treated in isolation, the zipper rift model has the weakness that much of the proximal evidence cited in favour of snowball Earth (iron deposition, isotopic data, thickness and synchronicity of LNGD and cap carbonates, severity of geochemical freeze-thaw signatures and weathering cycles) would need to be disputed outright as the result of repeated misinterpretation of LNGD and their stratigraphic context, and attributed largely to local phenomena without global climatic significance. This is possible, but less parsimonious than the existence of a common cause.

High tilt, polar wander, ice rings and impacts

If the Earth’s axis of rotation were tilted relative to its orbital plane by more than about 54° , then the poles would receive a greater annual heat flux than the tropics (Jenkins, 2004). The explanation of low paleolatitude Neoproterozoic glacial deposits via such an enhanced tilt of Earth’s spin axis has been proposed (Williams, 1972, 2000, Williams & Schmidt, 2004, Jenkins, 2004). The strongest observation in favour of a high orbital tilt Earth is that, although a single high paleolatitude glacial deposit would undermine the idea’s logical foundation, not one such deposit has been found (Evans, 2000, Fairchild &

Kennedy, 2007). It is worth noting, however, that this might result simply from the lack of any high latitude land masses at the time. Under a high tilt scenario axial rotation of the planet would have a much milder influence on the energy balance of any given latitude, and extreme seasonality might be expected to last over time scales of the order of months, up to 6 months in the extreme 90° (Williams & Schmidt, 2004). Some “sand wedge” features found in conjunction with LNGD have been interpreted as diagnostic of this kind of extreme seasonal cycle (Williams & Tonkin 1985), but these features may be equally likely to arise by temperature fluctuation over a much shorter timescale (Pierrehumbert, 2005). The problems with high orbital tilt as an explanation lie not in how it explains the LNGD, but in the processes it invokes but offers no evidence (or mechanism) to support, and in the other, geochemical lines of evidence that it fails to account for. Even under the extreme 90° orbital obliquity case, the 6 month tropical extreme winter would nevertheless be followed by an equivalently extreme summer - whereas formation of persistent glacial deposits depends on the amount of surviving summer sea ice, hence on relatively mild summers (Hoffman & Maloof, 1999). The probability of net growth of permanent summer sea ice under a high orbital obliquity regime therefore rests critically on the completely unconstrained hydrological cycle of an Earth divided (in the extreme case) into ice-covered and ice-free hemispheres. A high orbital obliquity regime would likely give rise to continual formation and destruction of glaciers at independent positions as the position of the winter hemisphere progressed across the Earth’s surface - hence it can offer no explanation for the apparent synchronicity (or at least the lack of extreme diachroneity (Evans, 2000)) of LNGD, nor for the periods during which they are absent. The latitude of Proterozoic evaporite formation is consistent with the kind of hydrological cycle that general circulation models predict would operate in a low obliquity world (Evans, 2003, 2005). But the biggest deficiency of the High tilt model is the lack of any mechanism to suddenly reduce orbital obliquity back to its present value - which would need to have happened by about 430Ma, (Fairchild & Kennedy, 2007). The Earth’s orbital tilt is particularly resistant to change due to its coupling with the Moon, and there is no acceptable mechanism to return the system to the contemporary state, particularly not so rapidly (Levrard & Laskar, 2003). High orbital tilt can explain preferential low latitude glacial deposits, but not Carbon cycle disturbances or apparent oceanographic trends, and begs far more questions than it answers. A mild change in tilt could be feasible if a mechanism was presented to rectify it, but the model as a whole cannot be considered an alternative to the snowball Earth hypothesis.

The correspondance between axial and magnetic north during the Neoproterozoic has been called into question, although the present correspondance between the Earth’s ice caps and its geomagnetic cores does appear to have been established by at least the late Ordovician (Smith, 1997), and perhaps the early Cambrian (Bertrand-Sarfati et al, 1995).

If the Earth's geomagnetic field had a large non-dipolar component, the paleolatitude inferred from remnant magnetism would be inaccurate. A scenario with either four or eight geomagnetic poles (Kent & Smethurst, 1998) would have greatest impact on remnant magnetism implying high apparent paleolatitudes, and minimal impact at equatorial paleolatitudes (Evans, 2000). A non-dipolar scenario is therefore unlikely to explain the abundance of low paleolatitude deposits, and similarly to the high obliquity model, cannot directly explain isotopic and geochemical evidence supporting snowball Earth.

The episodic collapse into the atmosphere of rings of ice orbiting the planet was proposed as a means by which low latitudes might be shielded from insolation, allowing glaciers to form (Sheldon, 1984). But ice accumulation, hence the shielding effect, would only operate on the winter hemisphere (Hoffman & Schragg, 2002), hence is unlikely to be relevant to the survival of summer sea ice necessary for glacial growth. Some of the extreme isotopic and biotic patterns attributed to snowball Earth, particularly those occurring during the Vendian event, have been argued to be the result of asteroid impact (e.g. Grey et al, 2003). Others have reinterpreted the tillites themselves as derived from the frequent asteroid impact events that probably occurred during the late Neoproterozoic (Oberbeck, 1993). Although asteroid impact events probably did occur frequently across deep time (Holland, 1984) they do not provide an explanation for the low latitude bias in the (proposed) glacial deposits, nor (at least directly) for the evidence of deep ocean anoxia or Carbon cycle disturbances.

Remaining uncertainties

What caused the global-scale glaciations?

Global-scale glaciation requires a severe decrease in either greenhouse or luminosity forcing. The latter is probably an insufficient explanation, ultimately because the temperature dependence of silicate weathering would raise CO_2 enough to buffer the reduced insolation (Tajika, 1999). The original proposition of a large, distintegrating land mass at the equator (Kirschvink, 1992a, Hoffman et al, 1998, Hoffman & Schrag, 2002) remains possible (Cawood, 2005) and has the desired effect in some model results (e.g. Godderis et al, 2003). But uncertainties in paleocontinental configuration make it difficult to tell whether this is the entire picture (Fairchild & Kennedy, 2007). In general, qualitative changes in Earth system processes are attributed to the biosphere - because life is the only part of the system that is directly creative (Vernadsky, 1926). The implicit assumption tends to be that evolutionary innovation at the end of the Neoproterozoic and further into the Phanerozoic had consequences that ultimately stabilised climate - proliferation of calcifiers (Ridgwell et al, 2004), attainment of steady state organic-inorganic Carbon balance (Rothman et al, 2003) being examples. But an equally plausible mechanism comes from the opposite

philosophical perspective - that life initiated the CO_2 drawdown by enhancement of silicate weathering and marine organic Carbon burial, causing climatic instability rather than buffering it (Lenton & Watson, 2004). This requires an evolutionary explanation for the increased presence of weathering organisms such as lichens on the Neoproterozoic land surface, and a quantitative assessment of how this might interact with the ice albedo feedback, not to mention an explanation of why this instability did not continue into the Phanerozoic.

Severity: The snowball-slushball debate

Slushball solutions in GCMs are contingent on unconstrained and often somewhat arbitrary assumptions about climate (Ikeda & Tajika, 1999, Pierrehumbert, 2005). These include tropical evaporation and heat diffusion (Pollard & Kasting, 2005), cloud formation and boundary-layer heat transport (Hyde et al, 2001) and meridional diffusivity (Tajika, 2003). Clouds have a net warming effect when the difference between surface and planetary albedo is small - as is the case for high levels of ice cover (Poulsen & Jacob, 2004, Pierrehumbert, 2005). Increased surface wind speed increases sensible heat exchange between the (warmer) ocean and (colder) atmosphere, resulting in cooling of the ocean and growth of sea ice (Lewis et al, 2007). Some GCM studies remain non-committal on the snowball-slushball debate (Baum & Crowley, 2003, Pierrehumbert, 2005). In general, spatial resolution is of use in determining the position and nature of the ice-albedo instability, but qualitative features of the Carbon cycle are treated as responsive rather than causal. Hyde et al (2000), for example, mimic the effect of CO_2 changes solely with a top-of-atmosphere radiative adjustment, thereby ignoring changing in silicate weathering or ocean-atmosphere CO_2 partitioning. Inclusion of sea ice dynamics probably prevents a stable open water solution - because (thinner) dynamic sea ice is more likely to spread via wind stresses than is sea ice with thickness determined only by local energy balance (Lewis et al, 2007). This, of course, assumes wind stresses to be significant, implying tangible latitudinal heat gradients.

Sea ice

A suggested compromise between open water and hard snowball solutions is the existence of low latitude sea ice that remains thin enough (around 2 metres) for photosynthetically active radiation to pass through it - as in modern Antarctica (McKay, 2000, Pollard & Kasting, 2005, Lewis et al, 2007). But the stability of thin sea ice is contentious. Vertical throughput of ice by basal freezing and surface sublimation may, at surface temperatures below ~ 12 celsius, be too small to keep the ice thin (Warren et al, 2002). Equivalently, because the level of solar radiation passing through thin ice is greater than the geothermal heat flux by a factor of ~ 50 (Mckay et al, 1985), sea ice that is too thin is likely to melt after the ocean warms, giving rise to open water (Pollard & Kasting, 2005, Lewis et al, 2007). It is arguable that repeating cycles of thin ice and open water are reasonable. The property of critical relevance to the whole debate is the albedo of thin sea ice and its affect

on local energy balance. For sea ice to remain thin and allow marine photosynthesis it probably needs to remain free from bubbles, therefore to freeze slowly with minimal brine inclusion (Mckay, 2000, Pollard & Kasting, 2005). Export of heat from the tropics needs to remain low, which, along with the requirement that (stable) thin ice must remain free from snow and dust, means that the activity of the tropical hydrological cycle is critical (Warren et al, 2002). For the flow of sea glaciers under their own weight (Pollard & Kasting, 2005), sea ice would probably need to be too thick to avoid progression to a hard snowball (Lewis et al, 2007). Atmospheric heat transport, snow cover on sea-ice, bubble formation and brine expulsion are all examples of crucial processes, relevant to sea ice thickness - therefore global scale stability- that do not fossilise. This makes the probability of glaciation remaining mild enough to permit marine photosynthesis difficult to assess. At any rate, ice thin enough for photosynthesis would likely remain in inland seas and (large) lakes protected from sea-glacier flow, even if the ocean was decimated (Pollard & Kasting, 2005). A planet with completely ice-covered oceans could still be tolerated by the biosphere.

The carbonate system

Ridgewell & Kennedy (2004) attempt a more complete synthesis and argue that the Neoproterozoic glacial events represent the last instance of an instability in climate caused by the sensitivity of marine carbonate Carbon deposition to shallow-shelf depositional area (therefore to sea level, therefore to global-scale glaciation). They postulate an inflection point relating continental $CaCO_{3(s)}$ area A to altitude H , with a topographic contrast in which $\frac{\partial A}{\partial H} \gg 0$ corresponding to the Neoproterozoic instability, and $\frac{\partial A}{\partial H} \leq 0$ corresponding to a Phanerozoic system with active biotic calcification, hence more buffered depositional “area”. Reduced depositional area resulting from a fall in sea level increases marine $[CO_{3(aq)}^{2-}]$, reducing the amount of $CO_{2(aq)}$ in direct equilibrium with the atmosphere through series of reactions summarised by $CO_2 + CO_3^{2-} + H_2O \rightleftharpoons 2HCO_3^-$, reducing $CO_{2(g)}$ (Ridgewell et al, 2003, 2004). In the Neoproterozoic this mechanism is severe, in the Phanerozoic active biotic calcification compensates for reduced depositional area to maintain a tangible carbonate burial flux. The positive feedback between CO_2 reduction and sea level fall through land ice formation was proposed as the determinant of glacial severity, and (unlike the Urey reaction) can work for non-steady state carbonate Carbon. This idea is probably the most mechanistically explicit means of integrating extremely cold climates and Carbon cycle disturbances, although it still lacks an explanation for the attenuation of the ice albedo instability. But the hypothesis is also slightly circular as a solution to the snowball-slushball debate, in that it requires a significant carbonate weathering flux (Ridgewell & Kennedy, 2004), hence non-glaciated parts of the land surface that are hot enough to provide a tangible carbonate weathering flux, hence a slushball solution. Although weathering can and does occur under contemporary glaciers (e.g. Skidmore et al, 2005), the assumption that

the carbonate weathering flux would be qualitatively unchanged by a global-scale glaciation implies that the temperature and ice cover changes were relatively mild to begin with.

The marine organic Carbon reservoir

Another plausible mechanism shown to prevent runaway glaciation is CO_2 release by remineralisation of a massive pool of dissolved inorganic Carbon (Peltier et al, 2007). Massive fractionation changes mean the Carbon cycle was almost certainly out of steady state, the justification for the proposed massive marine biosphere being a relatively long residence time in the organic pool in comparison to the inorganic (Rothman et al, 2003). This could equally be realised by the (dismissed) possibility of “the virtual absence of carbonate sedimentation” due to a small marine inorganic pool (Rothman et al, 2003). The latter scenario cannot be directly linked to CO_2 release, but might be expected during the glacial interval of a hard snowball. The proposed CO_2 release through remineralisation ignores CO_2 -drawdown by silicate weathering at low temperatures (Peltier et al, 2007), but still requires, at the same time, persistence of a massive marine organic Carbon reservoir even through extremely low temperatures and tangible sub-tropical ice cover. The latter implies relatively mild glaciation, giving rise to the circularity inherent in other partial ice-cover solutions.

Diachroneity and repetition?

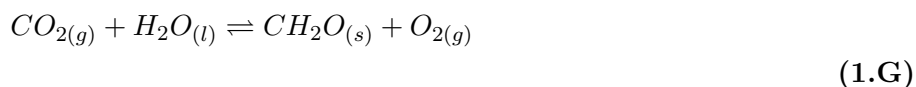
The likely occurrence of severe Paleoproterozoic glaciations at around 2.4 (Ga) underlines how Neoproterozoic glaciation models might be extrapolated accurately to the rest of Precambrian time (Kirschvink et al, 2000, Kopp et al, 2005), and arguably provides support for the (occasional) disposition of Earth’s climate to oscillation between glaciated and non-glaciated states. The oldest 741Ma and youngest 643Ma age estimates for the Sturtian glacial interval unequivocally invoke diachroneity if they are accepted (Frimmel et al, 1996). Even more conservative estimates incorporating error margins place some Sturtian LNGD at least 40 Myr apart (Fairchild & Kennedy, 2007). Using an average subsidence rate in conjunction with the (low) fraction of the thickness of Neoproterozoic strata comprised by LNGD, a crude estimate suggests that no more than 5 – 20% of the duration of the glacial prone era (750 – 580Ma) was actually ice-covered - implying it is unlikely that such large differences could reflect the same event, and that the Sturtian glacial interval was probably therefore diachronous (Fairchild & Kennedy, 2007). So on the one hand, there is a degree of concentration of LNGD deposition into discrete intervals (Evans, 2000), but on the other, there remains the possibility that Neoproterozoic glaciations represent an inherent climatic instability that may also have been realised at other times (Kopp et al, 2005). Despite this apparent susceptibility in Earth’s climate, since the end of the Ediacaran, global temperature fluctuations have remained comparatively mild

(e.g. Lenton et al, 2004). The question of how the extreme Neoproterozoic gave rise to the relative habitability of the Phanerozoic is both important, and largely neglected.

Role of the biosphere: Cause, effect, or both?

A biological trigger for snowball Earth?

The idea that biotic enhancement of terrestrial silicate weathering was necessary to trigger the snowball Earth events (Lenton & Watson, 2004, Hedges, 2004), raises both the philosophical issue of the role of evolutionary creativity in climatic regulation and extreme change (Watson, 2004), and the practical issue of how poor the constraints are on the relative biotic enhancement of silicate weathering over geologic time (e.g. Berner, 1994, Schwartzman, 1999). The presence of lichens on the Neoproterozoic land surface was hypothesized to accentuate the silicate weathering-derived CO_2 drawdown that ultimately resulted from the fragmentation of the Rodinia supercontinent. Hence the terrestrial biosphere, assumed to comprise lichen and associated soil bacteria, was suggested to have acted as a direct trigger for the Neoproterozoic glaciations (Lenton & Watson, 2004). A geochemical role for the increased flux of inorganic phosphate $PO_4^{2-}(aq)$ to the ocean resulting from lichen activity was hypothesized, in addition to the accentuation of the rate of CO_2 drawdown via the Urey reaction (1.C). Although nitrate $NO_3^-(aq)$ may sometimes be the nutrient limiting marine production over short timescales, phosphate $PO_4^{2-}(aq)$ is the principal limiting marine nutrient over geologic timescales, due the longer residence time of P (roughly 50,000 years) compared to N (roughly 3000 years) (Redfield et al, 1963, Libby, 1992, Lenton & Watson, 2000a). Due to the stoichiometry of photosynthesis at the planetary scale:



(Where $CH_2O_{(s)}$ is a label for total planetary fixed Carbon), the burial of marine organic Carbon $CH_2O_{(s)}$ before it is remineralised (according to a stoichiometry represented by the reverse of “reaction” (1.10)), represents a net withdrawal of 1 mol of C from, and the addition of 1mol of O_2 to, the atmosphere-ocean system (Lenton & Watson 2000a, 2000b). The runoff from drainage basins colonised by lichens that are actively weathering the land surface can reasonably be assumed (Lenton & Watson, 2004) to be high in $PO_4(aq)$ concentration relative to an uncolonised land surface - due to $PO_4(aq)$ release during selective mineral weathering by lichen (Landeweert, 2001). This process liberates P , N and micronutrients into aqueous solution and promotes their supply to the ocean. Therefore it was hypothesized that (geologically) rapid bursts of lichen - enhanced silicate weathering during the Neoproterozoic both enhanced and/or triggered glacial intervals by promoting CO_2 drawdown, and gave rise to the increase in atmospheric O_2 that later permitted

diversification of large metazoa (Lenton & Watson, 2004). Notwithstanding some of the (highly contentious) molecular clock evidence for early divergence (Hedges, 2001, 2004), the earliest documented lichen like symbiosis in the fossil record is not until 600 MA (Yuan et al, 2005), over 100 MA after the earliest of the LNGD, its diagnosis as a lichen remains equivocal, and it is probably intertidal/marine in life history. The hypothesized presence of lichens on the early Neoproterozoic land surface therefore requires theoretical justification, as does the magnitude of the hypothesized weathering impact.

The Neoproterozoic terrestrial biosphere

Deposits of probable lichens have been found in a shallow subtidal (suggesting a marine or intertidal life-history) environment at about 599 ± 4 Ma (Yuan et al, 2005) (Figure 3.1). Sets of microfossil samples from ~ 1200 and ~ 800 Ma have been documented in limestone of apparent terrestrial drainage basin origin, in conjunction with highly ^{13}C depleted carbonates - implying a tangible terrestrial biosphere producing total soil CO_2 of an order comparable to terrestrial vascular plants (Horodyski & Knauth, 1994, Kenny & Knauth, 2001). This evidence is bolstered by the apparent presence of microbial mats in terrestrial drainage basin-derived sediments (Prave, 2002). Theoretical considerations suggest that soil respiration as low as that observed in modern arctic biomes (around 0.001 times the soil respiration of contemporary temperate grasslands (Johnson & Vestal, 1991)) can still be sufficient to support tangible rates in the weathering flux of calcium and magnesium silicates (Keller & Wood, 1993). But by far the strongest evidence for an active terrestrial biosphere increasing in size over Precambrian time comes from the progressive increase in $^{87}Sr/^{86}Sr$ in marine carbonates (Sheilds & Veizer, 2002, Halverson et al, 2007), implying an equivalent increase in the ^{87}Sr influx from runoff.

Lichen evolution

A lichen is a symbiosis between a fungus, usually an Ascomycete, the “mycobiont”, and a green alga or cyanobacterium, the “photobiont” the latter being contained within the fungal hypha (e.g. Nash, 1996). The photobiont supplies the fungus with fixed Carbon (and in the case of some cyanolichens with fixed atmospheric Nitrogen $N_{2(g)}$) and in exchange (probably) receives a flux of micronutrients extracted from the abiotic environment by the fungus. The magnitude of the mycobiont to photobiont nutrient flux is contentious, therefore so is the evolutionary nature of lichenisation (Nash, 1996). Cyanobacterial photobionts generally exhibit a lower growth rate in the lichenised state than when free-living - meaning the symbiosis is often viewed as a controlled form of parasitism, whereby the fungus experiences disproportionate benefits (Ahmadjian, 1993). But lichenization can also be facultative - often occurring in environments in which the photobiont is capable of living autonomously (Nash, 1996). This could be because the fungus is simply exploiting the availability of photoautotrophs, or because the symbiosis has a mutualistic side. Con-

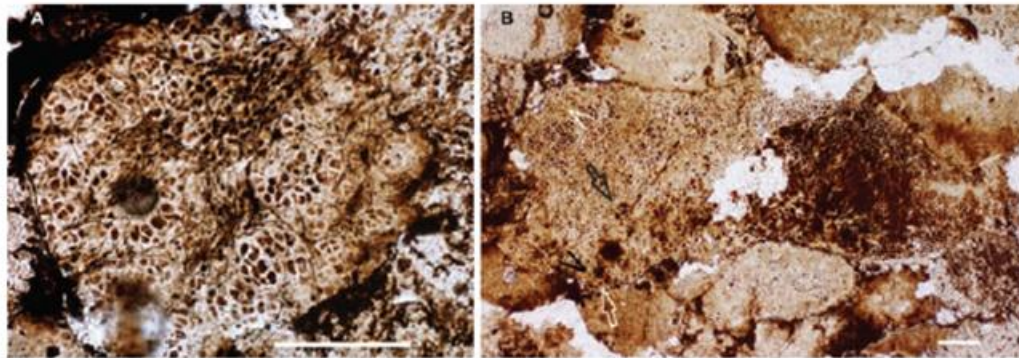


Fig. 1. Thin-section photomicrographs of two better-preserved specimens. (A) Coccoidal thallus divided by dense filaments in the middle. Further compartmentalization of coccoidal thallus by less densely packed filaments is visible at higher magnification (Fig. 2, A to C). (B) Coccoidal thallus with filaments (not discernable at this magnification; see magnified views of arrowed areas in Fig. 2, D to G) in the left part, but not the right part, of this specimen. Scale bars, 100 μm .

Figure 1.9 - Probable Neoproterozoic lichens deposited in a shallow marine environment (from Yuan et al, 2005).

sistent with the latter is the observation that lichenisation permits photobionts to colonise environments in which they are incapable of existence in the free living form (e.g. Boucher, 1982), particularly high light intensity environments in which they are protected from photoinhibitory stress by existence within the fungal thallus (Nash, 1996). This indicates a benefit to the photobiont (at least in terms of ecological abundance) of a symbiosis than may have originated in it being parasitised by the mycobiont. When viewed in this way, some lichen symbioses therefore illustrate the broader evolutionary principles of different mechanisms being responsible for the origin of a trait than for its persistence, and how an initially costly or even maladaptive trait can give rise to fitness benefits once it has become established (e.g. Maynard-Smith & Szathmary, 1995).

Lichens undergo vegetative asexual reproduction involving the coupled reproduction of both partners. Differentiation involves formation of soredia containing both photobiont and mycobiont cells, and fragmentation without obvious morphological change (Nash, 1996). Soredia occur in algal lichens, where small groups of algal cells surrounded by fungal filaments, and are dispersed by wind via structures called soralia. Equivalent coupled reproduction (i.e. reproductive structures containing both partner species) occurs in outgrowths called isidia and, in cyanolichens, fragmentation of vegetative fungal hyphae, wrapped around cyanobacterial cells (Eichorn et al, 2005). Reproduction of the photobiont is highly reduced during lichenisation, and it is assumed that genetic exchange between them is minimal or nil, and that they reproduce vegetatively, analogous to an organelle (Ahmadjian, 1993, Nash, 1996). Sexual reproduction appears to be confined to the mycobiont - which may undergo meiotic division followed by sexual fusion and spore formation in a manner equivalent to autonomous fungi, then reassociation with a photobiont partner (Nash, 1996). Strong selectivity is exhibited by the mycobiont for a specific photobiont (Yahr, 2004), presenting the opportunity for lichenisation after separate, potentially sexual, reproduction by each symbiont. Molecular sequence data suggests that asexual lichen species may periodically split from an ancestral sexual form, but maintain an ecological "species complex" with the ancestor and perhaps even periodically return to the sexual mode of reproduction (Grube & Kroken, 2000). This represents an ambiguous blurring between the traditional biological species concept (e.g. Ridley, 1996) and the alternation of generations between sexual and vegetative morphs of free-living fungi. The evolutionary concept of a species, as well as that of an individual, may therefore be inadequate to describe the lichen symbiosis.

Lichenisation is polyphyletic and probably extremely ancient (Ahmadjian, 1993, Nash, 1996, Raven, 2002, DePreist, 2004). Most lichenised fungi fall within the Ascomycota, although rarer basidiolichens are also documented (Nash, 1996). The divergence of green algae from mosses and vascular plants is rooted at around 1000MA by molecular clock analysis of nuclear protein sequences (Hedges et al, 2001), and has been inferred to in-

diccate colonisation of land surface at around 600 MA (Heckman et al, 2001). The same techniques suggest divergence of fungi from animals at 1547MA (Hedges et al, 2004). The basidiomycete-ascomycete split had occurred by 400 MA (at the onset of a phylogenetic radiation of fungi in conjunction with the colonisation of land by vascular plants) and may have happened much earlier (Taylor & Berbee, 2006). Cyanobacteria diverged from gram positive Actinobacteria up to 2558 MA (Batistuzzi et al, 2004). Molecular clock dating (with all of the clauses and caution that this technique requires before its conclusions are interpreted) of highly conserved nuclear proteins suggests that the same species of mycobiont has repeatedly switched (algal) photobiont during its evolutionary history, whilst maintaining a lichenised life habit (Piercy-Normore & DePreist, 2001), illustrating how lichenisation is flexible and facultative (at least for the fungus), and can be initiated relatively quickly over evolutionary time. It is therefore realistic to hypothesize that green algae, fungi, and cyanobacteria were present at the onset of the proposed Neoproterozoic glaciations, perhaps on the land surface in the case of the latter two, and that if these species coexisted the evolution of lichenisation was a likely result. Consistent with this idea, members of the Ediacaran macrobiota, that appear from 630Ma onwards have been postulated to be marine and intertidal lichens (Retallack, 1994). Nevertheless, the presence of terrestrial lichen during the Neoproterozoic remains only a hypothesis - the first unequivocal terrestrial lichens not being present until around 400Ma (Taylor et al, 1995, Taylor & Wilson, 2004), after the earliest fossil evidence (Raven & Edwards, 2001) for land plants.

Lichen physiology and ecology

There is no biome on Earth that does not contain lichens. The hardiness of lichens is illustrated by the survival of desiccated lichen soredia in space (Sancho et al, 2005). The boundary conditions for growth of a lichen species of some sort illustrates the inadequacy of treating the lichen symbiosis as a single biological entity - they are as wide as the boundary conditions for life on Earth (Nash, 1996, Purvis, 2000). Lichens known as cryptoendoliths are able to survive in arctic and antarctic environments experiencing sub-zero temperature conditions by forming hydrated, translucent, gel-like zones in porous granite and crystal-like structures in sub-surface marble (Purvis, 2000). In such environments, lichens exhibit high intracellular concentrations of Calcium oxalate CaC_2O_4 in the form of hydrated crystals, which have been hypothesized to function in osmoregulation (Seaward, 1997), and in refraction of harmful ultra-violet light wavelengths (Clark et al, 2001). The huge boundary conditions permissive for lichen growth are illustrated in tolerance to stress due to extremes of all main photosynthesis-limiting environmental variables:

(a) Temperature: Temperature extremes damage all life, predominantly due to loss of protein function after denaturing (e.g. Stryer, 1975). Desert lichen are capable of surviving

surface temperatures of 55°Celsius, arctic lichen of -13° (Nash, 1996, Clark et al, 2001). Osmolyte production limits the potential for intracellular damage by ice - crystal formation, and some lichens may survive being frozen for periods of up to 3.5 years (Kappen, 1973). Tolerance to both extreme cold (Larson, 1983) and extreme heat (Kershaw, 1985) by different lichens is significantly reduced if the lichen experiences the extreme heat change at high thallus water potential. This indicates lichens' extreme sensitivity to the external hydrosphere, of relevance to the fluctuating osmotic conditions likely on a Neoproterozoic Earth.

(b) Water. The poikilohydry (rapid equilibration of cellular water potential to that of the external environment) of lichens is probably the major constraint on growth imposed by the abiotic environment (Nash, 1996). Nonetheless, lichens are able to tolerate irregular and extended intervals of desiccation by entering a "Cryptobiotic" dormancy-like state in which detectable metabolic activity ceases (Purvis, 2000).

(c) $O_2 : CO_2$ stress: photorespiration. Ribulose-1,5-biphosphate Carboxylase Oxygenase ("Rubisco"), is the enzyme that catalyses the first major step of the Carbon fixation reactions, or "dark" Calvin cycle reactions, of photosynthesis (e.g. Taiz & Zeiger, 1998). The production of Rubisco's substrate, Ribulose-1,5 biphosphate (RUBP) requires energetic intermediates nicotinamide adenine dinucleotide phosphate (NADPH) and adenosine triphosphate (ATP). These are produced using the energy in the proton gradient across chloroplast thylakoid membranes - energy that ultimately derives from photo-oxidation of water and cyclical electron transport during the light reactions of photosynthesis (e.g. Taiz & Zeiger, 1998). Under "normal" photosynthesis, RUBP is carboxylated (CO_2 is incorporated into it), and the product, 3-phosphoglycerate, enters the Calvin cycle - resulting in net photosynthetic Carbon fixation. The oxygenase activity of Rubisco (thought to be a relic of evolution in a low oxygen environment (e.g Stern et al, 2003)), upsets the stoichiometry of the first carboxylation step, producing 3-phosphoglycollate in addition to (less) 3-phosphoglycerate. 3-phosphoglycollate cannot enter the rest of the calvin cycle and (although some scavenging mechanisms exist in vascular plants to recover the reduced Carbon contained in it) is therefore a waste of the metabolic energy used to produce RUBP. This physiological impairment can substantially decrease growth (at least of vascular plants) in environments with a high ambient $O_2 : CO_2$ ratio, in which the oxygenase activity increases (Taiz & Zeiger, 1998).

Mechanisms exist to concentrate CO_2 at the active site of Rubisco and therefore reduce the damage to productivity done by photorespiration. Amongst the most efficient of these concentrating mechanisms are the pumps within the membranes of cyanobacterial and algal cells (Taiz & Zeiger, 1998). ATP produced during the light reactions is used to actively

import $CO_{2(aq)}$ and $HCO_{3(aq)}^-$ (the latter of which is converted to CO_2 by the enzyme Carbonic anhydrase) into the cell, causing its intracellular concentration to approach $50mM$ in some cyanobacterial cells (Ogawa & Kaplan, 1987). This prevents the autonomous cells of green algae and cyanobacteria from experiencing photorespiration, unless previously acclimatised to extremely high CO_2 and then suddenly transferred to high O_2 conditions (Taiz & Zeiger, 1998). These physiological properties within the free-living photobionts of some lichen means that hypothesized inhibition of lichen growth by excessively high $O_2 : CO_2$ (Lenton & Watson, 2004) is at odds with physiological expectations. Conversely however, increased photosynthetic productivity has been observed in some algal lichen after artificial reduction of ambient O_2 and increase in thallus water content (Snelgar & Green, 1980) - interpreted by the authors as indicating apparent photorespiration. But the same authors refuted the possibility of general widespread photoinhibitory activity in green algal lichen after a more comprehensive study of thirteen species (Snelgar & Green, 1981). Consistent with this is the growing skepticism about how widespread Carbon-concentrating mechanisms are in lichen algal photobionts (Smith & Griffiths, 1998, Maguas et al, 1995) and the observation that many lichen-forming algae have recently been found to lack the Carbon-concentrating mechanisms previously assumed to exist (Raven et al, 2005). Studies on a cyanolichen demonstrated that although exposure to high light intensity (resulting in high CO_2 uptake) followed by transfer to darkness, did result in net CO_2 release (symptomatic of photorespiration), photorespiration as a cause was negated by the extremely low O_2 level used (Coxson et al, 1982). The theoretical potential for photorespiratory inhibition of Carbon fixation in lichens remains reasonable, but the inhibition of lichen photosynthesis by excessive $O_2 : CO_2$ has never been documented, and the atmospheric O_2 level at which it would occur is therefore unconstrained.

(d) Light stress The “light harvesting complexes” are groups of proteins responsible for directing light to the chlorophyll reaction centres of photosynthetic bacteria and plant and algal chloroplasts. When the chlorophyll reaction centre receives a photon, it is raised to an excited state in which it becomes temporarily oxidised. Subsequent electron transport produces a cross-membrane proton gradient that is used to produce ATP and NADPH. Excessive light can result in damage to the reaction centres and impede photosynthesis and growth; “Photoinhibition” (Teiz and Zeiger, 1998). Because the lichen photobiont is contained within the fungal thallus, incident light received by it is lower than surficial light (Nash, 1996). The factor by which light received by the photobiont is lower than than in the external environment is (like other lichen stress sensitivities) highly contingent on hyphal hydration status, probably due to changes in intracellular refraction patterns (Nash, 1996). The reduction can be 54 – 79% when dry, but is reduced to 24 – 54% when fully hydrated (Ertl, 1951). Accessory pigments such as carotenoids and zeaxanthins exist in lichens as in other photoautotrophs to prevent excess photons from reaching and damaging the

chlorophyll reaction centres (Nash, 1996). The Mycobiont may also produce intra-hyphal crystals to protect the photobiont from excessive visible and ultra-violet radiation (Clark et al, 2001). At low light intensities, lichen exhibit a lower value light saturation point - i.e. become CO_2 -limited, rather than light limited, at a lower light intensity (Kershaw, 1985). Such acclimatisation to low light intensities is mechanistically similar to that seen in vascular plants, with lichen in low light environments having fewer photoprotective pigments and thinner thalli to maximise photosynthetic yield (Nash, 1996).

Enhancement of silicate weathering by lichens

Weathering entails an increase in the reactive surface area available for the reaction of a given mineral. Abiotic weathering involves the physical breakup of rock at a series of spatial scales, biotic weathering involves both enhancing this process, as well as creating microenvironments in the weathering interface that reduce the activation energy of weathering reactions. Rocks are cracked by the expansion of freezing water during frost wedging and salinity changes, and surficial layers are removed by physical erosion (e.g. Berner & Berner, 1987). At the molecular scale, this increases the reactive surface area available for the chemical reactions of minerals with water, including the silicate weathering reactions (1.A) that comprise the first stage of the Urey “reaction”. These processes are significantly enhanced by the activity of the biosphere. Reactive surface area is increased by plant root wedging, physical expansion of fungal hyphae, expansion of microbial osmolytes, ice nucleation (Kieft, 1988), organic acid production, and animal activity (Schwartzman, 1999). The rate of bacterial weathering of feldspars is increased under conditions of PO_4 deprivation (Bennett et al, 2001). Tangible microbial communities giving rise to carbonate weathering and sulphate release persist beneath contemporary glaciers, implying that the bacterially-driven weathering flux may remain substantial amid terrestrial ice cover (Skidmore et al, 2005). But a large (though uncertain) contribution to terrestrial weathering in contemporary environments comes from the growth and physiological activity of lichens.

Abundant evidence exists for active enhancement by lichen of silicate rock weathering (Jackson & Keller, 1970 McCarroll & Viles, 1995, Banfield & Barker, 1996, Schwartzman, 1999, Aghamiri & Schwartzman, 2002, de los Rios et al, 2003). However the factor by which weathering rate is increased above the abiotic rate is contentious, as is the separation of this factor from the cumulative biotic enhancement of weathering over geologic time (e.g. Schwartzman, 1999). Lichens, like free-living fungi, secrete organic anions and protons to increase reactive surface area on the silicate minerals upon which they grow (e.g. Landeweert, 2001). Because they are poikilohydrous, lichens probably derive osmotic benefit from ice nucleation (Kieft, 1988) - which therefore represents a further, unknown mechanism by which they may increase reactive surface area through physical break up of rocks. It is estimated that, through soil hydration and elevated reactive surface area, the activa-

tion energy of silicate breakdown (ie the first stage of (1.6)) is reduced by rough one half by lichen colonisation (Schwartzman, 1999). Colonisation by lichens liberates nutrients, particularly P and N , and increases reactive surface area - promoting colonisation by bacteria and free-living fungi (Barker & Banfield, 1996). Recruitment of bacterial species in antarctic biomes takes the form of a hydrated, colloidal “biofilm” gel that may promote collective nutrient availability (de los Rios et al, 2003). Microbial respiratory CO_2 dissolves into aqueous solution in soils, significantly increasing soil CO_2 over the global atmospheric partial pressure, probably ultimately increasing silicate weathering over geologic timescales (Keller & Wood, 1993). Differential accumulation of nutrient weathering products within pores of lichenised rocks parallels the nutritional needs of the lichen but varies hugely, between a factor of 0.28 to 16 over the abiotic rate (Schwartzman, 1999). Colonisation of a bare rock surface and the initiation of a soil structure by lichens is also, of course, necessary for the ecological succession to vascular plants. Lichens therefore represent a large component of the net biotic weathering enhancement factor used in Carbon cycle modelling (Berner, 1998). This parameter is uncertain because of the difficulty in separating biotic and abiotic contributions to the weathering rate of a given surface, but is between 10–100 at the global scale over geologic timescales (Schwarzman, 1999). Lichens are therefore usefully viewed as triggering a form of ecological positive feedback, of increasing nutrient availability and soil bacterial species recruitment, which increases weathering through a community level biotic enhancement - but which remains unquantified to any degree of certainty, especially over geologic time.

Survival of multicellular eukaryotes

I use the term “hard snowball” to correspond to a high ice-cover, equilibrium (as opposed to steady-state) solution of the ice albedo feedback. A key assumption underlying this work is that such a solution does not necessarily correspond to a complete lack of habitable refugia. Ice-free land surface would probably occur under a hard snowball scenario, as well as thin-ice-covered, geothermally-heated inland lakes and shallow seas (Pierrehumbert, 2005). A critical unconstrained parameter is cloud water content, which, if raised sufficiently, may permit diurnal tropical melt pools (Pierrehumbert, 2005). (Although this change is probably unrepresentative of the dry atmosphere likely in a hard snowball scenario, it serves to illustrate the uncertainty in crucial parameters). In this light it is worth recalling that contemporary ice-mat communities support cyanobacterial, microbial and eukaryotic growth (Vincent, 2004). Biotic refugia are an uncontroversial proposition for an open water scenario (e.g. Peltier, 2007). But perhaps such refugia are possible under a thin tropical ice scenario, in which glacial movement causes open water channels to periodically appear, regardless of how thick the average level of ice cover tends to be (Halverson et al, 2004). An uncontested expectation is a significant negative impact on productivity for glacial scenarios of all levels of severity. The original interpretation of the Carbon isotope

data in this regard (Hoffman et al, 1998) has been withdrawn, but alternative scenarios are ambiguous because they violate the steady state Phanerozoic archetype (Rothman et al, 2003, Peltier et al, 2007). Prokaryotic communities show no evidence of having been decimated (e.g. Corsetti et al, 2004), but the evidence may be artifactual because the biotic samples may not originate at the site of deposition (Hoffman, pers comm, cited in Pierrehumbert, 2004). Extrapolation from the contemporary Arctic suggests that the expected devastation of prokaryotic communities may have been over-played (Vincent, 2004). The diversification of Eumetazoa during the Ediacaran period and subsequent Cambrian explosion has attracted a range of possible explanations, but few have received more attention than the simultaneous rise in atmospheric oxygen (e.g. Nursall, 1959, Margulis et al, 1976, Runnegar, 1982). The respiratory energy yield from glucose metabolised anaerobically is estimated at between 3 – 12% of the aerobic value, and the physiological energy yield for growth per respiratory substrate in aerobic organisms is greater than anaerobic organisms by a factor of up to six (Catling et al, 2005). Considerations of this sort explain why contemporary metazoans capable of anaerobic metabolism tend to have small body sizes, and why anaerobic physiology is probably a derived character state in most if not all such species (Hochanka et al, 1973, Gaidos et al, 2007). In this light, Canfield et al (2007) attribute diversification of aerobic animal metabolism to increased photosynthetic O_2 production after the Gaskiers event, citing as evidence decreased reactive:total Fe , and increased ^{34}S fractionation after termination of the glacial deposits. Equivalently, Gaidos et al, (2007) propose a selection pressure for feeding on large particles of suspended organic matter in a C -depleted ocean and/or predating on other marine metazoa, followed by a positive feedback in niche differentiation amongst marine metazoa. The latter mechanism might conceivably go hand in hand with the marine C -depletion through organic matter remineralisation (Peltier et al, 2007) and/or increases in marine organic Carbon burial. An equivalent mechanism of escalatory coevolution in the Eumetazoa, mechanistically independent from O_2 , might arise from a restructuring of macroecology by the Ediacaran macrobiota and/or increased potential for differentiation associated with a larger body size (Butterfield, 2007). All of these explanations, however, effectively move the question back in time, by failing to provide an explicit mechanism for why the Ediacaran macrobiota diversified in the first place. Although all of the proposed mechanisms may be logically consistent in themselves, and may plausibly have operated during the late Precambrian and early Cambrian, it is becoming apparent that confusion arises when hypothesized mechanisms to *allow* macroscopic diversification are confused with hypothesized mechanisms to *drive* it (e.g. Conway-Morris, 2006, Butterfield, 2007). All proposed explanations to date for the radiation of macroscopic animal life entail the assumption that macroscopic form will emerge once some physical or ecological constraint is lifted - i.e. that it is already adaptive in an evolutionary sense. Part of this thesis will involve questioning this assumption, by noting that although conditions such as reciprocal coevolution and (in particular)

relatively high atmospheric Oxygen were almost certainly *necessary* for the physiology and ecology of differentiated, macroscopic animal form to operate, these conditions may not, alone, be *sufficient* for such form to increase from rarity by natural selection.

Research questions

The second and sixth chapters of the thesis address the connections between Neoproterozoic glaciation events and the evolution of life history strategies in macroscopic eukaryotes - by relating multi-level selection trade offs to the evolution and proliferation of symbioses such as lichens in the Neoproterozoic abiotic environment (chapter 2), and by examining the effect of extreme glaciations on the ecology and evolution of costly macroscopic heterotrophic form (chapter 6). The middle chapters examine constraints on the snowball Earth problem from a more direct geochemical perspective - firstly with an attempt to quantify the impact of biologically-enhanced silicate weathering on CO_2 levels and thus improve constraints on the biological trigger hypothesis (chapter 3), then with an assessment of atmosphere-ocean fractionation and tectonic constraints on the duration of the glacial interval (chapter 4), with an assessment of the role of the biosphere in the probability of snowball glaciations occurring repeatedly over Earth history (chapter 5).

Chapter 2: Theoretical justification for hypothesizing the presence of Neoproterozoic terrestrial lichens

Summary

I hypothesize that the fitness of members of a costly trait group can be higher than that of autonomous individuals when the group context allows tolerance of fluctuating abiotic environments. I represent this in a simple cost-benefit parameterisation similar to Hamilton's rule but incorporating the effect of the abiotic environment. This requires a more efficient physiological division of labour in groups, the benefits of which "cheaters" cannot experience (although they do benefit from being within the group in a generic way). Groups experience a stronger selection pressure than individuals for homeostasis with respect to reproductively-limiting variables, because their greater longevity exposes them more frequently to suboptimal physical conditions, and greater physical size means they spatially encompass a larger fraction of any resource/nutrient gradient. Groups achieve homeostasis by differentiation into compartments with specialist functions, e.g. cell types. Such differentiation is more limited in individuals due to their smaller size and shorter lifespan, hence so is the range of physical conditions over which homeostasis can be sustained. Groups also sequester larger absolute quantities of resource than individuals, and group death is less frequent, hence the population dynamics of groups cause resource/nutrient availability to fluctuate with greater amplitude than that of individuals - meaning that groups are also more likely to give rise to fluctuating abiotic conditions. I show that a trait providing increased tolerance (α) to fluctuation ($|V - V_{opt}|$) in a limiting abiotic variable (V), at relative fitness cost (C), can increase from rarity if the condition $\alpha \cdot |V - V_{opt}| > C$ is met. Collectively increasing the amplitude of fluctuation in a reproductively limiting environmental variable, is a potential mechanism for altruists to increase from rarity and limit the growth of cheaters. Once altruists reach intermediate frequencies, a positive feedback process can be initiated in which a differentiated group enhances physical fluctuation beyond the tolerance of any "cheat", and in so doing enhances the selection pressure it experiences for homeostasis. This idea may help explain the spread of lichens on the Neoproterozoic land surface, in that symbioses in which nutrient/Carbon flow was less restricted between partner species (i.e. symbioses in which the mycobiont phenotype was more altruistic) may have been able to tolerate a wider range of deleterious abiotic conditions. ¹

¹(The work described in this chapter was published in 2006 as "Fluctuation in the physical environment as a mechanism for reinforcing evolutionary transitions". Boyle, R.A. & Lenton, T.M. *Journal of Theoretical Biology* 242. 832-843.)

Introduction

During Earth history there have been several qualitative re-organisations in the way that some lineages transfer genetic information between generations. These “evolutionary transitions” occur when natural selection starts to act on a spatially larger group composed of ancestrally autonomous individuals (Szathmary, 1989, Maynard-Smith & Szathmary 1994). This principle holds at spatial scales from hypercycles (Maynard-Smith, 1983) through multicellular organisms to kin groups (Hamilton, 1964, 1972). The group units of selection that result are prone to parasitism by “cheater” individuals that evade the reproductive cost of group membership by increasing their own short term fitness, to the detriment of the group. Social group structures may be adaptive under a range of situations, e.g. when an appropriate balance between within group reproduction and between group dispersal is met, or when kin selection exceeds kin competition (e.g. (Michod, 1997, Nowak, 2006). But the balance between these processes remains sensitive to prevailing physical conditions and ecological context, consequently so does the fitness of a gene giving rise to a costly cooperative phenotype. The work in this chapter is concerned with explaining the persistence of evolutionary transitions despite this inherent and unavoidable vulnerability to cheater genotypes. I argue that groups are able to replicate over an amplitude of environmental fluctuation that would be fatal or highly deleterious to a single autonomous individual. Actively increasing the amplitude of fluctuation in such physical variables is suggested as a viable “policing” strategy for the group to limit reproduction of cheaters. In this regard, I note that fluctuating physical conditions probably coincided with some evolutionary transitions - cycles of saturation and dessication may even have been necessary to concentrate reactants during both the origin of a nucleic acid genome, and even for the emergence of homeostatic systems such as the Oklo reactor (Maynard-Smith, 1983, Maynard-Smith & Szathmary, 1995).

The key elements of the hypothesis are as follows. For a given individual, being part of a co-ordinated group increases the range of its tolerance to deviation of one or a number of essential physical variables from optimum (relative to the tolerance range of an individual with an autonomous life history). This results from the evolution of a group-level physiology that is able to buffer abiotic environmental fluctuation by functions such as storage, transport or detoxification. Such a physiology requires a degree of homeostasis that a system can only evolve by differentiation into a number of microcosms, each of which perform a separate function. This level of differentiation is, in turn, only possible or adaptive at the greater spatial and temporal scales over which the group reproduces. Of course, individuals are composed of microcosms just as are groups; a cell consists of distinct classes of organelles just as a multicellular organism consists of distinct organs. But the potential for diversification is greater in a group than in an individual - because its larger size permits a greater range of microcosms to develop, and because the capacity for autonomous physio-

logical function is greater in the individuals that make up a group than in the component parts (be they organs or organelles) that make up those individuals. Therefore, I argue, the potential that the group has to protect its component parts from external fluctuation by maintaining internal homeostasis is greater than that of any one individual, making its tolerance within the range over which the variable fluctuates similarly greater. Hence, while extreme directional changes in the abiotic environment may be tolerable to individual parasitic genotypes, or even enhance selection for them, in a fluctuating environment no single “cheat” genotype will be able to maintain a sufficient relative frequency to invade the group, because they lack a homeostatic property with respect to the given variable that the group is able to achieve. Prokaryotic species may be extremophilic in specified directions, but no one bacterial species encompasses the range of chemical microcosms present in a multicellular eukaryote.

The hypothesis is justified on grounds of size, timescale, and likely optimal strategies for minimising kin competition. By definition, groups are larger and reproduce more slowly than the autonomous individuals of which they are composed. The greater longevity of groups means they are more likely to encounter greater temporal variation in limiting resources or other deviation from physiologically optimal conditions, (for example as a consequence of seasonality or fluctuation in weather conditions), than that experienced by more short-lived autonomous individuals. Additionally, because of their larger size, groups will be more likely to experience spatial heterogeneity and will encompass larger gradients in a given resource or nutrient than will individuals. Such factors will provide a selection pressure, greater than that experienced at the individual level, for the sequestration of resources for periods of sub-optimality and the creation of microcosms for processing toxins etc, a pressure dealt with by spatial/temporal differentiation. Furthermore, differentiation into distinct niches will be adaptive for competitively inferior individual genotypes and beneficial for the group because it will decrease kin competition. Therefore, regardless of whether the early evolutionary dynamics of the group are dictated by kin selection, or by adaptation of group-forming individuals that retain a degree of their ancestral autonomy (as apparent to a degree in some kin-selected traits (Griffin & West, 2002)), differentiation into microcosms is a reasonable possible result.

Increased capacity for physiological homeostasis in groups

The environmental factors that create the selection pressure for diversification into microcosms will also make it easier for such features to evolve. Separate bacterial microcosms and morphs can arise solely as a consequence of individual selection and spatial heterogeneity (Rainey & Travisano, 1998). Therefore compartmentalisation, a prerequisite for evolutionary transitions (Maynard-Smith & Szathmary, 1995), may predispose the system to phenotypic divergence - and perhaps, as a result, physiological robustness with respect

to reproductively-limiting variables. Increased cellular compartmentalisation in eukaryotes relative to prokaryotes, diversification into cell types after the transition to multicellularity, formation of reproductive/worker castes in social insects, and divergence into sterile and fertile, dominant and subordinate individuals within kin groups, are suggested as examples of this pattern. In each of these cases, the group survives across a greater range of physical conditions than any one of the individuals of which it consists.

To illustrate the hypothesis, consider a tumour growing within a microenvironment inside a multicellular system. The tumourigenic cheat cells reproduce within this microenvironment by depriving neighbouring cells of nutrients, respiratory substrate, oxygen etc, hence impose a cost on the group. Suppose also that an essential resource starts to fluctuate beyond the tolerable range within this microenvironment. In some instances co-operative cells will die as a consequence of this fluctuation just as will tumour cells. But if the fluctuation can be buffered by active transport from or to an organ containing a store of the resource elsewhere in the multicellular system, the impact of the fluctuation will be less dramatic. In some circumstances the tumour will benefit from this buffering mechanism just as much as the co-operative cells, and one could say that homeostasis in the resource in question is a trait that has been successfully parasitized. However, one way in which tumour cells differ from those of the rest of the body is via cell junction formation, a process likely to play a role in the acquisition of malignancy (e.g. Yamasaki et al, 1999). If the buffering process requires a signalling mechanism that functions through cell junctions absent in the tumour, the whole tumour will die or experience dramatically curtailed growth if the fluctuation continues. Although individual tumourigenic genotypes may have been able to adapt to extreme levels of resource were the change directional, no single cell within the tumour will possess the capacity to be coupled to the organ performing the buffering function, so no single tumour genotype will be able to cope. The essence of the hypothesis is that evolutionary transitions in individuality result in properties analogous to such cell junctions, properties that cannot be parasitized by cheat individuals, regardless of their frequency within the group. The capacity to form cell junctions and achieve physiological co-ordination with neighbouring cells may thus be more than merely a metaphor for such a trait. Similarly, a mechanism for the multicellular system to bias the environment so that fluctuation is enhanced bears a parallel to the administering of chemotherapeutic drugs in discrete doses in order to medically treat such tumours, in that the wild type cells have a greater capacity for recovery. The ability of social insect colonies and social groups of mammals to sequester a range of resources in quantities that no individual could achieve, or hunt a variety of prey unavailable to any one individual are similar examples. The division of labour in a group comprises a larger phenotypic space. In some instances the benefits from these properties are available to cheats. But if a check on group membership or an analogous property exists that restricts the range of group properties from which the

cheat can benefit, then the group will be able to survive should one resource/prey suddenly fluctuate deleteriously, whereas any one specialist individual will be unable to exploit those properties of the group that derive from individuals with different capabilities to itself.

Relevance of multi-level selection to inter-species symbioses

Whilst symbioses may not be examples of group formation in the strict sense, they do constitute a pooling of genetic resources and a loss of reproductive autonomy by each partner, therefore they are arguably a transition between levels of selection (Maynard-Smith & Szathmary, 1995). In a symbiosis in which each partner contributes a resource at levels the other is unable to obtain, a critical stoichiometry between the nutrients provided by each partner is likely to be vital for successful function of the mutualism (Sterner & Elser, 2002). An adaptive nutrient stoichiometry may only be achievable in a fluctuating environment if both partners are sufficiently mutualistic. In a lichen, for example, the $C : P$ ratio must be high enough to meet the needs of the mycobiont (i.e. - there must be enough reduced Carbon available), but not so high that photobiont growth becomes PO_4 limited. Lichens, like all symbioses, exist on a genetic continuum between mutualism and parasitism (Van Baalen & Jansen, 2001, Hyvarinen et al, 2002). Imagine a cheater fungal genotype that evolves to wholly or partially restrict the supply of P (obtained by the fungus) to its photobiont. Should the steady state abiotic level of one of the nutrients suddenly drop, the cheater mycobiont genotype will be less likely to adequately compensate for the change by elevating supply to its photobionts than will a more mutualistic fungal genotype with a higher initial P flux to its partner - because, by definition, the phenotypic plasticity required to do so is less than in a more altruistic genotype. This idea could apply equally under a sudden excessive increase in P (or N), in which cases symbioses with cheat photobiont genotypes partially restricting carbohydrate supply to the fungus would be selected against, because the fungus would approach Carbon limitation as its growth rate responded to the sudden glut of inorganic nutrient. Dynamics of this sort will affect the continuum of any symbiosis subject to fluctuating resource availability. I think there may frequently exist an adequate window of mutualism in which the system is able to compensate for fluctuating resource availability, and should either partner evolve too far toward the cheater end of the continuum, the symbiosis will become maladaptive in the presence of such fluctuation.

Enhancement of fluctuation in physical variables by groups

Evolutionary transitions in individuality may also correspond to significant changes in the impact that life has on the physical environment, such that the amplitude of fluctuation in certain limiting physical variables is increased as a function of group abundance. Life will have a stronger influence upon its environment when biota are confined to a microcosm, in which uptake of resources/nutrients and excretion of waste products will be concentrated

in a small space. Given that compartmentalisation of living material into such microcosms was probably necessary both for successful coevolution of a large, coordinated (RNA) hypercycle, and for concentration of metabolic reactants within protocells (Eigen, 1971, Bresch, 1980, Maynard-Smith & Szathmary, 1995), it seems reasonable to assume that a consequence of some transitions in individuality was a significant increase in the impact of the post-transition group on the (micro)environment in which it evolved, when compared with pre-transition autonomous individuals. This idea may be understood in a simple generic sense based on arguments of spatial and temporal scale, and on negative feedback from the physical environment. Groups' larger size means they displace a greater absolute quantity of any given physical resource or nutrient. Similarly, because groups survive longer than any given individual, the release of such sequestered resources upon group death will be less frequent. Therefore the population dynamics of groups causes more dramatic fluctuation of such resources/nutrients than that of individuals, with a more peaked distribution of availability in time and space. If the "cheat" life habit experiences the same physical environment as the group (e.g. if it is a cell growing on the exterior of the multicellular system it is parasitizing), it may be unable to tolerate fluctuations in the availability of essential substances - fluctuations that are non-fatal to the group due to the buffering functions mentioned above. For example, the origin of swarming and other social behaviour in insects may have resulted in a sudden increase in resource sequestration per individual, relative to an autonomous life history. Upon death of the colony, release of these resources will be more concentrated in time and space than would the release of an equivalent quantity of resource by the same number of individuals living independently, hence will cause resource fluctuation of an increased amplitude. This argument might just as well apply to a comparison between a unicellular and a multicellular system.

A further reason to expect the group to elevate the amplitude of physical change, as opposed to causing a dramatic unidirectional change, involves negative feedback from the physical environment (Lenton, 1998). If the change induced by a group is directional, but triggers a response in the physical environment that counteracts this change and therefore makes the environment less suited to group reproduction, then the system will oscillate as group numbers rise and fall. This process is thought to have occurred following colonisation of the land by vascular plants. This probably required the symbiosis with mycorrhizal fungi (e.g. Wilkinson, 2001). Once vascular plants achieved terrestrial abundance, a dramatic decrease in atmospheric Carbon dioxide was induced, due to the resultant biotic enhancement of silicate weathering (Berner, 1990, Schwartzman, 1999, Lenton et al, 2004). This caused a decrease in temperature, which in turn decreased biological productivity. It is plausible that repeated cycling through this negative feedback loop (Lenton & Watson, 2000) would lead to fluctuation in the availability of a variety of nutrients, as a result of the impact of temperature on physical weathering processes and the activity of the hydrological cycle

over geologic time.

Figure (2.1) shows a schematic of the hypothesized mechanism. Suppose that any dramatic physical change elicited by the post-transition biological system is countered by a negative feedback process within the physical environment (for example, the sequence: “increased vascular plants \rightarrow increased silicate weathering \rightarrow decreased CO_2 \rightarrow decreased temperature \rightarrow decreased vascular plants” described above). If this occurs, any sufficiently sudden and dramatic biologically triggered physical change will lead to an oscillation, as the environmental effect of that change feeds back on the biological cause (e.g. as above - and within appropriate limits - “decreased vascular plants \rightarrow decreased weathering \rightarrow increased CO_2 \rightarrow increased vascular plant productivity”). All biologically significant nutrients and resources are influenced by such negative feedback processes (e.g. Lenton, 1998, Schwartzman, 1999).

A simple model

Model outline

Three simple differential equations describe the relative abundance of altruist and cheater genotypes and of the level of an independently fluctuating abiotic variable. The fitness of each genotype is the rate of reproduction per individual of that genotype relative to the other. The total population size varies; the absolute number of individuals of either genotype in any generation, is that number in the previous generation, multiplied by the genotype’s fitness. The key influences (i.e. cost, benefit, abiotic impact) are parameterised in order to determine their relative importance in the outcome of the evolutionary dynamics.

Parameterisation

Consider a population of a theoretical haploid, asexual, group-forming species, the reproduction of which is limited by an essential environmental variable, V . This variable fluctuates independently over time, about the optimum level for growth of the species, V_{opt} . Let the fitness of a gene causing an altruistic individual phenotype involving contribution to the group be F_g . F_g is determined by the replication fidelity R , the advantage of group membership relative to an autonomous life history β , and the reproductive cost of the cooperative phenotype C . Within the group there are cheater individual genotypes that parasitize any given group trait, hence experience β without incurring C . Replication of both the group as a whole, and of parasitic cheater individuals, is decreased by deviation of the focal variable V from the species’ optimum value V_{opt} . Positive and negative deviations from this optimum are assumed to be equally deleterious. Therefore the relative fitness (here assumed synonymous with the geometric rate of increase per generation) of a gene in a co-operative individual, F_g , is therefore the product of the replication fidelity, benefit of

being in the group context, and various demographic parameters, as described by equation (2.1):

$$F_g = \beta \cdot R \cdot (\lambda - (C + m + |V - V_{opt}|)) \quad (2.1)$$

Where λ gives the species' birth rate and m the mortality rate when $V = V_{opt}$ (other forms of intraspecific competition, as well as density dependence, are ignored). Parasitic cheater individuals of genotype P avoid the cost of group membership but share the same basal fecundity λ and mortality m , giving them relative fitness F_p :

$$F_p = \beta \cdot R \cdot (\lambda - (m + |V - V_{opt}|)) \quad (2.2)$$

If membership or non-membership of the group has no bearing on the response to fluctuation in V , then parasitic genotypes will increase in frequency by a factor of C each generation, because β , the only beneficial consequence of the transition, is fully available to "cheats". However, suppose that an additional consequence of the transition is greater tolerance α of deviation of V from optimum, incurring a greater cost C , but dampening the physiological impact of fluctuation in the physical variable. In this case the fitness F_g of a co-operative genotype becomes:

$$F_g = \beta \cdot R \cdot [\lambda - (m + C + (1 - \alpha) \cdot |V - V_{opt}|)] \quad (2.3)$$

Whether or not such a trait is adaptive is a function of the proportion of the time that $V \neq V_{opt}$. Because the β , R , m and λ terms are the same for both genotypes, the condition for the co-operative genotype to have higher relative fitness $F_g > F_p$, is dictated only by the tolerance of fluctuation, magnitude of fluctuation experienced, and relative fitness cost of the extra tolerance. Substituting the parameters discussed, co-operative fitness superiority $F_g > F_p$ therefore simplifies to:

$$\alpha \cdot |V - V_{opt}| > C \quad (2.4)$$

Expressing the condition that if α , the increased tolerance to deleterious fluctuation in V that altruistic individuals within the group have relative to cheaters, exceeds the relative fitness cost of this decreased sensitivity, then this genotype will have higher relative fitness if the environment is sufficiently variable. Genotype P might be considered analogous to K-selected life history strategy within the window $V = V_{opt}$, whereas genotype G equivalent to an r-selected "generalist" with respect to variable V . It is perhaps improbable that the environment will vary just enough to limit cheat reproduction but not so much as to be outside the habitable window for the group. However, should a further consequence of an evolutionary transition be elevated fluctuation in the physical environment, a positive

feedback process may be initiated, by which (within limits) the group makes the environment more variable, and benefits from this variability by the decreased reproduction of cheat individuals. This process will apply only in situations in which the cheat genotype is incapable of achieving this extra homeostatic ability regardless of its frequency within the group. Once the fluctuation reaches such a level as to cause condition (2.4) to no longer hold, group reproduction will decline, before the group eventually self-limits through the variability it is able to induce. I encompass extra deaths (i.e. above m) as a result of deleterious fluctuation in V , within the fitness term by allowing negative fitness values in sufficiently deleterious environments. The absolute frequencies of the group-forming genotype G and parasitic cheater genotype P are scaled by their starting frequencies (denoted by a zero subscript), and their respective fitness values as they change over time, as described by (2.5) and (2.6):

$$G_t = G_0 \cdot F_g^t \tag{2.5}$$

$$P_t = P_0 \cdot F_p^t \tag{2.6}$$

Where subscripts denote time t and time zero generations as shown. The respective rates of change over time of the absolute frequencies of the two genotypes are given by differentiating (2.4) and (2.5), and imposing the constraint that total population size $G+P$ cannot exceed carrying capacity K . This gives the time derivative for the altruistic genotype $\frac{dG}{dt}$, and for the cheater genotype, $\frac{dP}{dt}$, respectively in (2.7) and (2.8):

$$\frac{dG}{dt} = G_0 \cdot F_g^t \cdot \ln(F_g) \cdot \frac{dF_g}{dt} \cdot \left(1 - \frac{G+P}{K}\right) \tag{2.7}$$

$$\frac{dP}{dt} = P_0 \cdot F_p^t \cdot \ln(F_p) \cdot \frac{dF_p}{dt} \cdot \left(1 - \frac{G+P}{K}\right) \tag{2.8}$$

The only determinant of the relative abundance of each genotype that varies systematically with time is the impact that fluctuation in V has on the fitness terms:

$$\frac{dF_g}{dt} = -\beta \cdot R \cdot [(1 - \alpha)] \cdot \frac{dV}{dt} \tag{2.9}$$

$$\frac{dF_p}{dt} = -\beta \cdot R \cdot \frac{dV}{dt} \tag{2.10}$$

The environmental variable V oscillates about V_{opt} with an entirely abiotically determined amplitude τ according to:

$$V = V_{opt} + \tau \cdot \sin\left(\frac{\Pi}{2} + t\right) \quad (2.11)$$

(Where t is a timestep of length one generation). If the group alters the physical environment such that the amplitude of the oscillation exceeds τ , by a factor ϕ of the group's abundance, then (2.11) becomes:

$$V = V_{opt} + \tau \cdot \sin\left(\frac{\Pi}{2} + t\right) \cdot (1 + \phi \cdot G) \quad (2.12)$$

Where ϕ is the effect on V per individual of genotype G , so that:

$$\frac{\partial V}{\partial G} = \tau \cdot \sin\left(\frac{\Pi}{2} + t\right) \cdot \phi \quad (2.13)$$

Differentiating (2.12) gives the total amount of fluctuation in the variable within a system in which the background variability is enhanced by group activity:

$$\frac{dV}{dt} = \tau \cdot \cos\left(\frac{\Pi}{2} + t\right) \cdot (1 + \phi \cdot G) + \tau \cdot \sin\left(\frac{\Pi}{2} + t\right) \cdot \phi \cdot \frac{dG}{dt} \quad (2.14)$$

But as $G \rightarrow 0$, (i.e. when the altruist genotype is at rarity), the G term in (2.12) disappears, hence:

$$\frac{dV}{dt} \rightarrow \tau \cdot \cos\left(\frac{\Pi}{2} + t\right) \quad (2.15)$$

For the group-forming genotype G to invade a population of potential "cheat" individuals that will parasitise it should it increase from rarity:

$$\frac{dG}{dt} > \frac{dP}{dt}$$

Because V is the only part of the system varying systematically over time, this is equivalent to:

$$\frac{dG}{dF_g} \cdot \frac{dF_g}{dV} \cdot \frac{dV}{dt} > \frac{dP}{dF_p} \cdot \frac{dF_p}{dV} \cdot \frac{dV}{dt} \quad (2.16)$$

Substituting terms, re-arranging and simplifying gives:

$$(1 - \alpha) < \frac{P_0 \cdot F_p^t \cdot \ln(F_p)}{G_0 \cdot F_g^t \cdot \ln(F_g)} \quad (2.17)$$

Equation (2.17) describes a necessary condition for the frequency of the co-operative genotype to increase from rarity: the detrimental effect of fluctuation in V on genotype G must be less negative than the genotype's demographic inferiority in the population. Therefore relative physiological robustness and demography alone must be sufficient to

cause G to reach a frequency at which it can influence V via the positive feedback process (i.e. $\frac{\partial V}{\partial G}$) described above. After this point, if genotype G is to approach fixation, the deleterious impact of the fluctuation that genotype G induces must have a lesser impact on its own frequency than on cheaters P :

$$\frac{\partial G}{\partial |V - V_{opt}|} > \frac{\partial P}{\partial |V - V_{opt}|} \cdot \frac{\partial |V - V_{opt}|}{\partial G} \quad (2.18)$$

(Noting that the partial derivatives of both genotypes with respect to $|V - V_{opt}|$ will be negative). As absolute growth rate slows whilst the system approaches carrying capacity, genotype G will continue to increase in relative frequency as extra deaths due to deviation in V occur disproportionately in genotype P . Finally, if suboptimality in V causes extra deaths in both genotypes, then for G to go to fixation (where $\Sigma = G + P$) these extra deaths must preferentially occur in the parasitic genotype P :

$$\frac{\frac{dP}{dt}}{\frac{dG}{dt}} < \frac{\partial \Sigma}{\partial |V - V_{opt}|} \cdot \frac{\partial |V - V_{opt}|}{\partial G} \quad (2.19)$$

Inequality (2.19) implies that genotype G goes to fixation before the entire population goes extinct due to the deleterious fluctuation in V , (note that the partial derivative of total population size will be negative, as will the full derivative $\frac{dP}{dt}$ under conditions in which G is amplifying fluctuation). Inequality (2.19) says that the negative impact of altruistic genotype G on cheater genotype P must be more negative than the impact of genotype G on the population as a whole. This situation will persist until G self-limits, by reaching an absolute frequency sufficient to drive $|V - V_{opt}|$ high enough that relation (2.4) no longer holds. In simplifying (2.18) all terms cancel except α , meaning that if the group reaches a frequency at which it can influence the environment, the frequency of parasitic P individuals will be driven down until G self-limits, a positive value of tolerance α being the only proviso. If the absolute frequency of G required for self-limitation through V is higher than the carrying capacity K then G will go to fixation and P will go extinct, if not then (2.19) will not be realised and an equilibrium will be reached at which growth of both genotypes is limited by the degree of suboptimality in V .

Results

Sensitivity analysis

Figure (2.2) explores the impact of each biotic parameter on the relative viability of the two genotypes, within environments in which the abiotic variable V fluctuates at different abiotic amplitudes τ . The values chosen for other constants are given in Table (2.1). All plots show the results of different simulations (one per datapoint) over 100 generations, from an initial population of one individual of each genotype. Figure (2.2A) shows how the

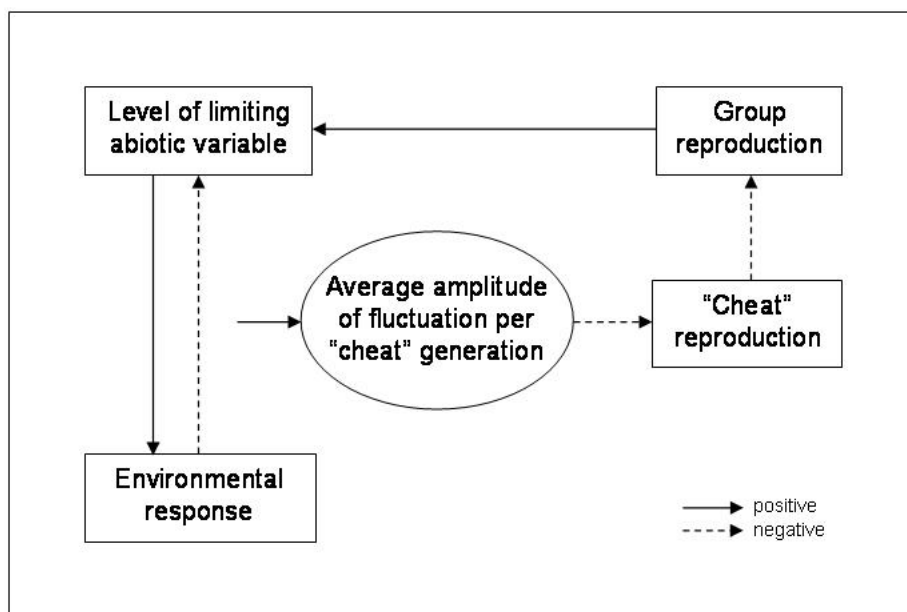


Figure 2.1. A directional biologically elicited physical change in a given variable can be converted into an oscillation in conjunction with a negative feedback process in the physical climate that acts on that variable. Boxes represent the magnitude of the processes shown. Arrows represent positive or negative feedback according to sign.

value of tolerance α (X-axis) impacts upon the relative frequency of the G (group-forming) genotype (Y-axis), with cost C and enhancement of environmental fluctuation ϕ set to zero. The various curves differ in the magnitude of τ , the amplitude of abiotic fluctuation in V . Increasing α causes incremental increases in G 's relative frequency, with a gradient dictated by the amplitude of abiotic variability τ . Because C is zero, both fitness functions become identical when τ is zero, and relative frequencies remain at their starting values. Figure (2.2B) shows how increased cost C decreases the relative frequency of G with tolerance α fixed (at 0.25) with gradient again determined by the value of τ . Figure (2.2C) shows equivalent results but for $C = 0.25, \alpha = 0.25$, and variable magnitudes of ϕ , the increase in fluctuation in V caused per individual of genotype G . The influence of this parameter is highly sensitive to abiotic variability τ . At $\tau = 0.5$ increased enhancement ϕ actually has a slight negative impact on the relative frequency of G . At this tolerance α value, the increase in fitness that the altruist genotype G incurs as a result of extra variability is insufficient to overcome its inferior growth rate. This results from demographic changes due to the logistic formulation of the model (discussed below). At higher values of abiotic variation τ , enhancement ϕ incrementally increases the relative fitness of G , but as is evident from the plots, G is much more sensitive to tolerance α and cost C than to variation enhancement ϕ . As might be expected intuitively, ϕ is most influential in the dynamics of G at intermediate values of τ , because this is when the relative frequencies of both genotypes are most sensitive to $|V - V_{opt}|$.

Environmental variability and absolute population size

The proposed mechanism includes scenarios in which genotype G induces an abiotic change deleterious both to itself and to genotype P , but increases in relative frequency because its superior tolerance means its absolute frequency declines more slowly than that of the cheater genotype P . If this involves extra deaths, it presupposes a decrease in absolute population size. If it involves changes in birth rates, it presupposes the total population taking longer to reach carrying capacity. The idea is therefore potentially highly sensitive to absolute population size and initial demographic conditions. Figure (2.3A) shows the relative frequency of altruist genotype G for different values of the abiotic amplitude of fluctuation τ , again after 100 generations - from starting frequencies G_0 and P_0 of one individual per genotype. The curves differ in the value of ϕ , the increase in fluctuation induced per G individual. As fluctuation τ becomes larger, the relative frequency of G increases, with a gradient dictated by ϕ . Figure (2.3B) shows results from the same simulations, but plots the total population size $\Sigma = G + P$. Comparison of Figures (2.3A) and (2.3B) shows how at this combination of α and C values, if G is to approach fixation, the environmental variation $|V - V_{opt}|$ must be so great as to effectively drive the population extinct. When α takes larger values, and/or C lower values, this need not happen (below). Amplifying environmental variation in a deleterious direction is a risky strategy requiring a

substantial tolerance advantage in order to be adaptive. This figure thus emphasizes why a strategy of the sort described is only realistically likely to be associated with evolutionary transitions - incremental evolution through these parameter values is not possible, and a dramatic and sudden increase in physiological tolerance is therefore a prerequisite for using the environment as a policing strategy in this way. As I have argued above, the origin of multicellularity and of social groups both fulfil this criterion. Figure (2.3C) relates the model's results to the prediction made by relation (2.4) showing the relationship between cost C and $\alpha \cdot |V - V_{opt}|$ over a series of simulations in which $\alpha = 0.6$, $\tau = 1$, $\phi = 0.01$. $\alpha \cdot |V - V_{opt}| = C$ at the point where the two curves meet, and condition (2.4) is realised as an inequality to the right of this point. Note that the high sensitivity to the magnitude of the cost parameter C manifests as a strong non-linearity; G either rapidly tends to unity at permissive C values (altruists approach fixation), or to zero (cheaters go to fixation, before dying due to the absence of altruists once C is too high. That is, for fixed values of tolerance α , enhancement ϕ and abiotic variability τ , the relative frequency of genotype G approaches either zero or extinction, depending on whether or not condition (2.4) is realised (And provided enhancement and abiotic amplitude are both non-zero and within the permissive ranges identified in Figures 2.2C and 2.3A).

Invasibility

TABLE 2.1 <i>Constant</i>	<i>Value</i>
β	1.0
R	1.0
K	1000
m	0.1
λ	1

Figure (2.4) compares the results of single 100 generation simulations, to test the criteria identified above for group genotype G to invade, within a more realistic context in which a single G individual arises in a population of 99 P individuals, where cost $C = 0.2$, and tolerance $\alpha = 0.7$. In each set of two plots A-C, plot (i) compares the relative frequency of G (circles), P (stars), with the level of V (solid line, relative to the optimum $V_{opt} = 1$), the (constant) threshold C (dashed line), and the value of $\alpha \cdot |V - V_{opt}|$ (dot-dashed line). Note the increased size of the Y-axis through Figures A, B and C. Figure (2.4A) illustrates the dramatically lower relative and absolute frequency of G in an environment with low variability where $\tau = 0.1$, in which frequencies of the G genotype do not differ appreciably from their values in a constant environment (G has relative and absolute frequencies of 0.006 and 6 individuals respectively with $\tau = 0$ (not shown), versus 0.0069 and 7 individuals in fig. A where $\tau = 0.1$). Note that $\alpha \cdot |V - V_{opt}|$ is much lower than C , hence condition (4) is not realised. Figure (2.4B) shows how the G genotype is able to exploit its higher tolerance

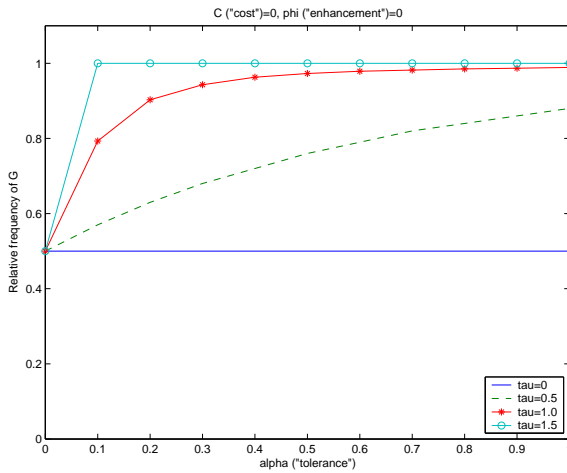


Figure 2.2(a). The impact of each parameter on the relative frequency of the group-forming G genotype after 100 generations in environments of different τ (baseline abiotic variability). Starting relative frequencies of 0.5 and absolute frequencies of 1, for both genotypes. Impact of α (tolerance to deviation of V from optimum), $C = 0$, $\phi = 0$.

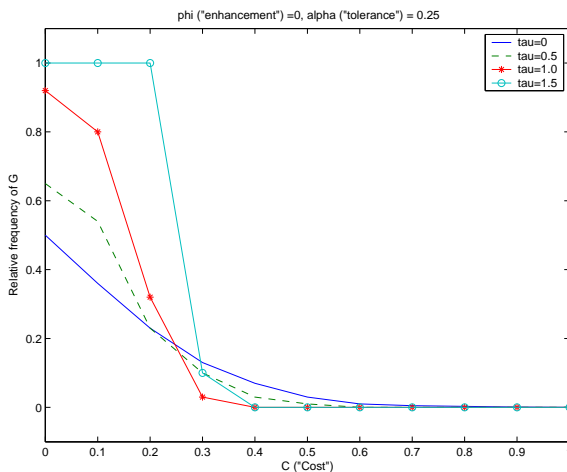


Figure 2.2(b) Impact of C (Cost of group membership), $\alpha = 0.25$, $\phi = 0$.

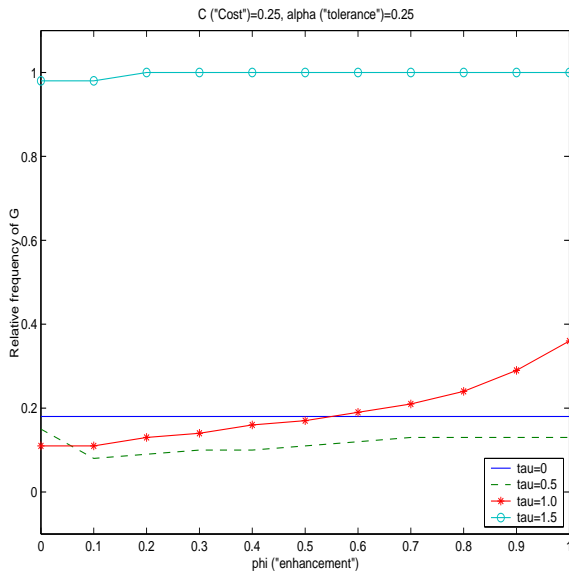


Figure 2.2 (c) Impact of ϕ , (enhancement of fluctuation in V per individual of genotype G). $C = 0.25$, $\alpha = 0.25$.

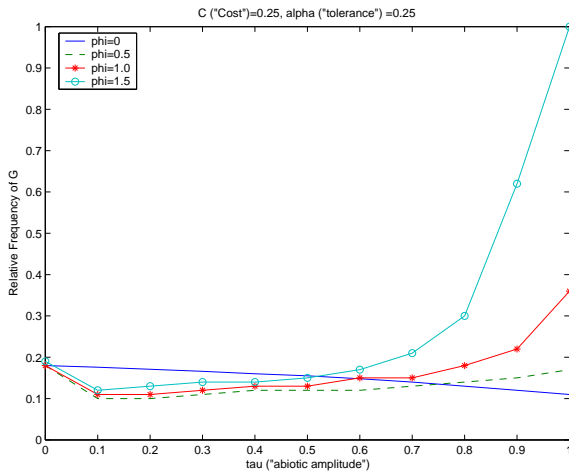


Figure (2.3). Impact of abiotic variability τ on the relative frequency of G at different ϕ values.

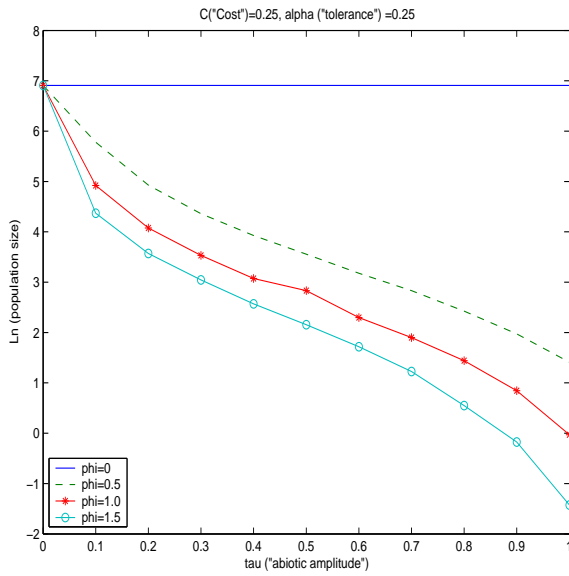


Figure 2.3B Impact of abiotic variability τ on the total population size Σ at different ϕ values.

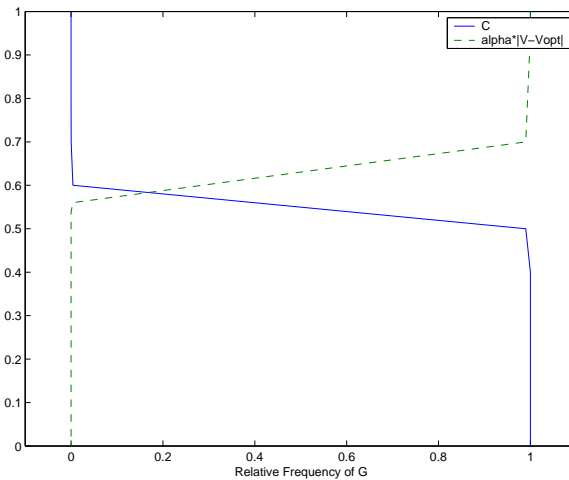


Figure 2.3C Relation between the relative frequency of G (x-axis), and the relative magnitudes of C and $\alpha \cdot |V - V_{opt}|$, where $\alpha = 0.6$, $\tau = 1$, $\phi = 0.01$.

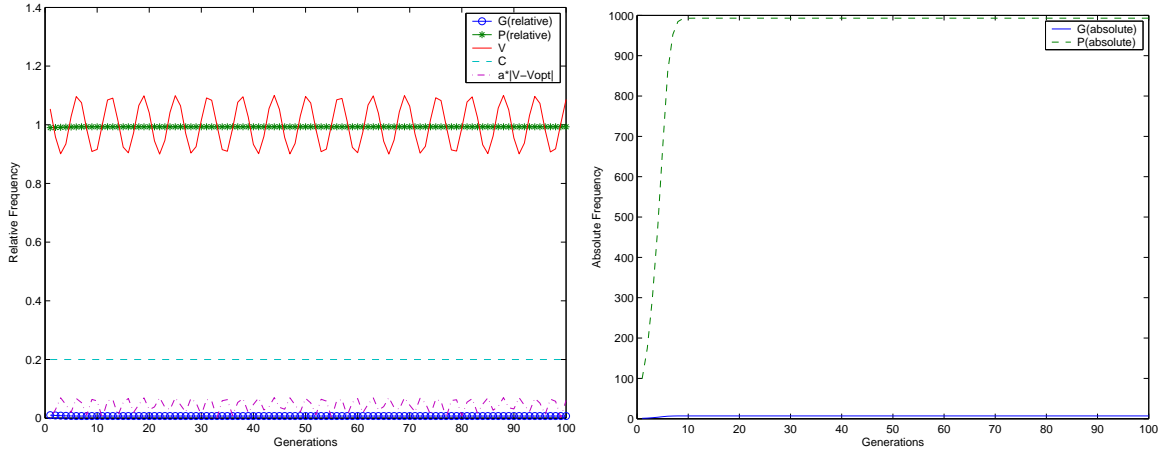


Figure (2.4)(a). Single simulation results, Cost $C = 0.2$, tolerance $\alpha = 0.7$. Left - relative Frequencies, Right absolute Frequencies. (Note the increasing size through A-C of the y-axis in part (i)). $\phi = 0$, $\tau = 0.1$ (slight biotic enhancement, weak abiotic variation).

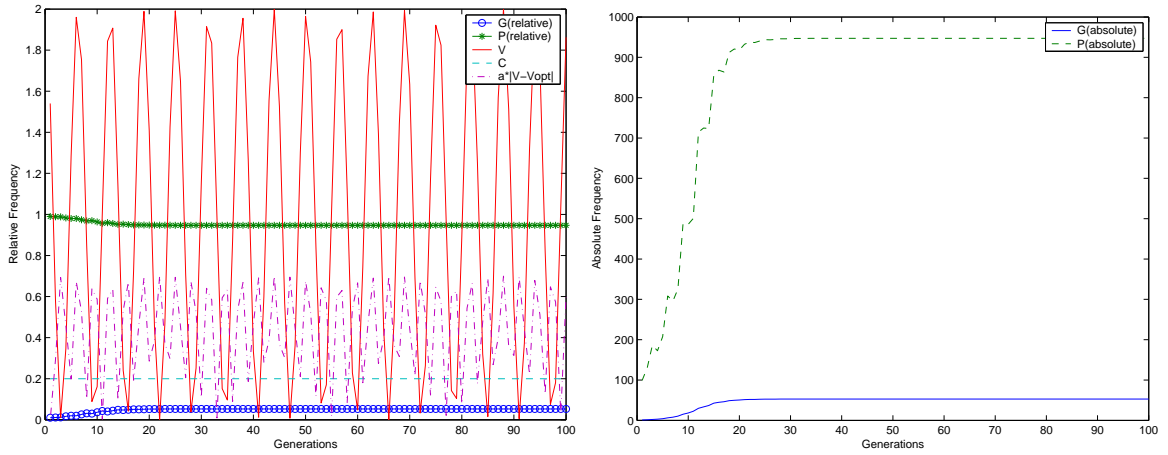


Figure 2.4B. $\phi = 0$, $\tau = 1.0$ (slight biotic enhancement, strong abiotic variation).

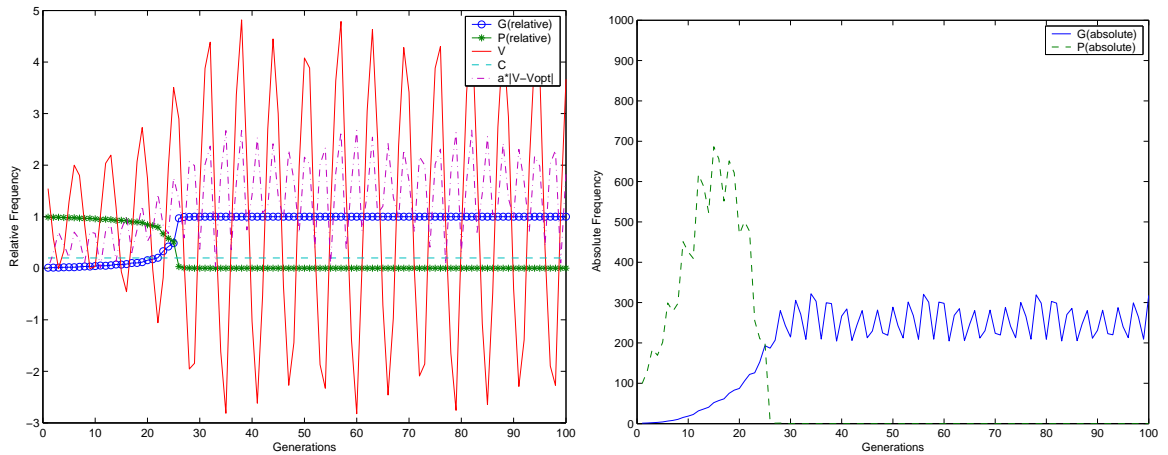


Figure 2.4C $\phi = 0.01$, $\tau = 1.0$ (slight biotic enhancement, strong abiotic variation).

as a function of the baseline variability in the the environment. Note that $\alpha \cdot |V - V_{opt}|$ is driven above the C threshold once abiotic variability $\tau = 1$, and at the same time G starts to persist at tangible (but low) frequencies. Figure (2.4C) shows that if in addition to its superior tolerance G is able to increase $|V - V_{opt}|$ by a factor 0.01 per individual, then it can drive P extinct by amplifying this variation. Note that the fluctuation in V reaches, and is sustained at, a greater magnitude than that prior to the fixation of G (Figure 2.4C(i)). Note also that G self-limits; its absolute frequency remaining below the carrying capacity K (Figure 2.4C(ii)), as a result of the deleterious fluctuation that the G genotype is itself causing.

Discussion

The effect of a trait group on the abiotic environment is density dependent - therefore it cannot be invoked to explain the increase from rarity of a trait for such an effect. Furthermore, neither high tolerance $\alpha = 1$ or strong enhancement of fluctuation $\phi \geq 1$ is likely to be realistic outside rare microenvironments in which fluctuation is low in the first place, removing the selective advantage of a physiological tolerance trait like α . However, as the environment becomes more variable, even a relatively modest tolerance α value can give the group G a dramatic fitness advantage. Whilst an increase in relative tolerance of a tenth remains a relatively large change, the reader is asked to consider the difference in spatial scale between the pre-transition and post-transition systems when assessing the realism of the values chosen. Any cell within an ancestral multicellular organism is more likely to be shielded from external fluctuations because of the co-operative's greater physical size, even prior to the evolution of the homeostatic physiological systems that will further protect it. If the process described is to be relevant, either the physiological robustness must evolve first, or the group must reach the required intermediate frequencies by genetic drift. The realism of the latter supposition is strengthened by the increased influence of drift in the small populations within the microcosms that characterise many evolutionary transitions, right back to the cycles of condensation thought to be required for the origin of a genetic code (Maynard-Smith & Szathmary, 1995). Additionally, the contrast in spatial scale between such microcosms and larger more well mixed environments, is more conducive to the biota achieving localised environmental effects of an order necessary to realise condition (2.4), because resource/nutrient sequestration and release by an organism has a greater influence on its environment when contained in a partially closed system (Lenton, 1998). Furthermore, because the group's greater physical size means it displaces a greater absolute quantity of resource within a smaller space than an equivalent number of autonomous individuals, its impact on the dynamics of such a resource will be similarly greater. All this means that the magnitude of change in resource concentration the group causes is likely to be dramatically greater than the impact of an autonomous individual. I therefore ar-

gue that evolutionary transitions are reasonably described by the parameter values used, whereby the group persists at low frequency, and amplifies variation to drive the “cheat” genotype extinct (enhancement $\phi = 0.01$, tolerance $\alpha = 0.7$). Nonetheless, the greater physical size of the group comes at the cost of a similarly dramatic decrease in short-term fitness, so a high value of tolerance α must also correspond to a high value of cost C .

Hence, a two-stage process is proposed: A transition in individuality occurs and results in enhanced physiological robustness, causing the responsible trait to increase in frequency if the environment is sufficiently variable for this robustness to be adaptive. Once an appropriate frequency is reached, positive feedback with the environmental variable allows the group to approach fixation. In a situation in which the environment is already varying at intermediate amplitude due to abiotic causes, then population sizes of autonomous individuals are likely to be subject to frequent crashes, further accentuating the influence of genetic drift. The kind of environment in which physiological robustness is advantageous is therefore also one in which a trait for such robustness may be more likely to gain, by chance, a relative frequency sufficient to exploit this robustness. Outside such environments, the physical system is unlikely to permit conditions (2.4) or (2.17) to be realised, making the emergence of a trait of this sort rare, and confined to dramatic changes in the structure, function and abiotic impact of life, such as transitions in individuality.

The fact that the group, G , induces a change deleterious to itself in order to purge cheats, means it also limits its own growth - and therefore the magnitude of this change. A transition in individuality should initially cause a dramatic increase in fluctuation through a positive feedback process, in which the fluctuation increases the relative fitness of altruist genotypes compared to cheaters. Then, as it becomes too great for the group to tolerate, the abundance of the group should decline to a steady state as the group self-limits through the fluctuation. The resulting magnitude of environmental fluctuation will be greater than prior to the transition. This pattern corresponds well to figure (2.4C). If the hypothesized mechanism occurs, I expect such a pattern to be seen in the geologic record at times of major transitions in individuality. I now discuss two candidate intervals.

Consider the colonisation of the land surface by vascular plants after the transition to multicellularity, in symbiosis with mycorrhizal fungi. This resulted in an increase in the efficiency of weathering of inorganic Phosphorous (Lenton, 2001), in addition to an increase in bulk silicate weathering described above. Only the post-transition “group” was able to achieve this - the plant providing reduced Carbon and increasing physical weathering via root growth, the mycorrhizal fungus able to selectively weather Phosphorous by acidification of the soil and chelation of the cations to which inorganic phosphates are bound (Landeweert, 2001). The consequence of increased Phosphorus weathering efficiency is increased export of phosphorus to the oceans, which causes increased marine production and increased burial

of marine organic Carbon. This burial is the principal source of atmospheric oxygen over geologic timescales (Lenton & Watson, 2000). The rise in oxygen, in turn, decreases plant growth by increasing photorespiration and fire frequency. This closes a negative feedback loop by limiting Phosphorus weathering (Lenton & Watson, 2000, Lenton, 2001). A plant-induced rise in Oxygen in the Devonian and Carboniferous has been inferred separately from Carbon isotopes (Hayes et al, 1999) and rock-type abundance data (Ronov, 1976). Models driven by such data predict a peak oxygen level of 25-35% around 300 Ma (million years ago) (Lenton, 2001, Berner, 2001). Fossil evidence shows a continuous presence of forests since 350 Ma, placing an upper limit on fire frequency and therefore oxygen, while a continuous charcoal record constrains the lower limit on atmospheric Oxygen at around 15% (Lenton & Watson, 2000). Models suggest atmospheric Oxygen underwent a damped oscillation within these bounds, reaching a minimum in the late Triassic around 200 Ma before rising again to a secondary peak in the Cretaceous around 100 Ma (Lenton, 2001, Berner, 2001).

Applicability to Neoproterozoic lichen symbioses

The same processes linking Phosphorous weathering to atmospheric Oxygen may also have been operating as far back as the Neoproterozoic era 1.0-0.55 Ga (billion years ago). During this era, a photobiont-mycobiont symbiosis in the form of lichens probably evolved (Hedges, 2004, Yuan et al, 2005). This would had two major environmental consequences. Firstly, a lichen can colonise disparate niches unavailable to fungi or cyanobacteria alone, meaning the productivity and size of the terrestrial biosphere may have suddenly increased after the origin of lichens. This would have enhanced bulk silicate weathering, drawing down atmospheric Carbon dioxide and decreasing the temperature. This in turn could have started the global scale oscillation between extreme greenhouse and icehouse states that has been proposed to explain Neoproterozoic glacial deposits (Lenton & Watson 2004, Hedges, 2004). Secondly, in a similar manner to the plant colonisation described above, selective weathering of Phosphorous by lichens (Landeweert, 2001), may have caused a net increase in atmospheric Oxygen (Lenton & Watson, 2004). During times of extreme glaciation, productivity was decimated and hence Oxygen would have declined. However, there was an overall increasing trend in Oxygen that provided a necessary condition for the Cambrian explosion (Lenton & Watson, 2004). Given the polyphyletic nature of the lichen life history (e.g. Nash, 1996), the million year timescales over which climatic feedbacks of this sort occur is of the same order as that over which one might expect evolution of lichens, following overlap of separate mycobiont and photobiont populations. Thus the pattern following the evolution of these symbioses is one of overall increases in Oxygen and decreases in Carbon dioxide and temperature, with signs of oscillation and stabilisation at new levels. This is not dissimilar to the consequence of a transition in individuality predicted by my simple model. But do such symbioses correspond directly to a transition in

the level of selection? I think so, for two reasons. Firstly, the loss of autonomy at short term fitness cost involved in a symbiosis bears a strong parallel to formation of group structures between relatives of the same species (Maynard-Smith & Szathmary, 1994). Secondly, it has been noted (Axelrod et al. 2004), that the concept of relatedness can be extended from that of a statistical property of the locus in consideration, to a more dynamic measure of social context in which arbitrary relatedness indicator traits coevolve with kin-selected loci. Although traditionally regarded as a mutualism, recent modelling of bipartite and tripartite (fungus, cyanobacteria and alga) lichen symbioses implies that cyanobacterial growth may be actively limited by fungi where non-zero metabolic cost results from the cephalodia in which they are contained, and that the phenotypic plasticity of lichens is consistent with a controlled form of (fungal) parasitism (Hyvarinen et al, 2002). It is important to note that, despite the fact that neither partner was capable of autonomous colonisation of the land surface, the appropriate comparison in terms of altruism is not between the symbiosis and free-living component species, but between parasitic and mutualistic symbiotic genotypes. The latter are selected in fluctuating, unpredictable environments, because their capacity for physiological homeostasis is greater. It is not correct to regard the symbiosis as having higher fitness than autonomous species, but it is correct (in some environments) to regard mutualism as a preferable survival strategy to parasitism.

Were lichens really present on the Neoproterozoic land surface?

Retallack (1994) has argued that marine and intertidal lichens and unlichenized fungi may have comprised a significant part of the Ediacaran macrobiota dating from 630 – 542Ma. The compaction properties of some specimens (in comparison to younger vascular plant specimens in equivalent media) suggests that their structural strength exceeded that of soft-bodied forms (equivalent to modern jellyfish or worms), and may have been as great as that of modern tree trunks. The raised compressions the specimens exerted on the substrate imply that this implicit structural strength is not artefactual, because strength derived from sand or other material that became incorporated into the specimen would manifest as molds or casts, rather than the raised compressions observed. The body size of many Ediacara is significantly greater than most early metazoa, and leaflike forms and tubular meshworks of cells make some specimens completely inconsistent with other examples of animals, and entirely consistent with lichens (Retallack, 1994). Chitin fibrils present in some contemporary fungi would provide appropriate resistance to compaction, and lichens today display an appropriate range of morphological diversity (Herrera et al, 1992, Retallack, 1994). Nevertheless, the assemblage referred to in this study dates from 560Ma (Retallack, 1994), well before the hypothesized lichens of the early Neoproterozoic (Lenton & Watson, 2004), and fungi or a stem group to the metazoa remain reasonable possible identities for the Ediacara. There is evidence for progressively increasing, silicate-specific, terrestrial weathering fluxes throughout the Neoproterozoic (Sheilds, 2007). This

pattern may be explained by changes in weatherability (Godderis et al, 2003), but it is at least consistent with a terrestrial biosphere that biases weathering activity towards silicates, therefore to the presence of lichens by extrapolation from the present day ecology (Schwartzman, 1999). Overall however, the evidence for terrestrial lichens during the Neoproterozoic is, as yet, circumstantial, the oldest unequivocal terrestrial fossil lichens not appearing until 400Ma (Taylor et al, 1995). It is therefore important to note that their geochemical implications remain, for the moment, strictly confined to the realm of theory.

Positive feedback between genotype frequency and abiotic states

In a more general sense, I argue that it is plausible that fluctuating abiotic conditions can reinforce, and be reinforced by, the biological traits that give rise to them. The process hypothesized here between physical variables and biological genotypes is loosely analogous to that involved in kin-selected altruism between relatives, in that an otherwise maladaptive trait can increase in frequency as a result of a positive feedback process to which it itself contributes. In this instance the ratio between the contribution made by a genotype to abiotic fluctuation, and the demographic benefit the genotype incurs as a result of this fluctuation, could be considered loosely analogous to kin-relatedness between the two processes - in that it expresses the probability that a sub-optimal trait, G , and a change in the fitness landscape (here, in the variable V) that this trait is able to induce, will successfully co-evolve. If I now relate this ratio to the ratio between the fitness benefit the post-transition “group” obtains by altering the environment and the cost of the environment-altering trait, (as described by (2.4)):

$$\alpha \cdot |V - V_{opt}| : C > \frac{1}{\frac{|V_{biotic} - V_{opt}|}{|V_{biotic} - V_{opt}| + |V_{abiotic} - V_{opt}|} : \frac{G}{G+P}} \quad (2.18)$$

Where $V_{abiotic}$ denotes the variable V uninfluenced by the activity of the group genotype (i.e. as described in (2.11)), and V_{biotic} the variable under circumstances in which the altruist trait group accentuates the abiotic variability (as in (2.12)). This condition bears qualitative similarities to Hamilton’s rule, $k > \frac{1}{r}$ (Hamilton, 1964), where k is ratio of gain to the recipient of altruism to loss to the altruist, and r is the relatedness between the recipient of the altruism and the altruist, and is arguably therefore an example of the same qualitative class of dynamics $\alpha \cdot |V - V_{opt}| : C > \frac{1}{\frac{|V_{biotic} - V_{opt}|}{|V_{biotic} - V_{opt}| + |V_{abiotic} - V_{opt}|} : \frac{G}{G+P}} \in \frac{b}{C} > \frac{1}{r}$. In this instance the post-transition group corresponds to a more energetic system (that is, a higher level of entropy production (e.g. Kleidon & Lorenz, 2004)), in which the physical variation increases the relative fitness of the entity able to induce it. A transition between levels of selection is likely to cause the above condition to be realised, because (I think) it involves a dramatic increase in physiological robustness. If this robustness is sufficient for $\alpha \cdot |V - V_{opt}| > C$, the group will increase in frequency. If it reaches a frequency at which it can amplify environmental variation, positive feedback between this variation and

the group's frequency will help purge the group of "cheats", and as a result further increase group viability. Due to its self-sustaining nature, a positive feedback process of this sort may be a powerful way for the group to persist despite the inherent parasitic tendencies of the individuals of which it is composed.

Chapter 3: A biological trigger for snowball Earth?

Summary

The ice albedo instability can usefully be discretized with respect to its interaction with the Carbon cycle, because it operates over a much shorter timescale and because even slushball solutions require a discontinuity in planetary ice cover relative to temperature. A global scale glaciation, triggered solely by biotic enhancement of silicate weathering, requires either an instability threshold at relatively mild temperatures ($\sim 10^\circ C$) and/or the Proterozoic biosphere causing a degree of weathering enhancement equivalent to or greater than the contemporary biosphere. The latter possibility is more plausible than has previously been assumed - given $Sr^{87/86}$ data implying increasing terrestrial runoff with localised, silicate-specific, weathering surges, and lichen/microbial enhancement of soil pCO_2 . Furthermore, an appreciation of the fraction of silicate weathering regimes that are kinetically (rather than substrate-supply) limited in the contemporary biosphere is necessary before a relation between terrestrial biomass and weathering enhancement can be made - there is no reason to suppose low Neoproterozoic terrestrial biomass necessarily implies correspondingly low weathering enhancement, particularly if there was an abundance of more readily eroded terrains. The temperature dependency of silicate weathering results in an increasing amount of thermodynamic work being required of the biosphere to induce a given CO_2 reduction at decreasing temperatures. But the evolutionary incentive to perform such work may increase if nutrient availability becomes erratic. The extremely large weathering enhancement required probably implies that either an increase in uplift or a hiatus in degassing rate, not a biological trigger, ultimately caused the Neoproterozoic glaciations. CO_2 drawdown was probably accentuated by lichen/bacterial enhancement of silicate weathering rate - perhaps sufficiently to tip planetary energy balance past the ice albedo discontinuity, and convert a cold, partial ice cover state to jump to a true equilibrium high ice cover state. The phrase biological “amplifier” is therefore suggested as more meaningful than “trigger” with respect to snowball Earth. The relation derived here between a discretized albedo/temperature instability and Schwartzman’s biotic weathering enhancement factor may be of use in constraining key parameters empirically.

Introduction

The chemical composition of the oceans is, on average, well-suited to the nutrient stoichiometry required by the marine biosphere (Redfield, 1958). This is in stark contrast with the relatively poor baseline nutrient availability in uncolonised, desiccated terrestrial rock surfaces. The terrestrial biosphere therefore needs to invest more energy in extracting

nutrients from their environment. A key part of this process is the weathering of rocks (which may actually turn out to be necessary for the PO_4 influx required to maintain the marine Redfield ratio (Lenton & Klausmeier, 2006)). The occurrence of biotic enhancement of silicate mineral weathering during the Neoproterozoic, possibly in conjunction with enhanced marine organic Carbon burial due to P export to the oceans, was proposed to have triggered the apparent global-scale glaciations (Lenton & Watson, 2004). The relevance of CO_2 drawdown via marine production has been elaborated upon and reinterpreted in terms of a slushball scenario, involving CO_2 fluxes derived from remineralisation of marine organic matter (Peltier, 2007). But this scenario neglected the role of terrestrial silicate weathering of any tangible magnitude (Peltier et al, 2007, supp mat.). The role of biological enhancement of silicate weathering in atmospheric CO_2 dynamics has been examined in some detail (Bernier et al, 1983, Volk, 1987, Schwartzman, 1999) but has not been explicitly related to the snowball Earth problem. Too many empirical uncertainties remain in terms of the present day biological enhancement of silicate weathering rate for conclusive falsification of the biological trigger hypothesis to be possible. However, some progress can be made by constraining the relationships between global-scale snowball Earth glaciation and the influence of land life on the Carbon cycle. This chapter is a sensitivity analysis to the key parameters in Lenton & Watson's hypothesis, and an attempt to quantify the relationship between them in order to aid their experimental measurement.

Model outline

Existing temperature, weathering and tectonic functions are related to each other in order to examine how sensitive the initiation of a snowball is to key unknowns. The Earth's energy balance is expressed using a planetary albedo that is discretized on either side of the ice albedo discontinuity (see figure 1.1). An atmospheric opacity function derived from the results of a higher resolution global climate model is used to express the impact of the (assumed) dominant greenhouse gases CO_2 , CH_4 , and H_2O . The threshold value of $CO_{2(g)}$ that corresponds to a given glaciation entry temperature is determined simply by solving for the CO_2 . Steady state CO_2 is implicitly assumed to result from the relative rates of terrestrial silicate weathering and tectonic outgassing being in balance, and it is assumed that such a balance would occur on either a biotic or an abiotic Earth (though the actual steady state CO_2 partial pressure on an abiotic planet would be higher). Schwartzman's measure of biotic silicate weathering enhancement, relative to the abiotic rate, is therefore used to determine the weathering enhancement factor corresponding to a given CO_2 /temperature glacial entry threshold. This enhancement factor is related to the present day using global productivity functions from the GEOCARB and COPSE models.

Planetary temperature

The mean radiative temperature of the planet T can be related in a simple way to the solar luminosity S , planetary albedo α , and Stefan boltzman constant σ , by requiring that the electromagnetic radiation emmitted from the Earth's surface balances the radiative influx from the Sun, and the greenhouse effect follows a simple grey-atmosphere approximation:

$$T^4\sigma = \frac{(1 - \alpha)S}{4}\left(1 + \frac{3}{4}\tau\right) \quad (3.1)$$

The factor $\frac{1}{4}$ is the ratio of the area of the disc receiving incoming solar radiation to the sphere emitting it, and planetary albedo α is the ratio of reflected to received radiation at the top of the Earth's atmosphere. The Stefan Boltzman constant σ relates the energy radiated by a surface per unit time to the fourth power of its absolute temperature (e.g. Green, 2002). The Earth's temperature differs from that expected of a blackbody radiator (one which absorbs without reflection all incident electromagnetic radiation) of the same size, as a function of the greenhouse effect. Greenhouse warming results from the absorbtion and subsequent re-emission, by atmospheric gases, of infra-red radiation emitted by the Earth's surface. Atmospheric re-emission occurs in all directions, causing some energy to return to the planet's surface. This gives rise to a net warming effect that is a function of the atmosphere's optical depth τ (without specification to wavelength - referred to as the "grey atmosphere approximation") (Chamberlain, 1980, McKay & Lorenz, 1999, Lenton, 2000). The factor $3/4$ in front of optical depth τ results from approximating the infra red radiation flux by the first two terms $P_0 + P_1 = 1 + x$ of a legendre polynomial expansion $P_n(x) = \sum_{r=0}^{r=m} (-1)^r \frac{(2n-2r)!x^{n-2r}}{2^n r!(n-r)!(n-2r)!}$ (where m is the integer part of $n/2$, e.g. King et al, 2003), then integrating over the upward and downward limits of the atmospheric infra red flux, whilst assuming that at the top of the atmosphere the optical depth $\tau = 0$ (i.e. all of the radiation is in the visible (Chamberlain, 1980)). The solar luminosity flux received from the sun S is measured in units of Watts per square metre. Variation in solar luminosity flux over time can be related to the present day value $S_0 = 1368Wm^{-2}$ by time t billion years before present and $t_0 = 4.6$ billion years being the age of the Earth, using the formula of Gough (Gough, 1981, Kasting, 2005):

$$S_{(t)} = \frac{S_0}{1 + 0.4(t/t_0)} \quad (3.2)$$

With $S_{(t)}$ the solar luminosity experienced at time t billion years before present.

Discretized ice albedo instability

Once a discontinuity has been reached in the impact of surface ice cover on planetary energy balance, models suggest that equilibrium is reached within a timescale of the order of years (Hall, 2004). Pierrehumbert (2005) found that a maximum of 20 years was suf-

ficient for surface ice cover and planetary energy balance to come into equilibrium with an imposed dramatic reduction in greenhouse forcing (Pierrehumbert, 2005). Conversely, the highest useful temporal resolution relevant to the Urey reaction and the dynamics of atmospheric CO_2 over geologic timescales is of the order of thousands of years (Walker et al, 1981, Berner et al, 1983, 1994). Therefore, changes in planetary albedo due to the dynamics of the ice albedo feedback (which operates over the short timescale $t_{(IAF)}$) can be assumed instantaneous with respect to the dynamics of the Carbon cycle (which operate over the much longer timescale $t_{(CO_2)}$, $t_{(CO_2)} \gg t_{(IAF)}$). The albedo experienced by the temperature changes relevant to the Carbon cycle, $\alpha_{(t_{CO_2})}$ is therefore a discrete value that is the net consequence of more short term changes, as stated by equation (3.3):

$$\alpha_{(t_{CO_2})} = \int \frac{\partial \alpha}{\partial t_{(IAF)}} \partial t_{(CO_2)} \tag{3.3}$$

The existence of an ice albedo discontinuity is suggested simply by the facts that an ice-covered surface reflects more incident electromagnetic radiation and that lower temperatures give rise to increasing ice cover. A runaway feedback occurs in any cybernetic (dynamically-controlled) system when the product of the interacting differential coefficients exceeds one (Riggs, 1976) - so the occurrence of a runaway global glaciation requires $\frac{\partial T}{\partial ice} \frac{\partial ice}{\partial \alpha} \frac{\partial \alpha}{\partial T} > 1$. Whether or not this is plausible in the real Earth system and, more particularly, the temperature and ice-cover combination that this circumstance corresponds to and whether it incorporates open ocean water, remains a contentious issue. The plausibility of such a slushball solution is likely influenced strongly by latitudinal heat diffusion, cloudiness and ocean-driven heat transport (Ikeda & Tajika, 1999, Poulsen, 2001, Donnadieu et al, 2004, Bendtsen & Bjerrum, 2002, Pierrehumbert, 2005, Lewis et al, 2007). But even a slushball scenario requires a discontinuity in the ice albedo system and a progression to a quasi-equilibrium high ice cover state. The snowball-slushball debate is therefore about the temperature severity and radiative transfer properties of the high ice cover state, rather than its existence. The stability of such a quasi equilibrium steady state is an unresolved debate beyond the scope of this work. For example, the apparent susceptibility of thin sea ice solutions to progressive thickening and an eventual hard snowball scenario (Lewis et al, 2007), suggests that thin ice as a compromise to the snowball-slushball debate (Pollard & Kasting, 2005) may not be reasonable - taking the argument back to the basis of the ice-albedo discontinuity. Here I simply discretize the planetary albedo to its value either side of the unstable temperature region. The initiation of a runaway ice albedo feedback occurs when planetary temperature T drops below a lower threshold ice free value T_f , i.e. $T \leq T_f$. At this point, planetary albedo instantaneously jumps from its ice free value $\alpha = \alpha_f = 0.3$ to the higher value corresponding to the ice-covered state $\alpha = \alpha_i = 0.7$ (values from (Caldeira & Kasting, 1992, Pierrehumbert, 2005), equation (3.4)). This causes

a dramatic change in planetary energy balance, giving rise to extremely cold temperatures. As is integral to the snowball Earth problem (Kirshvink, 1992), exit from the ice covered state (equation (3.5)) requires an external (greenhouse) forcing sufficient to raise planetary temperature above a threshold upper limit for the ice covered state, $T \geq T_i$. If planetary temperature is greater than the ice free threshold $T > T_f$ or less than the ice covered threshold $T < T_i$, the albedo remains in its current state (equation (3.6)). The idea that planetary albedo jumps between one of two possible values when temperature enters an unstable interval $T_i < T < T_f$ is an example of hysteresis (dependence of system dynamics on the previous state), involving a “non-linearity with memory” in the language of control theory (Riggs, 1976). This sort of simplification may therefore be of general applicability in simplifying the interaction between Earth system variables that adjust over different timescales. Equations (3.4)-(3.6) describe how, if temperature enters the unstable region $T_i < T < T_f$, the planetary albedo α jumps to its alternative value:

$$\frac{\partial \alpha}{\partial t_{(CO_2)}} (T_i < T < T_f), \frac{dT}{dt} < 0 = \alpha_i - \alpha_f \tag{3.4}$$

$$\frac{\partial \alpha}{\partial t_{(CO_2)}} (T_i < T < T_f), \frac{dT}{dt} > 0 = -\alpha_i + \alpha_f \tag{3.5}$$

$$\frac{\partial \alpha}{\partial t_{(CO_2)}} (T > T_f), (T < T_i) = 0 \tag{3.6}$$

Grey atmosphere greenhouse approximation

The optical depth of the atmosphere is assumed to be the result of additive interaction between the opacity contribution of greenhouse gases water $H_2O_{(g)}$, Carbon dioxide $CO_{2(g)}$ and methane $CH_{4(g)}$, $\tau = \tau(H_2O) + \tau(CO_2) + \tau(CH_4)$. The optical depth function τ is derived from a linear regression on various results of a radiative convective climate model (Kasting et al, 1993, Lenton, 2000). The assumptions of additive interaction between the optical depth contribution of different gases and of non-wavelength specificity in opacity to radiation might quantitatively alter the results of a high resolution modelling study examining the snowball slushball debate, but are unlikely to alter the qualitative conclusions I wish to draw here concerning the interaction between the ice albedo feedback and the Carbon cycle. The optical depth due to atmospheric $CO_{2(g)}$ is a function of its mixing ratio, $CO_2(\text{atmospheres})$, with sensitivity constant and exponent derived from CO_2 perturbation at constant temperature and water vapour (Lenton, 2000):

$$\tau(CO_2) = 1.73(CO_2)^{0.263} \tag{3.6}$$

The infra-red optical depth due to water is a function of its vapour pressure, which is in turn related to relative humidity and temperature by the Clausius Clapeyron equation (e.g. Saltzman, 2002). The relation between vapour pressure and infra red opacity is derived from a perturbing a radiative convective model with varying solar luminosity whilst holding CO_2 , CH_4 and temperature constant, giving (Lenton, 2000):

$$\tau(H_2O) = 0.0126(H(P_0e^{-(L/RT)}))^{0.503} \tag{3.7}$$

With relative humidity $H = 0.62$ (lower than the surface average of $H = 0.77$, but more representative of the atmosphere as a whole, particularly at declining temperatures (Lenton, 2000)), water vapour saturation constant $P_0 = 1.4 \cdot 10^{11} \text{Pa}$ (Nakajima et al, 1992), latent heat energy absorbed per mole of water upon transition from the liquid to vapour $L = 43655 \text{Jmol}^{-1}$, molar gas energy-temperature relation constant $R = 8.314 \text{Jmol}^{-1} \text{K}^{-1}$, and temperature $T^\circ \text{K}$. This function is a useful approximation to the perturbation results within the temperature range of glacial initiation $0 - 40^\circ \text{C}$ (Kasting et al, 1993, Lenton, 2000). Infra red optical depth due to variation in the mixing ratio of methane CH_4 was derived from an equivalent model perturbation in which CO_2 and H_2O were held constant, then performing a linear regression on the results of variable solar luminosity, in order to achieve the function appropriate for modern (habitable) temperature (Lenton, 2000).

$$\tau(CH_4) = 2.404(CH_4)^{0.326} \tag{3.8}$$

Sensitivity analysis

The role of biological weathering will be related to an unstable temperature/albedo region at a parameterised threshold temperature for glacial initiation, T_f . Recall that when temperature falls below this threshold $T \leq T_f$, the albedo jumps to the ice covered value $\alpha \rightarrow \alpha_i$ and the qualitative change in energy balance causes (I assume) a runaway glaciation to an equilibrium, high ice-cover state. For steady state luminosity and non- CO_2 greenhouse forcing, this transition point $T = T_f$ corresponds to a unique low CO_2 value, required to trigger global scale glaciation, $(CO_2)_{tr}$. It is useful to relabel this greenhouse forcing in terms of the rest of the temperature function at the transition point. Inserting the threshold temperature $T = T_f$ and albedo $\alpha = \alpha_f$ into equation (3.1) and substituting in equations (3.6-3.8) for $\tau = \tau(H_2O)_f + \tau((CO_2)_{tr}) + \tau(CH_4)_f$, where the non- CO_2 optical depth contributions of water $\tau(H_2O) = \tau(H_2O)_f$ and methane $\tau(CH_4) = \tau(CH_4)_f$ are equal to their (assumed unique) values at the transition point, I use equation (3.6) to solve

for $(CO_2)_{tr}$:

$$(CO_2)_{tr} = \left(\frac{1}{1.73} \left(\frac{16T_f^4 \sigma}{3(1 - \alpha_f)S} - \frac{4}{3} - \tau(H_2O)_f - \tau(CH_4)_f \right) \right)^{\frac{1}{0.263}} \quad (3.9)$$

Figures (3.1) and (3.2) show the results from this zero dimensional system of varying solar luminosity (X-axis in figure (3.1) units of Watts per square metre (Wm^{-2})) over the range it is predicted by Gough's formula (equation (3.2)) to have taken over the last 100 million years (Myrs), on the CO_2 value corresponding to the bifurcation point when it is assumed to occur at various values $0^\circ C \leq T_f \leq 14^\circ C$. In each case, the temperature threshold T_f was parameterised at a fixed value at the start of the model run, water and methane optical depth were dictated respectively by equations (3.7) and (3.8), with methane initially held at its pre-industrial value of $CH_4 \sim 650$ parts per billion (ppb), and relative humidity held at its initial value $H = 0.62$. Luminosity was varied over $0.5Wm^{-2}$ increments, and equation (3.9) was used to solve for $(CO_2)_{tr}$. This (admittedly crude) approximation suggests that global scale glaciation is relatively easy to initiate at Proterozoic luminosity, but it should be remembered that the fainter Sun would have given rise to a baseline CO_2 value significantly higher than the present day (Walker et al, 1981), meaning that, when the time dimension is brought into the problem of initiating a snowball Earth, a large CO_2 drawdown ~ 1320 ppm is needed (Donnadieu et al, 2004). However, setting up this condition in the system used here requires knowledge of the biological weathering enhancement factor that I am attempting to estimate. The work discussed here therefore focuses on a steady state comparison with the present, the quantitative details of which are likely to be subject to future revision.

Solar luminosity

Figures (3.1) and (3.2) show the effect of variation in solar luminosity flux S on the CO_2 partial pressure corresponding to the bifurcation point, $(CO_2)_{tr}$, at different threshold temperatures T_f . As might be expected intuitively, increases in the solar luminosity flux caused susceptibility to global scale glaciation to decrease steadily over Precambrian time. The greenhouse effect necessary to reproduce a given temperature increases further back in time - because the temperature dependency of silicate weathering causes the Urey reaction to adjust to a higher CO_2 steady state (Walker et al, 1981). The highest values for the temperature threshold $T_f = 14^\circ C$, $T_f = 12^\circ C$ and $T_f = 10^\circ C$ produce glaciation at partial pressures as high as 500 to 1000 parts per million CO_2 within the 600–800Ma time interval of interest, suggesting it is relatively easy to send the system into a global ice-covered state. The threshold temperatures $T_f = 0 - 6^\circ C$ require a substantial CO_2 drawdown to at or below its recorded pre-industrial value. Tajika (1999) discussed the effect of the lower Neoproterozoic solar luminosity flux on the susceptibility to global glaciation - arguing

that the lower Neoproterozoic solar flux would likely be offset by higher CO_2 , because it would cause a lower baseline silicate weathering rate, via the temperature dependencies of the reaction (Tajika, 1999). Further, the gradual changes in temperature expected from estimates of changes in solar flux are inconsistent with the 1000–1,000,000 year timescales of climate transit that are implicit in the Neoproterozoic geological data (Tajika, 1999). The temperature function used here supports both these conclusions. The lower value of the solar luminosity flux during the Neoproterozoic (and probably to a greater extent in the Paleoproterozoic (Kopp et al, 2005)) increases susceptibility to runaway glaciation, and under some parameter choices may be a prerequisite, but is insufficient as a cause in its own right due to homeostasis in the Urey reaction (Walker et al, 1981), and because the expected changes would be too gradual.

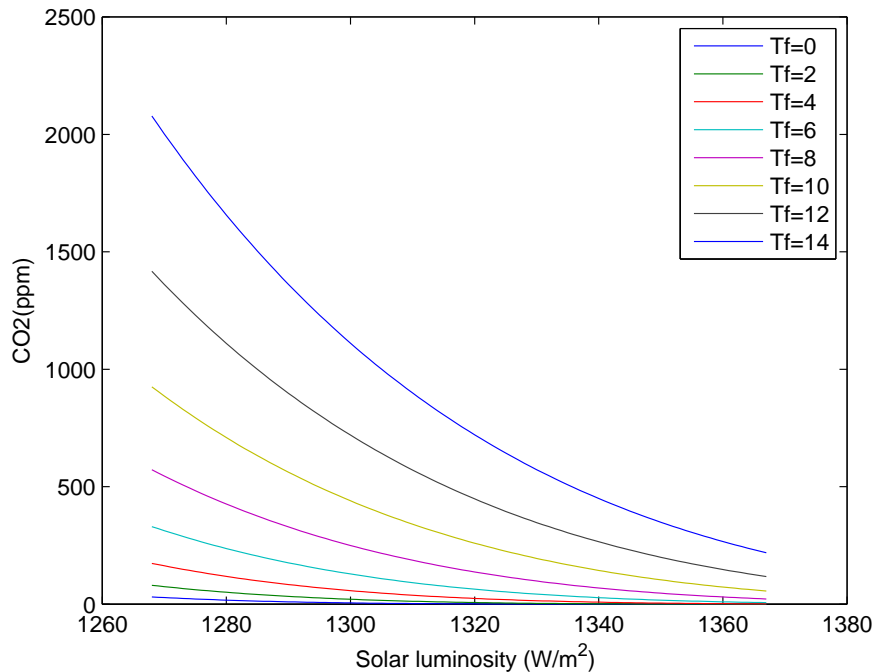


Figure 3.1 - The Solar luminosity fluxes (X-axis, units of Wm^{-2}) and CO_2 partial pressures (Y-axis, parts per million) corresponding to the switch point to global glaciation, at variable temperature thresholds T_f values of this switch point. Values shown are for ice free albedo $\alpha_f = 0.2289$, required for steady state $T = 15$ celsius for preindustrial $CO_2 = 280$ ppm.

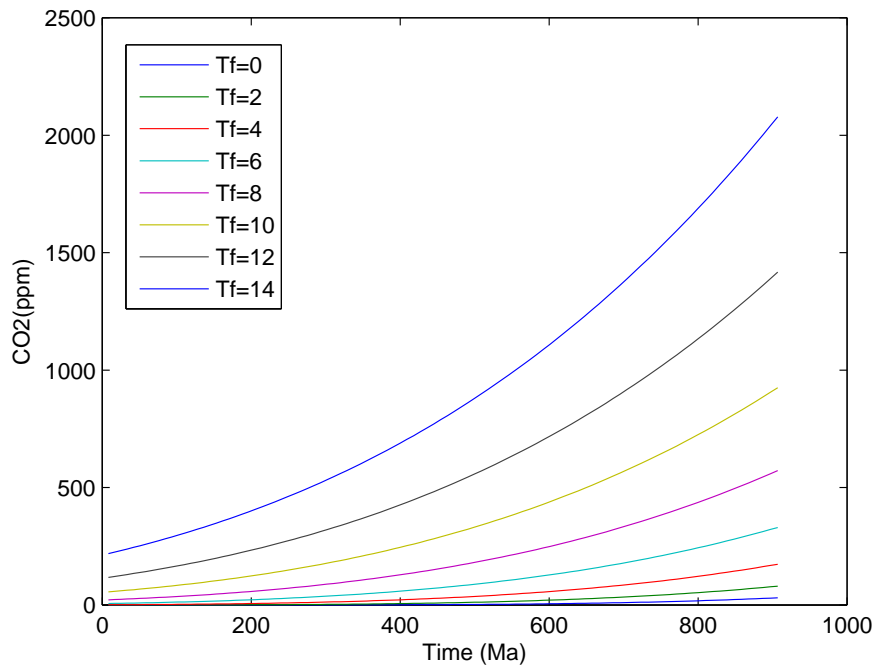


Figure 3.2 - The same results shown in figure 3.1 but with a comparison between CO_2 partial pressures (Y-axis, parts per million) and the time before present (X-axis, Ma) corresponding to the Solar luminosity fluxes shown. Recall the proposed timing of the Sturtian ($\sim 740 - 647$ Ma), Marinoan ($\sim 660 - 635$ Ma) and Gaskiers ~ 580 glaciation intervals (Fairchild, 2007).

Atmospheric methane

Figure 3.3 illustrates the $(CO_2)_{tr}$ (Y-axis, parts per million) and methane CH_4 (X-axis, parts per million) value combinations that are possible at various glacial initiation temperatures (In the figure legend in degrees celsius) when luminosity is fixed at the magnitude corresponding to 600Ma (by equation 3.2). The figure indicates that methane partial pressures much higher than the (assumed, e.g. Kasting (2005)) pre industrial partial pressure of around 0.65parts per million, are sufficient to prevent global scale glaciation, regardless of the magnitude of CO_2 drawdown or temperature susceptibility. Below this level, increasing CH_4 causes a roughly log-linear relationship between the CO_2 -drawdown factor required for the bifurcation temperature T_f to be reached. Methane’s greenhouse effect has been presented as a partial alternative to high CO_2 solutions for the “faint young sun” problem (Kasting, 2005). Relatively low growth of methanotrophic bacteria due to ocean anoxia and low SO_4^{2-} , and increased methanogenic degradation of marine organic matter prior to the evolution of fecal pellets, have been proposed to justify relatively high atmospheric CH_4 partial pressures (100 – 400ppm) throughout the Proterozoic, possibly with a significant role in greenhouse warming (Pavlov et al, 2003). A role for methane in a mechanistic explanation for the Carbon cycle perturbations that accompany late Neoproterozoic glacial deposits (LNGD) has been proposed repeatedly, but the climatic effect and scale of change suggested in the methane reservoir has been subject to frequent revision. Methane release from soil permafrost during deglaciation, followed by its anaerobic oxidation in conjunction with bacterial sulphate reduction (discussed in chapter 1), was presented as a mechanism to explain the cap carbonates (Kennedy et al, 2001, Boetius et al, 2000). However, HCO_3^- generation via this process would quickly become SO_4^{2-} -limited (Hoffman & Schrag, 2002), and the rapid carbonate precipitation proposed is in any case probably negated by the paleomagnetic reversals observed in cap carbonate strata (Fairchild, 2007). Of more direct relevance to the work in this chapter is the idea that destabilisation of a methane greenhouse was a causal factor in the Paleoproterozoic global glaciations (Kopp et al, 2005), and potentially in the final stages prior to a runaway ice albedo feedback during the Neoproterozoic snowball Earth glaciations themselves. Short term methane release by clathrate destabilisation supposedly temporarily raised temperature, giving rise to a silicate weathering surge sufficient to tip the system below T_f (Schrag et al, 2002, Hoffman & Schrag, 2002). This hypothesis may, however, require an unrealistically long (~ 1000 year) atmospheric lifespan for CH_4 (Pavlov et al, 2003). A more parsimonious scenario involves reduced production of the gas after an increase in the marine O_2 concentration at around 750Ma (Pavlov et al, 2003). Computational errors may have led to the magnitude of the greenhouse effect attributable to methane (previously estimated at a maximum of $\sim 12^\circ K$ for a 100ppm increase (Pavlov et al, 2003)) being over-estimated (Haqq-Misra et al, 2007). But the partial pressure and dynamics of atmospheric CH_4 nevertheless scale the required magnitude and possible climatic influence of a biological weathering trigger, as illustrated

in Figure (3.3).

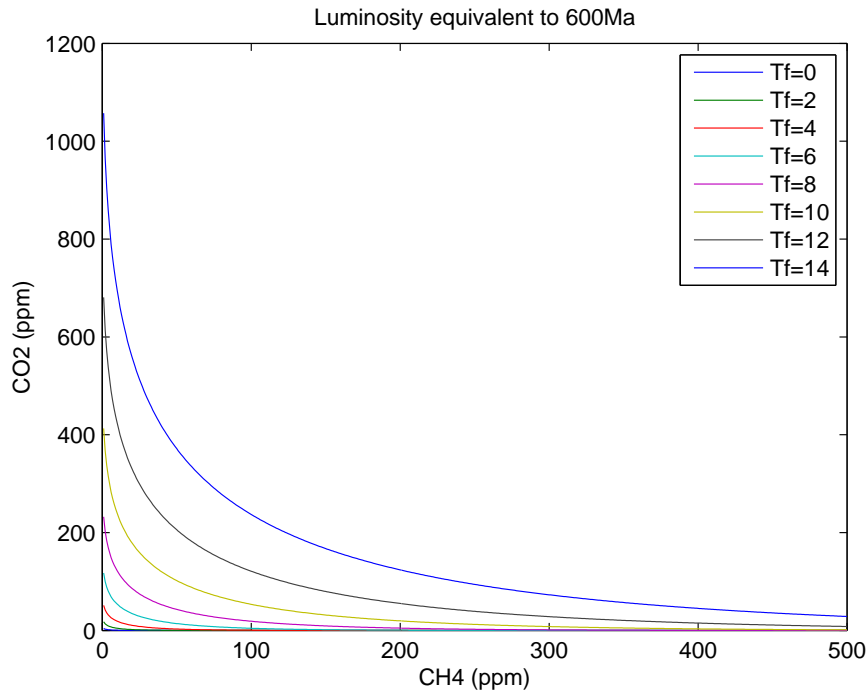


Figure 3.3 - (a) Different methane CH_4 partial pressures (X-axis) over the range of glaciation threshold temperatures T_f (Legend, celsius) at different (fixed) CO_2 partial pressures (Y-axis, parts per million). The amount of CO_2 drawdown required to initiate a global-scale glaciation asymptotes to zero as its effect is compensated for by the greenhouse effect of increasing methane CH_4 . Solar luminosity is equivalent to 600Ma

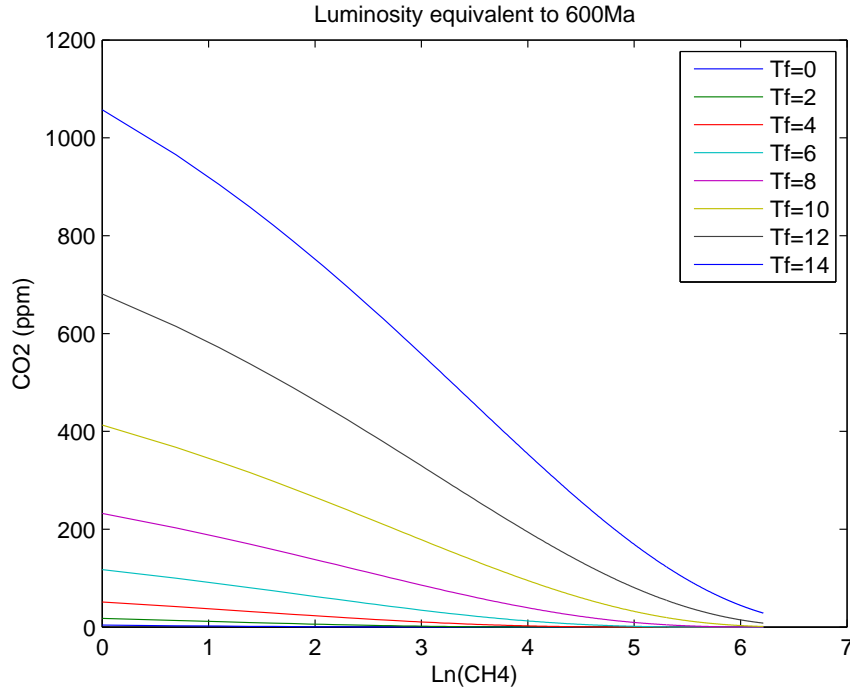


Figure 3.3 (b) - The same solutions as show in figure 3.3 (b), but X-axis now shows natural log of CH_4 partial pressure.

Relative humidity

The shape of the dependence of outgoing longwave radiation (OLR) on temperature encapsulates most fundamental climate phenomena (Pierrehumbert, 2002). Increasing temperatures give rise to increasing atmospheric water vapour, hence less outgoing longwave radiation. Water vapour flattens the curve of outgoing longwave radiation against temperature, in theory giving rise to an asymptotic maximum OLR value at which all the water is in the atmosphere and a runaway greenhouse may occur, as is thought to have been the case for Venus (Kasting, 1988, Pierrehumbert 2002). Hydrology therefore dominates all aspects of the snowball Earth problem. Figure (3.4) shows the impact on the CO_2 partial pressure/bifurcation temperature combinations at the initiation point T_f , of an extreme range of relative humidity changes (X-axis). Although the water optical depth function used here was not specifically designed to cope with such a range, alternative formulations are unlikely to alter the qualitative conclusion that a much greater CO_2 drawdown factor is required to cause a snowball Earth if high atmospheric humidity persists right up to the initiation temperature. It is more difficult to induce the climate to enter the globally ice-covered state when relative humidity remains at its present value right up until the bifurcation point, due to the strong greenhouse effect of water. This zero dimensional treatment underplays the significance of atmospheric hydrology in the snowball Earth problem. Changes in humidity are likely to be the main driver of the pole-equator heat gradient,

as well as changes in cloud cover, therefore of the stability of ice formation at different latitudes, therefore of the temperature of the bifurcation point T_f itself - for an isothermal planet, $T_f = T_i = 0^\circ C$ (Pierrehumbert, 2002). Of more direct relevance to Lenton & Watson's biological trigger hypothesis is the contrast between mineral supply-limited, and chemical kinetic-limited, silicate weathering (West et al, 2005). Only the higher weathering rates of the latter, kinetic-limited regimes may be subject to the CO_2 negative feedback of Walker et al, (1981). A crucial aspect of biotic weathering enhancement may be drawing significant quantities of water into the weathering interface by, for example, localised ice nucleation, as has been observed in lichens (Kieft, 1988). The baseline silicate weathering rate is dependent on temperature primarily through the impact of temperature on precipitation - and when surficial evaporation exceeds local absorbed solar radiation, the silicate weathering thermostat can break down entirely, because increased temperature fails to yield (equivalently) increased weathering rate (Pierrehumbert, 2002). Water vapour dynamics are therefore the most important unknown in all deep time paleoclimate problems (Pierrehumbert, 2002) - and the relevance of the conclusions drawn here may be subject to future revision based on knowledge of how water vapour behaves in a snowball Earth.

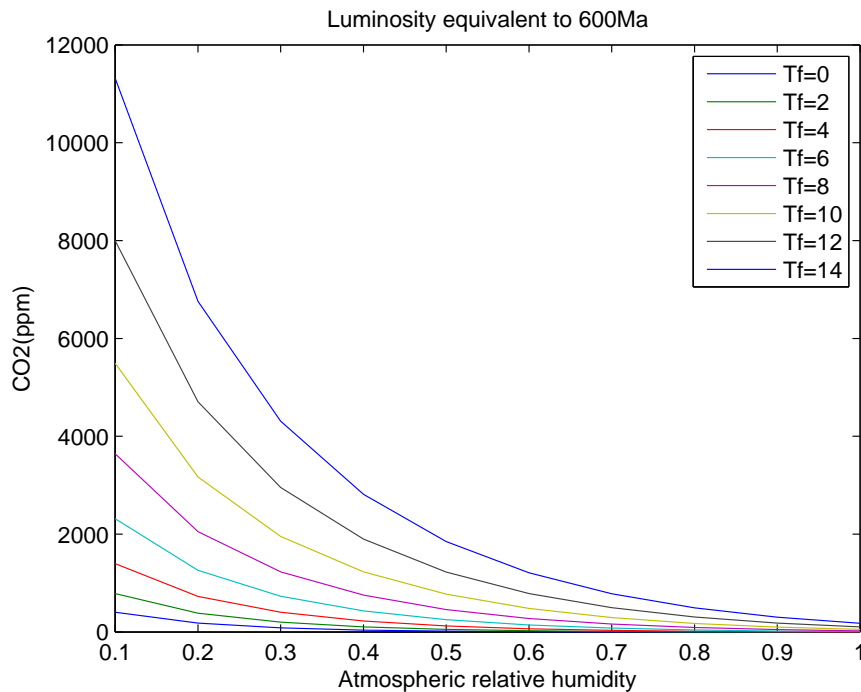


Figure 3.4 - The impact of atmospheric relative humidity (X-axis) on the CO_2 partial pressure (Y-axis), corresponding to the bifurcation point, when it occurs at different temperatures (Legend, celsius). Solar luminosity was held constant at $S = 1300.16 W m^{-2}$, equivalent to 600Ma. The values shown should be compared with the interval permissive for glaciation $0 < H < 0.45$ (Pierrehumbert, 2002) in the results of global climate models with conservative estimates of outgoing longwave radiation due to other greenhouse gases, and atmospheric (cloud) albedo.

Biotic enhancement of silicate weathering

Organisms within the terrestrial biosphere differ from their marine counterparts in that the macronutrient composition of the abiotic surroundings does not bear a close correspondence to their physiological requirements, in contrast to the situation in the oceans (Redfield, 1958, Arrigo, 2005). Life on land therefore must do significant thermodynamic work in order to extract the nutrients (particularly PO_4 and metal cations) they require from rocks - the runoff flux from which may actually turn out to be necessary for keeping the marine stoichiometry close to its biotic optimum (Lenton & Klausmeier, 2006). There is consensus that the biosphere invests energy in enhancing rock weathering rate. Bacteria selectively colonise P -rich parts of silicate rocks (Rogers et al, 1998), including the “endolith” zone up to 3.0mm inside limestone substrates (Ferris & Lowson, 1998) and probably have a direct influence of the chemical composition of runoff from dark, low-productivity subglacial environments (Skidmore et al, 2005). Microbial colonisation of silicate rocks may, as a rule, mirror the microbes’ nutritional requirements, with even erosion-resistant P -rich minerals being weathered more rapidly than less resistant P -poor substrates in situations in which the nutrient is scarce (Bennett et al, 2001). Runoff fluxes of Ca and Mg increase with increasing vegetation (Gislason et al, 1996). Fungi and lichens are thought to particularly enhance runoff from silicate minerals (Jackson & Keller, 1970, Chen et al, 2000, Kappen, 2000) primarily by secreting organic acids that dissolve P -rich rock components (Landeweert et al, 2001). Additionally, production of osmolytes and ice formation nuclei cause the water potential of soil and rock substrate microenvironments to fluctuate (Kieft, 1988, Zachariassen & Kristiansen, 2000), probably contributing to an increase in reactive mineral surface area (Schwartzman, 1999). Notwithstanding the extensive empirical evidence for biological weathering enhancement, the factor by which weathering is elevated above the abiotic rate at the present day (E_0) remains uncertain (Schwartzman, 1999). Recall the (calcium and/or magnesium) silicate weathering reactions discussed in chapter 1 (Ca/Mg) $SiO_{3(s)} + H_2O_{(l)} + 2CO_2 \rightleftharpoons 2HCO_3^- + (Mg/Ca)_{(aq)}^{2+} + SiO_{2(aq)}$ (with Ca/Mg denoting either cation). The bicarbonate $HCO_3^-_{(aq)}$ anions derived from these reactions reach the ocean through water table runoff from terrestrial weathering. There they form precipitates of carbonates (predominantly calcite $CaCO_{3(s)}$), i.e. $2HCO_3^- + Ca_{(aq)}^{2+} \rightleftharpoons CaCO_{3(s)} + H_2O_{(l)} + CO_{2(aq)}$ (e.g. Ridgwell & Kennedy, 2004). If a given fraction of the $CaCO_{3(s)}$ so-formed escapes remineralisation and is buried - hence is isolated from the atmosphere-ocean system until its subsequent return via degassing, then the net consequence is a withdrawal of 1mol of CO_2 , collectively referred to as the Urey reaction (Walker et al, 1981) $(Ca/Mg)SiO_{3(s)} + 2CO_{2(g)} \rightleftharpoons (Ca/Mg)CO_{3(s)} + SiO_{2(aq)} + CO_{2(aq)}$. The biotic silicate weathering enhancement factor, E , is defined as the relative increase in the global rate of the Urey reaction observed on the real Earth, above the rate that would be expected if the planet were abiotic, i.e. a value of $E = 1$ corresponds to zero biotic weathering enhancement and the reaction rate being equal to a planet Earth without life

(Schwartzman, 1999). Changing HCO_3^- concentrations between vegetated and barren basalt produce variable results for the present day enhancement factor E_0 , from $E_0 \simeq 3$ (Cawley et al, 1969) to $2 < E_0 < 5$ (Moulton & Berner, 1998), to $E_0 \simeq 10$ (Gislason et al, 1996), up to as high as $10 < E_0 < 100$ (Cochran & Schwartzman, 1995). An empirical problem is the presence of microbial life on land surfaces previously assumed to be abiotic (Thomson, 1984, Thorseth et al, 1992). But a greater contributor to the uncertainty surrounding the value of the contemporary enhancement factor E_0 is probably extrapolation to the global average Urey reaction rate from a variety of very different local weathering regimes. The Urey reaction weathering thermostat discussed above is only relevant to planetary temperature when atmospheric $CO_{2(g)}$ is of first order impact on the weathering rate - i.e. when the reaction is kinetically limited, rather than (for example) limited by the supply of new material by erosion (West et al, 2005, Sheilds, 2007). Many contemporary weathering regimes may be rate-limited by mineral supply, which in practice may amount to limitation by the fraction of the time the rock experiences continuous contact with water (Schwartzman, 1999, Sheilds, 2007). Hence, regardless of the activity of the terrestrial biosphere in enhancing substrate pH , CO_2 or local reactive surface area, if the baseline rate of uplift and/or precipitation rate is so low that weathering is supply limited, not kinetically limited, then neither weathering nor its biotic enhancement is of relevance to the Urey reaction or to atmospheric CO_2 . Future empirical measurements of global biotic enhancement E will likely focus more specifically on the Urey reaction, and in so doing will reduce uncertainty by comparing separate, kinetically-limited weathering regimes. This issue is discussed further in the concluding section.

Chemical weathering of Ca and Mg silicates can be expressed in terms of an Arrhenius relationship (describing the effect of temperature changes on the reaction rate constant) with planetary temperature. If the reaction proceeds at rate R_0 when temperature is T_0 , and at rate R when temperature is T , then the effect of temperature on the relative reaction rate is (Walker et al, 1981, Schwartzman, 1999):

$$\frac{R}{R_0} \propto e^{\frac{E}{R^*} \frac{(T-T_0)}{TT_0}} \tag{3.10}$$

Where $E \simeq 50kJmol^{-1}$ is the activation energy for the weathering reaction (Walker et al, 1981) and $R^* = 0.008314kJmol^{-1}$ is the gas constant (e.g. Marshall et al, 1988). (Note temperature-dependent weathering rates R and R_0 are not the same as the gas constant R^* expressing energy change per mole). The temperature dependency in relation (3.10) is simplified in terms of a single parameter $b = \frac{E}{R^*} \frac{1}{TT_0}$ relating weathering rate to temperature deviation $\Delta T = T - T_0$. Using $T_0 = 385^\circ K$ and $T = 288^\circ K$, I get $b = 0.0542$ (used below). To the kinetic temperature dependency must be added a relationship between weathering rate and runoff from precipitation, which is itself assumed to scale with temperature deviation $\Delta T = T - T_0$ from a standard in the same way as the Arrhenius

dependence (Manabe & Stouffer, 1980, Manabe & Wetherald, 1980, Walker et al, 1981, Berner, 1994, Schwartzman, 1999):

$$\frac{R}{R_0} \propto e^{c(T-T_0)} \quad (3.11)$$

Where $c = 0.017$ (Walker et al, 1981). Finally, weathering rate depends on the concentration of the reactant CO_2 at the rock substrate, which can be expressed in terms of an exponent of the ratio of CO_2 to a standard value, $CO_{2(0)}$ (Walker et al, 1981, Berner, 1992, Schwartzman, 1999):

$$\frac{R}{R_0} \propto \left(\frac{CO_2}{CO_{2(0)}}\right)^a \quad (3.12)$$

The value of the CO_2 exponent a is subject to a high degree of uncertainty because it must encompass many different types of weathering regimes, and because incorporated within it is a dependence of weathering on pH , which itself scales with CO_2 . The weathering reaction depends on the formation of Carbonic acid, via the equilibrium $H_2O_{(l)} + CO_{2(g)} \rightleftharpoons H_2CO_{3(aq)}$, which has equilibrium constant $K_1 = \frac{H_2CO_3}{CO_2}$, then on the equilibrium $H_2CO_{3(aq)} \rightleftharpoons HCO_{3(aq)}^- + H_{(aq)}^+$, with equilibrium constant $K_2 = \frac{HCO_3^- \cdot H^+}{H_2CO_3}$ (Schwartzman, 1999). In a system in continuous reaction with water that is saturated with CO_2 and continuous with the atmosphere, $HCO_{3(aq)}^- = H_{(aq)}^+$. Therefore, the equilibrium constants can be used to obtain a relationship between rock hydrogen ion concentration $H_{(aq)}^+$ and atmospheric CO_2 , because $H^+ = (K_2 H_2CO_3)^{\frac{1}{2}} = (K_2 K_1 CO_2)^{\frac{1}{2}}$ (Schwartzman, 1999). This is important in terms of silicate weathering rate, because under these conditions, the rate of dissolution has been shown to vary with $(H^+)^n$, with $0 < n \leq 1$ (Sverdrup, 1990, Berner, 1992, Brantley & Chen, 1995, Blum & Stillings, 1995). The likely range for the CO_2 dependency is $0.25 < a < 0.4$ (Walker et al, 1981, Schwartzman, 1999). All of the parameters discussed are subject to high levels of empirical uncertainty, and the act of averaging these key weathering parameters to the planetary level is necessarily slightly arbitrary. But this is not likely to affect the qualitative outcome of this modelling exercise - which is to assess the order of magnitude of the difference between biotic and abiotic silicate weathering regimes on the approach to a snowball glaciation.

Snowball Earth and the biotic Urey reaction enhancement factor E

Schwartzman (1999) noted that the balance (required for steady state CO_2) between tectonic outgassing rate D , and terrestrial silicate weathering rate per unit area, W , and available weatherable land surface area A , (i.e. $D - WA = 0$), must hold regardless of whether the terrestrial biosphere exists or not, hence is of use in quantifying biotic en-

hancement of weathering. In comparing biotic and abiotic scenarios, it is important to make the distinction between sensitivity to perturbation and steady state condition. For example, if incremental change in biotically-impacted parameters has only a mild impact on absolute silicate weathering rate in comparison to equivalent parameter changes on an abiotic planet, this does not necessarily mean that the overall biological weathering enhancement is low. The magnitude of all fluxes would be influenced by that fact that (for example) an abiotic planet Earth would be much hotter. A useful metaphor is a thermostat - the magnitude of biological weathering enhancement is best indicated by how much colder the temperature setting is relative to the abiotic value - rather than how sensitive the thermostat is to incremental changes of the dial (Schwartzman, 1999).

Combining temperature, runoff and CO_2 formulations of the sort discussed above means that the weathering flux per unit time for a biotic planet, W_β , of calcium and magnesium silicates can be parameterised in terms of these variables and scaled by a baseline magnitude $W_{\beta 0}$ (Walker et al, 1981, Schwartzman, 1999):

$$W_\beta = W_{\beta 0} \left(\frac{CO_{2\beta}}{CO_{20}} \right)^a e^{(b+c)(T_\beta - T_0)} \quad (3.13)$$

Where the constants $a = 0.25$, $b = 0.056$, and $c = 0.017$ give respectively the sensitivity to CO_2 , Arrhenius kinetic temperature sensitivity, and sensitivity to runoff/hydrology changes (Walker et al, 1981). A sensitivity analysis for these parameters has been conducted elsewhere (Walker et al, 1981, Schwartzman, 1999), and will not qualitatively effect the conclusions I wish to draw about biotic weathering enhancement. Therefore, at steady state $\frac{dCO_2}{dt} = 0$, $T = T_0$ and $CO_2 = CO_{20}$, then the flux is equal to its baseline value $W = W_0$ (with $W_0 = 6.65 \cdot 10^{12}$ moles per year at present). Recalling the assumption that biological weathering enhancement primarily results in a greater baseline flux value W_0 , rather than a (significant) change in the parameters a , b , or c , then the weathering flux W_{ab} on a theoretical abiotic planet Earth experiencing the same solar luminosity, takes the same sort of form:

$$W_{ab} = W_{ab0} \left(\frac{CO_{2ab}}{CO_{20}} \right)^a e^{(b+c)(T_{ab} - T_0)} \quad (3.14)$$

Where the “ ab ” subscripts denote the value of the variable for a theoretical abiotic planet Earth. Schwartzman (1999) noted that because the steady state (required between degassing D and weathering W per unit land area A) could be applied to ratio of the abiotic to the biotic values of these fluxes, as stated in equation (3.15);

$$\frac{D_{ab}}{D_b} = \frac{A_{ab}}{A_b} \frac{W_{ab}}{W_b} \quad (3.15)$$

then the present day value of the biotic enhancement of silicate weathering, $E_0 = \frac{W_{b0}}{W_{ab0}}$,

could be usefully expressed in terms of these fluxes by rearranging equation (3.15) and using equations (3.13) and (3.14) respectively to substitute for W_b and W_{ab} :

$$E_0 = \frac{D_b}{D_{ab}} \frac{A_{ab}}{A_b} \left(\frac{CO_{2ab}}{CO_{2\beta}} \right)^a e^{(b+c)(T_{ab}-T_\beta)} \quad (3.16)$$

Schwartzman's equation (3.16) thus describes a relation between the biotic:abiotic ratios of these variables required for steady state CO_2 , and is an average over the present day global weathering fluxes in a variety of weathering regimes - with all the approximations that this entails. Equation (3.16) describes how the assumed higher temperature T_{ab} and/or a higher atmospheric CO_2 level CO_{2ab} on a theoretical abiotic planet Earth are equivalent to the assumption of a high contemporary weathering enhancement factor E_0 . The biosphere has no influence, of course, on the tectonic degassing flux D or on the baseline land surface area A . There is therefore no reason to suppose that $D_b \neq D_{ab}$ or that $A_b \neq A_{ab}$. (Although the biosphere may affect the weatherability of the land surface area, this factor can probably be absorbed into changes in soil conditions and/or the baseline flux values, discussed below). It is nonetheless important to retain these tectonic factors in any measure of biotic weathering enhancement in order to emphasise their role in setting the steady state value of CO_2 - maintaining low CO_2 in the face of higher degassing fluxes requires an increased amount of thermodynamic work of the terrestrial biosphere. The numerical value of the current silicate weathering enhancement factor E_0 is poorly empirically constrained and may in theory vary by up to two orders of magnitude, but realistically is estimated to be about $E_0 \approx 100$, assuming an abiotic planetary temperature $T_{ab} = 50 - 60^\circ C$ (Schwartzman, 1999). Implicit in Schwartzman's formulations are a Precambrian weathering enhancement factor significantly lower than the Phanerozoic value, and a much hotter planetary temperature history in which some of the evidence for (predominantly Paleoproterozoic) glaciations are attributed to asteroid impacts (Schwartzman 1999). All of these assumptions may turn out to be unreasonable (as discussed below) and only empirical studies comparing biotic and (genuinely) abiotic silicate weathering reactions in kinetically-limited regimes can resolve the uncertainty. The approach taken in this work will be to compare the enhancement factor required for a biological weathering-triggered planetary glaciation, E_{Tr} , with the (uncertain) present day enhancement factor. Substituting into equation (3.16) the CO_2 and temperature conditions (discussed above) corresponding to the bifurcation point at which global glaciation occurs, so that $T_\beta = T_f$ and $CO_{2\beta} = CO_{2Tr}$, and retaining the tectonic terms corresponding to a biological trigger scenario, so that $D_b = D_{Tr}$ and $A_b = A_{Tr}$, then dividing through by equation (3.16) as it stands, we get the ratio $\frac{E_{Tr}}{E_0}$, of the biotic silicate weathering enhancement required for a biologically-triggered planetary glaciation (E_{Tr}), to the present day value of the enhance-

ment factor (E_0):

$$\frac{E_{Tr}}{E_0} = \frac{D_{Tr}}{D_b} \frac{A_b}{A_{Tr}} \left(\frac{CO_{2\beta}}{CO_{2Tr}} \right)^a e^{(b+c)(T_\beta - T_f)} \quad (3.17)$$

Where $CO_{2\beta}$ and T_β refer to the present day (biologically-altered) planetary CO_2 and temperature values. Note that because I have scaled by the present enhancement factor (i.e. because equation (3.17) can also be expressed in the rather more untidy form $\frac{E_{Tr}}{E_0} = \frac{\frac{D_{Tr}}{D_{ab}} \frac{A_{ab}}{A_{Tr}} \left(\frac{CO_{2ab}}{CO_{2Tr}} \right)^a e^{(b+c)(T_{ab} - T_f)}}{\frac{D_{ab}}{D_{ab}} \frac{A_{ab}}{A_b} \left(\frac{CO_{2ab}}{CO_{2\beta}} \right)^a e^{(b+c)(T_{ab} - T_\beta)}}$), we no longer need to know the temperature and CO_2 conditions corresponding to a theoretical abiotic planet. This eliminates a major source of uncertainty in the work of Schwartzman (1999) from the consideration of the snowball Earth problem attempted here, at the cost of losing some information on the absolute magnitude of the fluxes.

What was the required enhancement factor?

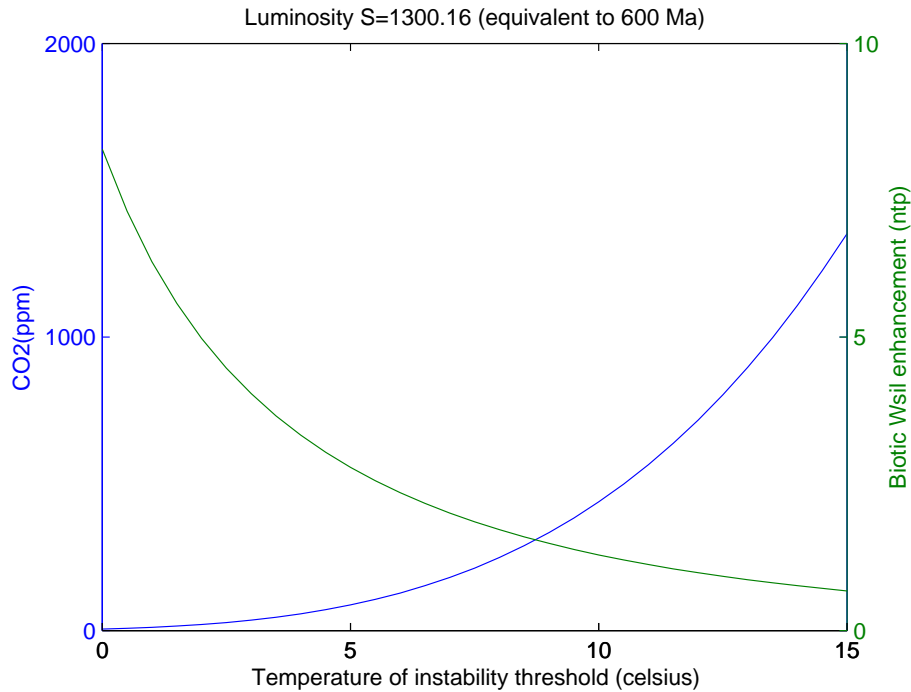


Figure 3.6 - Values of atmospheric CO_2 partial pressure (Left Y-axis, blue line) and biotic enhancement of silicate weathering rate relative to the present day $\frac{E}{E_0}$ (Right Y-axis, green line) corresponding to the entry point to a snowball global-scale glaciation, at different temperatures of this switch point T_f (X-axis, celsius). Results refer to a Solar luminosity flux $S = 1300.16 W m^{-2}$, corresponding to 600 Ma (I.e. between the putative Marinoan and Gaskiers glacial intervals). Note that this result assumes that the tectonic forcings relevant to biological weathering enhancement are equal to their present day values, i.e. $\frac{D_{Tr}}{D_b} \frac{A_b}{A_{Tr}} = 1$ in equation (3.17).

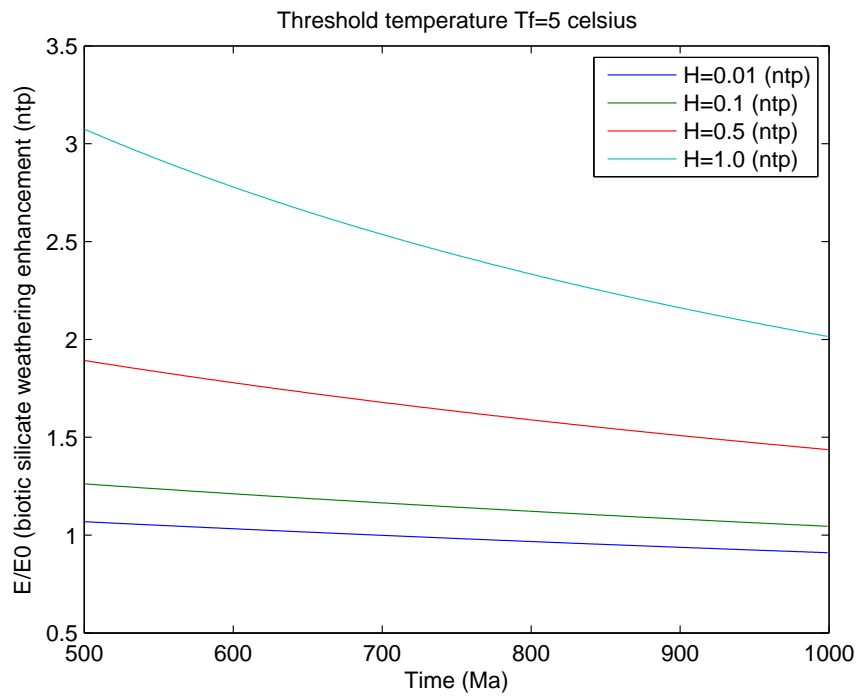


Figure 3.7(a) - The impact of atmospheric relative humidity (legend, normalised to present day value $H = 0.62$) on the biotic weathering enhancement factor (Y-axis, normalised to present) necessary to draw the temperature down to a $T_f = 5^\circ C$ bifurcation point, at solar luminosity values corresponding to various timepoints before the present (X-axis, Ma).

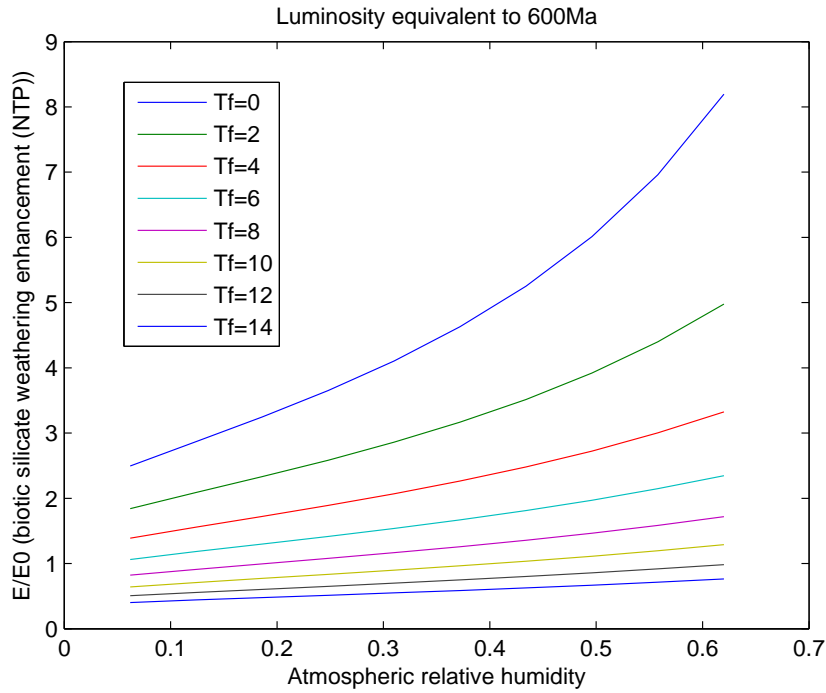


Figure 3.7 (b) - The impact of atmospheric relative humidity (X-axis, absolute value shown, altered by successive factors of 0.1 – 1.0 of the baseline value $H = 0.62$) on the normalised biotic enhancement of silicate weathering (Y-axis) corresponding to the bifurcation point, when it occurs at different temperatures (Legend, celsius). Solar luminosity was held constant at $S = 1300.16Wm^{-2}$, equivalent to 600Ma.

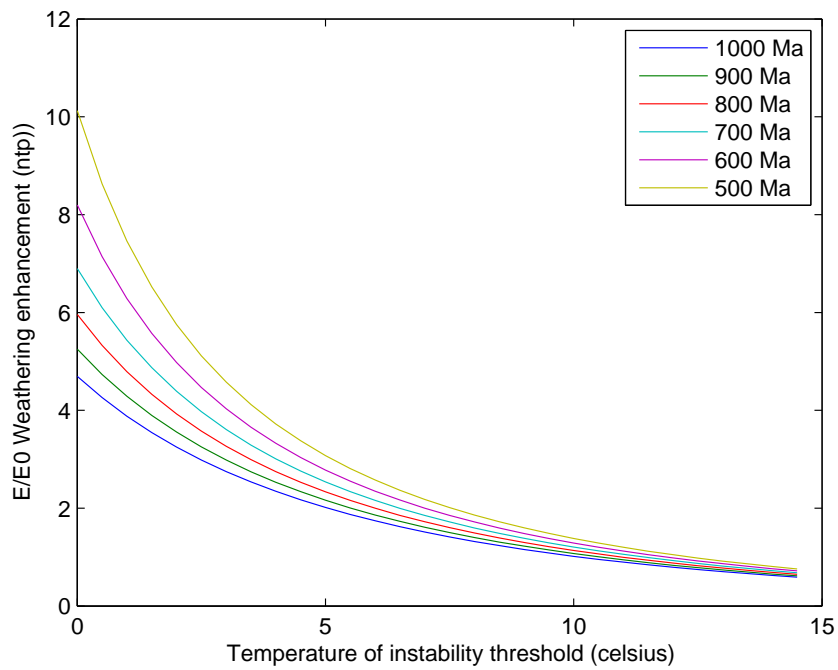


Figure 3.8- The impact of variable solar luminosity corresponding to the time points indicated in the figure legend (1000 – 500Ma) on the relative silicate weathering enhancement factor $\frac{E_{Tr}}{E_0}$ (Y-axis) required to initiate global glaciation at a range of temperature instability thresholds (X-axis).

Figure (3.6) shows the biological weathering enhancement factor that is necessary to cause CO_2 drawdown corresponding to global glaciation at various temperature thresholds. The right Y-axis (green line) shows the value of the biotic silicate weathering enhancement factor, in comparison to the value $E_0 \approx 100$ it takes at present, required to give rise to a biologically-triggered snowball Earth-scale glaciation. Note that the values of $\frac{E_{Tr}}{E_0}$ shown refer to a situation in which the tectonic forcings are equal to their present day values, i.e. $\frac{D_{Tr}}{D_b} \frac{A_b}{A_{Tr}} = 1$. This is a crucial assumption that is of extreme importance to the results (Figure 3.7, below). At the present day degassing rate D and available surface area for silicate weathering A , figure (3.6) illustrates how a biological trigger for snowball Earth requires either that a limiting case global glaciation occurs at relatively mild planetary temperatures (right hand side of figure (3.6)) or that the precambrian weathering enhancement factor that resulted from lichen colonisation of the Neoproterozoic land surface was significantly greater (i.e. 5 – 10 fold) than the factor’s present day value, (left part of the figure). Note that the gradient of the enhancement curve steepens as temperature becomes progressively lower- the enhancement necessary to induce a given CO_2 drawdown becomes higher as temperature is reduced. The direct cause of this is the minus sign before the T_f variable in equation (3.17), but the result can be thought of more intuitively as resulting from the temperature dependence of weathering. Weathering enhancement is measured with comparison to a fixed value that refers to present day temperature. As weathering is reduced via the temperature dependency, its impact on CO_2 similarly declines. Consequently, a given CO_2 reduction requires a greater weathering increase, hence a greater amount of enhancement activity by the terrestrial biosphere. Figures (3.7) and (3.8) show respectively the influence of relative humidity and solar luminosity of the enhancement factor-threshold temperature relationship. These plots emphasise how any conclusions about the activity of the terrestrial biosphere must be scaled by these abiotic variables.

Tectonic constraints

Figure (3.9) shows the impact of the degassing rate:land area ratio between a snowball initiation scenario and present day (the parameter $\frac{D_{Tr}}{D_b} \frac{A_b}{A_{Tr}}$ in equation (3.17)). As equation (3.17) suggests, any measure of weathering enhancement in comparison to the present $\frac{E_{Tr}}{E_0}$ must be scaled by the first order dependence on these tectonic parameters - biological weathering enhancement can trigger a snowball glaciation much easier at lower degassing rate D and/or increased land surface area A . For example, figure (3.9(a)) shows that in order to trigger an ice-albedo discontinuity at instability temperature $T_f = 5^\circ C$, then a degassing:land area value of $\frac{D_{Tr}}{D_b} \frac{A_b}{A_{Tr}} = 1$ requires weathering enhancement $\frac{E_{Tr}}{E_0} \simeq 3.5$, a ratio of $\frac{D_{Tr}}{D_b} \frac{A_b}{A_{Tr}} = 2$ requires $\frac{E_{Tr}}{E_0} \simeq 6$ and if the degassing/area balance is lowered as far as $\frac{D_{Tr}}{D_b} \frac{A_b}{A_{Tr}} = 0.2$, glaciation can be achieved at $\frac{E_{Tr}}{E_0} \leq 1$, i.e. at or less than the present day value. Note that the shape of the curve of the enhancement factor against temperature in figure (3.7) differs between values of $\frac{D_{Tr}}{D_b} \frac{A_b}{A_{Tr}}$; ultimately a result of the temperature dependence of weathering - meaning that a unit CO_2 reduction requires more energy at low CO_2 values than at high values (indicated in figure (3.6)). How reasonable are these tectonic estimates?

Both available land area A and degassing rate D correlate with the rate at which tectonic plate movement causes new continental crust to form at mid ocean ridges (i.e. the sea floor spreading rate), the latter via the direct plate movement, the former via the increase in continental uplift that often results from that plate movement. Consequently, the time derivatives expressing the change in terrestrial land area and the change in volcanic outgassing are of the same order, and can be balanced with each other using a sensitivity constant (Schwartzman, 1999). Normalised degassing rate is assumed to scale linearly with seafloor spreading rate SR , $\frac{D}{D_0} = \frac{SR}{SR_{(0)}}$, based on the assumption that most CO_2 outgassing occurs after decarbonation of subducted sediments (Berner, 1991, 1994, Franck & Bounama, 1997, Franck et al, 1999). Estimates of relative changes in seafloor spreading rate SR depend upon the assumptions made about continental growth over Earth history. Similarly, estimates of Precambrian continental growth formation vary by orders of magnitude, differing from linear interpolation across the history of the Earth, to dramatically different estimates of the fraction of the present crust that had already formed by the mid Paleoproterozoic (2000Ma) Rino et al (2004). Episodic continental growth models incorporating changes in Mid-ocean ridge activity give rise to peaks in continental crust formation at 1700 – 1800Ma and 1100 – 1500Ma, and imply a relatively low formation rate of new continental crust during the Neoproterozoic (Rino et al, 2004, figure 3.10). A linearly-interpolated continental growth rate (i.e. the rate of formation of new continental crust has remained constant over Earth history) produces a seafloor spreading rate of at most $\frac{SR}{SR_{(0)}} \simeq 5$ for the early Neoproterozoic, and more realistic continental growth models incorporating the bias toward continental formation in the earlier Precambrian (i.e. ~ 700 Ma)

give $\frac{SR}{SR_{(0)}} \simeq 1.1$ (Franck & Bounama, 1997). Conversely, a low baseline degassing flux D appears to be a necessary condition for Neoproterozoic glaciations (Tajika, 2003). A reduction to $D = \frac{1}{2} - \frac{1}{4}$ of the present rate D_0 was required to explain glaciation in a spatially resolved energy balance model with $0 < T_f < 5^\circ C$, using estimates of weathering and marine organic Carbon burial implicit in $\delta^{13}C$ data (Tajika, 2004). A resolution to the requirement for low degassing rate at the same time as seafloor spreading rate at or greater than its present value is likely to be found in changes in subduction, and the assumption that the carbonate Carbon was not at steady state (Rothman et al, 2003) hence shallow shelf precipitation (Ridgwell & Kennedy, 2004) limited CO_2 release from the decarbonation of subducted materials. However, any pre-glacial reduction in tectonic outgassing would have occurred gradually throughout the Proterozoic. The climatic changes implicit in the Neoproterozoic are of the order of 100,000 year to millennial (Hoffman & Schrag, 2002), so any hiatus in degassing is likely to have been too gradual to be a complete explanation, because it would have been compensated for within the CO_2 -weathering thermostat. More importantly, no continental crust formation model implies a dramatic difference between the early ~ 730 Ma and late ~ 580 Ma Neoproterozoic glaciations (Figure 3.10), so a change in degassing rate cannot explain the apparent repeated switching between glacial and non-glacial conditions. A low baseline CO_2 degassing rate is probably a necessary condition for Neoproterozoic glaciation events (Tajika, 2003, 2004). But the occurrence of glaciation-deglaciation cycles, and the Sr (Fairchild & Kennedy, 2007) and implicit Carbon isotopic (Tajika, 2004) evidence for high weathering fluxes, mean that a low degassing rate is not a sufficient condition for the occurrence of a Neoproterozoic snowball Earth.

The parameter A is a label for surface land area available (i.e. incorporating changes in relief) for the silicate weathering reaction, so that $\frac{A}{A_0}$ gives the relative abundance of silicate rocks on the Earth's land surface in comparison to the present day. Increased continental relief will lead to enhanced erosion, and in some circumstances the formation of mountain belts will lead to increased continental precipitation, probably including enhanced silicate weathering (Berner, 1994). One means of estimating changes in land substrate area available for weathering is through changes in isotopic abundance of marine strontium $^{87}Sr/^{86}Sr$ with respect to a standard, the deviation from which is assumed to scale at first order with the impact of terrestrial silicate weathering (Holland, 1984, Berner, 1994, Bergman, 2003). Within this approach, the contribution to seawater $^{87}Sr/^{86}Sr$ (assumed represented by marine carbonates) expected from reaction with mid-ocean ridge basalts alone, R_{ocb} , is calculated by assumed mass balance for the total atmosphere and ocean Sr reservoir, MSr . Equation (3.17) shows the expected value for mid-ocean ridge basalt Sr at (arbitrary) timepoint t , $R_{ocb(t)}$ from the Geocarb II model (Berner, 1994):

$$R_{ocb(t)} = R_{ocb(t-1)} + \frac{F_{b0} \frac{SR(t)}{SR(0)} (R_{bas} - R_{ocb(t-1)}) + F_{riv0} (R_{riv} - R_{ocb(t-1)})}{MSr} \quad (3.17)$$

Where F_{b0} is the present day mass flux of strontium between basalt and seawater, $\frac{SR(t)}{SR(0)}$ is the normalised seafloor spreading rate, F_{riv0} is present day flux of Sr into oceans from rivers, R_{riv} and R_{bas} are the present day $^{87}Sr/^{86}Sr$ of (respectively) marine basalt and river runoff. Berner (1994) held each of the Sr specific fluxes constant at these present day values. Using as a reference the $^{87}Sr/^{86}Sr$ of marine basalt calculated from equation (3.17), R_{ocb} , as well as an sensitivity parameter L , Berner (1994) calculated the relative rate of uplift of new surface land area:

$$\frac{A}{A_0} = 1 - L \left(\frac{R_{ocb} - Sr_{obs}^{87/86}}{R_{ocb} - 0.7} \right) \quad (3.18)$$

Where $Sr_{obs}^{87/86}$ is the observed value of $^{87}Sr/^{86}Sr$ in marine carbonates, which indicates (within the assumptions of Sr mass balance (Berner, 1994)) the impact of collective terrestrial weathering on marine $^{87}Sr/^{86}Sr$, and L is a sensitivity parameter expressing the proportionality between continental uplift and marine Sr composition, by default, $L = 1$ (Berner, 1994). Neoproterozoic values for $Sr_{obs}^{87/86}$ reach a maximum of $Sr_{obs}^{87/86} = 0.71$ (Sheilds & Veizer, 2002, Halverson et al, 2007, Figure (1.6)). Setting $R_{ocb(t)} = R_{ocb(t-1)}$ in equation (3.17) and solving for $R_{ocb(t-1)}$ using the present day values of the fluxes/ratios ($F_{b0} = 0.92 * 10^{16}$, $R_{bas} = 0.703$, $F_{riv0} = 3.3 * 10^{16}$, $R_{riv} = 0.711$, (Berner, 1994)), it is possible to get an estimate of the expected $^{87}Sr/^{86}Sr$ from the seawater basalt reaction - under different assumptions about the baseline seafloor spreading rate $1.1 < \frac{SR(t)}{SR(0)} < 5$ (Franck & Bounama, 1997). With spreading rate $\frac{SR(t)}{SR(0)} = 1$, I get $R_{ocb} = 0.7093$, with $\frac{SR(t)}{SR(0)} = 5$, $R_{ocb} = 1.32$. Using these values in equation (3.18), I respectively get $\frac{A}{A_0} = 1.075$ and $\frac{A}{A_0} = 0.016$. Finally, using $\frac{D_{Tr}}{D_b} = \frac{SR(t)}{SR(0)}$ and $\frac{A_{Tr}}{A_b} = \frac{A}{A_0}$, I arrive at the (huge) interval within which the tectonic balance $\frac{D_{Tr}}{D_b} \frac{A_b}{A_{Tr}}$ may lie:

$$\left(\frac{1.1}{1.075} = 1.023 \right) < \frac{D_{Tr}}{D_b} \frac{A_b}{A_{Tr}} < \left(\frac{5}{0.016} = 312.5 \right) \quad (3.19)$$

This massive potential range in degassing/land area balance dominates the changes between possible values of weathering enhancement $\frac{E_{Tr}}{E_0}$ (equation (3.17)). It is this uncertainty that ultimately limits the work in this chapter to a sensitivity analysis, and prevents conclusive falsification of the biological trigger hypothesis of Lenton & Watson (2004). The range in $\frac{D_{Tr}}{D_b} \frac{A_b}{A_{Tr}}$ might be reduced by using alternative values of Berner's uplift sensitivity parameter L , or by relaxing the assumption of steady state Sr , however such a treatment

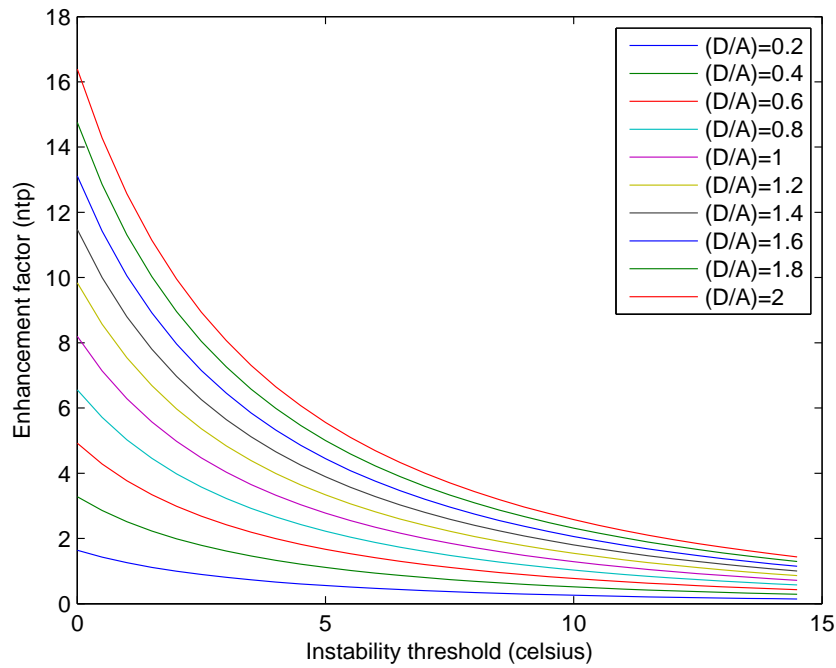


Figure 3.9 (a)- The importance of the steady state tectonic forcings in making conclusions concerning biotic weathering enhancement. Y-axis shows normalised biotic weathering enhancement factor $\frac{E_{Tr}}{E_0}$, X-axis instability threshold temperature T_f . Legend shows the ratio (between a snowball Earth scenario and present), of the degassing flux/available a land surface area $\frac{D_{Tr}}{D_b} \frac{A_b}{A_{Tr}}$. Luminosity fixed at value corresponding to 600Ma.

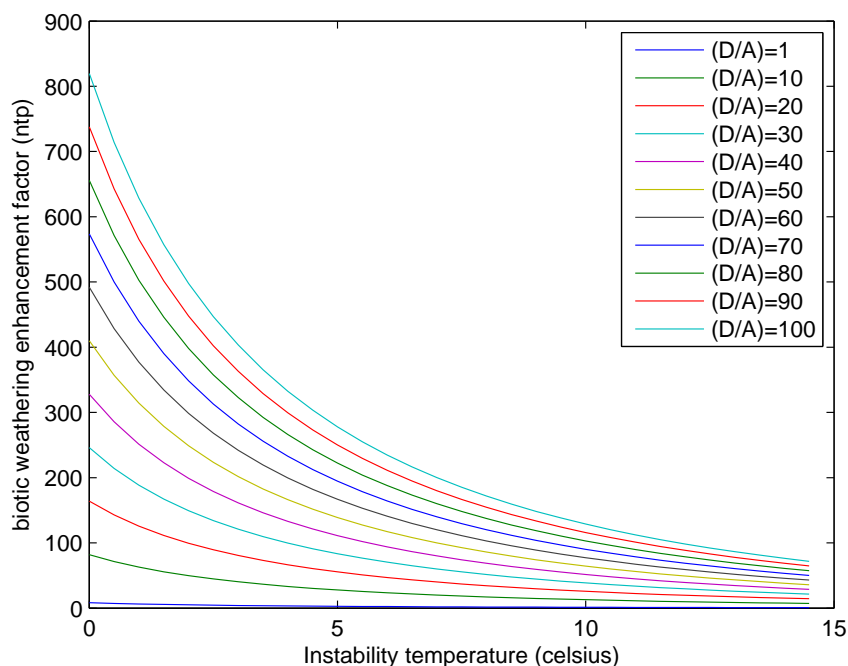


Figure 3.9 (b) - The same plot as figure (3.9(b)) but legend shows larger (and less realistic) range of values for the tectonic parameter $\frac{D_{Tr}}{D_b} \frac{A_b}{A_{Tr}}$.

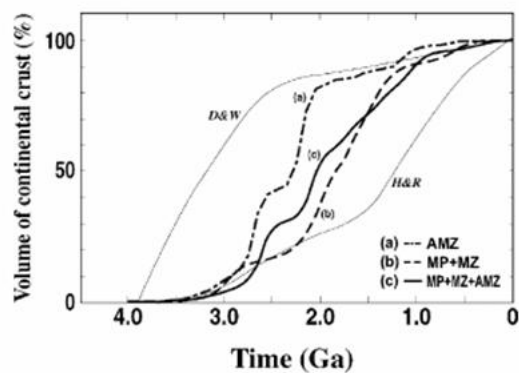


Fig. 11. Continental growth curve estimated from the age population of detrital zircons in the river sands; MP (the Mississippi), MZ (the Mackenzie), and AMZ (the Amazon). The continental growth curves are different between the continents. The summarized continental growth curve of two continents indicates episodic growth of continental crust at ca. 2.7 and 2.0 Ga. Two earlier growth curves of continental crust are also shown; D&W (Dewey and Windley, 1981) and H&R (Hurley and Rand, 1969).

Figure 3.10 - Estimates of continental crust formation over time by ages estimates derived from radioactive decay of U in igneous crystals of the mineral $ZrSiO_4$ (Rino et al, 2004). The authors propose periodic stratification then subduction within the mantle as an explanation for the surges in outgassing rate.

would be without empirical support for the Neoproterozoic, so the approach taken here is to acknowledge the uncertainty and explore its implications for biotic weathering enhancement, should it become better constrained in the future. Figure (3.9) shows the value of enhancement $\frac{E_{Tr}}{E_0}$ for different values of $\frac{D_{Tr}}{D_b} \frac{A_b}{A_{Tr}}$, illustrating how an instability temperature threshold $T_f = 5^\circ C$ (for example), implies a factor of $\frac{E_{Tr}}{E_0} \simeq 40$ for $\frac{D_{Tr}}{D_b} \frac{A_b}{A_{Tr}} = 10$, and $\frac{E_{Tr}}{E_0} \simeq 180$ for $\frac{D_{Tr}}{D_b} \frac{A_b}{A_{Tr}} = 60$. Both of these values, of course, still place an extreme requirement on biological silicate weathering in order for the idea to work. But figure (3.9) also shows the more modest combination of parameter choices $\frac{E_{Tr}}{E_0} \simeq 6$ for $\frac{D_{Tr}}{D_b} \frac{A_b}{A_{Tr}} = 2$. A more conservative estimate such as this might be realistic if available land surface area A_{Tr} is specified to be the reactive, weatherable surface area, rather than the land area produced by changes in continental uplift. In this case, the lower limit in relation (3.19) might be reduced because the relative (effective) surface area $\frac{A_{Tr}}{A_b} = \frac{A}{A_0}$ would be significantly higher.

Weatherability, biotic soil CO_2 concentration and physiological constraints

Basalt (a fine-grained volcanic rock containing $\sim 50\%$ SiO_2 and $5 - 15\%$ MgO , CaO and FeO) weathers rapidly, at around eight times the rate of more coarse-grained granitic rocks (Dessert et al, 2003). The concentration of large volumes of basalts in an equatorially-positioned, fragmenting supercontinent, may have provided sufficient CO_2 drawdown to trigger snowball events within the $800 - 500$ Ma solar luminosity range (Donnadieu et al, 2004, Li et al, 2003). For the purposes of this study, this is a potential abiotic increase in weatherability (loosely defined here as the relative rate of silicate weathering per unit land surface), that would be lumped into a higher effective land area prior to glaciation (increased $\frac{A_{Tr}}{A_b}$ in terms of equation (3.17)) - because the granularity of basalt-rich rock provinces effectively increases the reactive surface area, and the steady state atmospheric CO_2 level has been raised by degassing of the rock basaltic lavas (Godderis et al, 2003). An increase in the fraction of the land surface that was basaltic in composition, or an increase in continental surface area: volume ratio as a result of supercontinent fragmentation, are both tangible potential causes of CO_2 drawdown via an increase in silicate weathering rate per unit land surface (Godderis et al, 2003, Dessert et al, 2003, Li et al, 2003, Donnadieu et al, 2004). Incorporating these effects into the surface area estimate would add little to the conclusions from studies incorporating a spatial dimension - a relatively low basaltic trap fraction of total continental land mass is thought to be potentially sufficient to induce glaciation (between 1% and 8% , (Godderis et al, 2003)), depending on latitudinal continental configuration, temperature thresholds, and relief. These factors might substantially reduce the absolute increase in surface area necessary for glaciation (i.e. reduce the lower limit in relation (3.19)), but their parameterisation requires high resolution modelling outside the scope of this work.

A land surface colonised by life weathers faster than an abiotic surface because life actively increases weatherability - by physical break up, increasing the fraction of rock substrate in contact with water, metabolically-induced pH changes, etc - the factors that actually comprise enhancement E . One such factor that can usefully be extracted from the aggregate enhancement variable is the enhancement of soil CO_2 concentration above the atmospheric level via the effect of the metabolism of the terrestrial biosphere. Volk (1987) was the earliest to formulate an explicit description of how weathering strictly depends on CO_2 in soil, rather than the averaged atmospheric value, after which he developed a relation between normalised terrestrial production $\frac{\Pi}{\Pi_0}$ and soil CO_2 , CO_{2soil} (Volk, 1987):

$$\frac{CO_{2soil}}{CO_{2soil(0)}} = \frac{\Pi}{\Pi_0} \left(1 - \frac{CO_{20}}{CO_{2soil0}}\right) + \frac{CO_2}{CO_{2soil0}} \quad (3.20)$$

Where zero subscripts denote the present day value of the variable. In order to derive this relationship, Volk assumed that the atmosphere-soil diffusive exchange coefficient k_{soil} ,

and the fraction of terrestrial production released as respiratory CO_2 , f_{root} , remained constant. (He assumed that $\frac{f_{root}}{k_{soil}} = \frac{CO_{2soil0}-CO_{20}}{\Pi_0} = \frac{CO_{2soil}-CO_2}{\Pi}$, allowing him to eliminate the constants $\frac{f_{root}}{k_{soil}}$ and obtain equation (3.20) (Volk, 1987)). But this assumption presents a severe problem for modelling a Neoproterozoic biosphere of dramatically changing mass and species composition, experiencing a very wide range of abiotic boundary conditions - these factors will, of course, not remain constant, but vary by orders of magnitude. Introducing such a dependency here would have the unhelpful effect of lumping all the uncertainty into a productivity factor in an innaccurate way, and move the focus away from weathering enhancement. In terms of the second issue, the contemporary vascular-plant dominated biosphere may not give rise to a particularly strong enhancement of weathering by respiratory CO_2 , because long term increases in local partial pressure are more likely to be absorbed into a productivity increase within the contemporary soil structure, with a tenfold increase in soil CO_2 above the atmospheric level resulting a relative weathering rate increase of only ~ 1.56 (Von Bloh et al, 2003). Therefore, here, I simply note that on an abiotic planet the “soil” (i.e. abiotic regolith) CO_2 concentration would not appreciably deviate from the atmospheric level, whereas the presence of life enhances soil CO_2 via respiratory release, by a concentration factor C , so that biological soil CO_2 concentration is $CO_{2\beta}C_0$ at present. The weathering enhancement required for a snowball, in comparison to the present value (3.17) can therefore be relabelled:

$$\frac{E_{Tr}}{E_0} = \frac{D_{Tr}}{D_b} \frac{A_b}{A_{Tr}} \left(\frac{CO_{2\beta}}{CO_{2Tr}}\right)^a \left(\frac{C_0}{C_{Tr}}\right)^a e^{(b+c)(T_\beta-T_f)} \quad (3.21)$$

Where the parameter a is the exponent relating weathering rate to CO_2 as discussed above (Walker et al, 1981). Figure (3.10) shows the effect of this concentration factor (normalised to the present day, vascular-plant dominated value C_0), on the weathering enhancement factor needed to initiate global scale glaciation $\frac{E_{Tr}}{E_0}$. I.e. the figure shows a partitioning between increasing CO_2 at the weathering interface, and other biological factors responsible for increased weathering (osmolyte release, non-Carbonic organic acid secretion, physical substrate break up, etc), so the value of E shown on the Y-axis is the enhancement factor due to influences other than respiratory soil CO_2 . As indicated, elevating the CO_2 at the weathering interface above the atmospheric level may reduce the necessary extra enhancement factor by several orders of magnitude. Note that $\frac{C_{Tr}}{C_0} > 1$ implies an extremely large absolute enhancement factor, because vascular plant root respiration is thought to accentuate CO_2 concentrations in contemporary soils by a factor of $C_0 \sim 10$ (Von Bloh et al, 2003). However, lichen and bacterial enhancement of local CO_2 concentration may cause substantive pH reduction, as well as enhance baseline weathering rate (Jackson & Keller, 1970, Chen et al, 2000, Bennet et al, 2001). Although it is (presumably) unlikely that the global scale and spatial extent of a lichen/bacterial terrestrial biosphere would approach that of a Phanerozoic system, localised CO_2 concentration, particularly

in the kinetic-limited silicate weathering regimes relevant to the Urey reaction (West et al, 2005), might have been sufficient for the development of a tangible effect on climate during the Neoproterozoic.

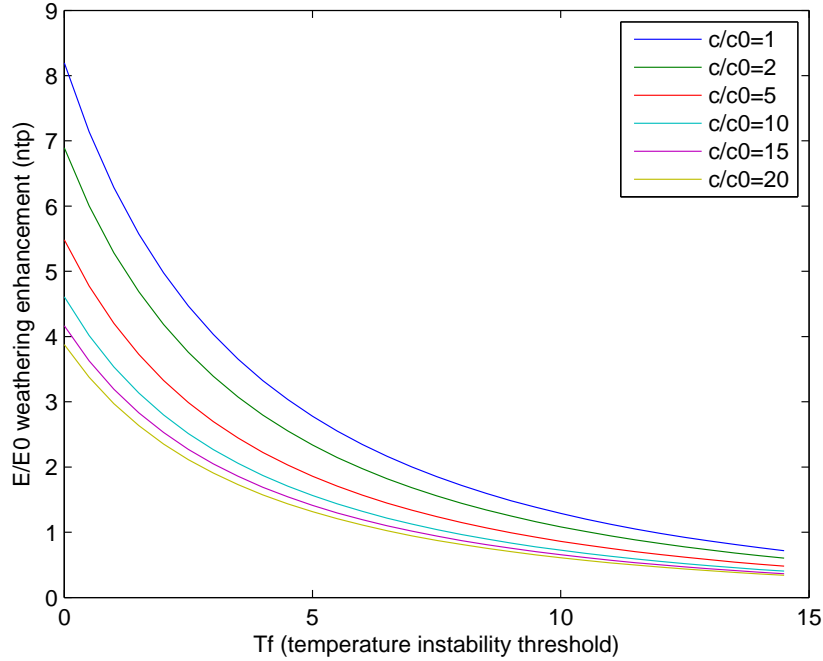


Figure 3.10 - The impact of biological weathering interface CO_2 concentration enhancement above the atmospheric level relative to the present day collective enhancement (by vascular plants), C/C_0 (legend), on the relative weathering enhancement $\frac{E_{Tr}}{E_0}$ (Y-axis) required to induce a snowball glaciation at various temperature threshold T_f values (X-axis). Luminosity value corresponds to 600 Ma.

Oxygen

It is worth recalling that the total biological enhancement of weathering E is, of course, the product of terrestrial biomass B and enhancement per unit biomass ε :

$$E = \varepsilon B \tag{3.22}$$

The relative extent of the terrestrial biosphere's coverage of land has been estimated previously in a normalised way using the deviation of temperature T , CO_2 and oxygen O_2 from their (vascular plant) optimum values (Lenton & Watson, 2000b, Bergman, 2003):

$$\frac{B}{B_0} = 2\Omega(1.5 - 0.5\frac{O_2}{O_{20}})(\frac{CO_2 - CO_{2Min}}{CO_{2\frac{1}{2}} + CO_2 - CO_{2Min}})(1 - (\frac{T - 25}{25})^2) \tag{3.23}$$

Where $\frac{B}{B_0}$ is the mass of the terrestrial biosphere relative to the present day, $O_{20} = 0.21$ is the present day atmospheric mixing ratio of oxygen, $CO_{2Min} = 10\text{ppm}$ is the minimum CO_2 under which the terrestrial biosphere can grow, $CO_{2\frac{1}{2}} = 183.6\text{ppm}$ is the partial pressure at which Carbon fixation proceeds at half its maximum rate, and the 25 in the third bracket is the temperature in degrees celsius at which maximum Carbon fixation occurs in vascular plants (Volk, 1987, Caldeira & Kasting, 1992, Bergman, 2003). The parameter Ω represents the relative progression of terrestrial colonisation of the Earth's surface in comparison to the present day - i.e. it is an (approximate) evolutionary history forcing (Bergman, 2003), and the factor of 2 is for normalisation, so that $\frac{B}{B_0} = 1$ under present day conditions. Of course, the terrestrial biosphere of interest to the snowball Earth problem was dominated by lichens, fungi and soil bacteria, hence its photosynthesis kinetics will differ from the Phanerozoic, vascular-plant dominated biosphere for which the function (3.23) was designed. However, although the *range* of environments that can be colonised by different lichen species is much wider than that of vascular plants (Nash, 1996), the ecological conditions at which production is *maximal*, in particular the optimum Carbon fixation CO_2 and temperature conditions, are not substantially different from vascular plants (Nash, 1983, Cowan et al, 1992, Nash, 1996). The first bracketed terms describes the photoinhibitory effect of O_2 partial pressures higher than the present day on terrestrial productivity at a macroscopic level (Lenton & Watson, 2000b). It is this aspect of the terrestrial growth function that is likely to introduce the most uncertainty, because the range of photoprotective mechanisms operating in lichens, as well as the range of ambient $O_2 : CO_2$ ratios in different environmental contexts is likely to result in very different photorespiratory properties in lichens in comparison to vascular plants (Nash, 1996). However, quantifying this difference requires empirical demonstration of photooxidation in lichens, and quantifying its impact on productivity.

Biological enhancement of silicate weathering relative to the present is equal to the product of the mass of the terrestrial biosphere B and the enhancement per unit biomass ε , (i.e. $\frac{E}{E_0} = \frac{\varepsilon}{\varepsilon_0} \frac{B}{B_0}$). Substituting this into the enhancement equation (3.17) and recalling that the productivity function (3.23) is constrained to be equal to 1 under present day conditions (i.e. $B_0 = 1$), I get a measure of biological weathering enhancement corresponding to the initiation of glaciation that incorporates physiology:

$$\frac{\varepsilon}{\varepsilon_0} 2\Omega(1.5 - 0.5 \frac{O_2}{O_{20}}) \left(\frac{CO_{2Tr} - CO_{2Min}}{CO_{2\frac{1}{2}} + CO_{2Tr} - CO_{2Min}} \right) \left(1 - \left(\frac{T_f - 25}{25} \right)^2 \right) = \left(\frac{CO_{2\beta}}{CO_{2Tr}} \right)^a e^{(b+c)(T_\beta - T_f)} \quad (3.24)$$

Using (3.24) I can solve for the normalised oxygen mixing ratio corresponding to the start of a snowball glaciation:

$$\frac{O_2}{O_{20}} = 3 - \frac{\left(\frac{CO_{2\beta}}{CO_{2Tr}} \right)^a e^{(b+c)(T_\beta - T_f)}}{\frac{\varepsilon}{\varepsilon_0} \Omega \left(\frac{CO_{2Tr} - CO_{2Min}}{CO_{2\frac{1}{2}} + CO_{2Tr} - CO_{2Min}} \right) \left(1 - \left(\frac{T_f - 25}{25} \right)^2 \right)} \quad (3.25)$$

Equation (3.25) therefore describes the O_2 mixing ratio expected at the switch point to glaciation T_f given a land biosphere growing according to a Michealis-Menten physiological function (Lenton & Watson, 2000b). Although the half-saturation CO_2 partial pressures might differ in a Neoproterozoic biosphere dominated by lichens, the most important free “parameter” likely to be qualitatively important to the results of (3.25) is the factor $\frac{\varepsilon}{\varepsilon_0} \Omega$ in the denominator. This is the product of the normalised enhancement of silicate weathering rate per unit terrestrial biomass, $\frac{\varepsilon}{\varepsilon_0}$, and the evolutionary forcing Ω (Bergman, 2003) which represents the relative colonisation of the land surface by the biota, in comparison to the present day, at which $\Omega = 1$. Therefore $\frac{\varepsilon}{\varepsilon_0} \Omega$ essentially represents the extent to which evolutionary innovation in the terrestrial biosphere is biased specifically towards the enhancement of silicate weathering. Figure (3.11) shows the oxygen mixing ratios relative to the present day value (Y-axis) given by equation (3.25) when glaciation occurs at different threshold temperature T_f values (X-axis), when the factor $\frac{\varepsilon}{\varepsilon_0} \Omega$ (legend) takes different values. The higher O_2 values shown are of the same order as that attributed to increased marine organic Carbon burial resulting from PO_4 export to the ocean, in conjunction with biological weathering enhancement (Lenton & Watson, 2004).

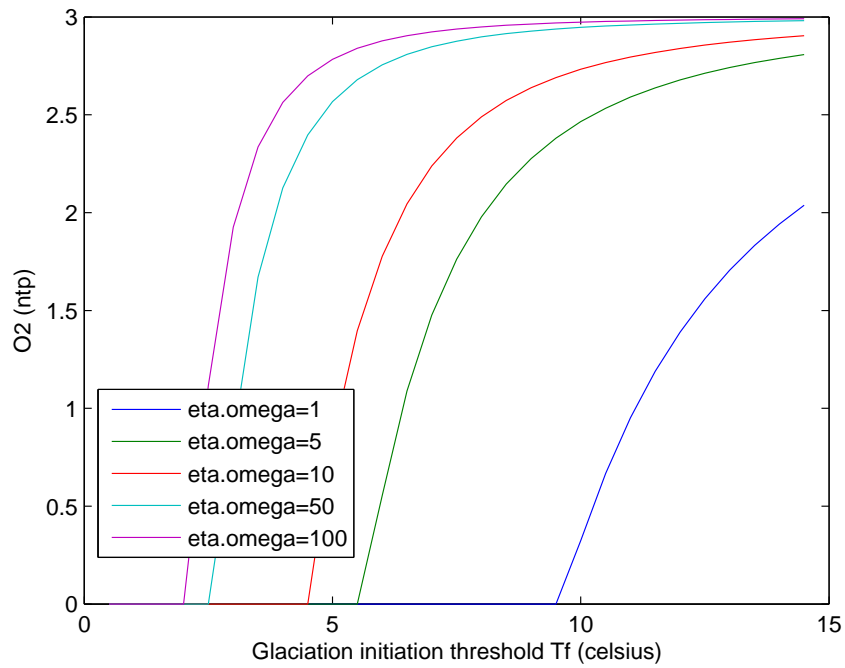


Figure 3.11 - The level of atmospheric oxygen (Y-axis, normalised to present day value) implicit from the biotic weathering enhancement function E/E_0 at different threshold temperature values T_f (X-axis, celsius). Legend shows differing values of the parameters $\Omega(\varepsilon/\varepsilon_0)$ in equation (3.25).

Discussion

This chapter has examined the sensitivity that biological enhancement of silicate weathering bears to various Earth system variables, in an attempt to quantify and constrain the hypothesis (Lenton & Watson, 2004) that weathering of the Neoproterozoic land surface by lichens caused sufficient CO_2 drawdown to trigger snowball Earth glaciations. Conclusive falsification of the hypothesis requires (a) direct experimental measurements constraining the present day biological enhancement factor, and (b) confident estimates of the planetary temperature at which the ice-albedo discontinuity gives rise to global scale glaciation. Neither of these pieces of information are available, limiting the work presented here to a theoretical sensitivity analysis. Bearing this clause in mind, some conclusions are possible about the feasibility of a biologically-triggered snowball Earth.

The magnitude of weathering enhancement required is dictated primarily by the balance between the rate of exposure of new land area suitable to take part in silicate weathering reactions, and the degassing of CO_2 due to tectonic activity. A higher degassing rate implies a higher baseline Urey reaction rate for the maintenance of the same planetary temperature. More available land area means net weathering rate is higher at the same weathering rate per unit area (Walker et al, 1991, Schwartzman, 1999). Figure (3.7) illustrates how both the shape and magnitude of the enhancement factor corresponding to a given temperature discontinuity are strongly influenced by the tectonic $\frac{D_{Tr}}{D_b} \frac{A_b}{A_{Tr}}$, the normalised ratio between rate of CO_2 degassing and the rate of uplift of new land substrate. Note that increased $\frac{D_{Tr}}{D_b} \frac{A_b}{A_{Tr}}$ results in a steepening of the curve relating weathering enhancement to temperature (Figure 3.7 (a) and (b)), as well as raising the point of intersection with the Y-axis (enhancement). This is due to the multiplicative interaction of two factors. Firstly, the fact that at higher $\frac{D_{Tr}}{D_b} \frac{A_b}{A_{Tr}}$, maintaining a given temperature by weathering-induced CO_2 drawdown requires a greater weathering rate. Secondly, at lower temperatures, the baseline weathering rate (whatever its value for steady state) is reduced by the Arrhenius dependency in the reaction, so the factor by which the baseline rate must be multiplied in order to achieve the same CO_2 reduction, is increased. So at high $\frac{D_{Tr}}{D_b} \frac{A_b}{A_{Tr}}$ and low temperatures, a relatively high baseline rate must be multiplied by an increasing enhancement factor to achieve the same temperature reduction. In practical terms, both of these issues amount to the assumption that enhancing a high abiotic rate requires more total biological work than enhancing a low abiotic rate. The validity of this assumption depends on the effect of a high abiotic rate on growth (nutrient availability etc), which have not been explicitly considered here. However, the idea can be defended with a metaphor. Consider a chisel impacting on a rock surface as a metaphor for biological weathering enhancement: A chiselling action of equivalent force does more to *increase* the reactive surface area of a coherent boulder with low surface area:volume ratio (a low baseline abiotic rate) than of a finely ground collection of stones of the same mass (a high baseline abiotic rate) - because

the reactive surface area in the former is significantly lower to begin with. Increased force and sharpness of the “chisel” (increased acid secretion, osmotic changes, hyal expansion, chelating activity) require increased thermodynamic work, regardless of the substrate on which it is impacting.

This argument serves to illustrate two conclusions that are apparent from the tectonic parameters in this study. Weathering-induced cooling requires more thermodynamic work from the biosphere at lower temperatures, because the baseline abiotic rate is decreased. Therefore if future high-resolution modelling studies give rise to a consensus that the Neoproterozoic ice-albedo discontinuity would not occur until planetary temperature reached relatively low ($\leq 5^{\circ}C$) values, then the biological trigger hypothesis requires an increasingly large and active terrestrial biosphere. Furthermore, a higher degassing:land area uplift balance $\frac{D_{Tr}}{D_b} \frac{A_b}{A_{Tr}}$ implies a higher baseline abiotic rate for steady state temperature, and therefore requires more thermodynamic work from the terrestrial biosphere to achieve an equivalent temperature reduction, by the arguments above. Therefore the biological trigger hypothesis implies an increasingly active Neoproterozoic terrestrial biosphere at higher degassing rates and lower uplift rates - so is (presumably) less plausible under these conditions.

A biological amplifier for snowball Earth

At the present day degassing/uplift rate balance, a biologically-triggered Neoproterozoic glaciation probably corresponds to a silicate weathering enhancement factor up to six times the present day $1 < \frac{E_{Tr}}{E_0} \leq 6$ (Figure 3.6). In order to assess the plausibility of this idea, it is necessary to consider the contrast between supply-limited and kinetically-limited silicate weathering regimes, and changes in the relative abundance of such regimes on the Earth’s surface over geologic time (West et al, 2005). West et al (2005) note the contrast between silicate weathering regimes in which weathering rate is limited by the supply of virgin rock substrate by mechanical erosion, and regimes in which rate is limited by kinetic constraints on the weathering reactions themselves. Only the latter, kinetically-limited regimes are of relevance to climate, because only in such regimes is weathering rate sensitive to atmospheric CO_2 (West et al, 2005). Hence the values of biotic weathering enhancement E discussed here should not be compared with the contemporary terrestrial biosphere as a whole, but with biological weathering enhancement in the kinetically-limited silicate weathering regimes of direct relevance to climate. More directly, these regimes are unlikely to be those stabilised by soil structures and colonised by vascular plants, because net physical erosion of virgin rock substrate may actually be lower in such regimes. Therefore, there may be no reason to expect a greater Neoproterozoic weathering enhancement factor than the present $\frac{E_{Tr}}{E_0} > 1$ to correspond to a terrestrial biosphere of the same or greater mass as that at present, because the present day relative abundance of, and biological

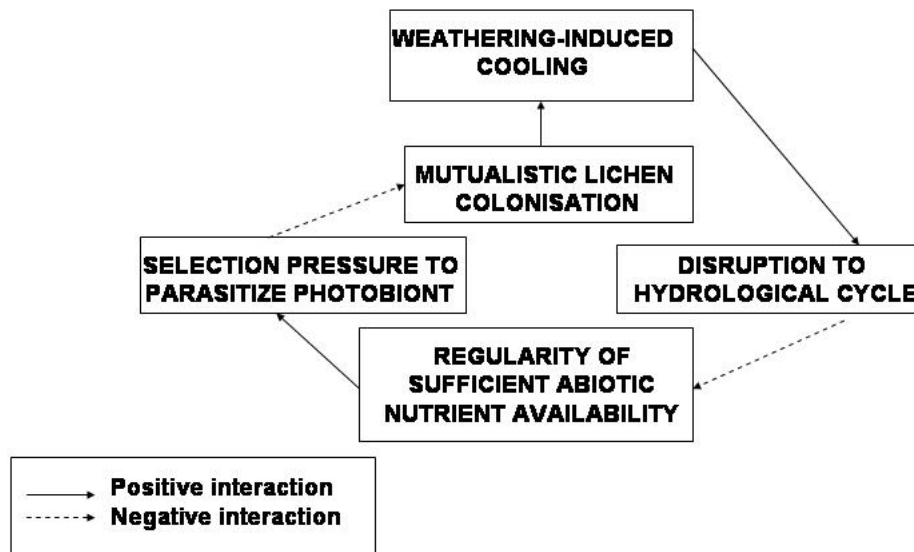


Figure 3.12 - Factors affecting the degree of weathering enhancement due to lichen colonisation under conditions of hydrological variability on the approach to the bifurcation point $T = T_f$. Solid arrows indicate positive feedback processes, dashed arrows negative feedback. A loop with an even number of negative feedbacks represents a net positive feedback.

activity within, kinetically-limited silicate weathering regimes may turn out to be relatively low. Only empirical studies comparing net denudation rate between kinetically-limited, soil-stabilised vascular plant-dominated biomes and lichen colonisation of recently eroded rock can resolve this issue. But there is certainly no clear cut relationship between the weathering enhancement factor and the mass of the terrestrial biosphere, and little reason to expect one.

Supply-limited regimes are characterised by slow physical erosion rate and complete chemical weathering, kinetically-limited regimes by more rapid erosion, and sometimes incomplete chemical weathering (West et al, 2005). At higher erosion rates, the relationship between silicate cation denudation flux and total physical erosion changes from a log-linear relationship (in the supply-limited, slow erosion regimes) to an explicit kinetic dependency (characteristic of the kinetically-limited, rapid erosion regimes). The increase in erosion rates sufficient to alter rate limitation from supply-limited to kinetically-limited are likely to depend upon temperature, CO_2 , and runoff - precisely the climatic controls that characterise the kinetically-limited regimes (West et al, 2005). Fluctuating or rapidly changing climates (like the formation or recession of glaciers during the start or finish of a snowball Earth) are likely to elevate erosion rates sufficiently to cause a significant increase in the fraction of the global silicate weathering flux that occurs in a kinetically-limited regime (West et al, 2005). This has several implications for the geophysiological meaning of snowball Earth having had a biological trigger. In the habitable state $T > T_f$, equatorial regions may be characterised by rapid erosion and kinetically-limited silicate weathering. This is particularly probable under the scenario of an enrichment of equatorial basaltic “traps” associated with the disintegration of the Rodinia supercontinent (Donnadieu et al, 2004). Terrestrial biological activity, primarily lichens and the soil bacteria associated with them, may accentuate what would already be a disproportionately high silicate weathering rate. CO_2 drawdown will cause cooling, and cover some weathering regimes in ice. If this cooling is not sufficient to give rise to a discontinuous switch to the equilibrium, high ice cover state, then ice cover progression may cease - because lower temperature and CO_2 will curtail weathering rate in kinetically-limited regimes, and erosion rate will occur more slowly in supply limited regimes due to the lower temperature and coupling to local ice-formation/melting cycles (i.e. in comparison to a hot, relatively porous “soil” structure in a highly weatherable, equatorial, porous volcanic basalt). A scenario of this sort would be consistent with a genuine slushball Earth - in which some ice formation occurs, but the ice albedo discontinuity is not reached and therefore largely irrelevant. However, in those remaining kinetically-limited weathering regimes, biological enhancement of weathering may compensate for the reduced baseline abiotic rate caused by the lower temperature. In cooler conditions, relatively low background PO_4 and cation availability may *enhance the evolutionary incentive* to extract nutrients from rocks by the mechanisms proposed

(Lenton & Watson, 2004, Landeweert et al, 2001). An increasingly erratic hydrological cycle may give rise to fluctuating abiotic nutrient availability, potentially selecting for lichen symbioses with a division of labour sufficiently mutualistic to survive this - by the evolutionary mechanisms proposed in chapter 2. The increased relative abundance of such lichens in comparison to free-living and/or parasitic fungi and cyanobacteria will give rise to increased biological weathering enhancement - because biotic colonisation of kinetically-limited silicate weathering regimes will be greater than for free living fungi, limited by Carbon substrate availability. This increased weathering enhancement will increase CO_2 drawdown, thus cooling, giving rise to an increasingly unpredictable hydrological cycle. This completes a net positive feedback loop (Figure 3.11), that may have been sufficient to tip a low ice cover, cool, planet Earth, into a genuinely snowball Earth regime in which the ice-albedo discontinuity occurred.

Chapter 4: Atmosphere-ocean CO_2 equilibration and glacial duration

Summary

Speciation between marine carbonate anions, of which $CO_{2(aq)}$ comprises a small fraction, causes an ocean at chemical equilibrium with the atmosphere to eventually become a net source of CO_2 when overall atmosphere-ocean reservoir size is increasing. This makes the length of open water “slushball” scenarios qualitatively shorter than “hard snowball” scenarios lacking atmosphere-ocean equilibration. The estimated duration of a hard snowball event can vary by orders of magnitude depending upon different assumptions about the magnitude of the degassing flux and the fraction of it that enters the atmosphere directly, with the latter parameter appearing to dictate the increase in glacial duration in comparison to a slushball. Furthermore, because slushball scenarios imply CO_2 exchange between the ocean and atmosphere, deglaciation becomes impossible if the ocean is a long term sink for CO_2 , making a return to habitable temperatures contingent on a carbonate weathering to burial ratio $R = \frac{W_{carb}}{B_{carb}} > 1$. If neither of these conditions are met, there is insufficient marine carbonate alkalinity for the atmospheric part of the CO_2 reservoir to increase. The duration of any snowball scenario is also, of course, sensitive to the temperature T_i at which glacial exit occurs. The simple relationship developed here is in agreement with studies using more complex models, and illustrates how the debate about glacial duration boils down to the choice of these parameters, rather than more explicit assumptions about climate. Under certain carbonate Carbon scenarios, slushball solutions are as unlikely to be recoverable as hard snowball solutions - just for different, but equally poorly constrained, reasons. The assumption that slushball scenarios are a more pragmatic synthesis of Neoproterozoic climate is therefore invalid without more information about the atmosphere-ocean apportioning of the CO_2 degassing flux and the influx:efflux balance of marine carbonate alkalinity.

Introduction: The Urey reaction and the global Carbon budget

Weathering of the CaO and MgO component of igneous rocks on the land surface has the net effect of converting a terrestrial silicate rock into a marine carbonate rock, moving 1mol of carbon from the atmosphere to the ocean floor at a rate that is sensitive to the level of atmospheric CO_2 (discussed in Chapter 1). The climatic importance of the buffering mechanism that results (Walker et al, 1981) must be scaled by the influence of other factors that cause total atmosphere-ocean CO_2 to deviate from steady state (Berner, 1994). In particular, the suite of marine factors that affect formation, remineralisation, subduction and decarbonation of sediments may cause degassing rate to deviate from any linear relation

with seafloor spreading and/or tectonic activity (Sundquist, 1993, Ridgwell & Zeebe, 2005). Tangible weathering activity probably does occur below glaciers today (Sharp et al, 1999). The long timescales of glacial formation and re-advance mean that contemporary glacial-driven weathering of silicates is likely to be supply limited, therefore less relevant to climate (West et al, 2005). Additionally, extrapolation from contemporary glacial environments may not always be useful. A million year timescale, global spatial scale glaciation would, by definition, reduce temperature sufficiently to significantly limit terrestrial weathering. Anything close to a hard snowball scenario would cause a hydrological cycle shutdown that would drastically decrease the time that (ice-free) rock surfaces were in contact with water - also effectively reducing substrate supply. Consequently, the work in this chapter focuses on the probable length of a Neoproterozoic global glaciation, using the underlying assumption that terrestrial silicate weathering is negligible, and that carbonate weathering is likely to have been substantially decreased. I explore, using as simple a model as is possible, the difference in dynamics between an atmospheric CO_2 reservoir that is isolated from the ocean (a hard snowball scenario) and an equilibrated ocean-atmosphere CO_2 reservoir (a slushball scenario). I will neglect changes in the strength of the biological pump (i.e. the difference between marine organic Carbon fixation and the net burial flux that escapes remineralisation). Such changes may be relevant to the initiation of glaciation (Rothman et al, 2003, Lenton & Watson, 2004), but I will assume that the reduction in marine biomass that would result from a snowball scenario would limit the effectiveness of the biological pump during the glacial interval. It is possible that if a sufficient radiative flux reaches surface waters, the marine biosphere may only experience a mild decrease in size during a slushball scenario (Pollard & Kasting, 2005). The importance of the results I present here concern the role of the inorganic marine Carbon cycle, and may therefore be subject to future revision, in the light of the expected behaviour of the marine biosphere. But at present, this behaviour is unconstrained and would introduce an uncertainty that may turn out to be irrelevant. The key factors I address are therefore (a) whether the ocean and atmosphere reach chemical equilibrium and (b) how the marine carbonate alkalinity balance is affected by the occurrence of glaciation.

The degassing rate in present day oceans is the sum of direct CO_2 volcanism at mid ocean ridges and tectonic “hot spots” as well as subduction-induced decarbonation of organic and inorganic carbonates (e.g. Tajika, 2003). This produces a degassing flux $D_0 = 6.65 \cdot 10^{12}$ moles per year (Berner, 1994). As discussed in the previous chapter, this is balanced by the net weathering rate of silicates on land $W_{sil0} = D_0$, meaning that the dynamics of atmosphere ocean CO_2 , as described in equation (4.1), can usefully be assumed to sum to zero, over multi-million year time scales:

$$\frac{dCO_2}{dt} = D - W_{sil} \tag{4.1}$$

The dynamics of CO_2 are also affected by changing total mass C_R of carbonate rocks, meaning that equation (4.1) is only an accurate representation of the system when carbonate Carbon is at steady state (Berner, 1994). carbonates are buried and compacted on the ocean floor after the deposition of organic Carbon captured by photosynthesis, or $CaCO_{3(s)}$ precipitated organically or inorganically. carbonates are eventually converted back into CO_2 - which is emitted in the gas phase by decarbonation and in solution after weathering W_{carb} :

$$\frac{dC_R}{dt} = B_{carb} - W_{carb} - D \quad (4.2)$$

In reality therefore, the effect of the silicate weathering flux in (4.1) is to drive aqueous CO_2 , into the ocean, and (implicitly) raise the value of the burial flux B_{carb} by moving 1 mole of CO_2 from the atmosphere to ocean sediments. For dynamic carbonate Carbon scenarios, it is appropriate to distinguish between the total ocean-atmosphere CO_2 reservoir, ΣCO_2 , (which increases as inorganic Carbon in crustal rocks C_R decreases, so that $\frac{d\Sigma CO_2}{dt} = -\frac{dC_R}{dt}$) and changes in the fraction Φ of that reservoir that is in the atmosphere $CO_{2(g)} = \Phi \Sigma CO_2$. The value of Φ is dictated predominantly by the biogeochemistry of the oceans (Sundquist, 1993), but its long term behaviour is poorly constrained and introduces significant uncertainty into long-term Carbon cycle modelling of the Phanerozoic Earth system (Bergman, 2003).

Differences between the duration of hard snowball and slushball glacial intervals

I hypothesize that ocean-atmosphere chemical continuity will significantly alter the duration of the glacial interval during a Neoproterozoic snowball Earth. Let the planetary temperature corresponding to the start t_0 of the global glacial interval be T_0 . Note that $T_0 \ll T_f$, because it is the temperature that the system jumps to when planetary energy balance instantaneously adjusts to the high ice-cover albedo value, i.e. after the switch to the high ice cover state has occurred. I label the temperature change needed to get to the exit threshold temperature T_i as a definite integral $T_0 + \int_{t_0}^{t_1} \frac{dT}{dt} dt = T_i$. I assume steady state luminosity and albedo (i.e. that the dynamics of temperature are dictated by those of CO_2 , so that $\frac{dT}{dt} = \frac{\partial T}{\partial CO_2} \frac{\partial CO_2}{\partial t}$). For a hard snowball scenario, the duration of the glacial interval is dictated solely by the fraction c of the CO_2 degassing flux D that enters the atmosphere directly, because the fraction $1 - c$ that enters the ocean does not affect climate because it does not come into equilibrium with the atmosphere. The time interval $t_{1hsb} - t_0$ needed to build up enough CO_2 to melt the ice is therefore:

$$(T_i)_{hsb} = T_0 + \int_{t_0}^{t_{1hsb}} \frac{\beta}{CO_{20}} D c dt \quad (4.3)$$

In a slushball scenario, the situation is more complex, and the time interval $t_{1slush} - t_0$ is dictated by the behaviour of the total reservoir size ΣCO_2 and the atmospheric fraction Φ , the dynamics of which over geologic time are both a function of each other (Ridgwell & Zeebe, 2005)

$$(T_i)_{slush} = T_0 + \int_{t_0}^{t_{1slush}} \frac{\beta}{CO_{20}} (\Sigma CO_2 \frac{d\Phi}{dt} + \Phi \frac{d\Sigma CO_2}{dt}) dt \quad (4.4)$$

This difference in expected time intervals therefore identifies the problem that I am attempting to solve with the work in this chapter. Note that both of the scenarios assume an equivalent low CO_2 starting value, to which the system decreased immediately after the initiation of glaciation (i.e. when the ice albedo discontinuity has just switched to the ice covered state and temperature was well below the melt threshold $T \ll T_i$), and from which the process of CO_2 buildup was required to begin. In both of the models used here, this CO_2 value was lower than 50 parts per million, and approached zero for some lower-bound choices of the initiation threshold temperature T_f . The negligible difference between starting CO_2 values of snowball and slushball model set ups was therefore unlikely to effect my conclusions.

Model description

Outline

I present a simple 3-box model (Figure 4.1) of the inorganic Carbon cycle in which the partitioning of Carbon between the atmosphere and ocean CO_2 reservoir and carbonate carbon in rock, C_R , is dictated by the chemistry of the oceans - primarily the effect of temperature and pH extremes on the solubility of CO_2 . A simple temperature function with a discretized ice albedo feedback is used to relate the box model to the CO_2 partial pressure needed to deglacierate at different (parameterized) exit temperatures. Under hard snowball scenarios the ocean chemistry has no impact on partitioning of CO_2 between atmospheres and oceans, which is dictated simply by the fraction of the degassing flux that enters each component of the reservoir. The silicate weathering flux is assumed negligible during the glacial interval. The magnitude of the carbonate weathering and burial fluxes are varied (but only effect the duration of the glacial in equilibrated slushball scenarios, because CO_2 is released/precipitated from the HCO_3^- component of the reservoir).

Temperature function

Temperature was described by encompassing radiative convective changes into empirically-constrained parameters (North, 1979, North et al, 1981). Greenhouse warming attributable to changes in atmosphere-ocean CO_2 was written in terms of a logarithmic sensitivity parameter derived from global climate modelling $\beta = 4.33$, by which temperature is re-

lated to changes in CO_2 - corresponding to about 3 degrees celsius warming per doubling of CO_2 (Berner, 1994, Oglby & Saltzman, 1990). The numerical value of this CO_2 -climate sensitivity parameter is a major source of uncertainty in climate science, and its extrapolation from the results of different global climate models (GCMs) somewhat arbitrary, particularly given conjecture that it may decrease at large reservoir sizes (Berner, 1994). The value of β used here may therefore introduce uncertainty into the temperature thresholds and numerical values of the CO_2 partial pressures determined. However, it will not alter any differences between hard snowball and slushball results, being the same in both representations. The zonally averaged planetary temperature was written as:

$$T = \frac{1}{B} \frac{S}{4} (1 - \alpha) - \frac{A}{B} + \beta \text{Ln} \left(\frac{CO_2}{CO_{20}} \right) \quad (4.6)$$

Where empirical radiative convective parameters $B = 2.09 W m^{-2}$ and $A = 203.3 W m^{-2}$ account for the sensitivity of temperature to average cloudiness and humidity, and are measured in units of watts per square metre (North et al, 1981). The solar luminosity flux S is again varied over Neoproterozoic time using the formula (3.2) (Gough, 1981). The mixing ratio of atmospheric greenhouse CO_2 was scaled by its pre-industrial value $CO_{20} = 280$ parts per million (ppm). Planetary albedo α was again discretized so that when temperature reached or fell below the initiation threshold T_f , the albedo instantaneously jumped from the ice-free to ice-covered value $\alpha_f \rightarrow \alpha_i$, when the temperature of a glaciated system exceeded the melt threshold T_i , albedo jumped back to its ice-free value $\alpha_i \rightarrow \alpha_f$ causing the qualitative changes in energy balance described in the previous chapter, equations (3.4)-(3.6).

Hard snowball

In a situation in which total sea ice cover prevents equilibration between the atmosphere and ocean, the duration of the glacial interval is dictated by the magnitude of the degassing rate D , parameterised as a fraction of its present day value $D_0 = 6.65 \cdot 10^{12}$ moles per year, and its partitioning between the atmosphere and ocean, dictated by the atmospheric fraction parameter c . It was assumed that both carbonate and silicate weathering fluxes would tend to zero in a hard snowball Earth scenario that was severe enough to cause chemical isolation between atmosphere and ocean. Although the magnitude of carbonate Carbon burial within an ice-covered ocean might be of relevance to the size and properties of post glacial cap carbonates (Fairchild & Kennedy, 2007), the magnitude of the carbonate burial B_{carb} is not relevant to the duration of a hard snowball in which ocean chemistry is decoupled from atmospheric CO_2 . Therefore, within an ice-covered ocean scenario, the dynamics of CO_2 in the atmosphere and ocean were separated, according to (respectively) equations (4.7) and (4.8):

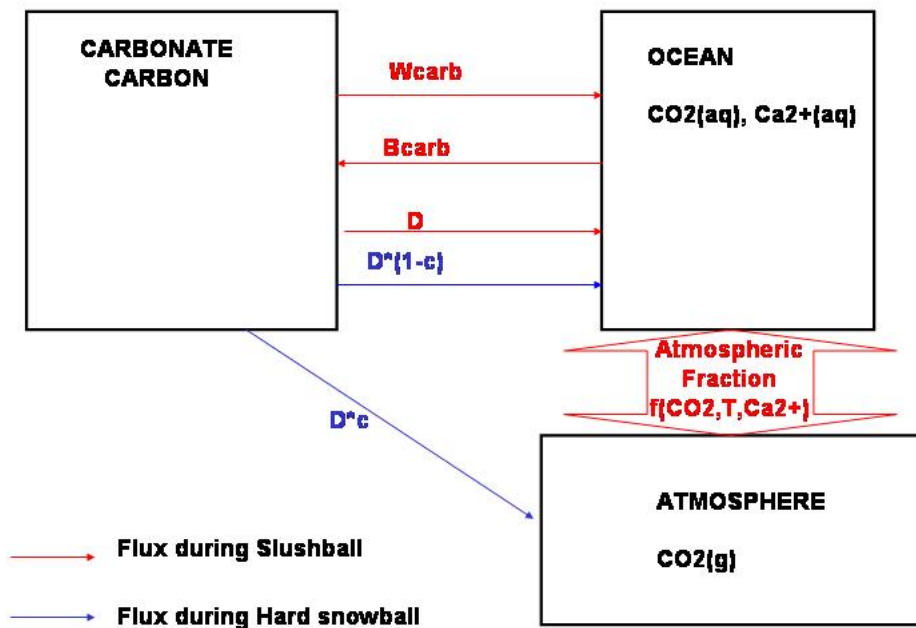


Figure 4.1 - Schematic of the minimal complexity 3-box model used for the work described in this chapter. Arrows of different colours denote the key assumptions about how fluxes in the inorganic Carbon cycle would have been different between a slushball scenario with atmosphere-ocean continuity, and a hard snowball, in which no atmosphere-ocean flux of CO_2 or alkalinity occurred during the glacial interval.

$$\frac{dCO_{2atm}}{dt} = c \frac{D}{D_0} \quad (4.7)$$

$$\frac{dCO_{2ocean}}{dt} = (1 - c) \frac{D}{D_0} \quad (4.8)$$

In the case of dynamic carbonate Carbon, the atmospheric fraction Φ of the CO_2 reservoir was a responsive variable, in that it merely tracked the relative changes in atmosphere versus ocean CO_2 :

$$\Phi = \frac{CO_{2atm} \cdot \frac{Mol_{atm}}{1,000,000}}{\Sigma CO_2} \quad (4.9)$$

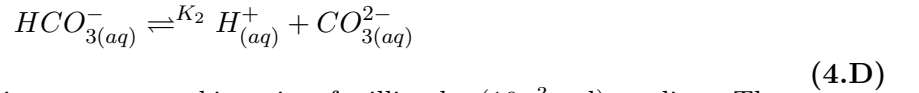
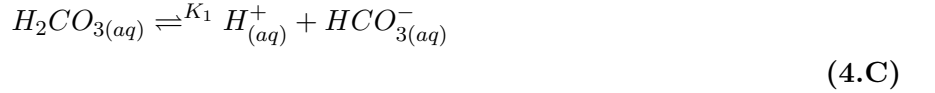
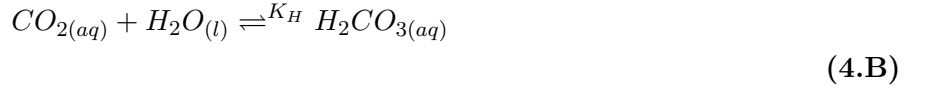
Where CO_{2atm} is the mixing ratio of CO_2 in parts per million, and $Mol_{atm} = 1.773 \cdot 10^{20}$ is the total molar volume of the atmosphere, which was assumed conserved (e.g. Saltzman, 2002). The total moles of CO_2 in the Earth system as a whole was initialised at the current value, $\Sigma CO_2 = CO_{2atm} + CO_{2ocean} = 3.193 \cdot 10^{18}$ moles (Lenton, 2000). However, in practice, non-steady state Carbon Carbon made little difference to glacial exit when chemical continuity between atmosphere and ocean was neglected.

Slushball

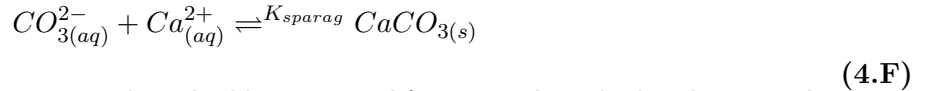
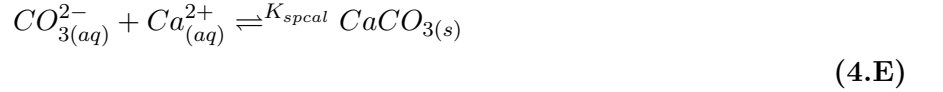
Slushball scenarios involved either steady state carbonate Carbon, in which the dynamics of the total ocean-atmosphere CO_2 reservoir was described by (4.1), or dynamic carbonate Carbon, the change in reservoir size (4.2). In both cases, the atmospheric partial pressure of $CO_{2(g)}$ was determined by explicit equilibration with ocean carbonate chemistry. Even for steady state carbonate Carbon, changes in the atmospheric fraction still differed between slushball and hard snowball scenarios, as a function of the impact of terrestrial carbonate weathering (and by implication climate) on ocean alkalinity.

Ocean carbonate chemistry

Partitioning between aqueous carbonate species used empirically-derived fits for the equilibrium constants of marine carbonate reactions. (As in chapter 1, for clarity chemical reactions are indexed by letter, equations by number). Atmospheric CO_2 dissolves in surface ocean waters as a function of its solubility, K_0 . Dissolved CO_2 molecules make up a low fraction of the total ocean reservoir, because $CO_{2(aq)}$ readily speciates into aqueous Carbonic acid $H_2CO_{3(aq)}$, as a function of the molecule's hydration coefficient K_H , which is then rapidly partitioned into the two main ions, bicarbonate $HCO_{3(aq)}^-$ and carbonate $CO_{3(aq)}^{2-}$, respectively formed by reactions involving equilibrium constants K_1 and K_2 . This speciation is shown in reactions (4.A)-(4.D):



Where all carbonate species are measured in units of millimoles (10^{-3} mol) per litre. The carbonate ion is also withdrawn from the ocean by the precipitation of calcium carbonate - the two major minerals of which, calcite and aragonite, were resolved. These were assumed to precipitate as a function of their respective solubility products (reactions (4.E) and (4.F)):



The equilibrium constants were described by empirical functions described and reviewed in Millero (1995). The solubility of CO_2 in seawater was given by (Weiss, 1974):

$$\begin{aligned} \ln(K_0) = & -60.2409 + 93.4157\left(\frac{100}{T_K}\right) + 23.3585\ln\left(\frac{T_K}{100}\right) + S0.02351 \\ & -S(0.023656\left(\frac{T_K}{100}\right) + 0.0047036\left(\frac{T_K}{100}\right)^2) \end{aligned} \quad (4.10)$$

Where $T_K = T + 273.15$ is planetary temperature in degrees Kelvin, S is salinity, held at the present day value $S_0 = 35$ grams $NaCl_{(aq)}$ per litre of seawater under non-glacial conditions, and raised to $S = 42.5$ during the glacial period. This salinity value is the maximum that the suite of equilibrium constants used here were designed to represent (Millero, 1995), to incorporate the maximum possible impact on ocean salinity of brine expulsion during sea ice formation (Pollard & Kasting, 2005, Lewis et al, 2007). The equilibrium constants K_0 - K_2 are measured in units of moles of reaction per kilogram of solution. The hydration of $CO_{2(aq)}$ was not resolved explicitly; it was assumed that virtually all ocean

CO_2 was in the form of Carbonic acid, i.e. that it was not necessary to differentiate between $CO_{2(aq)}$ and $H_2CO_{3(aq)}$ (Consistent with Millero, 1995). The first and second dissociation constants for Carbonic acid K_1 and K_2 (describing reaction 4.C and 4.D respectively) used a fit taken from Mehrbach et al (1973), refitted and adapted by Dickson & Millero (1987):

$$\text{Log}_{10}(K_1) = -\frac{3670.7}{T_K} + 62.008 - 9.7944\text{Ln}(T_K) + 0.0118S - 0.000116S^2 \quad (4.11)$$

$$\text{Log}_{10}(K_2) = -\frac{1394.7}{T_K} - 4.777 + 0.0184S - 0.000118S^2 \quad (4.12)$$

The carbonate solubility products were taken from Mucci (1983), with K_{spcal} and K_{sparag} representing equilibrium constants for precipitation of calcite and aragonite respectively:

$$\begin{aligned} \text{Log}_{10}(K_{spcal}) = & -171.9065 - 0.07793T_K + \frac{2839.319}{T_K} + 71.595\text{Log}_{10}(T_K) - 0.07711S \\ & + \sqrt{S}\left(-0.77712 + 0.0028426T_K + \frac{178.34}{T_K}\right) \end{aligned} \quad (4.13)$$

$$\begin{aligned} \text{Log}_{10}(K_{sparag}) = & -171.945 - 0.077993T_K + \frac{2903.293}{T_K} + 71.595\text{Log}_{10}(T_K) - 0.1008S \\ & + \sqrt{S}\left(-0.068393 + 0.0017276T_K + \frac{88.135}{T_K}\right) \end{aligned} \quad (4.14)$$

Dynamic carbonate Carbon

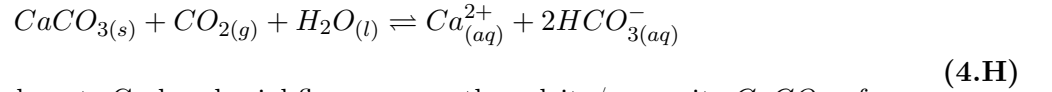
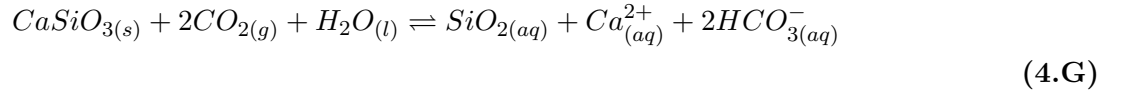
Changes in the partitioning between carbonate ions were calculated numerically, by adapting a method that estimated carbonate alkalinity iteratively by making an initial guess at ocean pH (Watson et al 1995), and coupling it to a dynamic carbonate alkalinity flux from a geochemical box model in which resolution of ocean carbonate speciation had been previously attempted unsuccessfully (Bergman, 2003). Dynamic carbonate Carbon scenarios involved the time derivative of the carbonate Carbon rock reservoir C_R being given by (4.2), and the total atmosphere-ocean CO_2 derivative being a sink for any carbonate Carbon that left this reservoir:

$$\frac{d\Sigma CO_2}{dt} = -\frac{dC_R}{dt} = D + W_{carb} - B_{carb} \quad (4.15)$$

Alkalinity Alk was defined as the normalised magnitude of the cation influx that would be required to conserve charge balance in the ocean, following the carbonate specific alkalinity definition on which the flux $\frac{dAlk}{dt}$ was based (Bergman, 2003). The total ocean alkalinity was defined by the function given by Millero & Sohn (1992):

$$Alk = [HCO_3^-] + 2[CO_3^{2-}] + [B(OH)_4] + [OH^-] - [H^+] + [SiO(OH)_3^-] + [MgOH^+] + 2[HPO_4^{2-}] + 3[PO_4^{3-}] \quad (4.16)$$

Where the square brackets denote the concentration of each ion, and the factor 2 or 3 in front of some ions accounts for the difference in charge (Millero & Sohn, 1992). The total alkalinity was scaled by its present day value of 2.237 millimoles (thousandth of a mole) per litre (Millero & Sohn, 1992). The time derivative of alkalinity was assumed to scale linearly with that of carbonate alkalinity. Neglecting the specific dynamics of B and PO_4 might introduce a degree of inaccuracy, but is unlikely to affect the comparison between hard snowball and open ocean scenarios. As described above, silicate weathering reactions were treated as a source of carbonate alkalinity to the oceans, and the burial reactions relevant to steady state in the Urey reaction were resolved explicitly. Weathering of silicate and carbonate rocks (reactions (4.G) and (4.H) respectively) provided bicarbonate HCO_3^- to the oceans (Saltzman, 2002):



The marine carbonate Carbon burial flux removes the calcite/aragonite $CaCO_{3(s)}$ from the ocean-atmosphere system, hence is effectively the reverse of reaction (4.H), driving the equilibrium from right to left. Because each mole of weathering reaction adds 2 moles of HCO_3^- to the ocean, a factor of 2 appears in the time derivative of carbonate alkalinity, Alk , that relates ocean Carbon chemistry to these fluxes (Bergman, 2003):

$$\frac{dAlk}{dt} = \frac{2}{ov} (W_{carb} + W_{sil} - B_{carb}) \quad (4.17)$$

The volume of the Earth's oceans, ov was assumed conserved at $ov = 1.37 \cdot 10^{21}$ litres (Libby, 1992). Although changes in shallow shelf depositional area, caused by changing ocean volume may significantly effect the marine Carbon cycle within a slushball scenario, the reduced ocean volume $\sim 1.36 \cdot 10^{21}$ that I estimate by subtracting the estimated volume of sea ice (Ridgwell & Kennedy, 2004), made little qualitative difference to the results and was therefore excluded. The main likely source of error in the approach used here was that variation in marine $CO_{2(aq)}$ concentration with depth and with latitude was neglected - i.e. as indicated in equation (4.17), concentration of carbonate alkalinity

was averaged over ocean volume, neglecting any marine stratification. Although there is significant stratification in the marine CO_2 reservoir with depth, that has some influence on the carbonate solubility products K_{spcal} and K_{sparag} in particular (Ridgwell & Zeebe, 2005), the magnitude of these sorts of effects (i.e. in terms of their potential impact upon net carbonate Carbon burial flux) are assessed, albeit in a parameterized way. carbonate alkalinity was initialised at its present day seawater concentration $Alk_{CO_20} = 2.204mmoll^{-1}$ (thousandths of a mole per litre) (Lewis & Wallace, 1998), then solved iteratively based on changes in these weathering fluxes. It was also necessary to include the dynamics of ocean calcium Ca^{2+} , which are also dictated by the weathering/burial reactions. The ocean-atmosphere Calcium reservoir was initialised at its present value $Ca_0 = 1.37 \cdot 10^{19}$ moles (Bergman, 2003), and its dynamics scaled by weathering fluxes according to:

$$\frac{dCa}{dt} = \frac{1}{ov}(W_{carb} + W_{sil} - B_{carb}) \quad (4.17)$$

It is worth emphasising that this was not intended to give a genuinely illustrative representation of all details of the Calcium cycle as a whole, but rather to help achieve a qualitative comparison between dynamic and steady state carbonate scenarios. Note also that silicate weathering was set to zero during the glacial interval for $T < T_f$. For example, the addition of a Magnesium cycle might change quantitative duration estimates but would have no qualitative impact of the comparative results. The carbonate weathering flux W_{carb} exhibited a square root dependency on atmospheric CO_2 (Berner, 1994, Bergman, 2003), and a temperature dependency developed to correspond to the surface of a pre-vascular plant Earth (Bergman, 2003):

$$W_{carb} = W_{carb0} \sqrt{\frac{CO_2}{CO_{20}}} (1 + 0.087(T - T_0)) \quad (4.18)$$

Where planetary temperature is expressed in celsius as a function of its deviation from present day $T_0 = 15^\circ C$. A number of different carbonate Carbon burial B_{carb} fluxes were used. The baseline flux (4.19) related carbonate burial to the normalised total aqueous CO_2 :

$$B_{carb} = B_{carb0} \frac{Ca}{Ca_0} \frac{(HCO_3^- + CO_3^{2-})}{(HCO_3^- + CO_3^{2-})_0} \quad (4.19)$$

Where Calcium Ca is expressed in moles, and the carbonate CO_3^{2-} and bicarbonate HCO_3^- are in moles per litre and scaled by their present day values $HCO_3^- = 1.772molL^{-1}$ and $CO_3^{2-} = 0.216molL^{-1}$ (Lewis & Wallace, 1998). The stability of the crystal structure of Calcium carbonates in the open ocean (i.e. whether they persist or dissolve) is expressed in terms of the saturation state $\Omega = \frac{[Ca^{2+}][CO_3^{2-}]}{K_{sp}}$, where square brackets denote concentrations of various species in solution, and K_{sp} is the solubility product de-

fined above (Ridgwell & Zeebe, 2005). The burial flux of Calcium carbonates is assumed to be proportional to $(\Omega - 1)^n$ when $\Omega > 1$, and the fraction of marine $CaCO_{3(s)}$ that dissolves when $\Omega < 1$ is proportional to $(1 - \Omega)^n$, n being a parameter expressing how strongly the stability of $CaCO_{3(s)}$ responds to a change in $CO_{3(aq)}^{2-}$ (Zhong & Mucci, 1993) (note that $\Omega - 1 < 1$). I.e. a low value of n implies that the Calcium carbonate burial flux will increase in magnitude in response to a relatively low increase in $CO_{3(aq)}^{2-}$, and that steady state $CO_{3(aq)}^{2-}$ will be restored without requiring a large CO_2 drawdown (via the set of reactions summarised in $CO_{2(aq)} + CO_{3(aq)}^{2-} + H_2O_{(l)} \rightleftharpoons 2HCO_{3(aq)}^-$). As discussed in chapter 1, the proliferation of coccolithophores and foraminifera during the Mesozoic may have resulted in a decrease in the value of n , that is a more efficient buffering of ocean carbonate chemistry as more work is invested by the biosphere in promoting $CaCO_{3(s)}$ precipitation (Ridgwell et al, 2003, Ridgwell & Kennedy, 2004). An abiotic ocean is thought to be characterised by $1.9 < n < 2.8$ (Zhong & Mucci, 1993), and the early Phanerozoic by $n = 1.7$ (Caldeira & Rampino, 1993, Munhoven & Francois, 1996). This entire range was covered by the different simulations shown below, but was found to be significantly less relevant to glacial duration than the balance between carbonate weathering and burial at different temperatures. The default value adopted was $n = 2.8$, corresponding to an ocean without biotic buffering. The saturation state was calculated separately for calcite and aragonite:

$$\Omega_{cal} = \frac{[Ca^{2+}][CO_3^{2-}]}{Ksp_{cal}} \quad (4.20)$$

$$\Omega_{arag} = \frac{[Ca^{2+}][CO_3^{2-}]}{Ksp_{arag}} \quad (4.21)$$

With the respective solubility constants defined in equations (4.13) and (4.14) above. The value of the saturation state was then averaged over all $CaCO_{3(s)}$ formed using the fraction of total carbonate burial made up by aragonite, $f_{arag} = \frac{1}{10}$ (Zhong & Mucci, 1993), producing the overall saturation state used in the carbonate burial flux B_{carb} :

$$\Omega = (1 - f_{arag})\Omega_{cal} + f_{arag}\Omega_{arag} \quad (4.22)$$

$$B_{carb(\Omega>1)} = B_{carb0}(\Omega - 1)^n \quad (4.23)$$

$$B_{carb(\Omega<1)} = B_{carb0}(1 - \Omega)^n \quad (4.24)$$

A critical parameter relevant to the feasibility of glacial recovery was the relative mag-

nitude of the carbonate weathering influx and carbonate burial efflux from the oceans. In some simulations therefore, carbonate burial was dynamic, as defined in (4.19), and carbonate weathering was related to it by a proportionality parameter R :

$$W_{carb} = W_{carb0} \frac{B_{carb}}{B_{carb0}} R \quad (4.25)$$

Solution method and convergence criterion

If two of the four ocean chemistry parameters (a) pH , (b) Alkalinity, (c) total CO_2 , $\Sigma CO_2 = CO_{2(aq)} + HCO_{3(aq)}^- + CO_{3(aq)}^{2-} + H_2CO_{3(aq)}$ and (d) atmospheric $CO_{2(g)}$ partial pressure, then the relationships between them are sufficiently well constrained that it is possible to calculate the other two (Millero & Sohn, 1992). The ocean chemistry subroutine used here to calculate ocean-atmosphere fractionation used alkalinity and total CO_2 in order to calculate pH via an iterative convergence criterion. Total alkalinity was defined as per equation (4.16), and was distinguished from carbonate alkalinity (Millero & Sohn, 1992):

$$Alk_{CO_2} = [HCO_3^-] + 2[CO_3^{2-}] = Alk - \Sigma B_i \quad (4.26)$$

Where $\Sigma B_i = [B(OH)_4] \dots$ etc, i.e. all bases other than carbonate and bicarbonate. The various components of carbonate alkalinity were calculated from the empirically-constrained fit (Millero & Sohn, 1992):

$$[CO_2] = \Sigma CO_2 - Alk_{CO_2} + \frac{(Alk_{CO_2} - \Sigma CO_2) \frac{K_1}{K_2} + \sqrt{Alk_{CO_2} (4 - \frac{K_1}{K_2}) + \Sigma CO_2 \frac{K_1}{K_2})^2 + 4(\frac{K_1}{K_2} - 4) Alk_{CO_2}^2}}{2(\frac{K_1}{K_2} - 4)} \quad (4.27)$$

$$[HCO_3^-] = \frac{\Sigma CO_2 K_2 - \frac{K_1}{K_2}}{K_2 - 4} \quad (4.28)$$

$$[CO_3^{2-}] = \frac{(Alk_{CO_2} - \Sigma CO_2) \frac{K_1}{K_2} - 4 Alk_{CO_2} + \sqrt{Alk_{CO_2} (4 - \frac{K_1}{K_2}) + \Sigma CO_2 \frac{K_1}{K_2})^2 + 4(\frac{K_1}{K_2} - 4) Alk_{CO_2}^2}}{2(\frac{K_1}{K_2} - 4)} \quad (4.29)$$

In order to calculate the value of the various species above, it was necessary to obtain a unique value of ocean pH and (non-carbonate) alkalinity. These were given by the empirical fits in the above functions (Millero & Sohn, 1992, Millero, 1994). Inorganic alkalinity sources were given by total boron concentration $\Sigma B = [B(OH)_4^-] + [B(OH)_3]$, in micro mol per litre, assumed to scale with salinity $\Sigma B = 0.01212S$, and experiencing partitioning by equilibrium constant $K_B = \frac{[H^+][B(OH)_4^-]}{[B(OH)_3]}$. Inorganic alkalinity was also, of course, affected by changes in the concentration of free $[OH^-]$ ions, dictated by the

dissociation constant of water $K_W = [H^+][OH^-]$. :

$$\Sigma B_i = Alk - \left(\frac{K_B \Sigma B}{H + K_B} \right) + [H^+] - \frac{K_W}{[H^+]} \quad (4.30)$$

The equilibrium constant K_B dictating boron speciation was a function of various inorganic ions, temperature, and salinity (Millero & Sohn, 1992, Millero, 1994):

$$\begin{aligned} \ln(K_B) = & 148.0248 + (137.194 + 0.053105T_K)\sqrt{S} + 1.62247S \\ & + \frac{1}{T_K}(1.726S^{1.5} - 0.0993S^2 - 8966.901 - 2890.51\sqrt{S} - 77.942S) - (24.434 - 25.085\sqrt{S} - 0.2474S)\ln(T_K) \\ & + \ln(1 - 0.001005S) + \ln\left(\frac{1 + [SO_4]K_{HSO_4} + K_{HF}[F] \cdot 0.00007 \frac{S}{35}}{1 + [SO_4]K_{HSO_4}}\right) \end{aligned} \quad (4.31)$$

With the concentration of dissolved sulphate related to salinity $[SO_4] = 0.0293 \frac{S}{35}$, and inorganic alkalinity equilibrium constants of sulphuric acid $K_{HSO_4} = \frac{[HSO_4][H^+]}{[H_2SO_4]}$ and hydrogen fluoride $K_{HF} = \frac{[F^-][H^+]}{[HF]}$ given by (Millero, 1994):

$$\ln(K_{HSO_4}) = 647.59 \frac{1}{T_K} - 6.3451 + 0.019085T_K - 0.5208 \sqrt{\frac{19.92S}{1000 - 1.0049S}} \quad (4.32)$$

$$\ln(K_{HF}) = 12.641 - 1.525\sqrt{T} - 1590.2 \frac{1}{T_K} \quad (4.33)$$

$$\begin{aligned} \ln(K_W) = & 148.9802 - 13847.26 \frac{1}{T_K} + (1.0495\ln(T_K) + 118.67 \frac{1}{T} - 5.977)S^{0.5} \\ & - 23.6521\ln(T_K) - 0.01615S \end{aligned} \quad (4.32)$$

The dynamics of phosphates, silicates and magnesium were neglected, these components merely being absorbed into the starting value $Alk_0 = 2.3089$ millimoles per litre (Bergman, 2003). Seawater temperature T is expressed in these function in Kelvin, and was constrained to a minimum of $T_K = 271.35$, equivalent to -1.8°C if planetary average temperature fell below freezing. I.e. it was assumed that the latent heat of dissolution provided by seawater salinity provided sufficient thermal inertia to prevent the oceans freezing regardless of the air temperature. All of the above functions required a unique value for hydrogen ion concentration $[H^+]$. An iterative method was used to solve for the $[H^+]$

value that would force the $[CO_2]$ to converge to within a range equivalent atmospheric values differing by less than 1 part per million. This, in turn, was achieved by iteratively repeating the calculation of carbonate alkalinity from total alkalinity, using estimates of $pH = -\text{Log}_{10}([H^+])$ corresponding to the carbonate equilibrium constants K_1 and K_2 , until the pH value implicit from each of these constants was in agreement. (These constants were calculated at the first time step using a “guess” of present day $[H^+]_0 = 7.0 \cdot 10^{-19}$ micromol/litre, then the loop allowed to iterate until an accurate value was reached). The H^+ in equilibrium with ocean carbonate chemistry at time $t + 1$ was given by:

$$H_1 = \frac{K_1[CO_2]}{[HCO_3^-]} \quad (4.33)$$

$$H_2 = \frac{K_2[HCO_3^-]}{[CO_3^{2-}]} \quad (4.34)$$

And the convergence criterion was set as:

$$\left| 1 - \frac{\sqrt{H_1 \cdot H_2(t+1)}}{\sqrt{H_1 \cdot H_2(t)}} \right| < 0.002 \quad (4.35)$$

If condition (4.35) was not true, then the hydrogen ion concentration was set to the new value $[H^+] = \sqrt{H_1 \cdot H_2(t+1)}$, and this value used to recalculate inorganic alkalinity (by equation (4.30)) thus carbonate alkalinity (by equation (4.26)), thus the relative partitioning between carbonate ions. Once the ocean $[H^+]$ had converged, the atmospheric CO_2 was calculated using the solubility constant K_0 (which is expressed in moles per kilogram per atmosphere):

$$CO_{2(g)} = \frac{1000[CO_2]}{K_0} \quad (4.36)$$

The atmospheric fraction Φ of the total ocean-atmosphere CO_2 reservoir was then recalculated according to equation (4.9) assuming a constant molar volume of the atmosphere. Finally, it was necessary to induce a condition to allow the system to converge when dealing with very large total ΣCO_2 reservoir sizes.

Figure (4.1) shows the effect on the atmospheric fraction of an artificially imposed reservoir size increase under present day luminosity conditions. This figure illustrates the familiar result that the atmospheric fraction of the CO_2 reservoir increases as a sigmoidal function of the total reservoir size. In effect, at relatively large total reservoir sizes, the ocean becomes increasingly acidified, and protonation of the carbonate ion causes the overall “equilibrium” $CO_{2(aq)} + CO_{3(aq)}^{2-} + H_2O_{(l)} \rightleftharpoons 2HCO_{3(aq)}^-$ to be shifted to the right. Although $CO_{2(aq)}$ still represents a small fraction of all carbonate ions, the atmospheric fraction increases because

the ocean effectively becomes saturated with CO_2 . This is, of course, part of the scenario originally invoked to explain cap carbonates within a “hard snowball” scenario (Kirschvink, 1992). Under these conditions, the values obtained for the equilibrium constants used above became unrepresentative, and the equilibration of CO_2 between the ocean and atmosphere became solely a function of the solubility K_0 and the amount by which the total CO_2 reservoir exceeded the total alkalinity. I.e. there came a point when marine carbonate alkalinity was sufficiently high that explicit resolution of all chemical speciation could be bypassed- because atmospheric CO_2 fractionation was determined only by the solubility. The computational criterion used to switch to this method of calculating atmospheric CO_2 was that $0.001[HCO_3^-] > [CO_3^{2-}]$:

$$(CO_{2(g)})_{0.001[HCO_3^-] > [CO_3^{2-}]} = \frac{1000(\Sigma CO_2 - Alk)}{K_0} \quad (4.37)$$

It was found that the numerical choice of this criterion made little qualitative difference to the results, and could be replaced with the condition $\Sigma CO_2 > Alk$, without loss of applicability.

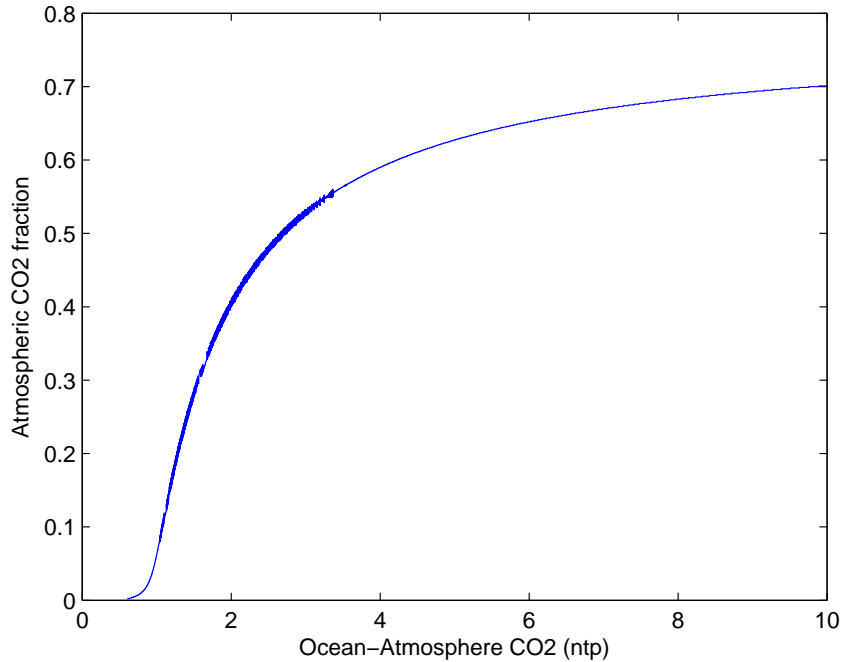


Figure 4.2. The relationship between atmospheric CO_2 fraction Φ (y-axis) and the total size of the ocean-atmosphere CO_2 reservoir (x-axis). The ocean chemistry was forced with an artificially imposed increase in total reservoir size ΣCO_2 with temperature fixed at $T = 288.15K$. “ntp” denotes normalised to present value.

Results

Figure 4.2 shows the effect on the atmospheric fraction Φ of increasing the total atmosphere-ocean reservoir size ΣCO_2 , demonstrating how, at high reservoir sizes, the atmospheric fraction reaches an upper limit as a function of the relative magnitude of the equilibrium constants, even when temperature is (artificially) held constant. At reservoir sizes close to the present, increasing the size of the total pool causes an increase in the atmospheric fraction, before starting to asymptote to a maximum fraction (which probably represents the limits of the applicability of the equilibrium constants used here). The imposition of a fixed temperature highlights the importance of total reservoir size ΣCO_2 as a variable in its own right, but, of course, limits the applicability of the results. The key point illustrated by figure (4.2) is that the ocean has a discrete capacity to absorb CO_2 , hence it is logical to suppose that an atmosphere at equilibrium with the ocean will experience different CO_2 dynamics than an isolated atmosphere - hence that hard snowball and slushball glacial intervals will have different durations. This is supported by the remaining results.

Degassing magnitude and apportioning

Figure (4.3) is the most important of the results shown in this chapter, because it indicates that the duration of a slushball glacial interval should be qualitatively shorter than that of a hard snowball, hence providing a simple test for distinguishing between the two scenarios, in line with previous more qualitative predictions (Hoffman & Schrag, 2002). This figure refers to steady state carbonate Carbon, so that the dynamics of atmospheric CO_2 were dictated by the various parameter choices according to (4.7); namely the fraction of the degassing flux that enters the atmosphere directly. The results refer to the duration of a glacial interval imposed by artificially decreasing atmospheric CO_2 in an incremental way (i.e. over timescales greater than $\sim 10,000$ years, allowing the system to equilibrate to that partial pressure). Luminosity was held constant at $S = 1300 W m^{-2}$ corresponding to 600Ma by equation (3.2). The atmospheric CO_2 level corresponding to deglaciation at this luminosity was around 30,000 parts per million, consistent with previous estimates in high resolution models (Hoffman & Schrag, 2002, Pierrehumbert, 2005). The Y-axis shows the length of time required to reach a glacial exit temperature fixed at $T_i = -20^\circ C$ (a lower limit, (Pierrehumbert, 2005), discussed below), the X-axis the magnitude of the CO_2 degassing flux D , relative to the present day value. Blue line shows the atmospheric fraction held constant at an approximate estimate of its present day value $\Phi_0 = 0.01614$ (Bergman, 2003). The only factor changing the amount of CO_2 in the atmosphere was the total reservoir size, which increased as a function of degassing rate D (set to the present day value). The blue line is therefore an unrealistic state to be used for comparison only - as it corresponds to a scenario in which the ocean is (implicitly) at equilibrium with the atmosphere, but carbonate Carbon (equation (4.2)) is at steady state, and the relationship

between atmospheric fraction and reservoir size shown in figure (4.1) is simply a flat line parallel with the X-axis, and the magnitude of the degassing rate is all that influences glacial duration at a given luminosity. It is clear that even at the present day value of D , glacial duration is still too long to fit even the most approximate estimates of glacial duration (3 – 30Ma, (Hoffman & Schrag, 2002)). An increase in the atmospheric fraction Φ of CO_2 is therefore needed to recreate glacial intervals of realistic duration - the question is whether this occurred in the context of a hard snowball or a slushball scenario.

The green line shows an atmospheric CO_2 fraction Φ fully equilibrated with the ocean chemistry, i.e. determined by equation (4.9) where $CO_{2(g)}$ was determined by equation (4.36). The red line shows a scenario in which the atmosphere was implicitly isolated from the ocean, and the atmospheric fraction simply responded to the relative apportioning of degassing D between the atmosphere and ocean according to (4.7), with atmospheric fraction of degassing flux $c = 0.5$, a conservative estimate designed not to bias the system to long glacial intervals (Pierrehumbert, 2005, Higgins & Schrag, 2003). Even with this scaling, it is clear that a slushball solution, in which the atmospheric CO_2 fraction is at equilibrium with ocean chemistry, produces qualitatively shorter estimates for glacial duration than does a hard snowball scenario. This conclusion depends on the choice of the parameter c , the atmospheric fraction of the degassing flux. The duration of a slushball depends only on the interaction between reservoir size and ocean chemistry, atmosphere-ocean apportioning of any changes in the reservoir size are, by definition, not relevant. Constraining the atmospheric degassing fraction c (discussed further in the concluding section, but assumed by default to scale roughly with relative planetary surface area $c \simeq \frac{1}{3}$ (Higgins & Schrag, 2003)) is therefore likely to be the point of departure in any attempt to resolve the snowball-slushball debate via different estimates of glacial duration.

Figure (4.4) shows how glacial duration of a hard snowball interval (i.e. with Φ given by (4.9) and atmospheric CO_2 given by (4.7)) is log-linear with the exit threshold temperature T_i (X-axis), with absolute duration (Y-axis, note natural log scale) dictated by the atmospheric fraction c of the degassing flux. Figure (4.4) reiterates the key point that attempting to resolve the snowball-slushball debate by estimates of glacial duration hinges on the choice of the atmospheric CO_2 degassing fraction. Figure 4.5(a) shows a slushball scenario in which the atmospheric fraction Φ is dictated by ocean chemistry; left Y-axis shows the duration in millions of years, right Y-axis shows the atmospheric CO_2 partial pressure (in bars). The X-axis shows the temperature threshold that corresponds to deglaciation. Figure 4.5(b) is virtually identical, but shows the results of all the different hard snowball scenarios shown in (4.3) (i.e. all the different parameter choices for the atmospheric fraction of the degassing flux c . The deglaciation partial pressures are identical in both systems, and are not shown in figure 4.5(b) for clarity). This illustrates how the parameter c is the factor by which a hard snowball scenario can be expected to have a shorter duration. This

issue is formalised in the concluding section. Table 4.1 shows in more detail the impact of ocean chemistry on the interaction between total atmosphere-ocean CO_2 , ΣCO_2 , the atmospheric fraction of the reservoir Φ , the atmospheric partial pressure and the duration of the glacial interval at different threshold temperatures. Table (4.1) refers to a steady state carbonate Carbon scenario. At the luminosity values chosen, an exit threshold warmer than $-4^\circ C$ required non-physical CO_2 partial pressures in the atmosphere. Warmer exit thresholds may be feasible (Pierrehumbert, 2005), but were not found in this study, due to a combination of the luminosity choice and the slightly arbitrary temperature function used. The key issue however, is that the qualitative conclusion that a slushball can be expected to be significantly shorter than a hard snowball nevertheless still holds.

Dynamic carbonate Carbon and atmospheric equilibration

Figure (4.6) shows the glacial interval duration produced from various degassing flux/exit temperature parameter combinations under a dynamic carbonate Carbon scenario in which CO_2 was determined by (4.2), and carbonate weathering W_{carb} and burial B_{carb} by (4.18) and (4.19) respectively. Y-axis shows duration of the glacial interval (Ma), X-axis shows the magnitude of the degassing flux D in comparison to the present day value. The duration of the glacial interval is dictated by the exit temperature threshold T_i (legend), with gradient dictated by the degassing magnitude D . A more meaningful depiction of the importance of carbonate dynamics is given by figure (4.7), which shows the expected glacial duration under various formulations of the marine carbonate Carbon burial flux B_{carb} . Longer estimates of duration of the glacial interval are obtained from using a dependency of B_{carb} on the ocean saturation state Ω the abiotic dependency $n = 2.8$ corresponding to a pre-Coccolithophore ocean (Ridgwell et al, 2003) implying a relatively weak dependency of the burial flux on ocean $CO_{3(aq)}^{2-}$, so that low ΣCO_2 causes a relatively weak negative feedback on the burial flux B_{carb} , meaning that the flux constrains atmospheric buildup. This reflects the wider issue of the strong relationship between the atmosphere-ocean fractionation of CO_2 , dictated by the balance R between carbonate weathering influx and carbonate burial (as defined in equation (4.25), explored in more detail in table 4.3 and figure (4.8). Finally, the duration of the glacial interval in hard snowball and two different slushball scenarios is shown in figure (4.9), for an arbitrary, but reasonable, set of parameter choices.

Plots and numerical results

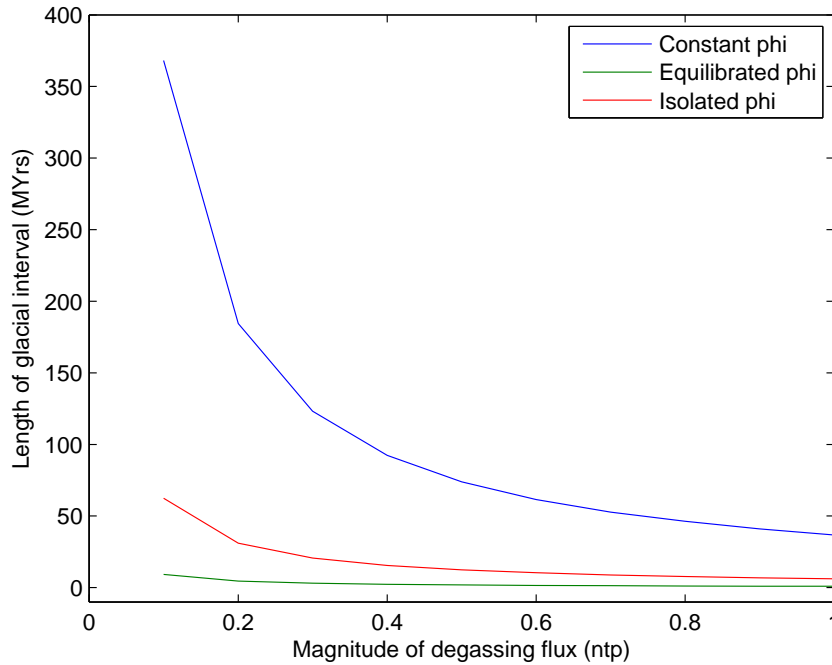


Figure 4.3. The impact of different scenarios for the ocean-atmosphere fractionation of on an artificially imposed glacial interval. A glaciation was forced by initialising the planetary albedo at the ice covered value. The exit threshold was constrained at -20 celsius, corresponding to an exit value of approximately 0.03bar (30000 parts per million), and luminosity held at $1300Wm^{-2}$, corresponding to $600MA$. “Constant phi” (red line) refers to the atmospheric fraction being constrained at its present value $\Phi = 0.01614$, “Equilibrated phi” to the atmospheric fraction resulting from a chemically continuous atmosphere and ocean (i.e. a slushball scenario) and “Isolated phi” to a hard snowball scenario in which the atmospheric fraction varied as a result of apportioning of the degassing flux as per equation (4.7) with the degassing atmospheric fraction at $c = \frac{1}{2}$. Y-axis shows the length of the glacial interval in millions of years, X-axis shows the CO_2 degassing flux normalised to the present value.

D fraction $c \setminus T_i(\text{celsius})$	-4	-6	-8	-10	-12	-14	-16	-18	-20
0.01	2440.6	1339.4	922.3	601.8	403.4	221.4	148.4	90.017	54.5
0.1	244.7	148.4	99.4	60.3	40.4	24.53	16.44	9.0	6.0
0.5	54.6	33.115	20.08	13.46	8.166	4.95	3.0	2.01	1.22
0.99	22.19	16.4	9.03	6.69	3.67	2.46	1.648	1.0	0.549

Table (4.1) - Duration of a hard snowball scenario (in millions of years) under different parameter choices for the exit threshold temperature T_i and fraction c of the CO_2 degassing flux entering the atmosphere directly. These results are equivalent to those expressed graphically on a natural log scale in figure (4.3).

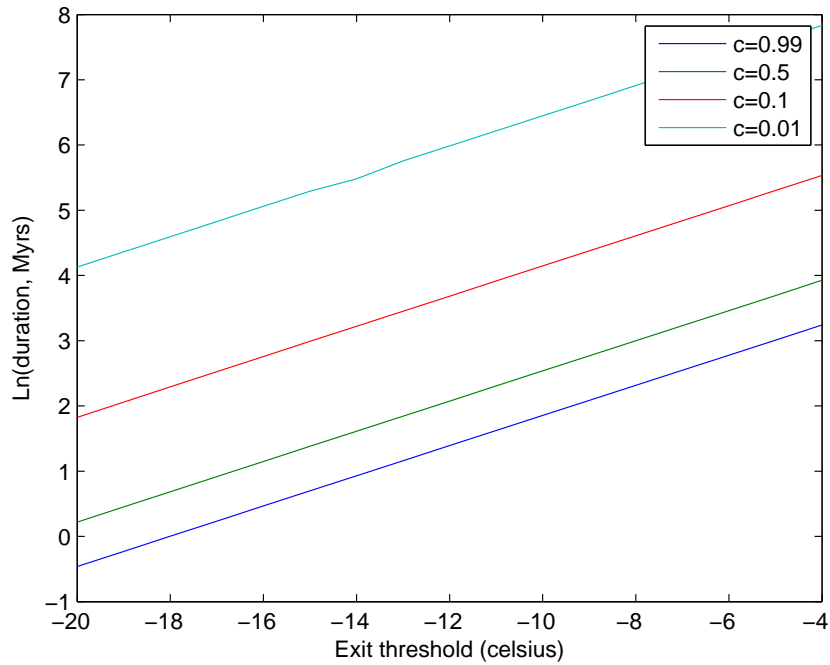


Figure 4.4 The impact of the atmospheric fraction c of the degassing flux (as discussed in equations 4.14 and 4.15) on the duration of a hard snowball lacking ocean-atmosphere chemical continuity, subject to different ice-albedo instability thresholds and with luminosity held at $1300Wm^{-2}$. Y-axis shows natural logarithm of the length of the glacial interval in millions of years, X-axis the value of T_i , the temperature threshold (in celsius) corresponding to an ice-covered planet, and the temperature that must be exceeded for deglaciation.

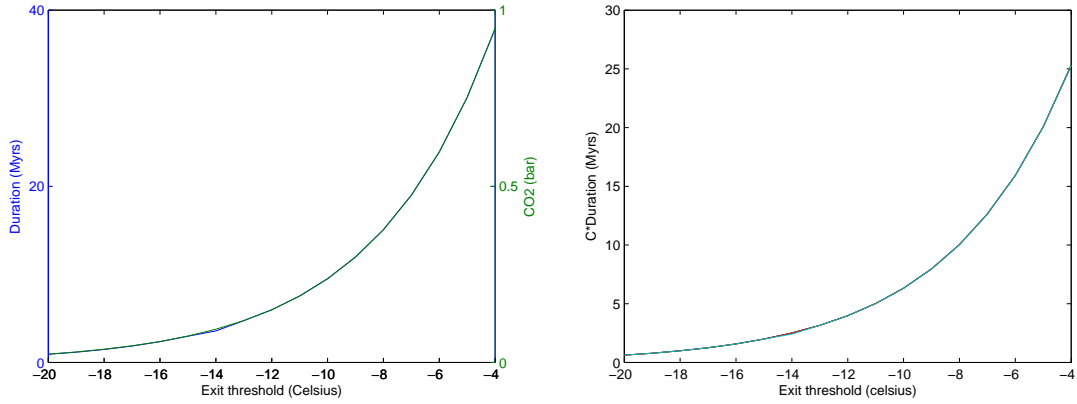


Figure 4.5 (a) Duration constraints of a glacial interval in which the ocean and atmosphere are chemically equilibrated but in which the dynamics of carbonate Carbon are set to zero $\frac{dR}{dt} = 0$ and therefore do not influence ocean carbonate speciation or atmosphere-ocean fractionation. X-axis shows the value of T_i , left Y -axis the length of the glacial interval in millions of years. Right Y-axis shows the value of atmospheric CO_2 in bars. Note further that the most reasonable estimates of glacial duration, exit CO_2 , and T_i coincide, at $T_i \approx 15$ Celsius, and that the identical shape to Figure 4.4(b), illustrating how glacial duration is linear with CO_2 when the ice-albedo system is discretized. **(b)** Under hard snowball conditions at constant degassing rate D , the atmospheric fraction of degassing rate, C , is the only determinant of glacial duration. X-axis is identical to Figure 4.4(a). Y-axis shows the length of the glacial interval in millions of years, multiplied by the atmospheric degassing fraction C . Note that multiple C value scenarios shown in figure 4.4(a) are shown in this plot; the same relationship with duration holds regardless of the parameter value - a feature amenable to testing in more complex climate models.

T_i (Celsius)	Length of glacial interval (Myrs)	ΣCO_2 (normalised)	Φ	CO_2 (ppm)
-20	0.926	2.922	0.448	23566
-19	1.168	3.433	0.480	29688
-18	1.478	4.077	0.509	37400.9
-17	1.867	4.890	0.535	47114.6
-16	2.359	5.916	0.557	59355.6
-15	2.978	7.202	0.577	74774.3
-14	3.758	8.825	0.593	94199.5
-13	4.742	10.870	0.606	118668.9
-12	5.981	13.477	0.617	149496.5
-11	7.541	16.693	0.626	188334.6
-10	9.507	20.782	0.634	237261.1
-9	11.976	25.934	0.64	298899.8
-8	15.076	32.424	0.645	376551.9
-7	18.980	40.6	0.649	474374.2
-6	23.900	50.9	0.652	597612.1
-5	30.098	63.876	0.654	752868.7
-4	37.906	80.223	0.656	948455.6

Table 4.2 Conditions at glacial exit for a continuous atmosphere and ocean with steady state carbonate Carbon.

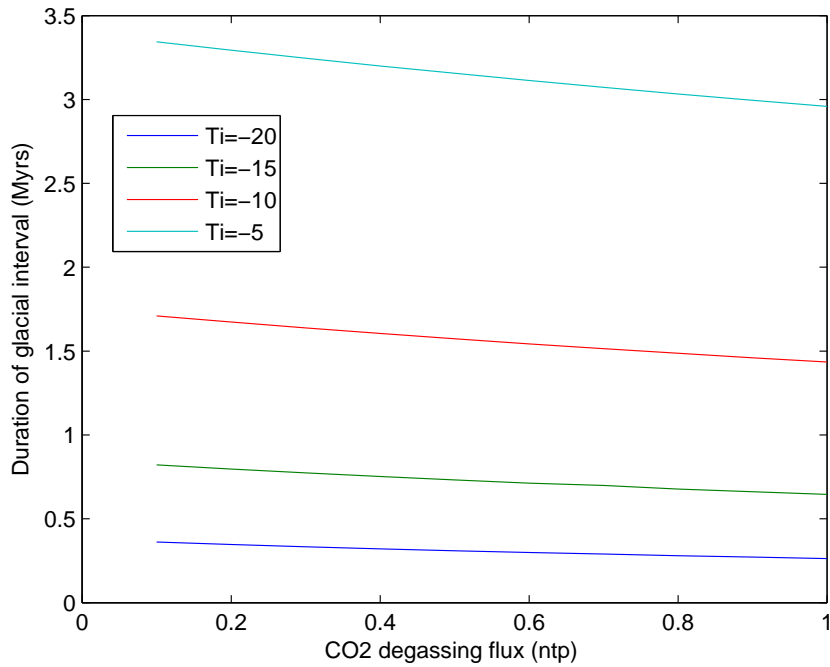


Figure 4.6 Impact of degassing rate D (X-axis) on the duration of the glacial interval in which carbonate weathering W_{carb} and carbonate burial B_{carb} are dynamic, given by equations 4.49 and 4.47 respectively. Note that carbonate Carbon burial B_{carb} was non-zero only when the calcite-aragonite apportioned value of $CaCO_3$ saturation, Ω_{total} , given by equation (4.40) was greater than unity. Duration of the glacial remains linear in CO_2 , but not necessarily in degassing rate, under this sort of dynamical scenario.

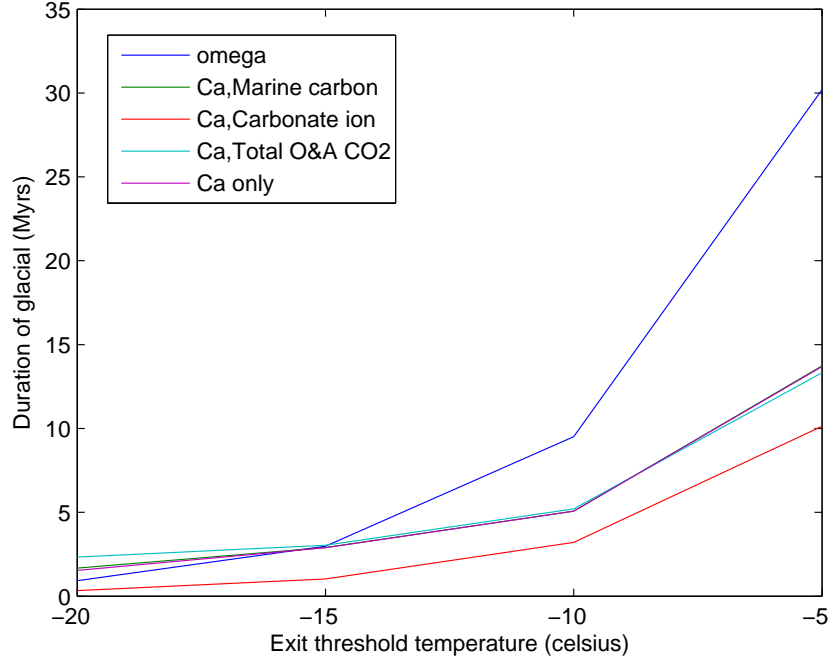


Figure 4.7 The impact of various marine carbonate Carbon burial functions on the duration of a glacial interval in which carbonate weathering W_{carb} is held constant at its present value. X-axis shows the exit threshold temperature T_i in celsius, Y-axis the duration of the glacial interval in millions of years. Luminosity held at $1300Wm^{-2}$, corresponding to 600MA. “omega”, (blue) refers to $B_{carb} = B_{carb(0)}(\Omega_{total} - 1)^{2.8}$, “Ca, Marine Carbon”, to $B_{carb} = B_{carb(0)} \frac{[Ca^{2+}]}{[Ca^{2+}]_0} \cdot \frac{([HCO_3^-] + [CO_3^{2-}])}{([HCO_3^-]_0 + [CO_3^{2-}]_0)}$, “Ca, carbonate” to $B_{carb} = B_{carb(0)} \frac{[Ca^{2+}]}{[Ca^{2+}]_0} \cdot \frac{[CO_3^{2-}]}{[CO_3^{2-}]_0}$, “Ca, total O&A CO_2 ” to $B_{carb} = B_{carb(0)} \frac{[Ca^{2+}]}{[Ca^{2+}]_0} \cdot \frac{\Sigma CO_2}{\Sigma CO_2(0)}$, “Ca” to $B_{carb} = B_{carb(0)} \frac{[Ca^{2+}]}{[Ca^{2+}]_0}$.

Table 4.3 The impact of the carbonate weathering:burial ratio parameter on the duration of an imposed glacial interval during which carbonate burial is held constant at its present value $B_{carb} = B_{carb(0)}$. carbonate weathering was related to carbonate burial by the ratio R , via equation 4.41 $W_{carb} = W_{carb(0)} \cdot \frac{B_{carb}}{B_{carb(0)}} \cdot R$. For scenarios in which $R < 1$, marine CO_2 remained too low for exit from the glacial period. Luminosity $L = 1313 Wm^{-2}$. Note that as the normalised carbonate weathering:burial ratio R , declines, normalised degassing rate D becomes increasingly important in order to build up adequate CO_2 to end the glacial interval, which is not possible in scenarios marked “n/a”. These duration estimates are in agreement with the idea that a relatively low degassing rate D is required for glacial entry (Tajika, 2004).

Table 4.3(a), $T_i = -20$ celsius. Duration figures are in millions of years (Myrs):

$R = \frac{W_{carb}/W_{carb(0)}}{B_{carb}/B_{carb(0)}}$	Duration $\frac{D}{D_0} = 1$	Duration $\frac{D}{D_0} = 0.5$	Duration $\frac{D}{D_0} = 0.1$	Duration $\frac{D}{D_0} = 0.01$
2.0	0.495	0.618	0.841	0.915
1.9	0.516	0.713	1.026	1.139
1.8	0.580	0.841	1.316	1.508
1.7	0.663	1.027	1.837	2.236
1.6	0.772	1.317	3.045	4.323
1.5	0.925	1.840	8.918	n/a
1.4	1.155	3.052	n/a	n/a
1.3	1.538	n/a	n/a	n/a
1.2	2.301	n/a	n/a	n/a
1.1	2.665	n/a	n/a	n/a
1.0	2.963	n/a	n/a	n/a

Table 4.3(b), $T_i = -15$ celsius.

$R = \frac{W_{carb}/W_{carb(0)}}{B_{carb}/B_{carb(0)}}$	Duration $\frac{D}{D_0} = 1$	Duration $\frac{D}{D_0} = 0.5$	Duration $\frac{D}{D_0} = 0.1$	Duration $\frac{D}{D_0} = 0.01$
2.0	1.490	1.984	2.70	2.939
1.9	1.665	2.288	3.297	3.660
1.8	1.861	2.702	4.233	4.851
1.7	2.126	3.299	5.912	7.194
1.6	2.479	4.237	9.803	13.923
1.5	2.974	5.923	28.736	n/a
1.4	3.490	7.857	n/a	n/a
1.3	3.938	9.426	n/a	n/a
1.2	4.333	n/a	n/a	n/a
1.1	4.721	n/a	n/a	n/a
1.0	5.019	n/a	n/a	n/a

Table 4.3(c), $T_i = -10$ celsius.

$R = \frac{W_{carb}/W_{carb(0)}}{B_{carb}/B_{carb(0)}}$	Duration $\frac{D}{D_0} = 1$	Duration $\frac{D}{D_0} = 0.5$	Duration $\frac{D}{D_0} = 0.1$	Duration $\frac{D}{D_0} = 0.01$
2.0	4.742	6.315	8.598	9.358
1.9	6.065	7.2734	10.495	11.66
1.8	7.248	8.602	13.477	15.452
1.7	8.159	12.071	18.834	22.920
1.6	8.889	16.287	31.263	44.406
1.5	9.495	18.963	93.735	n/a
1.4	10.011	20.897	n/a	n/a
1.3	10.459	22.466	n/a	n/a
1.2	10.859	n/a	n/a	n/a
1.1	11.242	n/a	n/a	n/a
1.0	11.541	n/a	n/a	n/a

Table 4.3(d), $T_i = -5$ celsius.

$R = \frac{W_{carb}/W_{carb(0)}}{B_{carb}/B_{carb(0)}}$	Duration $\frac{D}{D_0} = 1$	Duration $\frac{D}{D_0} = 0.5$	Duration $\frac{D}{D_0} = 0.1$	Duration $\frac{D}{D_0} = 0.01$
2.0	24.999	20.056	27.31	29.728
1.9	26.754	23.136	33.345	37.043
1.8	27.944	43.981	42.825	49.096
1.7	28.851	53.431	59.854	72.841
1.6	29.581	57.671	93.355	141.127
1.5	30.187	60.349	299.736	n/a
1.4	30.703	62.283	n/a	n/a
1.3	31.152	63.852	n/a	n/a
1.2	31.546	n/a	n/a	n/a
1.1	31.934	n/a	n/a	n/a
1.0	32.232	n/a	n/a	n/a

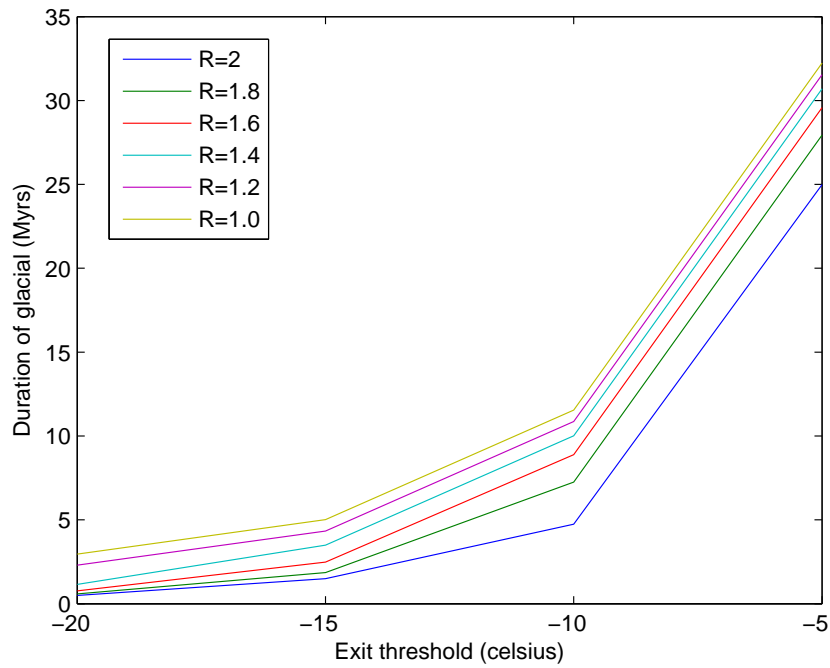


Figure 4.8 - The effect of ratio of carbonate Carbon weathering:burial fluxes $R = \frac{W_{carb}/W_{carb0}}{B_{carb}/B_{carb0}}$ (legend) on the duration (Y axis, millions of years) of a slushball scenario in which deglaciation occurs at different threshold temperatures (X-axis, celsius). Solar luminosity held constant at $S = 1300.16 W m^{-2}$, equivalent to 600 Ma. Degassing flux held constant at present value $D_0 = 6.65 \cdot 10^{12}$ moles C per year.

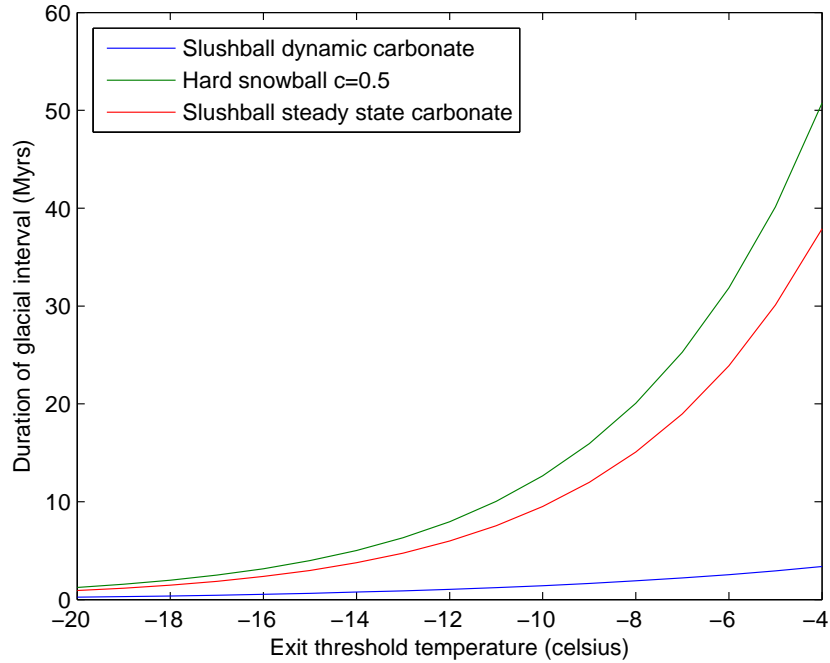


Figure 4.9 - Expectations of glacial duration under three realistic model scenarios. Y-axis shows duration of the glacial interval in millions of years, X-axis shows the glacial exit temperature T_i . Blue line shows CO_2 time derivative given by equation (4.24) with dynamic carbonate weathering scaled by a baseline $0.5 \cdot W_{carb(0)}$ i.e. half its present value. Carbonate burial B_{carb} was set to zero for temperatures below freezing. Green line shows a hard snowball scenario with CO_2 time derivative given by equation (4.11), silicate weathering set to zero below freezing, atmospheric CO_2 fraction Φ given by equation (4.16) and atmospheric degassing fraction $c = 0.5$ (equation 4.14). Red line shows a slushball scenario with atmospheric fraction Φ and CO_2 partial pressure determined by equilibration with ocean chemistry, but with carbonate Carbon held at steady state and CO_2 time derivative given by equation (4.11).

Discussion

Although the model used is of relatively low resolution and necessarily highly parameterised in places, the two conclusions that follow from the work in this chapter are very simple. First, a slushball scenario would be shorter in duration than a hard snowball, by a factor that scales with the fraction c of the CO_2 degassing flux that enters the atmosphere directly. I argue that this parameter, rather than any more complex formulation of (for example) the hydrological cycle, is the key to falsifying the snowball-slushball debate. Second, in order to be recoverable, a slushball scenario requires that a tangible reservoir of carbonate alkalinity persists in the ocean, despite severe glaciation - more specifically that carbonate weathering continues and/or $CaCO_{3(s)}$ precipitation is curtailed during the ice-covered interval. Assuming that carbonate weathering is essentially unaltered by glacial progression amounts to assuming a slushball *a priori*, so any model with this assumption is of no use in comparison between the two scenarios. I argue that the most realistic slushball scenario involves the influx of carbonate alkalinity to the ocean via carbonate weathering being significantly curtailed, by ice cover and low temperatures - in conjunction with an equivalent negative feedback on marine $CaCO_{3(s)}$ precipitation. The latter process assumes that $CaCO_{3(s)}$ precipitation, even before the origin of coccolithophores and the radiation of foraminifera, was linked to the marine biosphere, and therefore declined as lower temperatures reduced marine productivity.

Comparison with prior estimates of glacial duration

There is substantial uncertainty in estimates of the length of Neoproterozoic glacial intervals. Hoffman & Schrag give a range of between 3 – 30Ma (Hoffman & Schrag, 2002). This large range is consistent with estimates from *Ir* accumulation, for which the favoured length was estimated to be around 12Myrs (Bodieselitsch et al, 2005). At current degassing rates, my results show that duration of this order is compatible with a low glacial exit threshold $-16^\circ C > T_i > -18^\circ C$ if the atmospheric fraction $c = 0.1$, up to a milder constraint of $-8^\circ C > T_i > -6^\circ C$ as 99% of the glacial interval degassing flux is poured into the atmosphere. The actual values of these temperature thresholds are admittedly less accurate than the estimates that would result from a higher resolution modelling study, but are consistent with estimates from such studies (Pierrehumbert, 2005). Note that a planetary *average* temperature below freezing does not imply that all latitudes are this cold at all times throughout the year, hence may allow sufficient cumulative ice retreat for the reverse ice-albedo feedback to occur (Pierrehumbert, 2005). In this context, the parameterisation of the exit threshold of $T_i = -4^\circ C$ is conservatively warm, relative to previous estimates as low as $T_i = -15^\circ C$ even for contemporary luminosity (North et al, 1985). Glacial duration estimates of the order of 12Ma reproduce $-9^\circ C > T_i > -8^\circ C$ in my steady state carbonate slushball formulation, and both scenarios require about 0.3bar

CO_2 to melt the ice. It could be argued that a slushball, by definition, might be easier to melt regardless of CO_2 level, due to the reduction in planetary albedo by less advanced ice cover. But I suggest that such an argument is so circular as to be of little use, and that the key issue is the comparison between slushball and hard snowball Carbon cycle dynamics, at equivalent temperatures. In this vein, I write the difference in glacial duration for hard snowball Δt_{HSB} and slushball Δt_{SLUSH} scenarios, in terms of c , the atmospheric fraction of the degassing flux. Using $\Delta T = \frac{\partial T}{\partial CO_2} \frac{\partial CO_2}{\partial t} \Delta t$, and substituting $\frac{\partial CO_2}{\partial t}$ with (4.7) for a hard snowball, and the time derivative of (4.9) for a slushball, I can write the difference in expected duration of the two scenarios as:

$$\frac{T_i - T_{start}}{\frac{\beta}{CO_{20}} Dc} = \Delta t_{HSB} \tag{4.37}$$

$$\frac{T_i - T_{start}}{\frac{\beta}{CO_{20}} \Sigma CO_2 \frac{d\Phi}{dt} + \Phi \frac{d\Sigma CO_2}{dt}} = \Delta t_{SLUSH} \tag{4.38}$$

$$c \Delta t_{HSB} \simeq \Delta t_{SLUSH} \tag{4.39}$$

Figure (4.4) shows that, at least in the simple formulation presented here this relationship holds for a given solar luminosity, across a range of choices of the value of the parameter c , provided that carbonate Carbon is at steady state. Note that (4.39) is not algebraically true given the equations used here - it merely shows a good approximation to the results. This indicates that (for the CO_2 values appropriate to describing deglaciation), the duration of a slushball scenario can be assumed to be shorter than that of a hard snowball by a factor of $\frac{1}{c}$, i.e. by around a factor of 3, assuming the apportioning of the degassing fluxes mirrors relative planetary surface area (Higgins & Schrag, 2003, Pierrehumbert, 2005). Making this estimate more precise using (for example) the $\delta^{13}C$ of marine carbonates requires knowledge of any deviation the organic:inorganic fraction of the Earth's Carbon exhibited from its present day value of about $\frac{1}{5}$ (Fairchild & Kennedy, 2007), a deviation that was likely substantial and unconstrained throughout the period (Rothman et al, 2003). Furthermore, once the assumption of steady state carbonate Carbon is relaxed, a far greater range of duration values for the glacial interval become feasible (Table 4.2 and 4.3), and distinction between hard snowball and slushball on the basis of the Carbon cycle alone becomes more complex. In this case, information on the hydrological cycle is probably required, as well as knowledge of whether any proxies for hydrological variance correspond to the glaciated or transitional state (Allen & Hoffman, 2005). The key result of this work is that, for steady state carbonate Carbon during the glacial interval, the critical parameter dictating the increased duration of a hard snowball scenario is the atmospheric fraction of the (glacial) CO_2 degassing flux.

Balance between carbonate Carbon weathering and burial

The results in this chapter support the idea that a slushball scenario can reproduce realistic glacial duration estimates under certain parameter choices for the glacial exit temperature T_i , in a way that is consistent with previous studies (Hyde et al, 2000, Pollard & Kasting, 2005), in particular the importance of carbonate alkalinity balance in dictating glacial severity (Ridgwell et al, 2003, Ridgwell & Kennedy, 2004). I add to this work by emphasising that the ratio $R = W_{carb} : B_{carb}$ between carbonate weathering and burial must be greater than unity if a dynamic carbonate Carbon slushball scenario is to be recoverable. As described in Ridgwell et al (2003, 2004) and chapter 1, the impact of carbonate dynamics on glacial severity is dictated by the strength of the feedback linking $[CO_{3(aq)}^{2-}]$ and $CaCO_{3(s)}$ precipitation rate. Reduced sea level during the Neoproterozoic was proposed to have had a disproportionately high impact on $CaCO_{3(s)}$ depositional area, reducing the burial flux and raising the marine $[CO_{3(aq)}^{2-}]$ level. The temporary effect of this is to shift the equilibria of reactions 4.D, 4.C and 4.E to the left, giving rise to a (temporary) *rise* in $[CO_{2(aq)}]$, that is eventually corrected by a corresponding withdrawal of $[CO_{3(aq)}^{2-}]$ by an increase in the B_{carb} flux, a reversal of the shift in reaction equilibria, a decrease in total ocean Carbon and a net decrease in the fraction of the remaining Carbon in the form of $CO_{2(aq)}$, summarised by $CO_{2(aq)} + CO_{3(aq)}^{2-} + H_2O(l) \rightleftharpoons 2HCO_{3(aq)}$ moving to the right (Ridgwell et al, 2003, Ridgwell & Kennedy, 2004). The key issue of relevance to the snowball Earth problem is the idea that shallow shelf carbonate deposition rate was less actively impacted upon by the marine biosphere prior to the evolution of coccolithophores. Therefore a relatively large increase in $[CO_{3(aq)}^{2-}]$ was required in order for any increase in the carbonate burial flux, meaning that this increase, and the corresponding CO_2 draw-down, was large enough when it did occur to significantly contribute to glacial severity (Ridgwell & Kennedy, 2004). This idea may be a reasonable representation of a slushball scenario, and the results of this chapter do not contradict it. However this work highlights the potential importance of temperature in the existence (or not) of these feedbacks, and therefore in the climatic feasibility of a snowball scenario dictated by the carbonate alkalinity balance. Ridgwell & Kennedy (2004) assume that the carbonate weathering flux remains equivalent to the pre-vascular plant function from GEOCARB (Berner, 1994), and that carbonate Carbon precipitation occurs, regardless of the degree of ice-cover progression and sea level reduction. Whilst this may realistically describe the Neoproterozoic system, and can (as they note) explain cap carbonate formation over a multi-million year timescale, it amounts to assuming relatively mild temperatures, significant ice-free land surface, and marine biosphere of significant mass - i.e. a slushball scenario. Table (4.3) shows that under some combinations of the weathering to burial ratio $R = W_{carb} : B_{carb}$, a significant atmospheric CO_2 fraction cannot build up, and a dynamic carbonate Carbon, open water scenario would become unrecoverable. If both glacial severity and cap carbonate formation are dictated by carbonate precipitation dynamics, this probably requires

$R = W_{carb} : B_{carb} > 1$, no matter how severe the glaciation. Volumetrically significant abiotic $CaCO_{3(s)}$ precipitation is unlikely without extremely high $CO_{3(aq)}^{2-}$ (Barker et al, 2003), and prior to active biotic calcification was probably largely the result of precipitation during alkalinity release from dead plankton and bacterial cells (Riding, 2000). Because the biotic impact on $CaCO_{3(s)}$ precipitation prior to coccoliths was a metabolic byproduct that only manifested itself after death, it could not have been subject to natural selection, and must have remained linked to growth of the marine biosphere, and to temperature. The extensive uncertainty about the mass of the Neoproterozoic marine biosphere, in particular the problems with making any inferences from $\delta^{13}C$ data if carbonate Carbon is not at steady state, are another important unknown that may affect the implications of these results. $R > 1$ requires that if the carbonate weathering influx to the oceans decreased significantly as a result of lower temperatures or ice cover, the carbonate burial flux declined equivalently, so as to not withdraw all the dissolved Carbon from the glaciated ocean. Determining a relationship between temperature and marine $CaCO_3$ precipitation, in conditions representative of those before active calcifiers, is therefore important to assess the plausibility of the dynamic carbonate scenario.

Chapter 5: Changes in susceptibility to global-scale glaciation over Earth history

Summary

Global scale glaciations occurred during the Proterozoic but not during the Phanerozoic, and this difference cannot be solely attributed to increased solar luminosity. I show that if silicate weathering enhancement instantly returns to its pre-glacial maximum value after deglaciation, a subsequent glaciation will occur within 2 – 5Myrs. The qualitatively longer $\sim 40 - 50$ Myr interglacial interval between distinct Neoproterozoic snowball Earth events implies changes in weatherability occurred during the era. I hypothesize the need for a biotic “sucession time” to have elapsed after deglaciation, before biological silicate weathering enhancement activity could recover. The idea that this requirement dictated the length of Neoproterozoic interglacials is consistent with silicate depletion of cap carbonates. I also propose various mechanisms that may have reduced susceptibility to glaciation after the Neoproterozoic. An increase in the supply-limited fraction of silicate weathering regimes associated with the development of soils may have altered the overall climatic impact of the Urey reaction. An increase in the temperature sensitivity of silicate weathering enhancement during the replacement of Neoproterozoic, lichen-dominated land surfaces, with Phanerozoic, vascular plant-dominated ones, is implied by the broader temperature range that present day lichens have in comparison to plants. The coupling to coccolith growth could have buffered biotic marine $CaCO_{3(s)}$ precipitation with respect to temperature change. Where appropriate I suggest potential tests, but acknowledge the hypothetical nature of these ideas.

Introduction

The fact that ice-covered surfaces reflect more radiation than ice-free surfaces, combined with the fact that atmospheric greenhouse CO_2 exhibits dynamics over a longer timescale than those of surface ice cover (Hoffman & Schrag, 2002), means that the Earth’s climate is theoretically vulnerable to switching between ice-covered and ice-free equilibrium states (Peltier et al, 2007, Chapter 1, Figure 1.1, chapter 3, Figure 5.1). Intense silicate weathering (or equivalent CO_2 sink) may drive the system to the unstable region of ice-cover/energy balance “space” (lower dashed line, figure 1.1), whereupon the ice-albedo feedback results in an equilibrium high ice-cover state. This will manifest as a discrete switch with respect to the time scales of the Carbon cycle and the Urey reaction (Walker et al, 1981, Hoffman & Schrag, 2002). Removal of the weathering sink in the ice-covered state causes greenhouse CO_2 to build up again, eventually driving the system back to the initial low ice-cover equilibrium state (Kirschvink, 1992). For a given solar forcing, the CO_2 required

to deglaciate the high ice-cover state is vastly in excess of that required to maintain temperature in the ice-free region (Hoffman & Schrag, 2002, Pierrehumbert, 2005). Because silicate weathering rate is proportional to atmospheric CO_2 partial pressure (Walker et al, 1981), this means that any post glacial extreme greenhouse should, *in theory*, experience a correspondingly high silicate weathering flux (Kirschvink, 1992, Hoffman & Schrag, 2002). That is, *in theory*, glaciation must remove the silicate weathering flux, causing deglaciation, which must be characterised by an extreme greenhouse, which must cause high silicate weathering, which must cause reglaciation. I show below that the assumptions of sufficient silicate weathering and a discrete jump in planetary albedo are sufficient for the occurrence of this example of a self-sustained, non-linear oscillation, or “limit cycle”, (Saltzman, 2002). This scenario is shown in figure 5.1, in relation to the potential for a given temperature change to be amplified over shorter timescales by the ice albedo feedback. The question is whether the cycle has ever occurred in the real climate, and how the susceptibility to it has altered over the planet’s history. Paleomagnetic/geological data suggest that global-scale “snowball” glaciations occurred at least once (at about 2316Ma), probably on multiple occasions during the Paleoproterozoic (Kirschvink, 1992b, Kopp et al, 2005), and then again (as discussed in the introduction) during the Neoproterozoic (Hoffman et al, 1998, Hoffman & Schrag, 2002). Conversely, all recorded cycles of major glaciation during the Phanerozoic have been sub-planetary in their climatic scale and spatial extent (Hoffman & Schrag, 2002, Tajika, 2004). The lower solar luminosity flux of the Neoproterozoic relative to the Phanerozoic would have resulted in a lower silicate weathering flux, hence higher CO_2 for steady state planetary temperature, as a result of the temperature dependency of reaction kinetics (Tajika, 2004, Walker et al, 1981). This inherent homeostasis in the CO_2 -weathering buffer means that increased solar luminosity flux is not a sufficient explanation for why planetary-scale glaciation occurred during the Proterozoic, but not subsequently. I must therefore look for an alternative explanation as to why the planet has not experienced global-scale glaciation during the past 500 million years. I suggest that the silicate weathering flux, because it is closely linked to the evolution of the terrestrial biosphere, is most likely to have undergone a systematic change over this time period.

A simple model

Outline

Planetary temperature is described using a realistic solar luminosity forcing and an empirical parameterisation of radiative/convective properties of the atmosphere. Glacial entry and exit temperatures are held as fixed parameters. It is assumed that the requirements for oscillation between greenhouse and icehouse states are simply that CO_2 increases during the glacial period, and decreases during the inter-glacial period. Various functions describing the long term dynamics of CO_2 , particularly in terms of the mass and sensitivity of

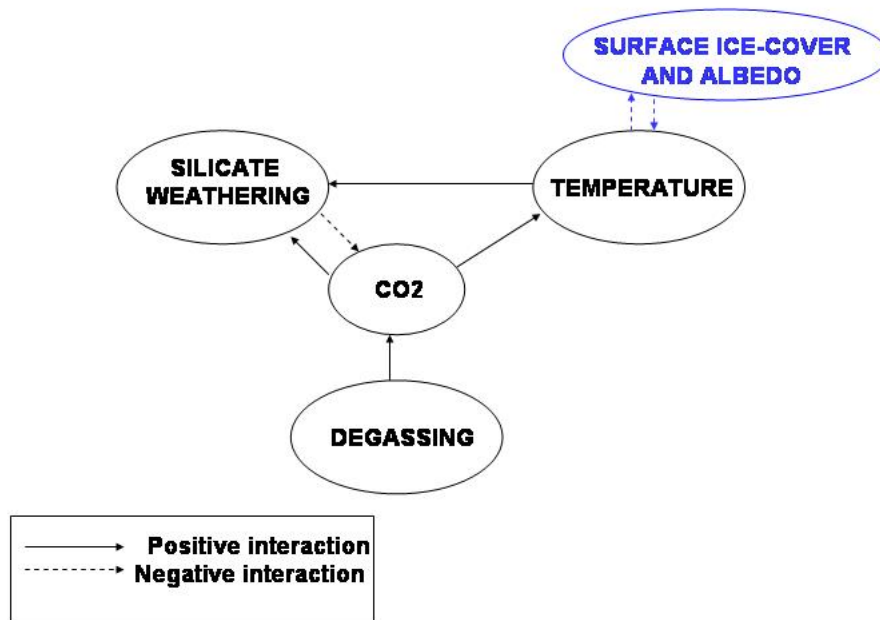


Figure 5.1 - The interactions required to predispose the Earth system to oscillation between icehouse and greenhouse states. The lack of a genuine oscillator in the present climate is probably due to a combination of progressively increasing solar luminosity flux (not shown) and (I propose) a decrease in the strength of the negative interaction between silicate weathering and CO_2 at the critical temperature corresponding to the bifurcation point, T_f . Over short (i.e. $< 100\text{yr}$ (e.g. Saltzman, 2002)) timescales, changes in temperature can be amplified by the surface ice albedo feedback (upper blue box/arrows, recall that two consecutive negative interactions constitute a net positive feedback (e.g. Riggs, 1976)). This may give rise to changes in planetary energy balance that are effectively discrete over the multi-millennial timescales across which the Carbon cycle adjusts. If these discrete changes cause temperature to drop to near ice-covered, or rise to extreme greenhouse conditions, the feedbacks shown in black are sufficient to dispose planetary temperature to oscillate between these two states.

biological enhancement of silicate weathering are used to examine the duration and severity of any such damped oscillation.

The energy balance aspect of the planetary temperature function can be represented by empirical radiative convective coefficients, and the greenhouse effect of CO_2 normalised using a sensitivity constant. This sort of formulation is intended to be representative of simple systems without a spatial dimension, whose long-term dynamics are dominated by changes in CO_2 . Temperature T can therefore be represented by an equation of the form of (5.1) (North, 1975, North & Coakley, 1979, North et al, 1981):

$$T = \frac{1}{B} \frac{S}{4} (1 - \alpha) - \frac{A}{B} + \beta \ln\left(\frac{CO_2}{CO_{20}}\right) \quad (5.1)$$

Where constants $A = 203.3 W m^{-2} C^{-1}$ and $B = 2.09 W m^{-2} C^{-1}$ are experimentally determined radiative-convective parameters (North & Coakley, 1979), and S is the solar luminosity flux, at present day $S_0 \simeq 1368 W m^{-2}$ (North et al, 1981) and for the work in this chapter is held constant at $S = 1305.6 W m^{-2}$, corresponding to 550Ma (Gough, 1981). In the ice free state the planetary albedo $\alpha \simeq 0.3$ (Caldeira & Kasting, 1992). Atmospheric CO_2 is related to its pre-industrial value $CO_{20} = 280$ parts per million by logarithmic sensitivity parameter $\beta = 4.33$ (North et al, 1981, Berner, 1994, Lenton, 2000). In the ice-covered state planetary albedo is set to $\alpha = 0.7$ (North et al, 1981), until such time as planetary temperature becomes warmer than the glacial exit threshold $T > T_i$, when the albedo jumps back to the ice-free value $\alpha_i = 0.3$ in the discretized way discussed in chapter 3. Over the millennial timescales relevant to the end of the Proterozoic I assume that the dynamics of temperature are dominated by those of CO_2 (i.e. that $\frac{dS}{dt} = \frac{d\alpha}{dt} = 0$), so that temperature changes as a function only of CO_2 , $\frac{dT}{dt} = \beta \frac{CO_{20}}{CO_2} \frac{dCO_2}{dt}$. I am therefore interested in the long-term balance between degassing D (via volcanism and decarbonation during mid-ocean ridge spreading) and withdrawal of CO_2 from the system via the Urey reaction. The time derivative of the atmosphere and ocean CO_2 reservoir is therefore of the form:

$$\frac{dCO_2}{dt} = D - W_{sil} \quad (5.2)$$

The flux W_{sil} is itself a time derivative, describing the moles of silicate weathering reaction occurring on the planet's surface per unit time (With the scaling factor $W_0 = 6.65 \cdot 10^{12}$ moles per year at present). Therefore I can use the chain rule and the approximation $\frac{\Delta T}{\Delta t} \approx \frac{dT}{dt}$ to describe the change in planetary temperature, ΔT , that occurs over an arbitrary number of timesteps, Δt :

$$\Delta T = \frac{\partial T}{\partial CO_2} (D - W_{sil}) \Delta t \quad (5.3)$$

Recall the discretized albedo that I proposed in chapter 3 as being a useful simplification for long-timescale approaches to the snowball Earth problem. For a given luminosity function, a sufficient condition for the planetary albedo to jump to its ice-covered value, and for a corresponding equilibrium, high ice-cover planetary state (i.e. a snowball Earth) to occur, was that planetary temperature reached, or dropped below, a given threshold temperature T_f . I noted in chapter 3 that the “snowball-slushball” debate concerned the real value of T_f in the Earth system, and the plausibility of it having ever been reached, rather than its existence per se. If the limit cycle that I describe above is to occur, CO_2 must decrease when temperature is warmer than the initiation threshold $T > T_f$ and increase when temperature is colder than the exit threshold $T < T_i$. Relations (5.4) and (5.5) describes how a sufficient condition for initiation of a snowball state is that silicate weathering exceeds degassing as temperature decreases from the habitable interval to approach T_f from the positive side. (A sufficient condition for homeostasis within the habitable region is that (5.5) is not realised). Relation (5.6) describes the requirement that degassing exceeds silicate weathering as temperature increases from the snowball interval to approach the degassing threshold (discussed in chapter 4) T_i from the negative side, and is necessary for a snowball Earth to be recoverable (Kirschvink, 1992). Although I have formalised the idea mathematically for consistency, the key point is the simple idea that CO_2 continues to decrease until temperature reaches the glaciation threshold, and then continues to increase until temperature reaches the deglaciation threshold.

$$T + \Delta T \leq T_f \tag{5.4}$$

$$\frac{\partial T}{\partial CO_2}(D - W_{sil})_{T \rightarrow +T_f} < 0 \tag{5.5}$$

$$\frac{\partial T}{\partial CO_2}(D - W_{sil})_{T \rightarrow -T_i} > 0 \tag{5.6}$$

A sufficient condition for oscillation between icehouse and greenhouse states is therefore that (5.5) and (5.6) are both simultaneously true of the Earth system. This disposition to switching between the two states has been highlighted throughout the course of work on the snowball Earth problem (Kirschvink, 1992, Hoffman & Schragg, 2002) and more recently explicitly described as a disposition to oscillation (Peltier et al, 2007).

Biotic silicate weathering enhancement

I focus on the impact of relative changes in terrestrial biomass B , and in enhancement per unit biomass ε on the silicate weathering flux W_{sil} , by scaling by the present day net silicate weathering flux (described previously and given by equation (3.13)), by changes in

the normalised silicate weathering biological enhancement factor, E_n . Recall from chapter 3 that the silicate weathering flux is the product of a baseline abiotic rate W_{ab} and a biotic enhancement factor E , so that at present day $E_0W_{ab0} = W_0$, and it is useful to normalise biotic enhancement:

$$E_n = \frac{EW_{ab}}{E_0W_{ab0}} = \frac{EW_{ab}}{W_0} \quad (5.7)$$

$$W_{sil} = E_n W_0 \left(\frac{CO_2}{CO_{20}} \right)^a e^{(b+c)(T-T_0)} \quad (5.8)$$

Where E_n , the normalised biotic enhancement of silicate weathering, is equal to the term $\frac{E}{E_0}$ from chapter 3, (with the “n” subscript, denoting normalisation to present, for notational convenience). The constants $a = 0.25$, $b = 0.056$, and $c = 0.017$ give respectively the sensitivity to CO_2 , Arrhenius kinetic temperature sensitivity, and sensitivity to runoff/hydrology changes, and planetary temperature T is expressed as a deviation from its present day value T_0 (Walker et al, 1981, Schwartzman, 1999, discussed in Chapter 3). This amounts to absorbing changes in the silicate weathering flux specifically due to CO_2 and temperature T into the baseline flux (5.4) (Walker et al, 1981), and changes specifically due to the biosphere into a separate part of the function. Consequently, the separation between biotic and abiotic components is not as strict as in chapter 3, or as in the work (Schwartzman, 1999) upon which it was based - because the importance of the biosphere in giving rise to the sensitivity constants in the (present day) baseline silicate weathering flux is uncertain. However, I make this simplification in order to focus specifically on terrestrial evolutionary history, and to make the weathering function more easily compatible with dynamic CO_2 and temperature. The terrestrial biomass B and enhancement per unit biomass ε are both normalised to the present day (i.e. equal to unity at present - a simplification that has been useful in previous Carbon cycle modelling (Berner, 1994, Bergman, 2003)). Hence the change in the weathering enhancement over time is the time derivative of $E_n = \varepsilon B$:

$$\frac{dE_n}{dt} = \frac{dB}{dt}\varepsilon + B\frac{d\varepsilon}{dt} \quad (5.9)$$

Identifying the problem

Figure (5.2) shows the results of driving this system with a weathering enhancement factor E_n that changes in a discrete way in response to the planetary temperature with an ice albedo instability threshold set at $T_f = 10^\circ C$, $T_i = -20^\circ C$. In the habitable region, $T > T_f$, biotic silicate weathering flux is set to $E_n \simeq 2$, which is just sufficient to trigger glaciation with the set of parameter choices described. This enhancement factor is the

result of a sensitivity analysis in which enhancement was incrementally decreased until reglaciation was possible. Although $E_n \simeq 2$ is arbitrary to my model, the key point is that it is the minimum required value to initiation glaciation. The issue I wish to explore is the impact of E_n returning instantly (or not) to this value after deglaciation. In the ice-covered state, the silicate weathering flux (5.8) is set to zero. Note that under the assumption that the habitable state instantly results in sufficient biotic weathering enhancement for triggering a glaciation, the system will, unsurprisingly, rapidly reglaciate. This occurs over a relatively short time period, of the order of 2 million years. Note that a weathering enhancement factor smaller than that shown would not be sufficient to trigger reglaciation, because the baseline flux would need to be larger to achieve an equivalent CO_2 drawdown - which could not be achieved without higher CO_2 and warmer temperatures, counteracting the drawdown (Walker et al, 1981, Tajika, 2004). Although the numerical value of the enhancement factor E_n is tied to the temperature function used here, I can still make a useful general conclusion about the system. Stated simply, if the habitable temperature state $T > T_f$ *instantly* results in a silicate weathering flux that is sufficient to drive the system into glaciation, the time between the exit of one glacial interval and the entry to the subsequent one is relatively shorter (of the order of ~ 3 Myrs or less) than the time interval thought to separate individual Neoproterozoic snowball Earth events $\sim 40 - 50$ Myrs or more (Hoffman & Schrag, 2002). If glacial initiation is linked to silicate weathering runoff, as an increasing amount of data suggests (Sheilds, 2007, Fairchild & Kennedy, 2007) then this suggests a lag time between the post-glacial extreme greenhouse conditions, and silicate weathering build up sufficient to cause another glaciation. I therefore divide the work in this chapter into two questions:

(1) Why did the Proterozoic system, given that it was susceptible to glaciation, not rapidly reglaciate?

(2) Why did global-scale glaciation happen in the Proterozoic but not the Phanerozoic?

Results

Why did the Neoproterozoic Earth not rapidly reglaciate?

Candidate variables

Tajika (2004) discussed the likely requirement for a lower baseline CO_2 /tectonic outgassing rate (0.25 – 0.5 times the present value), in order to initiate Neoproterozoic glaciation, as well as the converse problem of invoking lower degassing rate as the sole cause - in that it would require relatively long glacial intervals (Tajika, 2004). As described above, Tajika (2003) dismissed reduced solar luminosity as a cause of the snowball Earth events by

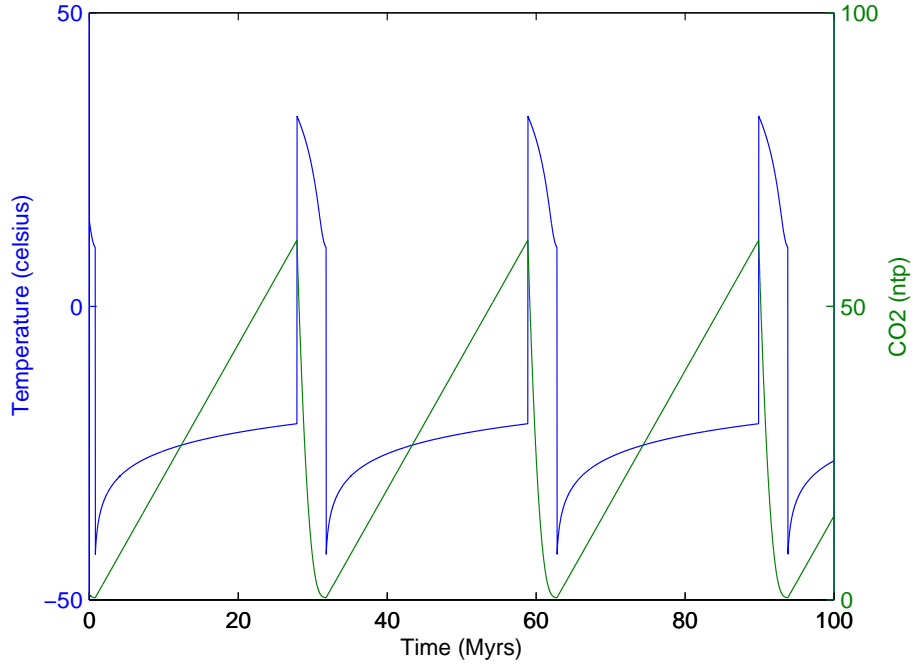


Figure 5.2 - If the habitable temperature state $T \geq T_f$ corresponds to a silicate weathering flux large enough to trigger a switch to the ice-covered state $T \rightarrow T_i$, then the Earth system is vulnerable to sustained oscillation between icehouse and greenhouse states. In this case the length of the interglacial separating snowball events is likely to be short (2 – 3 million years), because it is limited only by the time required for the silicate weathering flux to remove CO_2 from the ocean atmosphere system, as opposed to any additional time required for silicate weathering enhancement to increase to a sufficiently large value. Plot shows the simple temperature model described in the text, Y-axes show planetary temperature (celsius) on the left, and atmospheric CO_2 as a fraction of its pre-industrial value of $CO_2 = 280\text{ppm}$ on the right. X- axis shows time in millions of years. A 1Kyr timestep was used, and solar luminosity was held constant at $S = 1305\text{Wm}^{-2}$, corresponding to 550Ma (Gough, 1981) In the habitable state $T \geq T_f$ the silicate weathering flux (equation (5.8)) is multiplied by a constant scalar $E_n = 2$, in the ice covered state the silicate weathering flux is set to zero. The important point to note from this plot is that if the weathering enhancement factor in the habitable temperature state is instantaneously set to a *constant value, sufficient to trigger glaciation*, the length of the interglacial period is qualitatively shorter than the $\sim 50\text{Myrs}$ separating Neoproterozoic glaciation events. I propose that this implies that the time between Neoproterozoic glacial events was dictated, at least in part, by the time needed for a sufficient weathering enhancement factor to occur.

invoking the inherent homeostasis in the Urey reaction and the fact that changes in the solar flux would likely occur too gradually to account for separate Neoproterozoic glacial events (Tajika, 2003). These conclusions are relevant to the issue of rapid reglaciation. If a lower CO_2 degassing rate was the ultimate cause of glacial initiation in the first place then at the very least this places glacial duration toward the upper end of the estimated 3 – 30 Myr interval for glacial duration, and at most makes glacial exit problematic without some external (tectonic) forcing causing deglaciation rate to increase suddenly, before dropping back to a steady state magnitude. Episodic continental growth formation models can be derived from the age distribution of igneous continental crust particles, in turn calculated from $^{238}U \rightarrow ^{206}Pb$, and do imply a relatively low continental crust formation rate from around 1.0 Ga (Billion years ago) onwards, in addition to a hiatus from 2.3 – 2.5 Ga, corresponding to the Paleoproterozoic glaciations (Rino et al, 2004). These and other data implying low tectonic outgassing have been proposed as necessary (Tajika, 2004) to explain changes in glacial susceptibility over the Proterozoic. This may well be the case, but lower tectonic forcings are not a sufficient explanation for susceptibility to global glaciation during the Proterozoic for several reasons, stemming ultimately from the homeostasis inherent in the Urey reaction.

Firstly, there are the practical problems of extrapolating to global crustal formation rate from one restricted subset of igneous zircon deposits, and of assuming linearity between zircon deposition and continental crust formation rate, then between continental formation rate (as opposed to the conventional seafloor spreading rate, Berner, 1994) and degassing. But the main difficulty with such ideas is that the supporting data implies a similar (low) continental crust formation rate across the whole Neoproterozoic (Rino et al, 2004), so cannot explain the occurrence of multiple, distinct Neoproterozoic glacial events. Furthermore, the implicit low continental crust formation rate across the Phanerozoic (Rino et al, 2004, figure 3.10), which has clearly been habitable by comparison (Berner, 1994), is also irreconcilable with the idea of tectonic outgassing as the main driver of susceptibility to global-scale glaciation. Both low solar luminosity and low tectonic degassing rate may well be necessary conditions for glaciations on the scale of those that occurred during the Neoproterozoic. But both of these variables exhibit dynamics that are too slow to resolve distinct Neoproterozoic glacial events, and changes in both are likely to be compensated for by the negative feedback they will drive the CO_2 - weathering buffer (Walker et al, 1981, Tajika, 2003). Therefore these conditions cannot be a sufficient explanation. When a systematic change in the structure of the interactions between variables is needed, the biosphere is the most logical candidate, due to its capacity for innovation (Vernadsky, 1926). I therefore propose that the factor most likely to have changed over a sufficient magnitude and appropriate timescale, and most likely to have triggered a sustained decrease in glacial susceptibility over the Phanerozoic, is the biotic enhancement of silicate weathering.

A hypothesis

I discussed in chapter 3 my conclusion that at least some biotic enhancement of silicate weathering was needed to trigger global scale Neoproterozoic glaciation, albeit by accentuating a tectonically-driven change. A corollary of this is that with an entirely abiotic silicate weathering rate the system will not reglaciade, because biotic enhancement is needed to draw CO_2 down to the required low level. Note that this conclusion holds at lower CO_2 values corresponding to the approach of glaciation, so the issue of how high CO_2 is immediately after glaciation is less relevant. Biotic enhancement of silicate weathering is an aggregate property of lichens and associated soil bacteria (Schwartzman, 1999, Chen, 2000 Bennett et al, 2001). The nature of the interactions, both between and within species, that are necessary to sustain a significant weathering enhancement factor, are uncertain in an evolutionary sense. But I argue that two reasonable assumptions are (a) that the lichen symbiosis must be sufficiently mutualistic to survive over a range of abiotic conditions in order to spread across a significant fraction of the planetary land surface over multi-millennial time scales (Chapter 2, Boyle & Lenton, 2006), and (b) that sustained biotic weathering enhancement is more probable in a (lichen and microbial) soil community that exhibits some mutually beneficial interactions between lichens and associated soil bacteria (Bennett et al, 2001). I note that both of these properties will take many generations of social evolution to be achievable. This leads us to hypothesize that the lack of instant reglaciade during Neoproterozoic glacial events was a consequence of the decimation of the terrestrial biosphere during the glacial period, after which a tangible amount of (co)evolutionary time was necessary before biological enhancement of silicate weathering could become great enough again to drive the system into a subsequent snowball state. In short, regardless of how high the (abiotic) CO_2 forcing was at the end of one glacial event, the system still required biotic silicate weathering for another glaciation to occur, and this enhancement could not be achieved without terrestrial co-evolution over a multi-millennial “succession time”. I emphasise that the analogy with ecological succession is only intended as a metaphor aid to understanding, and the dynamics likely occurred over a significantly longer timeframe.

The growth of the terrestrial biosphere over geologic time is contingent on adequate nutrient/growth substrate availability - a condition that would, of course not be met if the land surface had been completely or partially ice-covered and/or experiencing sub-zero or near zero temperatures for the previous 3 – 30 million years of glaciation. Colonisation of virgin rock substrates by lichen and associated bacteria takes a tangible (but uncertain) number of generations (Schwartzman, 1999). I assume that at the immediate point after global glaciation has ended, the terrestrial biomass remains constant at an initial low value $B_0 = 0.01$ of the present day terrestrial biomass, until tangible, global scale growth of the terrestrial biosphere can occur, after a “succession” time t_s (Equations (5.10) and (5.11)). (Note that t_s

is measured in model timesteps (thousands of years), not generations, because the function $\frac{dB}{dt}$ is normalised and describes growth of net biomass in relation to present day, in contrast to the description of changing abundance of units of selection in chapter 2). I label the length of time that the land surface has been biologically colonised (i.e. since termination of the snowball state) as t_{biotic} years.

$$B(t) = B_0 + \int_0^t \frac{dB}{dt} dt \tag{5.10}$$

$$\frac{dB}{dt} = G_0 \cdot \frac{1}{2} \left(\frac{t_{biotic} - t_s}{|t_{biotic} - t_s|} + 1 \right) \tag{5.11}$$

Figure (5.3) shows the behaviour of the system with fixed values of enhancement per unit biomass $\varepsilon_{max} = 5$ and different values of the succession time t_s . As indicated in the figure, progressive change in the time interval required for a given enhancement factor to be achieved is sufficient for a qualitative change in the time interval between global scale glaciations.

How long would the biosphere take to re-establish weathering activity after glaciation?

The evolutionary “succession-time” t_s describes the time required for the emergence of a terrestrial biosphere, following one glaciation, with sufficient silicate weathering enhancement activity to cause reglaciation. It is important to note that the analogy with ecological succession and growth is a loose one. The time required for lichens to colonise virgin rock substrate today is around 40 years (Orwin, 1970) - instantaneous in terms of the timescales considered here. But the parameter t_s does not only measure the time required for growth of lichens over the land surface, but the time required for the development of a lichen-dominated terrestrial community that will, by natural selection of different genotypes within its component species, carry out significant silicate weathering enhancement over millennial timescales. The requirement for long time scales is of importance, because it implies persistence of the terrestrial biosphere over a range of abiotic conditions, a range that will become more deleterious (with respect to the hydrological cycle) as the glaciation threshold is approached. This persistence invokes high altruism via the mechanisms described in chapter 2. (A lichen symbiosis dominated by cheater mycobiont genotypes may be able to enhance silicate weathering transiently, but will self limit as the resultant temperature reduction causes fluctuation in water and nutrient availability). The inherent pressure toward cheaters may give rise to cycles of “failed” weathering enhancement - in which lichen symbioses enhance weathering, but cannot sustain the enhancement activity, because they cannot tolerate the deleterious conditions it causes. The evolution of a more

mutualistic system (i.e. with altruistic mycobionts), with such a tolerance, that can sustain CO_2 drawdown to the glaciation threshold at a global scale, will take significantly longer than simply the time to colonise bare rock surfaces. Lichenisation of a suitable versatility is a difficult evolutionary problem, because it must avoid the incentive experienced by each partner species to exploit the other. The time required for the evolution of such a system may well be of the order of hundreds of thousands of years, and may therefore partly explain the apparent lack of instantaneous reglaciation. This admittedly treats a terrestrial biosphere capable of triggering glaciation as a “black box”, but remains consistent with silicate depletion in cap carbonates. How realistic this idea is will be assessed by future constraints on net biotic weathering enhancement at present.

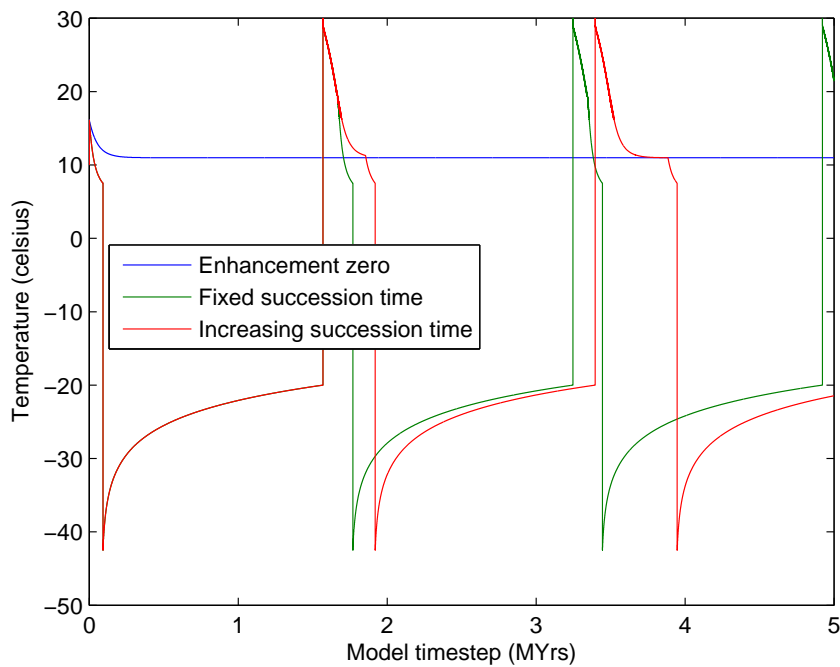


Figure 5.3 - The impact of the “succession time”, required for the growth and evolution of a terrestrial biosphere capable of triggering a global-scale glaciation, on the periodicity with which icehouse-greenhouse oscillation may be expected to occur. Y-axis shows planetary average temperature in celsius, X-axis shows model timestep in millions of years (Luminosity was held constant at $S = 1305.6Wm^{-2}$, corresponding to 550Ma). Blue line shows planetary temperature expected from the contemporary weathering rate function, with no additional enhancement. Blue and green line show a doubling of the biotic enhancement of silicate weathering above the present-day function (i.e. a doubling of the scalar W_0 by which the remainder of the function is multiplied) after habitable temperatures have persisted for a given succession time t_s . Green line shows temperatures resulting from a fixed succession time (of $t_s = 100Kys$), red line those resulting from increasing this value as a (linear) function of the model timestep.

I note that the cap carbonates overlying late Neoproterozoic glacial strata (LNGD) are depleted in silicates (Fairchild & Kennedy, 2007). This supports the idea that the post glacial greenhouse was sufficiently warm to accentuate carbonate weathering, but was in some way unsuitable for silicate-specific weathering surges. Given that CO_2 is a reactant in both carbonate and silicate weathering reactions, and that the rates of both reactions increase with temperature, there is no reason to expect carbonate weathering to be disproportionately increased relative to silicate weathering in any post snowball extreme greenhouse event. Furthermore, in a scenario in which the cap carbonates result entirely from precipitation of CO_3^{2-} and HCO_3^- already in the ocean of a slushball climate (Ridgwell & Kennedy, 2004), (as opposed to the equilibration of the ocean with atmospheric CO_2 sufficient to melt a hard snowball), one would still expect the greenhouse forcing sufficient to melt planetary-scale (slushball) ice cover to result in tangible silicate weathering fluxes, which would be detectable within cap carbonate deposits. *Sr* data suggests that such surges may have preceded glacial initiation (Shields, 2007), strengthening the tie with susceptibility to glaciation. Silicates tend to have a higher $^{87}Sr/^{86}Sr$ than do carbonates, in part due to relatively high concentrations of ^{87}Rb , which decays to the heavier *Sr* isotope (Bickle, 1994). There is a tendency for *Rb* and *Sr* to partition into different parts of silicate minerals, and perhaps for selective leaching of ^{87}Sr to occur, introducing variance into the $^{87}Sr/^{86}Sr$ expected from silicate weathering runoff. Nevertheless, when the seawater $^{87}Sr/^{86}Sr$ curve (Halverson et al, 2007) is normalised to the value expected from hydrothermal input at mid ocean ridges, and when the relative magnitude of the silicate and carbonate weathering fluxes $W_{sil} : W_{carb} \approx 45 : 55$, there is still strong evidence for a $^{87}Sr/^{86}Sr$ increase during the late Neoproterozoic, consistent with increased silicate weathering (Shields, 2007). This, in conjunction with cap carbonate Silicate depletion, implies pre-glacial silicate weathering enhancement (Lenton & Watson, 2004), and a post-glacial environment with higher (non-specific) chemical weathering (Kirschvink, 1992, Hoffman & Schrag, 2002). Furthermore, a post-glacial extreme greenhouse would necessarily involve tectonic and hydrological disturbances from the previous climate state, presumably giving rise to a highly variable erosion rate - thus equivalent variability in the kinetically limited fraction of silicate weathering regimes, therefore in the net Urey reaction rate (West et al, 2005). It is consequently difficult to envisage how a post-glacial extreme greenhouse could occur without resulting in a detectable silicate weathering increase, simply based on the expectation that the reaction kinetics would be expected to give rise to a higher reaction rate at increased temperature and CO_2 .

On a more practical level, it is self-evident that the sorts of (lichen and bacterial) physiologies conducive to surviving extreme glacial events in refugia are not necessarily the best adapted to rapid terrestrial colonisation and weathering enhancement during the post-glacial greenhouse, and that a significant number of generations must elapse before the

species composition of the terrestrial biosphere has altered sufficiently to cause significant weathering enhancement. A post-glacial rise in weathering flux does not, therefore, translate into repeated CO_2 drawdown and cooling, I think due to the requirement for a “succession” time within which the terrestrial biosphere could recover - consistent with the Silicate depletion of cap carbonates.

Why did global-scale glaciation happen in the Proterozoic but not the Phanerozoic?

As described above, it is unlikely that the answer to this question can be stated solely in terms of a lower solar or tectonic forcing. I suggest that the change in susceptibility may be the result of the activity of the biosphere, and present various candidate hypotheses.

Temperature sensitivity of weathering enhancement

The weathering enhancement per unit biomass ε is scaled by its maximum potential value ε_{max} by the deviation that planetary temperature T exhibits from the value $T_{max} \simeq 25^\circ C$, at which photosynthetic Carbon fixation is maximised (Lenton & Watson 2000b, Bergman, 2003). As discussed in chapter 3, although the climatic range across which distinct lichen species can maintain photosynthetic Carbon fixation is significantly greater than that of vascular plants, the temperature that maximises production in most species is not appreciably different (Nash, 1996). Hence I assume that regardless of whether I am modelling a Precambrian biosphere dominated by lichens and associated bacteria, or a Phanerozoic biosphere with a more elaborate soil structure dominated by vascular plants, T_{max} did not change sufficiently to qualitatively alter the results. But lichens of some form are present on every biome on Earth, whereas vascular plants exhibit a distribution more tightly restricted to latitude, particularly where they occur in Ecosystems of substantive biomass, containing a coherent soil structure. It is the difference in biomass that is the key issue here, the important point being that there is a difference between temperatures permissive for survival (including a short or erratic growth season, as in the contemporary arctic (e.g. Kappen et al, 1995)) and temperatures permissive for prolonged Carbon fixation (implying a relatively long growth season). In order to build up a tangible terrestrial biosphere dominated by vascular plants, of collective biomass equivalent to that at present, an average planetary temperature of around $8 - 10^\circ C$ or warmer probably needs to be sustained (Stanley, 1999), whereas the temperature range for lichen activity is much more variable. This leads us to a hypothesis concerning the change in glacial susceptibility from the Proterozoic, lichen dominated biosphere, to the contemporary Phanerozoic system dominated by vascular plants.

I hypothesize that a terrestrial biosphere dominated by lichens can maintain a given silicate weathering enhancement factor over a wider temperature range than can a terres-

trial biosphere dominated by vascular plants. This means that the Neoproterozoic, lichen-dominated biosphere was more likely to maintain biotic enhancement of silicate weathering down to the glaciation initiation threshold temperature T_i , than was the Phanerozoic biosphere, particularly as the latter became progressively more colonised by vascular plants from the Silurian onwards (Stanley, 1999). I now frame this idea in terms of the temperature sensitivity of the weathering enhancement factor per unit biomass, ε . I scale the deviation that temperature exhibits from T_{max} by a sensitivity parameter c , assuming that positive and negative excursions from the optimum temperature are equally damaging:

$$\varepsilon = \varepsilon_{max}(1 - c(T - T_{max})) \tag{5.12}$$

Figure (5.4) shows the results of a simulation in which temperature was described by (5.1) and solar luminosity S varied across values corresponding to the Proterozoic-Phanerozoic transition at $\sim 542\text{Ma}$, as described by equation (3.2) (Gough, 1981), and the sensitivity parameter c was incrementally decreased (Right Y-axis, green line). This scenario biases towards glacial susceptibility by using an initiation threshold of $T_f = 13^\circ\text{C}$, so that it is not “too easy” for biological changes to remove susceptibility to a snowball scenario. Left Y-axis (blue line) shows temperature as it oscillates between the threshold values $T_f = 13^\circ\text{C}$ and $T_i = -20^\circ\text{C}$, with a glacial interval duration dictated by the (fixed, present day) degassing rate D . The maximum potential enhancement factor was held constant at $\varepsilon_{max} = 5$, and normalised terrestrial biomass held constant at its present day value $B = 1$, $\frac{dB}{dt} = 0$. Though parameter choices are admittedly somewhat arbitrary, this serves to illustrate qualitatively the idea that a change in the temperature sensitivity of biological weathering enhancement can lead to a change in the stability of temperature relative to the glaciation threshold. As discussed in the previous chapter, the temperature at which lichen Carbon fixation is maximised approaches the value $\sim 20 - 25^\circ\text{C}$ of vascular plants, but different species of lichen can survive, and in some cases maintain net Carbon fixation over a temperature range from near freezing to above 35°C . This has implications for my work here comparing lichen-dominated and plant-dominated terrestrial biospheres. Implicit in equation (5.12) is that the temperature T_{max} at which maximum productivity is achieved will not qualitatively differ across most species of macroscopic photoautotrophs. However, prior to vascular plant colonisation of the land surface, a substantial change in temperature would not qualitatively alter biological weathering enhancement because a lichen dominated biosphere would be, probably through a change in species composition, significantly more likely to maintain tangible biomass and enhancement activity over a significant temperature range - by analogy with the ecological range of lichens compared with plants today. In short, the idea does not require that all lichens have a greater tolerance of temperature ranges than all vascular plants, but that different lichen species encompass, as a group, a wider temperature range for growth (Nash, 1996).

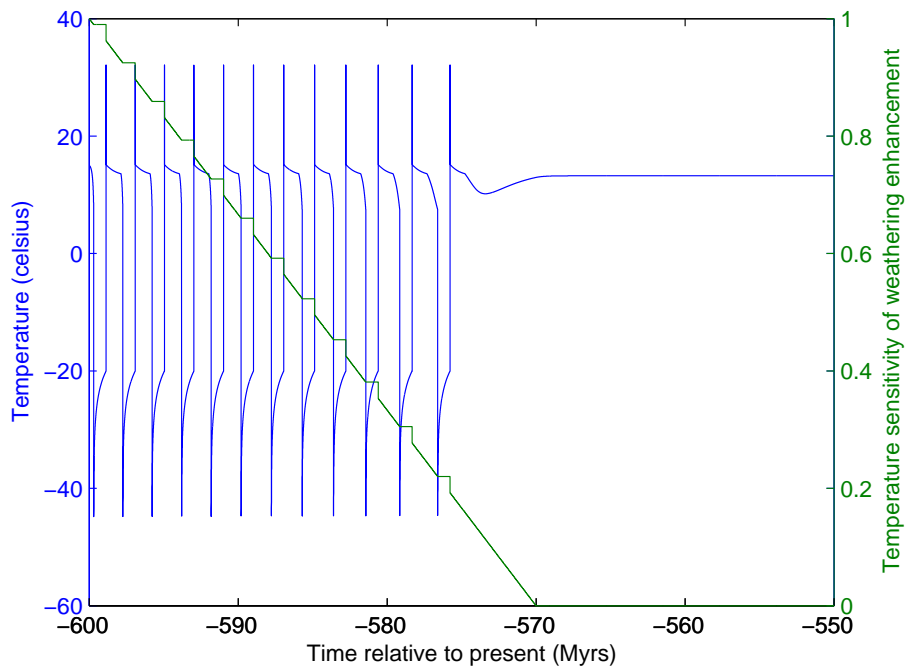


Figure 5.4 - Results of progressively inducing small reductions in the temperature sensitivity of silicate weathering enhancement, over a realistic range of luminosity values corresponding to the late Neoproterozoic. Left Y-axis shows average planetary temperature (celsius), right Y-axis the value of the parameter c as described above. X-axis shows the time in years relative to present.

Oxygen and photosynthetic efficiency

The oxygenase activity of Rubisco inhibits photosynthetic production, therefore can be reasonably expected to inhibit biological enhancement of silicate weathering that results from the growth of photosynthetic organisms. Hence rising Oxygen associated with the end of the Neoproterozoic glaciations (e.g. Kennedy et al, 2006) may have caused a reduction in biotic weathering enhancement, by imposing a cap on growth through photorespiration. The rise in atmospheric Oxygen that probably occurred from the late Neoproterozoic onward has been suggested to have imposed a limit on terrestrial biomass growth, hence biotic weathering enhancement (Lenton & Watson, 2004). I noted in chapter 3 that the fact that the lichens exhibit Carbon fixation in the aqueous phase, coupled with the lack of any strong evidence for photorespiratory activity in lichens, indicates that the Neoproterozoic, lichen-dominated terrestrial biosphere may have been less constrained by photorespiration. Therefore, the lack of immediate reglaciation is unlikely to have resulted solely from rising atmospheric oxygen. However, as vascular plants became increasingly spread over the Earth's land surface, photorespiration may have become an increasingly important consideration for growth (Bergman, 2003). Increased atmospheric oxygen may therefore have imposed a negative feedback on the growth/weathering enhancement of the terrestrial biosphere during the Phanerozoic, and in so doing reduced susceptibility to glaciation, in a way equivalent to that suggested by Lenton & Watson, (2004). In order to assess the plausibility of this hypothesis, I use the the function from chapter 3 relating terrestrial productivity to oxygen partial pressure (Bergman, 2003). Increased O_2 due to elevated marine organic Carbon burial (in turn due to increased PO_4 weathering influx to the oceans), has been suggested as a causal factor in the Cambrian explosion - being a necessary condition for macroscopic aerobic heterotrophs (Lenton & Watson, 2004). Oxygen can be related to temperature T , CO_2 , normalised (to present day) enhancement of silicate weathering per unit terrestrial biomass $\frac{\varepsilon}{\varepsilon_0}$ and relative colonisation of the land surface Ω by the relationship with the productivity function derived in chapter 3:

$$\frac{O_2}{O_{20}} = 3 - \frac{\left(\frac{CO_{2\beta}}{CO_{2Tr}}\right)^a e^{(b+c)(-T_f)}}{\frac{\varepsilon}{\varepsilon_0} \Omega \left(\frac{CO_{2Tr} - CO_{2Min}}{CO_{2\frac{1}{2}} + CO_{2Tr} - CO_{2Min}}\right) \left(1 - \left(\frac{T_f - 25}{25}\right)^2\right)} \quad (5.13)$$

One of the most simple scenarios by which biotic enhancement of silicate weathering could trigger a snowball Earth scenario involves a lichen-dominated Neoproterozoic terrestrial biosphere that is of relatively low biomass in comparison to the present day but which has a weathering enhancement factor per unit biomass significantly greater $\frac{\varepsilon}{\varepsilon_0} \gg 1$. Figure (5.5) (a) and (b) respectively show the value of atmospheric O_2 predicted by assuming that enhancement per unit biomass cancels $\frac{\varepsilon}{\varepsilon_0} \Omega = 1$, and overcompensates for $\frac{\varepsilon}{\varepsilon_0} \Omega = 2$ a lower net terrestrial biomass. The biotic weathering enhancement factor on the right Y-axis of

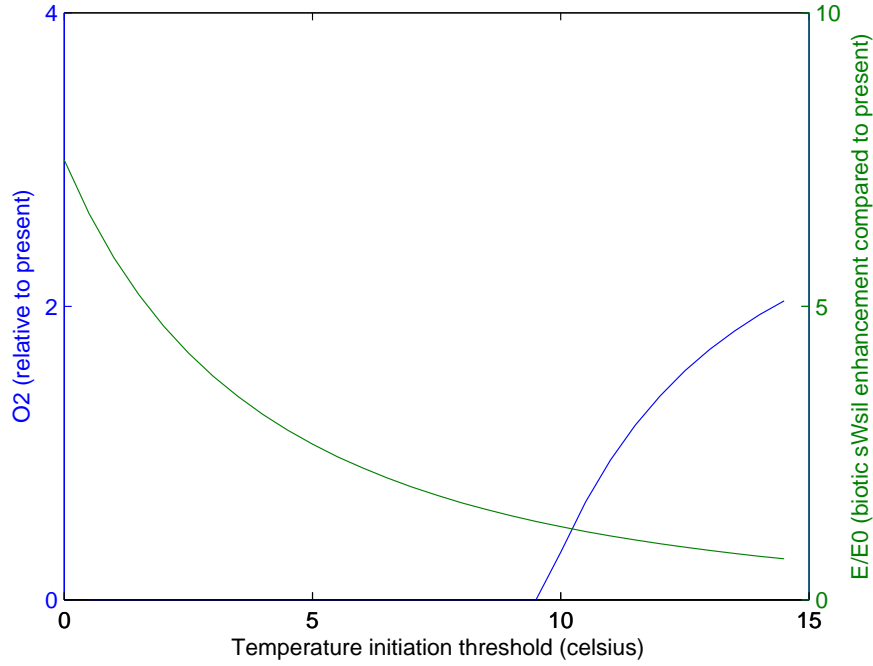


Figure 5.5 (a)- If a biologically-triggered snowball scenario occurred, the low CO_2 that this implies must necessarily go hand in hand with relatively low atmospheric oxygen. The above results were achieved by solving for oxygen within the function for relative growth of terrestrial biomass (see text). Left Y-axis shows the oxygen mixing ratio as a fraction of the present value, right Y-axis the enhancement of silicate weathering implicit (relative to the present day factor), X-axis shows the temperature at glacial initiation T_f . Figure (a) shows the results of assuming the enhancement per unit biomass ε completely compensates for the lower pre-phanerozoic value of the evolutionary colonisation forcing Ω , i.e. $\Omega\varepsilon = 1$. Figure (b) shows the results of assuming that the enhancement per unit biomass overcompensates for the lower total biomass $\Omega\varepsilon = 2$. The reason for this coupling stems from the expected photorespiratory inhibition of Rubisco at lower CO_2 partial pressures, which may potentially limit net Carbon fixation. The importance of this feedback is reduced as the total amount of fixed Carbon required to trigger glaciation declines - in other words, as the enhancement per unit biomass increases. It is reasonable that rising Oxygen could have limited biotic weathering enhancement (Lenton & Watson 2004), producing an equivalent pattern to figure 5.4. Nevertheless, the idea that reduced photosynthetic efficiency due to the increase in atmospheric O_2 could have caused the cessation of the Neoproterozoic glaciations requires the (improbable) assumption that lichens exhibit a similar photorespiratory response to vascular plants and have an equivalent enhancement per unit biomass.

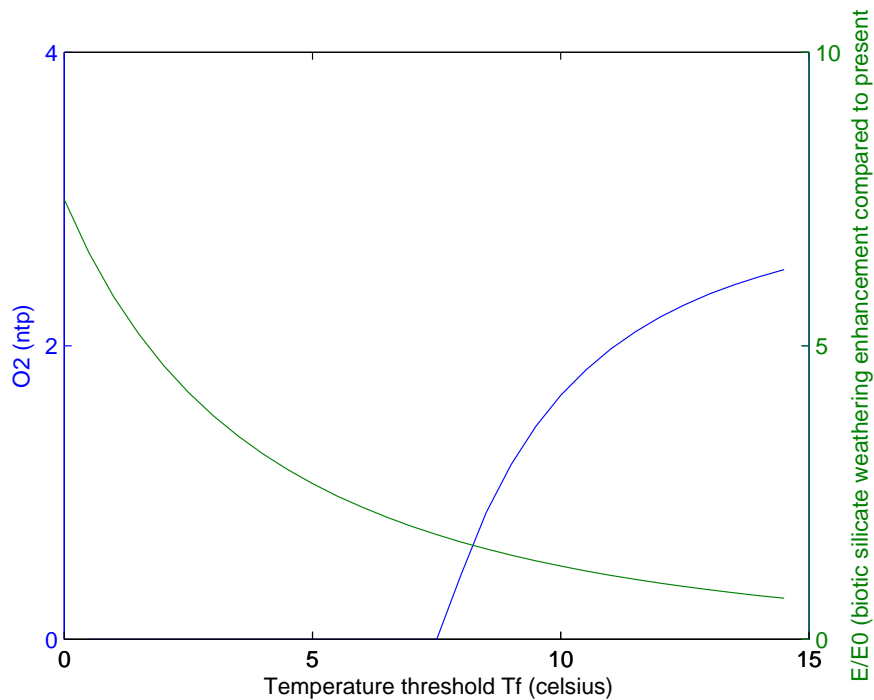


Figure 5.5 (b) shows the results of assuming that the enhancement per unit biomass overcompensates for the lower total biomass $\Omega\varepsilon = 2$. The reason for this coupling stems from the expected photorespiratory inhibition of Rubisco at lower CO_2 partial pressures, which may potentially limit net Carbon fixation. The importance of this feedback is reduced as the total amount of fixed Carbon required to trigger glaciation declines - in other words, as the enhancement per unit biomass increases. It is reasonable that rising oxygen could have limited biotic weathering enhancement as hypothesized in Lenton & Watson 2004, producing an equivalent pattern to that shown, but assessing the possibility requires a realistic constraint on the relationship between weathering enhancement and net terrestrial biomass.

both plots is (as discussed in chapter 3) the relative increase in the silicate weathering rate compared to an abiotic planet Earth. The relationship this factor bears to glacial susceptibility at different times in the past is quantified in chapter 3, and there is some overlap between the plots shown here and this relationship. However, an issue of relevance to susceptibility is the effect of increasing O_2 on productivity associated with the rise of vascular plants. Note that, according to the (generalised) productivity function (equation 3.23), increasing O_2 corresponds to reduced relative biological weathering enhancement, with the steepness of this relationship dictated by $\frac{\varepsilon}{\varepsilon_0}\Omega$, due to the physiological impact of Rubisco's oxygenase activity (Taiz & Zeiger, 1998). It is noteworthy that for $\frac{\varepsilon}{\varepsilon_0}\Omega = 1$ (Figure 5.5(a)) that present day oxygen levels $\frac{O_2}{O_{20}} = 1$ roughly coincide with the present day enhancement factor $\frac{E}{E_0}$ (at around $T = 12^\circ C$). This consistency between entirely separate physiological growth functions (Bergman, 2003), and weathering enhancement functions (Schwartzman, 1999), through the relationship (3.24) provides some support for the idea that contemporary high O_2 may limit terrestrial production (Lenton & Watson, 2004). If it can be assumed that at lower O_2 , more vascular plants would exist, and the weathering enhancement factor would be correspondingly higher, then high atmospheric Oxygen could reasonably be described as reducing the susceptibility to repeated snowball Earths at present. However, O_2 limits Carbon fixation; i.e. it limits biomass. The lack of any clear cut relationship between the silicate weathering enhancement factor E and the mass of the terrestrial biosphere was highlighted in chapter 3 - particularly in the light of changes in the kinetically-limited fraction of silicate weathering regimes. Without such a relationship, the strength of the influence of Oxygen on biological weathering enhancement cannot be further quantified. Even given this information, the question of the effect of Oxygen on glacial susceptibility requires data on the photorespiratory impact of different $O_{2(g)}$ partial pressures on the growth of lichen in order to be rigorously assessed. That said, the correspondance shown in figure 5.6 between a biotic weathering enhancement function (Schwartzman, 1999) and an entirely separate function describing the impact of oxygen on growth (Bergman, 2003), suggests that such an experiment may be worth undertaking.

Silicate weathering rate limitation and the growth of soils

In conjunction with the Oxygen and temperature sensitivity issues that I have noted are relevant to the spread of vascular plants, an important change may also have resulted from the associated spread of soils and soil-based ecosystems. The rate of export of some minerals is higher in lichen/moss -covered bedrock than in soil-covered temperate forests (Lamontagne, 1998). I noted previously the association between high net erosion and runoff rates with kinetic limitation of silicate weathering (West et al 2005). Only when silicate weathering is kinetically-limited does atmospheric CO_2 become relevant to the magnitude of the flux, hence only under such circumstances is the coupling between climate and the Urey reaction valid. Areas in which bedrock is covered by a solid structure are (probably)

associated with a reduced net runoff of weathering (and mineralisation) products (Lamontagne, 1998, Schwarzman, 1999). For example, leaf litter associated with conifer forests results in relative N immobilisation in comparison to lichen-covered bedrock (Lamontagne, 1998). Conversely, some studies have used the correlation between temperature and the runoff of weathering products to argue for a dominance of the magnitude of the global silicate weathering flux by its value in tropical regions (White & Blum, 1995). However, such studies are irrelevant to climatic impact estimates if they compare supply-limited and kinetically-limited regimes (West et al, 2005). Interestingly, even when tropical and polar drainage basins are compared, there is no clear climatic driver of the magnitude of Ca , Mg or K fluxes, which all correlate more strongly with variation within (rather than between) different watersheds (White & Blum, 1995). Of course, it is these Ca and Mg cation fluxes that are of strongest relevance to climate, via the Urey reaction. This is consistent with the idea that within-regime “noise” is dictated by the contrast between these two types of rate-limitation, with only kinetic limitation corresponding to climate in a predictable way. I present a theoretical but plausible distinction between soil-covered and bare rock silicate weathering regimes, and use it to argue that the Urey reaction rate decreased in magnitude and climatic impact after a lichen-dominated Proterozoic terrestrial biosphere was replaced during the rise of vascular plants.

The earliest tangible evidence of soils suggests a progressive increase in their abundance from roughly 500Ma onwards (Retallack, 2001). I propose that the spread of soils decreased the fraction of silicate weathering regimes that were limited by reaction kinetics, and in so doing reduced the sensitivity of the planetary silicate weathering rate to temperature and CO_2 . Because ecosystems with a tangible soil structure are characterised by slow net erosion rate and chemically complete erosion reactions, they are likely to be limited by substrate supply (i.e. erosion of the underlying rock) rather than by chemical and climatic factors. Biomes containing a substantive soil structure may have greater baseline concentrations of aqueous PO_4 , NO_3 immediately available, and consequently a greater biomass. But the rate of release of nutrients from unweathered bedrock is lower. Hence weathering is chemically incomplete and is limited by the supply of rock substrate - therefore its magnitude is largely decoupled from atmospheric CO_2 . In contrast, high, variable erosion rates and a fluctuating hydrological cycle mean that in largely uncolonised bedrock environments, weathering reactions are incomplete and are limited by kinetic factors (West et al, 2005). Only in such environments can the CO_2 -weathering thermostat be reasonably assumed to operate (West et al, 2005). What little available data there is suggests that soil-covered, vascular plant-dominated biomes are more compatible with supply-limited silicate weathering, and more sparse lichen/bacteria-dominated regimes with kinetic limitation. This amounts to a decrease in the planetary silicate weathering enhancement factor per unit biomass, because less of the terrestrial biosphere is directly active in terms of the Urey

reaction.

A mathematical exposition of this idea is not possible with the simple models used here, because it implies an entirely different function describing how atmospheric CO_2 changes over time, but would amount to a dramatic lowering of the effective baseline silicate weathering rate W_0 in equation (5.8). The result would be broadly similar to that shown for the increased biological temperature sensitivity (5.5), in that both this change, and a reduction in kinetic limitation of silicate weathering, would reduce the range of environmental conditions in which the Urey reaction was relevant to climate. For example, as a result of the proposed changes, kinetically-limited silicate weathering might have become only relevant to climate during those periods in Earth history in which supply-limited weathering in soil-covered biomes ceased, because (for example) temperature limited growth in such regimes. Under these circumstances, the effectiveness of the Urey reaction would be dictated by the extent, and impact, of how far planetary temperature departed from this critical temperature interval, in a manner qualitatively equivalent to that shown in equation (5.12) and figure (5.5). Although the result of these two changes would look similar, it is important to note that an entirely different range of (higher resolution) factors would become relevant to predicting atmospheric CO_2 in a system with a weaker Urey reaction buffer, therefore the approach used here would become inappropriate. The basic idea would be that silicate weathering would no longer be increased so directly by high temperature/greenhouse forcing. Only empirical studies determining the factors that limit silicate weathering rate in soil covered, and bare-rock environments can quantify this idea further.

Dynamic carbonate Carbon scenarios

As discussed in more detail in the previous chapter, the silicate weathering- CO_2 thermostat only operates in its simplest (and most effective) form (Figure 5.1) when a silicate weathering rate increase can be assumed to decrease atmospheric CO_2 . This assumption may become invalid when the carbonate Carbon rock reservoir C_R is changing in mass $\frac{dC_R}{dt} \neq 0$. In this case, the balance between carbonate weathering W_{carb} and carbonate burial B_{carb} (and the changes that occur within these fluxes with respect to temperature) can cause marine carbonate speciation to influence how atmospheric $CO_{2(g)}$ changes over time, making the situation more complex than shown in figure (5.1) (See chapter 4). The equations directly relevant to predicting atmospheric CO_2 then become:

$$\frac{dC_R}{dt} = B_{carb} - W_{carb} - D \tag{5.14}$$

$$\frac{d\sum CO_2}{dt} = -\frac{dC_R}{dt} \tag{5.15}$$

$$CO_2 = \Phi \sum CO_2 \tag{5.16}$$

With the atmospheric CO_2 fraction Φ a function of ocean temperature, pH and carbonate alkalinity, as discussed in chapter 4. The carbonate weathering and burial fluxes were related to their respective baseline values W_{carb0} and B_{carb0} via the deviation exhibited by temperature T from present day T_0 and CO_2 from present day CO_{20} , using the baseline fluxes discussed in the previous chapter (Bergman, 2003):

$$W_{carb} = W_{carb0} \sqrt{\frac{CO_2}{CO_{20}}} (1 + 0.087(T - T_0)) \tag{5.17}$$

$$B_{carb} = B_{carb0} \frac{Ca^{2+} (HCO_3^- + CO_3^{2-})}{Ca_0^{2+} (HCO_3^- + CO_3^{2-})_0} \tag{5.18}$$

The persistence of a tangible marine carbonate Carbon burial flux B_{carb} at temperatures low enough to significantly impair carbonate weathering W_{carb} can remove a large fraction of the aqueous marine CO_2 , thereby severely limiting the concentration of $CO_{2(aq)}$ in direct equilibrium with the atmosphere, because the fraction of total marine aqueous CO_2 made up by this species is small. Therefore, under scenarios in which the assumption of steady state CO_2 is relaxed and its dynamics described by equation (5.14), it is proposed that a high marine organic Carbon burial flux may provide sufficient reduction of CO_2 to drive the climate system colder than the glaciation threshold T_f . The role of the CO_2 - sink in figure (5.1) played by silicate weathering may become equivalent to the marine carbonate Carbon burial flux.

Just as the disposition to snowball-greenhouse oscillations can be removed if temperature-based negative feedback limits the silicate weathering flux at $T > T_f$, if the magnitude of the marine $CaCO_{3(s)}$ burial flux experiences an equivalent negative feedback, with temperature above the threshold $T > T_f$, the climate may no longer be susceptible to oscillation. This idea is illustrated in figure (5.6), the results of coupling the temperature function with discretized albedo to the ocean chemistry formulation discussed in chapter 4. At steady state degassing rate and with an identical (but temperature/ CO_2 -dependent) carbonate weathering function, if carbonate Carbon burial persists as temperature reaches and drops below the instability threshold T_f , the system undergoes sustained oscillation between snowball and extreme greenhouse states, in a manner equivalent to the original snowball Earth hypothesis, but with dynamic total carbonate Carbon (Kirschvink, 1992). If carbonate Carbon burial ceases at a warmer temperature than the bifurcation point T_f ,

temperature remains in the habitable region, although the relative abundance of marine carbonate species (not shown) may vary.

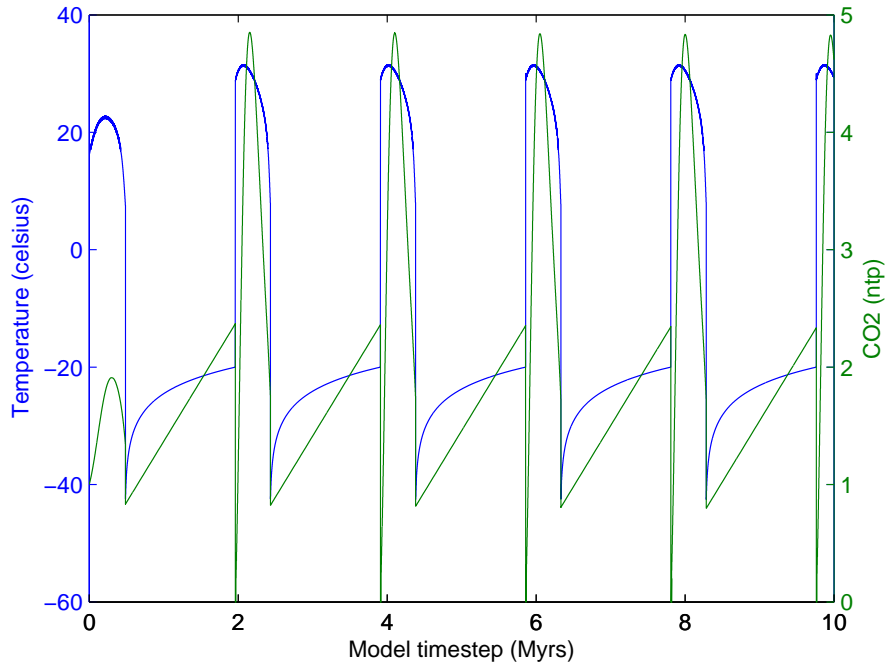


Figure 5.6 (a) - Disposition to snowball oscillations can also result from the relative positions of negative feedback on marine carbonate Carbon burial B_{carb} and the temperature initiation threshold T_f . Results are shown for an equilibrated atmosphere ocean scenario with solar luminosity held constant at $S = 1305.6 W m^{-2}$, corresponding to 550Ma, initiation threshold fixed at $T_f = 7.5$ celsius. Y-axis shows planetary temperature in celsius, X-axis shows model time step in millions of years. Green line corresponds to a scenario in which carbonate burial ceases before temperature drops below the threshold $T_{crit}(B) = 7.0$, blue line a scenario in which it continues until freezing $T_{crit}(B) = 0.0$. The large initial interglacial (first blue “spike”) is an artefact of the equilibration of the CO_2 -weathering system with the solar - luminosity used, causing a temporary rise in atmospheric CO_2 also seen in the steady state regime (green).

The reason that a systematic change in the temperature-based negative feedback on $CaCO_{3(s)}$ burial may have occurred during Earth history is that the magnitude of this flux is strongly influenced by the biosphere, hence subject to evolution. Ridgwell & Kennedy (2004) proposed that the lack of biologically-promoted open ocean $CaCO_{3(s)}$ precipitation prior to the evolution of foraminifera and coccolithophores would dramatically increase the sensitivity of the $CaCO_{3(s)}$ burial flux B_{carb} to the shallow shelf area suitable for deposition of $CaCO_{3(s)}$ precipitated in the photic zone, meaning that a reduction in this area (due to a reduction in sea level during glaciation) resulted in a very high marine CO_3^{2-} , hence a reduced CO_2 via the net change $CO_2 + CO_3^{2-} + H_2O \rightleftharpoons 2HCO_3^-$ (Ridgwell & Kennedy, 2004). This

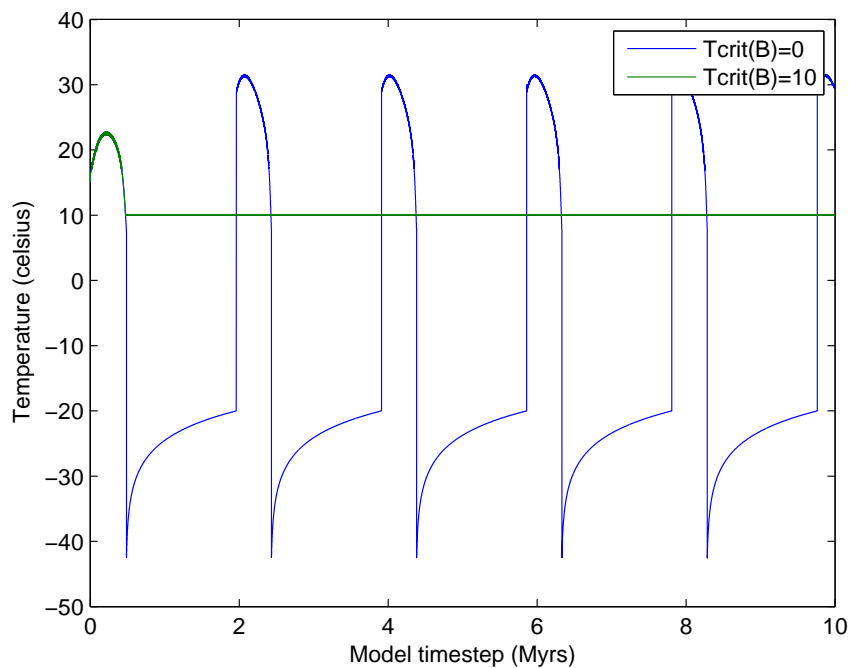


Figure 5.6 (b)- The same model set up as shown in figure 5.5 (a), but with the temperature results shown in isolation for clarity. Recall that the glaciation initiation threshold was held at $T_f = 7.5^\circ C$. Green line shows a scenario in which marine carbonate Carbon burial was set to zero when temperature decreased below $10^\circ C$, blue line a scenario in which this feedback did not occur until $7.5^\circ C$.

required two assumptions - first, a tangible carbonate weathering influx regardless of the temperature, second, a strong dependence of the $CaCO_{3(s)}$ burial flux on the CO_3^{2-} level in the photic zone. The ideas I suggest here require only the second of these assumptions, and are therefore more compatible with severe glaciation scenarios.

In the present day ocean, $CaCO_3$ precipitation is actively promoted by the biosphere. Coccolithophores (unicellular phytoplankton with $CaCO_3$ on their cell exterior), are thought to be responsible for around half of contemporary $CaCO_3$ precipitation, but did not originate until the Jurassic period $\sim 200 - 145$ Ma (De Vargas et al, 2004). A significant further contribution to present day carbonate precipitation is made by foraminifera - a group of zooplankton with a diverse range of carbonate shell morphologies. Radiation of the foraminifera occurred during the Carboniferous period $\sim 360 - 300$ Ma, but phylogenetic data has been used to propose a tangible Neoproterozoic foram community (Pawlowski et al, 2003). Were this the case, the argument that reduced shallow shelf depositional area could not have been compensated for by increased deep ocean $CaCO_3$ deposition during the Neoproterozoic (Ridgwell & Kennedy, 2004) might be weakened - the carbonate buffering of the era's ocean may have been more robust than previously assumed (Pawlowski et al, 2003). However, the dangers of extrapolation from molecular clock data in the absence of supporting fossils have been highlighted previously, and it is highly unlikely that significant biotic calcification (in the sense that the process is understood today; i.e. as a part of foraminifera ecology) occurred during the Neoproterozoic but escaped detection in the fossil record. In the absence of strong evidence for extensive Neoproterozoic biotic calcification, $CaCO_3$ precipitation has (reasonably) been assumed to have predominantly resulted from byproducts of bacterial metabolism during the snowball Earth period (Ridgwell et al, 2003). The key requirement of the mechanisms proposed here is that marine carbonate carbon burial did not exceed the (low) carbonate weathering influx during the glacial interval - i.e. there is a cap on the maximum possible magnitude of this burial flux. This is entirely consistent with $CaCO_{3(s)}$ precipitation as an incidental by-product of bacterial calcification. Photosynthetic uptake of CO_3^{2-} and HCO_3^- ions, and alkalinity release via metabolic sulphate reduction ($3.75SO_4^{2-} + 37.5H^+ + 30e^- \rightleftharpoons 3.75H_2S + 15H_2O$), denitrification ($2NO_3^- + 10e^- + 12H^+ \rightleftharpoons N_2 + 6H_2O$), the release of ammonium NH_4^+ , and the production of $CaCO_{3(s)}$ nucleation sites by various extracellular polymers, are all mechanisms by which bacterial activity promotes marine $CaCO_{3(s)}$ precipitation (Riding, 2000). A buffered marine carbonate system maintains roughly the same $W_{carb} - B_{carb}$ balance after reduction in available shallow shelf depositional area, a non-buffered system experiences a dramatic rise in CO_3^{2-} , biasing the various equilibria toward HCO_3^- (summarised as $CO_{3(aq)}^{2-} + CO_{2(aq)} + H_2O_{(l)} \rightleftharpoons 2HCO_{3(aq)}^-$) and reducing the marine $CO_{2(aq)}$ in direct equilibrium with the atmosphere (Ridgwell et al, 2003, Ridgwell & Kennedy, 2004). Via this positive feedback, a temperature reduction is amplified by reduced $CaCO_{3(s)}$ deposi-

tion, hence net $CO_{2(g)}$ drawdown - and the severity of snowball Earth events is dictated by the (lack of) buffering of marine $CaCO_{3(s)}$ deposition, hence by evolutionary change (Ridgwell & Kennedy, 2004). The key reason for proposing a more responsive buffering system during the Phanerozoic than the Neoproterozoic is that coccoliths and forams precipitate $CaCO_{3(s)}$ actively during their life cycle - and the process is therefore subject to natural selection, so that a decrease in the thermodynamic favorability of the reaction may (to some extent) be compensated for by organisms' ecological needs. This idea is consistent with Ridgwell's original slushball/carbonate buffering model (Ridgwell & Kennedy, 2004). Conversely, the majority of calcification that results from bacterial activity occurs upon alkalinity release from dead cells, and metabolic processes such as sulphate reduction may be less relevant (Bosak & Newman, 2003). Furthermore, the net rate of biotic $CaCO_{3(s)}$ precipitation is assumed to have qualitatively increased after the emergence of coccoliths and the radiation of foraminifera (Ridgwell et al, 2003). The key question is whether this greater degree of biotic calcification could persist (and cause snowball-greenhouse oscillation) when carbonate weathering and temperature were both sufficiently low to approach the bifurcation point. In the same way that the change in temperature sensitivity of silicate weathering enhancement (above) resulted from the group "lichens" maintaining weathering enhancement over a greater temperature range *collectively across all species*, so Proterozoic marine plankton and bacteria, collectively, could promote calcification over a larger temperature range, because marine carbonate Carbon burial was not so strictly tied *to a specific species composition* as it is in a marine ecosystem containing coccoliths and forams. Most coccolith species have an optimum temperature for growth at around $20^{\circ}C$, away from which bloom biomass declines sharply (Thierstein & Young, 2004). Species of foraminifera encompass a greater range of temperature optima, $\sim 4-20^{\circ}C$ (e.g. Mulitza et al, 1998) but their Proterozoic mass, species composition, and arguably even presence, is uncertain. The key difference making the Phanerozoic $CaCO_{3(s)}$ flux more directly sensitive to production was (I suggest) that Precambrian biotic promotion of $CaCO_{3(s)}$ deposition was a metabolic byproduct (Wright & Oren, 2004), whereas in the Phanerozoic active calcification made the process a necessary part of species' life cycles, meaning the magnitude of the flux was more directly related to ecological success. Nonetheless, it is critical to emphasize that because unambiguous radiation of actively calcifying species did not occur until the Mesozoic (e.g. Ridgwell & Zeebe, 2005), the carbonate buffering mechanisms proposed here can explain why the later Phanerozoic system was more buffered than that of the Proterozoic, but cannot offer any immediate explanation as to why the Neoproterozoic snowball Earth events ceased.

The carbonate buffering model was originally suggested as a means of integrating cap carbonate deposition with slushball glaciation scenarios. However, this synthesis required that the carbonate weathering flux remained at the baseline, pre-vascular plant value (equiva-

lent to that used in the GEOCARB and other models (Berner, 1994, Bergman, 2003)), and that substantive ice-free land mass persisted regardless of the severity of glaciation (Ridgwell et al, 2003, Ridgwell & Kennedy, 2004). Tangible weathering fluxes do indeed occur underneath glaciers, in part as a result of biotic activity (Skidmore et al, 2005), hence these assumptions may accurately represent a slushball scenario. However, the work in the previous chapter has shown that without significant input of carbonate alkalinity from weathering, and/or without significant curtailing of carbonate burial, then even a slushball solution may be unrecoverable. In short, significant ice-free land mass and large carbonate weathering flux are prerequisites for a slushball solution, so models in which these features are assumed to begin with cannot be considered tests of the snowball-slushball question. I suggest that the results shown in figure 5.5 indicate that the Ridgwell et al's carbonate buffering model is equally relevant to climate stability within hard snowball scenarios, in which case the buffering of carbonate deposition must occur with respect to changes in temperature, rather than just changes in ambient marine $[CO_3^{2-}]$. Oscillation occurs when biotic calcification prevents sufficient carbonate alkalinity build-up to stabilise atmospheric CO_2 . This amounts to the ability of the biosphere to promote calcification at low temperatures and when carbonate weathering influx is low.

Discussion

A system as intricate as the Earth's climate is affected by variables that adjust over many distinct timescales. Changes in boundary conditions qualitatively alter the long term dynamics of climate. Over time scales of the order of years, the surface ice albedo feedback is a function of local hydrology and atmospheric heat diffusion (North, 1975). But over millennial timescales, changes in planetary albedo can be simplified to discrete ice-covered and ice-free state changes, at the expense of losing information on the severity and point of occurrence of these states. A high resolution modelling study incorporating spatial changes in ice cover might detect the approach of a self-sustained, non-linear oscillation. For example, as the real part of the eigenvalue λ tended to zero within the system $\frac{du}{dt} = \lambda u$, (with u some vector describing the relevant variables), this would suggest that the onset of an undamped oscillation (i.e. the start or end of the snowball state) was approaching (Saltzman, 2002). This might be an accurate, quantitative *description* of the switch between snowball and greenhouse states, but (I think) it would not provide a parsimonious *explanation* as to why this switch happens in the real system. Furthermore, relating high resolution studies to deep time requires even more free parameters than used here, and determining in which parameter most of the uncertainty lies can become more difficult. In this chapter, I have attempted to simplify the situation, by noting that the reason for climate being susceptible (or not) to icehouse/greenhouse oscillation lies merely in the relative position of negative feedbacks between different variables, rather than in the particular dynamical description

that is most appropriate. I have assumed that the degassing flux will eventually cause cessation of any snowball glaciation (Kirschvink, 1992), and have treated susceptibility to entering a global scale glaciation as equivalent to susceptibility to oscillation between snowball and extreme greenhouse states. Thus, the problem can be boiled down to the idea that the atmospheric CO_2 steady state experiences a forcing that causes it to decrease, and that oscillation will occur if this forcing persists until temperature is below the bifurcation point $T < T_f$, and will not occur if this forcing experiences negative feedback at $T > T_f$. The occurrence of global scale glaciation in the Paleoproterozoic (Kopp et al, 2005) and Neoproterozoic (Hoffman & Schrag, 2002), but their absence from the Phanerozoic, suggests the introduction of such a negative feedback. The scenarios by which this may have occurred are:

- (1) An increase in the temperature sensitivity of biotic silicate weathering enhancement, such that enhancement was reduced as $T \rightarrow T_f$.

$$T_{MIN}(W_{sil}) < T_f \tag{5.19}$$

This requires the assumption that the abiotic silicate weathering flux alone was insufficient to drive the system into the snowball state. The evolutionary change relevant to the introduction of this feedback is the replacement of a terrestrial biosphere dominated by lichens and soil bacteria with one dominated by vascular plants growing within a soil substrate.

Additionally, the absolute weathering enhancement factor (without specificity to temperature) may have decreased due to:

- (a) An increase in the fraction of supply-limited silicate weathering regimes associated with soil growth and colonisation of more tectonically stable, low erosion environments, and/or;

- (b) A cap on net terrestrial biomass imposed by the rising atmospheric O_2 on the photosynthetic efficiency of vascular plants. This assumes that the growth of plants is more limited by photorespiration than that of lichens, whose photobionts tend to possess aqueous Carbon concentrating mechanisms (Nash, 1996). An implicit assumption in this idea is that the Phanerozoic biosphere has maintained a constant enhancement factor per unit biomass (i.e. since approximately the Silurian, (e.g. Schwartzman, 1999), and has experienced an upper limit on total biomass through photorespiration. The relative constancy of marine $\delta^{13}C$ since the end of the Neoproterozoic (Fairchild & Kennedy, 2007) might be assumed to support this idea, in that a constant marine organic Carbon burial flux implies a constant weathering-induced PO_4 influx to the ocean, hence constant biological weathering activity

(Lenton & Watson, 2000b, Lenton & Watson, 2004). An alternative means by which a CO_2 sink might have experienced negative feedback before climate entered the ice-covered state is:

(2) A negative feedback on carbonate Carbon burial occurring prior to temperature cooling below the temperature threshold for glaciation.

$$T_{MIN}(B_{carb}) < T_f \tag{5.20}$$

This is a development of Ridgwell et al's carbonate-buffering scenario in order to encompass hard snowball scenarios with extreme temperature fluctuations. The idea is simply that during the Neoproterozoic, $CaCO_{3(s)}$ was not tightly coupled to ocean temperature, because it was largely a byproduct of the release of alkalinity from dead bacterial cells. Hence, some carbonate Carbon burial occurred as long as there was tangible bacterial growth. The species composition of the marine biosphere may have changed as temperature decreased, but some precipitation of $CaCO_{3(s)}$ remained feasible. As proposed in previous work (Ridgwell & Kennedy, 2004), after marine calcification became more active (that is, a part of the life cycle relevant to survival and fecundity, hence subject to natural selection) after the radiation of foraminifera, then later of coccoliths, any cooling towards the bifurcation point $T \rightarrow T_f$ that was sufficient to limit production of these species would cause an equivalent relative reduction in the marine carbonate Carbon burial flux B_{carb} , perhaps enough to raise $CO_{2(g)}$ in the atmosphere, through a relationship of the form of equation (5.14).

The work in this chapter has separated these factors into two questions - why the susceptible planet did not instantaneously reglaciate, and why the subsequent Earth system appears to have become less vulnerable to global scale glaciation. It was important to make this separation in order to clarify my ideas above, but I note in conclusion that the ultimate reason that the planet is not currently experiencing a snowball Earth stems from a combination of the answers to both questions. The requirement for a biological "succession time" during which biotic weathering enhancement was required to recover from the glacial interval removed the vulnerability to an instant repeat glaciation. But the extreme glaciation event had effects other than the imposition of this requirement for the terrestrial biosphere to recover. I show in the next chapter that the snowball Earth events may have also directly triggered the proliferation of macroscopic, differentiated heterotrophs, including the ancestors of contemporary Metazoa. The idea that the proliferation of the first animals encouraged the growth of soils has been noted previously (McMenamin, 2004), as has the potential increase in reciprocal coevolution associated with the origin of predator prey systems (Butterfield, 2007). I note that these factors, in combination with the earliest examples of "herbivore"- "plant" (macroscopic heterotroph-macroscopic photoautotroph)

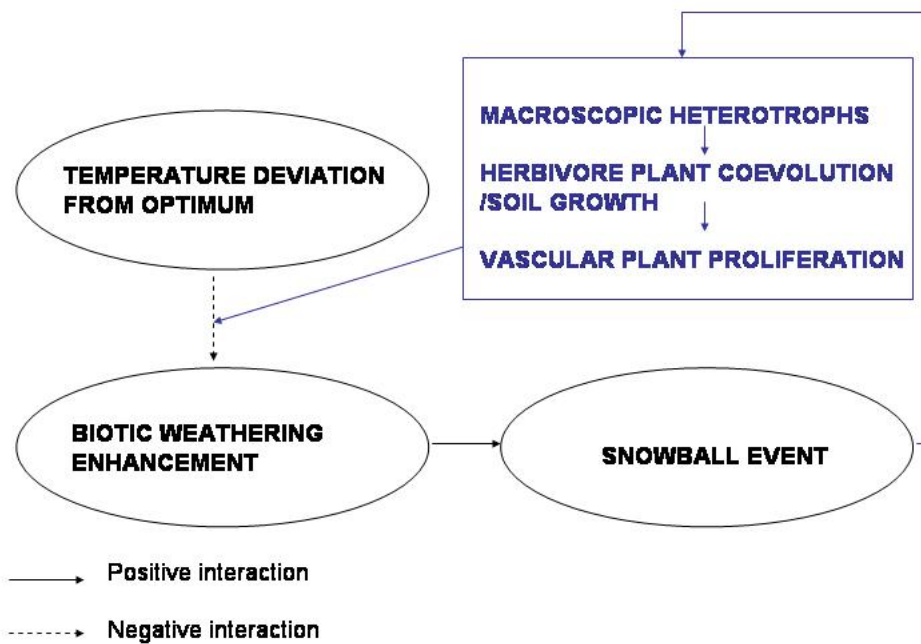


Figure 5.7 - Favoured scheme of cause and effect that lead to the reduction in susceptibility to global scale glaciation events towards the end of the Neoproterozoic. Dashed arrows indicate negative interaction, solid arrows positive interaction. The sequence of events shown in blue may have led to an increase in the strength of the negative interaction relating biological weathering enhancement and suboptimal temperatures, thereby reducing susceptibility to glaciation.

coevolution, in the sense that I understand it today, may have promoted the growth of a terrestrial photosynthetic biosphere sensitive to temperature fluctuation and requiring soils. As a result, the “animal” precursor ecosystems triggered by the snowball events may have promoted the growth of the “plant” precursor ecosystems that ultimately reduced susceptibility to such events. I sketch a possible sequence of cause and effect in figure (5.7).

Chapter 6: Neoproterozoic glaciations and the evolution of altruism

Summary

I hypothesize that a demographic and ecological effect of Neoproterozoic “snowball Earth” glaciations was to increase the fitness of group-level traits and consequently the likelihood of the evolution of macroscopic form. Extreme and repeated founder effects raised genetic relatedness - and therefore the influence of kin selection on the individuals within a group. This was permissive for the evolution of some highly costly altruistic traits, including those for macroscopic differentiation. In some eukaryotic species, the harsh and fluctuating abiotic conditions made a macroscopic physiology advantageous, perhaps necessary, for collective survival. This caused population wide group viability selection, whereby non-altruist “cheat” genotypes killed the groups they were in, and therefore themselves, by reaching fixation. Furthermore, dispersal between refugia would reach zero under anything near a “hard snowball”, which would protect altruists at high local frequency from the influx of cheats from neighbouring groups. I illustrate my hypothesis analytically and with a simple spatial model. I show how removal of between-group dispersal, in a population with initial between-group variation in cheat frequency, causes the relative frequency of altruists to increase whilst the population as a whole decreases in size, as a result of group death caused by cheat invasion. This may be of particular relevance to animal multicellularity because irreversible differentiation (highly altruistic in that it imposes a high fitness cost on the individual cell) is more prevalent than in other multicellular eukaryotes. The relevance of my hypothesis should be scaled by any future consensus on the severity of snowball Earth, but it is theoretically plausible that global-scale glaciations had a systematic influence on the level of selection during Earth history.²

Introduction

The Neoproterozoic era saw the most recent examples of global scale glaciation, followed by a qualitative increase in the taxonomic abundance and morphological diversity of macroscopic life during the Ediacaran period (Knoll, 2006, Vincent, 2004, Butterfield, 2007). The possibility of a causal connection between the Neoproterozoic glaciations and the evolution of the biosphere has been discussed for some time (e.g. Hoffman, 1998, Hedges, 2004, Vincent, 2004) but has lacked a mechanistic evolutionary basis. Similarly, a major gap in the “snowball Earth” hypothesis (Kirschvink, 1992, Hoffman et al, 1998, Hoffman & Schrag 2002) is its failure to explain how large celled, and potentially macroscopic Eukaryotes

²(The work described in this chapter was published in 2007 as “Neoproterozoic “snowball Earth” glaciations and the evolution of altruism” Boyle, R.A., Lenton, T.M. & Williams H.T.P *Geobiology* 5(4). 337-349).

could survive such an extreme climatic event. Many authors have used the assumption that the effect of a complete “hard” snowball Earth on life would have been intolerably harsh, as part of the motivation for investigating partial ice cover “slushball” solutions (E.g. Pollard & Kasting, 2005). But I argue herein that rather than presenting a paradox concerning how “complex” life could have survived a snowball Earth event, the demographic and ecological impact of a global-scale glaciation strongly favoured the evolution of group-level traits. Small, highly genetically related populations largely isolated from each other would have resulted in strong kin selection, relatively favourable to the costly “altruistic” life history strategies required for macroscopic differentiation. I argue that the “bottleneck and flush” style of evolution suggested as part of the original snowball Earth hypothesis (Hoffman et al, 1998) is entirely consistent with the levels of selection problem, and that causality between snowball Earth and the emergence of highly costly macroscopic form should be taken seriously as a hypothesis.

“Snowball Earth” as a geological pattern

The idea of glaciation at or near global in its spatial extent is not new (Harland & Rudwick, 1964), but has received recent attention via the “snowball Earth hypothesis” championed by Hoffman et al (Kirschvink, 1992, Hoffman et al, 1998, Hoffman & Schrag 2002). This hypothesis describes how glaciation supposedly results from extensive $CO_{2(g)}$ drawdown by weathering of low latitude continents, and eventually ends through $CO_{2(g)}$ build up from tectonic outgassing. Globally synchronous glacial tillites with primary equatorial remnant magnetism occur in three intervals during the late Proterozoic era at 710, 635 and 580 million years ago, although the synchronicity of the latter interval is more contentious (MA) (Evans, 2000, Fairchild, 2007). These date estimates are imprecise, ranging by 5 – 10 million years (Myr) or more, with estimates frequently overlapping within analytical error (Fanning & Link, 2004). Estimated duration of the glacial period is similarly imprecise, but in the region of 6 – 12 Myr (Hoffman et al, 2002). Some glacial tillites contain incompletely oxidised “banded” iron formations, invoking deep ocean anoxia and therefore an ocean at or near isolation from the atmosphere through surface sea ice cover. Most are overlain with metre thick “cap” carbonates, suggesting sudden exposure of the ocean to an atmosphere extremely high in CO_2 at the end of the glaciation. The Carbon isotope ^{13}C is enriched prior to some glacial periods then dramatically depleted during and immediately after (e.g. Kennedy 1996, Misi & Veizer, 1998, Kennedy et al, 2001, Rothman et al, 2003) with an equivalent pattern in ^{34}S (Veizer, 1998, Hurtgen 2002, 2005) - suggesting a crash in global productivity. Alternative models used to explain the paleomagnetic evidence include high orbital obliquity (Meert and Torsvik, 2004) and true polar wander (Kent & Smethurst, 1998) but are much less parsimonious than the idea of global-scale glaciation in integrating many of the other separate lines of evidence (Evans 2000, 2003, 2005). The latitudinal extent of ice progression remains equivocal. Glacial scouring - therefore hydrologic activity

(Rice & Hofmann, 2000, Hoffman & Schragg, 2002) has been used to invoke “slushball” solutions with some open tropical oceans (Hyde et al 2000, Baum & Crowley, 2001, Peltier et al, 2004, Pollard & Kasting, 2005), but is not necessarily impossible under a “hard snowball” with a minimal hydrological cycle including sublimation (Pierrehumbert, 2005, Baum & Crowley, 2003). The incompletely oxidised Iron sediments and cap carbonates argue for an ocean that is highly anoxic and largely sealed from the atmosphere.

A change in evolutionary tempo?

Biomarkers suggest the possible existence of eukaryotes as far back as the late Archean (Brocks et al 1999), and multicellular Eukaryotes can be identified from diagnostic cell division patterns, and later macroscopic form, from the Mesoproterozoic onward (Hofmann, 1990, Javaux et al, 2003, Knoll et al, 2006, Butterfield 2004, 2005, 2007). But there are no macroscopic animals prior to the late Neoproterozoic. The Mesoproterozoic 1800 – 850 Myr Eukaryotic fossil record documents the divergence of major Eukaryotic clades, but exhibits increasing but relatively low taxonomic abundance and little or no macroscopic differentiation. (Hofmann et al, 1990, Knoll, 2006, Huntley, 2006). During the Cryogenian period 850 – 635 MA encompassing the two most severe glaciations, acritarch taxonomic diversity crashed, before peaking sharply after the period’s ending (Knoll, 1994, 2006, Grey et al, 2003, Narbonne, 2005, Huntley et al, 2006). The subsequent early Ediacaran period 632 – 560 MA exhibits a marked increase in morphological diversification in algae (Xiao, 2002, 2004), (potential) animals (Xue et al, 1992, Li et al, 1998, Grotzinger, et al, 2000, Narbonne and Gehling, 2003), and unassigned macroscopic eukaryotes (Knoll, 2006, Butterfield 2007). Subsequent radiation of the Ediacaran biota 575 – 542 MA gave rise to the earliest examples of macroscopic differentiation into what are discernably organs (Xiao, 2004, Narbonne, 2005), prior to the rise of the Eumetazoa in the Cambrian explosion. Molecular clock studies have consistently found early divergence times for Eukaryotic phyla since their inception (Brown et al, 1972, Feng et al, 1997, Wang et al, 1999, Heckman et al, 2001, Hedges, 2001, 2004,). With some exceptions (Peterson et al, 2005, Peterson & Butterfield, 2005), molecular clock studies tend to place the origin of major animal clades significantly earlier than does the fossil evidence. However, the problems with making systematic inferences based on molecular clock results were discussed in the first chapter. Further, it is clear that eukaryotic differentiated multicellularity was present in algae and fungi significantly before any glacial event (Butterfield, 2000, 2005). Therefore it is incorrect to think of global scale glaciation as having been a necessary condition for the evolution of multicellularity or architecturally complex form. But after the glacial events, macroscopic form unequivocally became more taxonomically abundant and morphologically diverse. And I think it is also simplistic to assume that climatic events on the scale of the Neoproterozoic glaciations did not have a systematic influence on evolution.

Co-operation and altruism

There exist many circumstances where a population is better off collectively if each individual produces a costly extracellular substance that is available to the whole local population (e.g. a bacterial siderophore). The short term fitness benefit an individual genotype can gain by forgoing this cost and investing extra effort in its own reproduction but benefiting from production of the substance by its neighbours, increases its relative frequency - and therefore limits the level of the costly substance. This exemplifies the “tragedy of the commons” that the average fitness of the population is lower than that of a population in which all members acted altruistically and produced the costly substance. The definitive link that such “public goods” traits have with cell density and group phenotypes means that understanding when such costly traits are adaptive is important in describing the origins of multicellular and macroscopic form.

Natural selection frequently operates hierarchically on large groups of replicators (like multicellular organisms) that are composed of smaller individual replicators (like cells). Many traits have an evolutionary impact on both the bearer and on individuals with which the bearer interacts - such traits are referred to as “social”. Often, the trait value that maximises the fitness of the bearer is different to the trait value that has the greatest positive impact on other individuals - such as when genes for unrestricted cell growth lead to tumours in animals and plants. This leads to a tension between conflicting selection pressures at the individual and at the trait group levels. A trait that increases the fitness of the individuals with which the bearer interacts is termed co-operative, and a co-operative trait that imposes a fitness penalty on the bearer is termed altruistic (e.g. Lehmann & Keller, 2006), though of course no sentience is implied. If an individual interacts with an altruist, it receives a benefit, if it interacts with a non-altruist “cheat” individual, it receives nothing and may experience decreased fitness, depending upon its own genotype. Whether or not altruistic traits are adaptive depends on the nature of the relationship between the focal “actor” individual bearing the trait, and the “recipient” individual experiencing the trait’s results. There are a number of scenarios that can give rise to co-operation, all involving some constraint on the ratio $\frac{b}{c}$, of fitness benefit to recipient b , and fitness cost to altruist c . Each scenario involves some measure of the probability that an altruistic strategy will encounter and/or cause benefit to, a copy of itself. Different circumstances that can give rise to evolutionarily stable co-operation are (from Nowak, 2006):

(a) Kin selection $\frac{b}{c} > \frac{1}{r}$ (Hamilton, 1964). This process describes the effect on the fitness of an altruistic gene of the probability that the recipient of altruism also carries a copy of that gene. This probability is termed relatedness r , but is defined specifically with respect to the focal locus and measures the probability of a correlation in trait values - which is not necessarily identical to a correlation in descent. Kin selection is normally referred to

in the context of “Hamilton’s rule” $rb > c$ (Hamilton, 1964, 1972). The conditions under which kin selection is relevant to a given trait depend on the balance between kin selection and kin competition, and consequently on the demographics - other more complex forms of Hamilton’s rule have been derived to incorporate the influence of population viscosity under spatially continuous conditions (e.g. Van Baalen & Rand, 1998), as well as varying ploidy and sex ratios (Hamilton, 1972).

(b) Group selection (e.g. Sober & Sloan-Wilson, 1998). This is a means of expressing the way in which natural selection operates hierarchically on group replicators (such as multicellular organisms) that are themselves composed of smaller individual replicators (such as cells). In circumstances where trait values that increase the short term fitness of the smaller replicators simultaneously decrease the long term fitness of the larger replicators of which they are a part, then evolution of co-operation requires $\frac{b}{c} > 1 + \frac{n}{m}$, where n is the maximum number of individuals per group, and m is the number of groups in the higher level population (Traulsen & Nowak 2006). This condition arises from the assumption that a group of altruists will either split more frequently (“group fecundity selection”) or have a higher probability of survival (“group viability selection”) than will a group of cheats. It is arguable that in nature the probability of two individuals sharing a gene is reasonably approximated by $r \simeq \frac{m}{m+n}$ - i.e. that kin selection is an explicit genetic description of one type of group selection (Frank, 1998, Nowak, 2006).

(c) Reciprocity (Trivers, 1971). If an altruistic act by an individual increases the probability of that individual being the recipient of altruism, the trait may proliferate. Direct reciprocity requires $\frac{b}{c} > \frac{1}{w}$, with w , the probability of a repeated social interaction between the same two individuals, necessary to scale the mutual benefit from an interaction between two altruists by the probability that this interaction will happen again (Trivers, 1971, Axelrod & Hamilton, 1981). Reciprocity may also occur in other contexts, including a spatial framework $\frac{b}{c} > k$ where k is the average number of neighbours per individual (Nowak & May, 1992).

A mechanistic hypothesis

I hypothesize that global-scale Neoproterozoic glaciations caused unicellular eukaryotic individuals to experience high within-group relatedness and therefore strong kin selection ((a) above). Because between-group dispersal was at or near zero on a planet covered in ice, cheats could not spread over the population and individual strategies involving kin competition had a reduced fitness payoff compared to non-glacial conditions. The benefit of altruistic strategies was increased by the need for resource sequestration and accentuating disequilibrium with the environment, which (I think) is more efficient with the division of labour possible with macroscopic, organ level differentiation (Boyle & Lenton, 2006). After

reaching or approaching fixation by local kin selection, such multicellular scale physiology had consequences that made groups of altruists significantly more likely to survive the harsh abiotic conditions than groups of cheats - causing strong between-group viability selection (encompassed within (b), above). Therefore by reaching local fixation, cheat genotypes caused the group they were within to experience dramatically curtailed growth, or (more likely) dramatically lower survival probability. Snowball Earth thus gave rise to a uniquely strong sampling process favouring altruism, of kin selection within groups, and group viability selection between groups, a process that operated over a geological time scale and a global spatial scale.

Relatedness and founder effects

Snowball Earth would decimate the mass of the biosphere and scatter remaining populations into isolated refugia, in which individuals were descended from a number of “founder” individuals dramatically fewer than under non-glacial conditions. Fluctuation in hydrological and temperature conditions would shorten the growth season and make resource availability erratic - analagous to modern arctic biomes (e.g. Vincent, 2004). This would cause dramatic, repeated founder effects on a global spatial scale and a multi-million year temporal scale, leading to small, highly related populations with little or no dispersal between them. The promotion of the evolution of altruistic traits by repeated founder effects has been noted before (Cohen & Eshel, 1976, Eshel, 1977), though without tangible examples with sufficiently long duration and large spatial extent to have had an important influence on the history of life. In general, increasing demographic mobility (i.e. immigration and emmigration) has long been appreciated to impede the evolution of altruism by reducing the probability that the recipient of altruism also carries the altruistic gene (Wright, 1945, Eshel, 1971, Van Baalen & Rand, 1998). The amount of immigration required to hinder the evolution of altruism is negatively related to the size of the group (Cohen & Eshel, 1976). The biotic refugia present in a world nearly or entirely covered by ice would be small and intermixed with each other to a minimal extent, with complete between group isolation from each other during a “hard” (equatorial) snowball. Although the data do not allow us to specify a number of founder effect cycles, I think that uniquely high kin relatedness, fluctuating demographic conditions, and a spatial structure conducive to altruism are a reasonable description of the conditions prevailing on a planet with minimal biotic refugia interspersed with near global glacial cover.

The advantage of “cheating”

Altruism can evolve in viscous spatial populations by kin selection (e.g. Van Baalen & Rand, 1998), however under some conditions kin competition can outweigh kin selection (e.g. Griffin & West, 2002). Consequently, highly related populations are not always synonymous with increasing altruism. The balance between the the two processes depends on

the details of the trait and of the species, and the benefit to be gained from a non-altruistic strategy in terms of extra offspring. If productivity is low, and chances of dispersal to a new group are at or near zero, then a unicellular eukaryotic genotype that does not contribute to any higher level physiology would not have significantly more offspring than the relatives with which it was competing, i.e. survival becomes a more important component of fitness than does fecundity. More importantly, any detrimental impact non-altruist strategies had on the group might significantly decrease the survival probability of groups in which kin competition proliferated. Hence I think snowball Earth also reduced the fitness payoff for kin competition, swaying the balance of within-group evolution towards kin selection. In addition to processes sensitive to kin relatedness, reciprocal altruism is promoted by a small number of neighbours with low spatial demographic mobility (Nowak & May, 1992). Assuming the existence of some rudimentary cellular recognition mechanism, greatly reduced or absent between-group dispersal, and persistence of life in small populations, would increase the probability of repeated interaction between the same individuals. This means that the kin selection processes discussed may have been complemented by an element of reciprocity. Furthermore, if altruism is necessary for group survival, then in order to survive, non-altruist strategies must either avoid reaching fixation, or disperse to a new group before the death of any group that they come to dominate. Building a macroscopic Ediacaran “proto-animal” is a costly evolutionary innovation, probably requiring extensive terminal differentiation. In the majority of refugia, the ratio of the cost of altruism to the benefit would still be too high, cheats would reach fixation, and the group would go extinct. But not in all cases. And removal of virtually all between-group dispersal by the glaciations would mean only those rare groups where altruism was adaptive would leave descendants. Consequently, the species-wide relative frequency of altruistic strategies increased over a global spatial scale and multi-million year timescale.

Selection pressure for group level differentiation

The very existence of bacterial “public goods” such as siderophores demonstrates how a group of cells acting collectively can increase the average availability of a scarce resource through a scavenging behaviour linked to cell density. It is reasonable to suppose that the erratic, low energy hydrological cycle, and dramatic decrease in terrestrial weathering of a global scale glaciation would have made virtually all resources scarce and available only erratically during, increasing the evolutionary incentive for such group-level traits. We have argued (chapter 2, Boyle & Lenton, 2006) that the greater capacity of groups to undergo differentiation better predisposes them to tolerate fluctuation in the physical environment. Greater longevity and size makes groups more likely to encounter such fluctuation, giving rise to a positive feedback to exploit this potential to differentiate. I.e. under conditions likely prevailing on a snowball Earth, a macroscopic system of highly related eukaryotic cells would increase the likelihood of its survival and reproduction by differentiation into

organ structures that allowed it to (for example) sequester resources and maintain constant water potential. I think such a structure would leave significantly more descendants than a collection of autonomous single cells of equivalent size. Similarly, fluctuating climatic conditions will actively select for a latent reproductive stage in order to survive periods of suboptimal environmental conditions. Spatial heterogeneity and extreme gradients in redox conditions, water potential, temperature and resource conditions would be prevalent on a snowball Earth. Hence I propose that during the Neoproterozoic glaciations, the imposition of confined but heterogenous spatial structure, as well as harsh and fluctuating physical conditions, increased the fitness of differentiated group-level form with efficient division of labour. Within group kin selection was therefore complemented by between group viability selection for a division of labour efficient enough to survive the harsh conditions.

A simple model

Outline

A theoretical species contains two possible genotypes, altruists and cheaters (the former of which experience a fitness cost which the latter avoid, as above). A population of this species is subdivided into 100 groups. Each group has two neighbours, so that the total population resembles a ring of connected groups. The presence of at least one altruist is necessary for each group to remain alive, but (by definition) cheaters have a higher local replication rate because they do not experience the cost of group contribution. The replication rate of all individuals (regardless of genotype) within a group is proportional to the local relative frequency of altruists. Individuals can send new offspring to neighbouring groups (or not) according to a dispersal parameter, the impact of which on the cheater-altruist trade-off is examined.

I now illustrate analytically the two distinct phases that I propose describe the influence of snowball Earth on the evolution of life history strategies in relevant Eukaryotic species:

Phase 1: Repeated founder effects increase relatedness, altruism becomes necessary for group survival

Let t_{crit} be a sufficient number of generations for altruism to gain a sufficient impact on fitness that a group filled with cheats will go extinct. For example, t_{crit} could be a sufficient number of generations (of a species of unicellular eukaryotes) over which Hamilton's rule continuously holds, for a costly altruistic trait for multicellular aggregation to change from having a positive but trivial collective fitness payoff, to having a qualitatively higher fitness payoff such that a group of cheats would be at an extreme fitness disadvantage. A useful comparison is that between an essentially autonomous unicellular species with facultative multicellular grouping, and a species with a multicellular physiology sufficiently

co-ordinated and efficient that autonomous reproduction is either maladaptive or obsolete. I assume that such a physiology would impose extensive fitness penalties on individual cells, requiring many generations over which highly costly altruism was adaptive, in order to become established. I think this provided a constraint on the evolution of such traits. As mentioned, extreme glaciations would force eukaryotic species into small populations experiencing an erratic, short growth season, fluctuating hydrological cycle and only brief intervals of habitability. Extreme and repeated founder effects drove up relatedness causing strong kin selection. Such conditions would have had to hold for the required t_{crit} generations. Let E be some representation of the state of the abiotic environment that has influence on the fitness of altruistic traits. I lump all systematic change in the kin selection parameters over the focal time interval into the effect that the changing abiotic environment has on these parameters, so that (by the chain rule):

$$\frac{\partial}{\partial t}(rb - c) = \frac{\partial}{\partial E}(rb - c) \frac{\partial E}{\partial t} \tag{6.1}$$

Implicit in this formulation is my assumption that the strictly biotic constraints on the evolution of altruistic, macroscopic physiology (i.e. any constraint in terms of “laws of form”) did not systematically vary over the Neoproterozoic era (and in my opinion probably over all of Earth history) in any way that was not dictated by how different physiologies would fair in different abiotic environments. Certain physiologies (namely terminal organ-grade differentiation characterising animals today) could only evolve in abiotic environments that made the high fitness cost to the individual cell an adaptive trade off. Recalling that even in a permissive environment, many (t_{crit}) generations would be needed for such a costly macroscopic physiology to become co-ordinated enough for this trade off to be achieved, I require the abiotic environment E to allow Hamilton’s inequality to hold consecutively for this length of time:

$$\prod_{t=1}^{t_{crit}} \frac{1}{2} \left(1 + \frac{\int_0^t \frac{\partial E}{\partial t} \left(\frac{\partial}{\partial E}(rb - c) \right) \partial t}{\left| \int_0^t \frac{\partial E}{\partial t} \left(\frac{\partial}{\partial E}(rb - c) \right) \partial t \right|} \right) > 0 \tag{6.2}$$

Because snowball Earth operated over timescales unequivocally evolutionary (as opposed to ecological) in length, and because the dynamics of populations of proto-multicellular Eukaryotes were likely orders of magnitude faster than their modern descendents, I think this would have been possible during the Neoproterozoic glaciations. The requirement for altruism to become necessary for group survival is a prerequisite for the group viability selection I suggest below to be effective. But macroscopic form exists, multicellular animals and plants with excessive tumours die, so altruist frequency did gain such an influence at some point in Earth history. I think the radiation of the Ediacara immediately after a period demographically conducive to altruism is not merely coincidental. Finally, although ubiquitous small populations would increase the impact of genetic drift on evolution (e.g.

Wright, 1945), this does not preclude an additional directional trend, particularly under uniquely high relatedness conditions. Macroscopic form involving terminal differentiation is a physiological elaboration on mechanisms of differentiation present in bacteria and more simple Eukaryotes (e.g. Rainey & Rainey, 2003). I emphasise that I am not proposing any novel mechanism for the evolution of altruistic form, merely an abiotic environment that biased evolution towards strong kin selection and low kin competition, releasing an evolutionary constraint on highly costly group-level traits.

Phase 2: Complete removal of between group dispersal - “cheats” drive themselves extinct

If the presence of at least some altruists is a prerequisite for group survival, the non-altruist strategy that will leave most descendents is one that either remains at intermediate frequency (i.e. is further on the continuum towards altruism), or one that migrates to a new group before the death of the current one. An example of this trade off is disease - virulence is a strategy that gives a pathogen high fitness only in circumstances in which dispersal to a new host is possible before the death of the current one (e.g. Day, 2003). In a situation in which dispersal between individual groups is not possible - and, simultaneously the presence of altruists is a prerequisite for survival, cheat genotypes that reach fixation will die and only those that are less harmful to the group and/or remain at intermediate frequency will leave descendents. For example, if altruism constitutes storage of a resource of which there is no external supply over significant periods of time, then a cheat genotype that consumes the resource without sequestering it will out-compete an altruist genotype that sequesters a fraction of the resource available to it. But once the cheat genotype reaches fixation the resource supply will be exhausted and the whole group will die. A similar argument might be made for a patch of cells that required the presence of some altruistic terminally differentiated cells to form a boundary against a harmful external environment (such as one of fluctuating osmotic conditions). Without the possibility of between group dispersal, the death of all such altruists because they had been outcompeted by cheats would also constitute the death of the cheats. All macroscopic, multicellular form requires such altruistic strategies on the part of its constituent cells. And I think it is a reasonable assumption that emigration would be dramatically curtailed if not absent, in a world in which life was persisting in scattered refugia with the intermediate space nearly or entirely covered with ice.

Spatial implementation

A species exists in a population separated into G total groups. Each group has k neighbour groups, to which members of that group disperse with probability D per individual, per generation. I am interested in the way in which the j th genotype changes over time, because I will later label j as either altruist A or cheat S . The j th genotype has fitness F_j , by

which the genotype's frequency changes by each timestep, a starting frequency of N_{j0} and changes over time according to:

$$\frac{dN_j}{dt} = \frac{d}{dt}(N_{j0}F_j^t) = N_{j0}Ln(F_j)F_j^t \frac{dF_j}{dt} \quad (6.3)$$

The change in the genotype's frequency within a group $\frac{dN_j}{dt}_{group}$ is dictated by the interaction between those individuals already present (the within group dynamics) and the contribution of movement into and out of the group (the between group dynamics). The latter contribution is denoted by the operator $\frac{\partial}{\partial k}$:

$$\frac{dN_j}{dt}_{group} = (1 + Dk \frac{\partial}{\partial k}) \frac{dN_j}{dt} \quad (6.4)$$

The total change in the genotype's frequency $\frac{dN_j}{dt}_{total}$ across the whole population (i.e. over all G groups) is the sum of the changes in each group:

$$\frac{dN_j}{dt}_{total} = \sum_g^G (1 + Dk \frac{\partial}{\partial k}) \frac{dN_j}{dt}_g \quad (6.5)$$

For steady state global frequency of the j th genotype (i.e. all groups are experiencing the same balance of between and within-group dynamics, and the differences are dictated merely by starting conditions), over the whole population of G groups (the change over which is denoted by the operator $\frac{\partial}{\partial G}$), I can approximate with:

$$\frac{dN_j}{dt}_{total} = G \frac{\partial}{\partial G} (1 + Dk \frac{\partial}{\partial k}) \frac{dN_j}{dt} = 0 \quad (6.6)$$

There are four ways that this steady state for the j th genotype $\frac{dN_j}{dt}_{total} = 0$ can happen.

(1) Total extinction $G = 0$. Although under a global glaciation, this will encompass the majority of cases, it is not interesting to us because the species to which it happened did not leave descendents.

(2) No neighbours $k = 0$ and/or dispersal probability $D = 0$, without total extinction. As described, I think that a situation at or approaching a "hard" snowball Earth removed between group dispersal D and thus gave rise to the rare if not unique situation that the overall dynamics were the sum of the within group dynamics across all groups, without any immigration or emmigration:

$$\frac{dN_j}{dt}_{total} = \sum_g^G (1 + Dk \frac{\partial}{\partial k}) \frac{dN_j}{dt}_g = \sum_g^G \frac{dN_j}{dt}_g \quad (6.7)$$

(3) A global viscous population with the same change in genotype frequency over all groups:

$$\frac{\partial}{\partial G}(1 + Dk \frac{\partial}{\partial k}) \frac{dN_j}{dt} = 0 \quad (6.8)$$

I do not think that this happened during the Neoproterozoic glaciations, when the world was covered with ice. Even populations in close proximity would be confined to (for example) springs derived from separate and confined sources of volcanic heat, therefore not spatially continuous.

(4) A viable population within each group, with non-zero neighbours $k \neq 0$ and non-zero dispersal probability $D \neq 0$, experiencing a balance between the within and between group dynamics:

$$(1 + Dk \frac{\partial}{\partial k}) \frac{dN_j}{dt} = 0 \quad (6.9)$$

This describes a more comprehensive equilibrium encompassing a balance of between group and within group contributions to frequency change, an equilibrium relevant to most contemporary levels of selection problems. Whilst I think that situation (6.2) is most relevant to describing the impact of snowball Earth, (6.4) may also have briefly applied in some species during the Neoproterozoic glaciations.

Recall I am using the j th genotype N_j to denote either altruists N_A or cheats N_S . I want to write the fitness of these genotypes in terms of the relative frequency of altruists N_A , the benefit b to all members of a group (of total size $N_t = N_A + N_S$) due to the presence of altruists, and the cost c of altruism, that altruists incur per generation, but that cheats avoid. I therefore define the fitness of altruists and cheats respectively as. I use the local relative frequency of altruists as analagous to relatedness:

$$F_A = (\frac{N_A}{N_A + N_S})b - c \quad (6.10)$$

$$F_S = (\frac{N_A}{N_A + N_S})b \quad (6.11)$$

Balance between within and between group dynamics implies $(1 + Dk \frac{\partial}{\partial k}) \frac{dN_A}{dt} = (1 + Dk \frac{\partial}{\partial k}) \frac{dN_S}{dt} = 0$. Therefore, an equilibrium involving both within and between group processes, persisting over some arbitrary time interval $t_{end} - t_{start}$ implies:

$$\int_{t_{start}}^{t_{end}} \frac{dN_A}{dt} - \frac{dN_S}{dt} dt = \int_{t_{start}}^{t_{end}} Dk \frac{\partial}{\partial k} (\frac{dN_S}{dt} - \frac{dN_A}{dt}) dt$$

(6.12)

With (6.12) I can examine the implications of this dynamic equilibrium for the cost c and benefit b parameters, as well as the starting frequencies of altruists N_{A0} and cheats N_{S0} . It is useful to note that the relative frequency of altruists within the group, which appears in both fitness definitions (6.10) and (6.11) is equivalent to the average relatedness between the altruist and potential recipient of altruism as defined with reference to kin selection - i.e. $\frac{N_A}{N_A+N_S} = r$. Relabelling in this way, and substituting from (6.3), (6.10) and (6.11), the definite integral (6.12) implies:

$$[N_A - N_S]_{t_{start}}^{t_{end}} = [Dk(rb^t \frac{\partial N_{S0}}{\partial k} + N_{S0} \frac{\partial}{\partial k}(rb^t) - (rb - c)^t \frac{\partial N_{A0}}{\partial k} - N_{A0} \frac{\partial}{\partial k}((rb - c)^t))]_{t_{start}}^{t_{end}} \quad (6.13)$$

This means that over a steady state interval $t_{end} - t_{start}$, the within group difference in genotype frequency between altruists and cheats $N_A - N_S$, was balanced by a between-group component of that difference, with effect on both the initial frequencies and (probably to a lesser extent) the cost benefit parameters themselves. As I have discussed, selection pressure for differentiation into (for example) organs for resource sequestration in the harsh abiotic conditions would have driven up the benefit b for such altruistic traits, and high founder effects would have dramatically driven up r . But Snowball Earth would have been most significant in its effect on between group dispersal probability, an issue I now illustrate.

Numerical simulations

Consider a system of $G = 100$ groups, each with $k = 2$ distinct neighbouring groups, using the parameters benefit $b = 1$ and cost $c = 0.1$, and with relatedness defined by the varying within group altruist relative frequency $\frac{N_A}{N_A+N_S} = r$. Within each group, the frequency of a genotype at one generation is the product of its frequency and its fitness at the previous generation. The fitnesses of altruists and cheats were of the form of (6.10) and (6.11) respectively; i.e. altruists could potentially experience kin selection, but relatedness could be “diluted” by the reproduction of unrelated cheat individuals that benefitted from altruism but avoided the cost. Altruism was assumed necessary for group survival - and groups in which cheats reached fixation went extinct. Each group had a carrying capacity of 250 individuals, and was initialised with 25 individuals at the start of each simulation. An individual could potentially produce offspring both within its own group and in each of its neighbours, the latter according to the value of the reproductive dispersal probability D , per individual, per generation. The results I present refer to the end of a 200 generation simulation for various values of D . A group at its carrying capacity could not receive offspring from neighbouring groups, and an empty group was considered dead and therefore unsuitable for receiving offspring from adjacent groups. Genotype

frequency at a given timestep was the product of fitness and genotype frequency at the previous timestep. For non-zero dispersal probability D , this frequency contained a within group component, and an immigration component from each of the two neighbour groups. So in the G th group, with two neighbouring groups $G+1$ and $G-1$, from which individuals can add offspring according to reproductive dispersal probability D , at the t th generation, the number of altruists $N_{A_t,G}$ was:

$$N_{A_t,G} = \left[\left(\frac{N_{A_{t-1},G}}{N_{A_{t-1},G} + N_{S_{t-1},G}} \right) b - c \right] \cdot [N_{A_{t-1},G} + D \cdot (N_{A_{t-1},G+1} + N_{A_{t-1},G-1})] \quad (6.14)$$

With the first square bracketed term being altruist fitness within the G th group, as defined in (6.10), the second bracketed term being the frequency in the focal group and the neighbouring groups, with the latter scaled by dispersal probability D . The cheat genotype benefited from the presence of altruists according to their density, but lacked the fitness cost:

$$N_{S_t,G} = \left[\left(\frac{N_{A_{t-1},G}}{N_{A_{t-1},G} + N_{S_{t-1},G}} \right) b \right] \cdot [N_{S_{t-1},G} + D \cdot (N_{S_{t-1},G+1} + N_{S_{t-1},G-1})] \quad (6.15)$$

Of course, the results from any such spatial set up depend on the starting frequencies. I present results from three initialisations: (a) Continuous linear variation in initial altruist frequency, so that the first group began with 1% altruists, the second 2% etc. This caused relative genotype frequencies in neighbouring groups to be similar. (b) Heterogenous non-random variation in initial frequencies, with the relative frequency of each genotype negatively correlated with that of neighbouring groups. This was achieved with the (admittedly arbitrary) set up of the first group 1% altruists (therefore 99% cheats), the second group 98% altruists and 2% cheats, the third 3% altruists and 97% cheats, and so on, (c) Random initial altruist frequency (with cheat frequency $1 - \text{altruist frequency}$ as above).

Figures 1 and 2 show the results for various dispersal probabilities D . Figure 6.1 shows the final value of Hamilton's condition $rb - c$. This approaches 1 for zero between group dispersal but rapidly declines due to incremental cheat invasion when between group dispersal is at positive values. This decline is sharpest in scenarios (b) and (c) in which groups with high relative altruist frequency are neighboured by groups filled with cheats, and less sharp in conditions of continuous gradation over the population (a). The reason that $rb - c$ is able to reach such high values for $D = 0$ or extremely low dispersal probabilities rests in the variable population size (itself derived from my assumption of non-zero altruist frequency being a prerequisite for survival), and is illustrated in figure 6.2. At zero and extremely low dispersal probabilities population size drastically declines (around 5 groups from the starting 100), because groups in which cheats reach fixation die without the

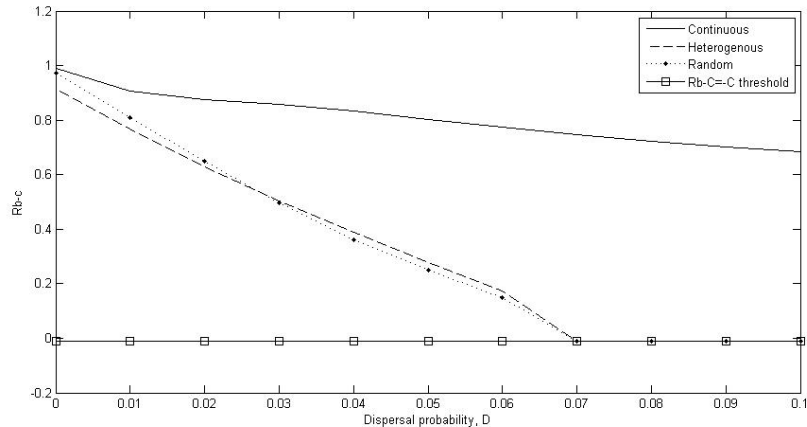


Figure 6.1. Increased mixing between groups reduces the probability of Hamilton’s condition being realised over a range of initial between group genotype frequencies. Y axis shows $rb - c$ using relatedness $r = \frac{N_A}{N_A + N_S}$ averaged over the whole population. “Continuous” (solid line) means each group has similar initial genotype frequency to its two neighbours, “heterogenous” (dashed line) means groups initialised at high relative altruist frequency are adjacent to groups initialised at low altruist frequency, “Random” (dotted line) refers to (pseudo)random initial frequencies of altruists in each group. Line marked with squares shows threshold of zero benefit for altruism. Note that the continuous experiment shows a lower sensitivity to low but non-zero between-group dispersal, because it takes longer for cheats to spread across the population.

opportunity to re-disperse, and the only remaining groups are those with high altruist frequency. As dispersal increases slightly population size increases, as cheats reach higher relative frequency across the population but reach local fixation less frequently. At dispersal probabilities of around $D = 0.3$ and higher, population size again becomes limited as cheats reach local fixation in a wider number of groups. I emphasise that this model is only intended to be illustrative. The key point is that in a system with within-group kin selection and group viability selection operating between groups, complete or near complete removal of dispersal strongly favours altruists.

Discussion

The temporal correlation between the glaciations and the emergence of complex animal life has been commented upon repeatedly (Hedges, 2004, Butterfield, 2007, Canfield et al, 2007). Butterfield (2007), for example, attributes diversification of the post Ediacaran biosphere to a restructuring of macroecology caused by the introduction of the Eumetazoa, but does not address the reason for Ediacaran diversification before the Cambrian explosion. Canfield et al (2007) attribute diversification of aerobic animal metabolism to increased photosynthetic O_2 production after the Gaskiers event, citing as evidence decreased reactive:total Fe , and increased ^{34}S fractionation after termination of the glacial deposits.

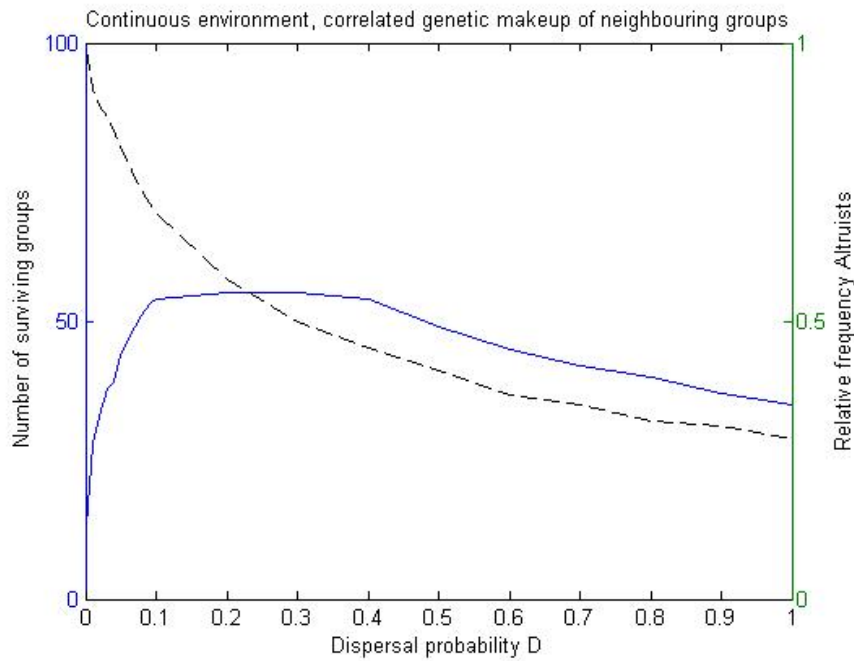


Figure (6.2). Low between group dispersal probability perpetuates spatial variation in genotype frequencies, protecting altruists from cheats in neighbouring groups. Right Y axis (dashed line) shows final relative altruist frequency averaged over the whole population, left Y axis (solid line) shows the number of groups from the original 100 surviving after the 200 generation simulation in which initial relative genotype frequencies were correlated between adjacent groups. At zero dispersal probability most groups go extinct as cheats reach local fixation, but in the small remaining population, altruists dominate. As the population becomes more continuous a larger number of groups survive but cheat frequency becomes higher, until at around $D = 0.3$, cheat fixation starts to decrease the size of the population despite the capacity for reproduction in neighbouring groups. Nonetheless, it is clear that altruists at relatively high local frequency are favoured by extremely low and zero dispersal values (see text).

Increased atmospheric Oxygen will indeed cause aerobic heterotrophic metabolism on a macroscopic scale to become more adaptive, and might arguably have been a necessary condition for the radiation of the Eumetazoa, as is popularly acknowledged (e.g. Lenton & Waton, 2004, Canfield, 2007). But macroscopic metazoan forms are necessary in the first place for evolution to alter their physiology. The capacity of a multicellular (proto) animal to differentiate in a co-ordinated, organ-scale manner, is necessary before natural selection can make the Oxygen assimilation of such an organism more efficient. Increased atmospheric oxygen will not give rise to this capacity to differentiate, therefore was not a sufficient condition for the evolution of macroscopic animals. Similarly, Baker (2006) argues that the impact of climatic stress on the “heat shock” chaperone protein HSP-90 caused increased expression of latent genetic diversity in animal signal transduction pathways, increasing the rate of the evolution of developmental complexity and contributing to the Cambrian explosion. This hypothesis may also be true, but requires a level of pre-existing developmental complexity in order for evolution to iterate on a theme. The existence of such potential for developmental complexity is, I think, the pattern that requires an explanation. The mechanism I present herein describes the broader, more systematic influence that I think global-scale glaciation would have had on the evolution of physiology and form across many taxa.

Requirements for evolution of multicellular and macroscopic form

The emergence of multicellular form requires separation of a germ line and a soma, exploiting the evolutionary advantages of multicellularity by top-down physiological control probably requires sexual reproduction (Wolpert, 1994, Maynard-Smith & Szathmary, 1995, Kerzberg & Wolpert, 1998, Wolpert & Szathmary, 2002). The first step towards the evolution of multicellularity requires formation of cell clusters (Kerzberg & Wolpert, 1998, Pfeiffer & Bonhoeffer, 2003). Cells on the exterior of such clusters are more likely to die in harsh environmental conditions, perhaps forming a protective barrier between inner cells and the environment. The earliest germline-soma separation may have been into one cell line predisposed to phagocytose neighbouring cells, and one cell line significantly less predisposed to do so (Kerzberg & Wolpert, 1998). Once such a mutation occurs, those cells that phagocytose their neighbours will, of course, leave many more descendents. Any developmental separation between the two cell lines early in development of the cluster will result in the germ line accumulating significantly less mutations than the soma; hence mutations disruptive to the higher level structure will not be passed on to descendents. This feature, coupled with increased relatedness due to passing through the egg cell bottleneck each generation, means that once it arose, the germline-soma separation was probably self sustaining (Wolpert, 1994, Kerzberg & Wolpert, 1998). But why should this separation have occurred in the first place? It is reasonable to suppose it would be adaptive for cells on the interior of a cluster to phagocytose dead cells on the exterior that had died as a

result of (for example) low resource availability, but why should the cells on the exterior not behave similarly before reaching the point of starvation? If the first eggs were cannibalistic, the germline-soma separation is best described as evolution of a somatic mutation for restraint from cannibalism. This is an extremely altruistic trait. Pfeiffer & Bonhoeffer (2003) show that spatial clustering may have promoted multicellularity in clusters of unicellular organisms with rudimentary co-operative behaviour, by reducing average probability of interaction with non-cooperators, but acknowledge that the reason for the existence of such clusters in the first place is unknown. Changes in the cell cycle giving rise to multicellularity have been attributed to unspecified ecological signals before (Wolpert, 1994). But there has been no systematic consideration of the types of trait made most adaptive by long term abiotic pressures occurring around the time of emergence of the earliest Metazoa. Regardless of the physiological basis for the first germline-soma separation, I think that the evolution of an altruistic soma is a major evolutionary step that remains incompletely explained. I propose that the first multicellular clusters of the Ediacara (and implicitly therefore, the ancestors of the Metazoa) were imposed on the biosphere by constraints on space and resource availability in the abiotic environment, and that extremely high within cluster relatedness resulted from strong founder effects - promoting the evolution of an altruistic soma through exceptionally effective kin selection. Subsequent elaboration of physiology by organ level differentiation was probably achieved by qualitative genomic changes in the regulation of development (e.g. Wilkins, 2002), many of which required costly terminal differentiation - further promoted by this persistently high relatedness. I.e. high relatedness within multicellular clusters of the first animals, as well as being the result of passing through an egg cell bottleneck, preceded and promoted the separation into a germline and a soma, as well as other costly group-level traits. Furthermore, the presence of highly related multicellular clusters was not initially an adaptation, but was imposed by extreme abiotic pressures.

Falsifiability: Analogues for a snowball Earth biosphere

Temporal resolution of both the geologic evidence for glaciation and the biological evidence for macroscopic differentiation is too coarse for the idea I present here to be anything other than a hypothesis, the relevance of which should be scaled by any future consensus on the severity of the Neoproterozoic glaciations. The strength of the founder effects and dispersal restrictions that I propose would be greatest under a complete “hard snowball”, but still likely prevalent under a “slushball” if the hydrological cycle caused isolation into refugia and decimated net productivity. I fully acknowledge that the only appropriate test is an empirical one - the presence of diverse macroscopic Ediacaran “animal” forms with organ-level differentiation prior to the Sturtian glaciation at 710 MYA would, of course, refute my idea. But none have been found, despite multicellular forms in other taxa. Furthermore the qualitative transition in altruism that I propose may in fact be an internal change - such

as a highly costly change in cellular compartmentalisation, gene duplication or resource storage, which only later gave rise to the macroscopic form for which it was necessary. A more realistic means of falsifying my idea may therefore be to examine the evolution of co-operative traits in existing extreme environments.

Modern Arctic and Antarctic bacteria and Eukaryotes tolerate extreme temperature decreases and extreme osmotic fluctuation, and decrease the risk of mechanical damage through ice crystal formation by a range of cellular and biochemical strategies, frequently being capable of maintaining significant enzymatic activity at near freezing temperatures (Vincent, 1988, Deming & Huston, 2000, Rothschild & Mancinelli, 2001). Communities consisting of a range of microbial extremophiles and Eukaryotic algae also persist within brine channels separating crystals of sea ice (Thomas & Dieckman, 2002). A particularly useful analog for the communities likely present during a snowball event is provided by that of the thick sea ice shelves of the modern Arctic and Antarctic. Most of the biomass in these communities is contained within microbial mats, dominated by prokaryotes but including micro-algae and some micro-invertebrates (Vincent et al, 2004). A range of microcosms provide niches for halophilic and halophobic, aerobic and anaerobic microbiota. Algae and cyanobacteria exhibit extensive diversification in light-harvesting photosynthetic pigments as well as photoprotective pigments; matching the range of light intensities and wavelengths penetrating different depths in water bodies amongst and below the ice. Sediment communities form microbial “ice mats” around the layers of gravel in the ablation zone - consisting of loosely bound communities of cyanobacteria and diatoms (Vincent, 1988, Hawes et al 1993). Formation and destruction of these gravel communities is frequent but erratic, matching the dynamics of ice formation and melting. Population densities are low but highly variable - mirroring the erratic hydrological cycle.

The evolutionary implications of global scale glaciation on communities of this sort have been considered before (Vincent, 2004, Hedges, 2004). Nisbet & Fowler (1999), as well as Vincent (2004), note that the steep redox gradients within communities below the ice could accentuate differentiation within microbial mats - suggesting that this factor, as well as the relative stability of extracellular DNA under the ice-cooled conditions, might have facilitated lateral gene transfer and symbiosis. Most consideration has been given to the Paleoproterozoic glaciations - diversifying selection under conditions of low productivity, as well as strong chemical nutrient gradients, having been proposed as a mechanism for eukaryogenesis (Vincent, 2004). However, to my knowledge, there has been no systematic consideration of the type of evolutionary strategy that is most adaptive in the extreme demographic conditions prevailing in these refugia. Spatial heterogeneity of the kind present in these biomes has been suggested to give rise to altruistic low growth rate, high growth yield strategies in bacterial biofilms - films with a lower average growth rate but a more coherent structure being able to achieve a larger size (Kreft, 2004). Imposition of spatial

heterogeneity is sufficient to cause morphological differentiation in bacteria (Rainey & Travisano, 1998), including co-operative group level differentiation detrimental to individual short term success (Rainey & Rainey, 2003). It is therefore reasonable to hypothesize that the extreme resource and oxidative gradients within such arctic environments may cause equally extreme differentiation in (say) bacterial colonies today. The mechanisms I suggest for eukaryotes would be merely an extension of this idea over a longer timescale and conditions of higher kin relatedness. Additionally, any similar event causing the decimation of the biosphere and isolation into distinct refugia could in theory increase the fitness of group level traits. If similar demographic conditions resulted, an analagous evolutionary effect of the Paleoproterozoic Makganyene glaciation (Evans et al, 1997), perhaps increasing the developmental complexity of (unicellular) eukaryotes, may also be plausible.

The cost of altruism: Specific influence on animal evolution?

This work has focused on altruism in a generic sense, but the data suggests that the group-scale trait of greatest direct relevance to Snowball Earth is the origin of animals, particularly the organ-grade differentiation present in their ancestors in the Ediacaran macrobiota - i.e. terminal, organ-grade differentiation in large heterotrophs. It is important to note the particular impact of snowball Earth on the evolution of macroscopic heterotrophs, because the restriction on cellular potency required of the individual cell is far greater than in plants or fungi - which obtain their nutrients in a continuous way from the environment, as opposed to (more) discrete feeding events. It might be argued that overcoming the cost of organ-grade differentiation is an inevitable consequence of the imposition of a single cell reproductive bottleneck (i.e. the evolution of sexual reproduction) in that this life history will result in high genetic relatedness between neighbouring cells, favouring altruism by kin selection. I argue, however, that sexual reproduction is not a sufficient condition for terminal differentiation in large heterotrophs.

Extrapolation from contemporary sponges, mosses and fungi, based on the assumption that the mode of sexual reproduction that these species exhibit is ancestral, implies that the earliest sexual reproduction may have been facultative, or at least without a rigid generation time for the sexual phase of the life cycle (e.g. Brown, 1999). (Note that this assertion remains compatible with a relatively early protostome-deuterostome split at 670Ma (Ayala et al, 1998) assuming that the outgroup displayed sexual reproduction at least as simple as that of modern sponges). Asexual revertant mutants would be abundant, and would experience mutation (equivalent to “somatic” mutation in modern metazoa) diluting kin relatedness. (In this sense, an asexual revertant mutant would simply be a cell that continues to grow regardless of developmental cue from the colony). Regardless of cellular ancestry, there would exist a strong selection pressure for asexuality, over the relatively short timescales relevant to cellular replication. This would reduce local relatedness at

the focal locus. The reader is reminded that the term “relatedness” used herein refers specifically to the locus responsible for altruism, so two neighbouring cells descended from the same recent cellular bottleneck could easily become effectively unrelated if a revertant asexual mutation occurs - because relatedness refers to the locus responsible for altruism (or not). Extreme and repeated founder effects would counteract this incentive to asexual “cheating” strategies, by raising relatedness and all loci. In some lineages, this effect may have been sufficient to convert a facultative sexual life-history into an obligate one. In short, even if the key altruistic trait sufficient for metazoa and their ancestors is in fact sexuality, rather than internal terminal differentiation, snowball Earth might have helped sexual reproduction become an obligate part of the life history, and in so doing reduced the probability of future asexual revertant mutants.

Even in contemporary multicellular organisms that experience obligate sexual reproduction, the ubiquitous incentive to cheat still occurs - indicated by the high frequency of tumours in animals and plants. This is because natural selection is blind to its future consequences - a gene for prolific cellular reproduction regardless of the developmental context (i.e. an oncogene) will always have higher fitness than its peers in the *short term*, regardless of its *long term* implications for collective reproduction. This incentive to short term high reproduction imposes a high cost of altruism from the perspective of the individual cell, regardless of whether the cellular population has recently experienced a sexual bottleneck. Being part of an organism demands sub-maximal reproduction from the component cells, which imposes a fitness penalty relative to maximal reproduction. Furthermore, mutation at the locus responsible for altruism constitutes a reduction in kin relatedness, (because, as discussed above, relatedness refers to the focal locus and is not necessarily the same as descent). Only an extreme forcing that will increase relatedness at the focal locus, repeatedly and over timescales of the order of gene (rather than organism) reproduction, will permit fixation of costly terminal differentiation. And only an extreme disturbance in habitability, such as snowball Earth, can provide this. Tangible examples of highly costly traits that may have been too costly to be adaptive before the context of snowball Earth include:

- 1) Restraint from cannibalism of neighbouring cells.
- 2) Metabolically expensive extracellular adhesion substances.
- 3) The conversion of ancestral facultative sexual reproduction into obligate sexual reproduction involving a fixed (group) generation time, specifically in macroscopic colonies of heterotroph cells - i.e. restraint from the short term cell-scale selective incentive toward asexuality.

4) Terminal cellular differentiation, i.e. the evolution of an altruistic soma, including caspase-based apoptosis.

Although sexual reproduction has been suggested to have been present in Algae at 1200Ma (Butterfield, 2000), and there exists varying degrees of eukaryotic multicellularity in unassigned pre-Edicaran “problematica” (Butterfield, 2007), there is no evidence for obligate sexual reproduction (i.e. a single cell bottleneck and a fixed colony generation time) in (precursorial) animals prior to the earliest snowball events. The presence of apparent sexual sponges at 580Ma (Li et al, 1998) is consistent with a sudden increase in morphological complexity in the aftermath of the final glacial events. But sponges today reproduce both sexually and asexually, and lack the organ-grade differentiation present in Bilateria.

Certain differentiated organ-level structures impose a qualitatively greater short term fitness cost on the individual cell than multicellularity per se, because they involve a greater decrease in potency than does a trait causing (say) cellular adhesion, but permitting some retention of reproductive autonomy. A cell that permanently differentiates into a macroscopic organ, and in so doing makes itself sterile, makes a greater short-term fitness sacrifice than a cell that undergoes reversible differentiation within a multicellular structure, but retains the potential ability to independently reproduce if that structure breaks down. This idea may be relevant to why there were multicellular algae and fungi before the Neoproterozoic, but no multicellular (ancestral) animals. Cells of higher plants and other photoautotrophs undergo extensive differentiation, but retain a far greater degree of developmental plasticity than do the differentiated cells of animals, in which potency becomes far more restricted (e.g. Weigel & Jurgens, 2002). One cannot extrapolate too precisely from the development of those multicellular Eukaryotes present today to that of their relatives from 500 MA. But I suggest it is useful to view the individual cell as incurring a greater short term fitness cost in macroscopic heterotrophic form than in photoautotrophic form, because the former involves a greater restriction on the number of possible future developmental fates the cell can adopt. I.e. animals have been more successful in mediating the levels of selection conflicts inherent in multicellular form than other multicellular Eukaryotes, but this has been achieved by making terminal cellular differentiation (and hence cellular altruism) more intrinsic to development. Consequently, macroscopic heterotrophic Edicara (and the Metazoa that some such taxa probably gave rise to) may have actually required the unique evolutionary conditions of strong kin selection and low incentive to cheat, provided by snowball Earth, in order to gain tangible fitness values.

If the evolutionary effects that I postulate here are reasonable, snowball Earth may have temporarily increased the degree of altruism that was adaptive and promoted an increasing degree of terminal differentiation. This paved the way for larger, more elaborate form and irreversibly redirected eukaryotic evolution.

Chapter 7: Conclusions

An unfortunate feature of deep time studies is that any conclusions reached are limited to being, at best, hypotheses that are consistent with a limited available set of data. Some schools of scientific thought are (quite reasonably) more cynical towards hypotheses that cannot be tested more easily, with smaller scale experiments over shorter time scales. But a starting assumption of this work is that human knowledge and understanding of past climate and evolution can still be advanced by considering what *might reasonably be expected* to have occurred given current understanding, even if it may never be possible to know for certain what *did* occur. From this point of view, modelling can be regarded as a test of the usefulness of current understanding, in addition to a means of fitting a single relationship to a single data set in a more restricted way (e.g. Pierrehumbert, 2005). The reader is asked to consider the conclusions from this perspective, and to entertain the idea that the *shape of the relationship* between two unknowns is still a useful result. Although the work in this thesis is admittedly abstract and speculative, it is not untestable - particularly if the current sample size of one planet-scale climate system can be increased in the future. Future information from extraterrestrial systems should eventually allow falsification of ideas linking planetary-scale climatic homeostasis and the presence of life, perhaps including some of the contributions made here. The first part of this concluding section summarises the key findings from each chapter, stating where appropriate what data may help to falsify each idea. The second part places these conclusions in the context of the wider understanding of coevolution of life and the environment at a planetary scale.

Summary of findings

Variable environments and multi-level selection

Chapter 2 showed that the hypothesized presence of lichens on the land surface of the Neoproterozoic Earth (Lenton & Watson, 2004), prior to their fossil detection at about 600 Ma (Yuan et al, 2005), was entirely reasonable from an evolutionary perspective. This conclusion was justified by the idea that the potential for phenotypic differentiation is increased by the formation of a social structure, because differentiation can occur at both the ancestral (within-individual) level, and the new (between-individual) level. The division of labour in the lichen symbiosis permits the fixation of Carbon, and often Nitrogen (possible in photobionts), in the same system as is responsible for the obtaining macronutrients by rock weathering, and spore formation strategies to avoid (predictable, short-term) deleterious conditions (possible in mycobionts). The symbiosis has a level of self-sufficiency relative to the abiotic environment that no partner species could achieve individually, making it likely better equipped to live on the Proterozoic Earth than symbioses in which the mycobiont genotype operates in a more exploitative (parasitic) way. But, as in any symbiosis,

there is a strong evolutionary incentive for one partner to parasitize the other if its contribution becomes unnecessary for survival. For example, in the presence of an external Carbon source the mycobiont would have no need of its photobiont's photosynthetic activity, and it would make evolutionary sense to restrict its nutrient supply - that is, to develop a controlled form of parasitism. I noted in chapter 2 that an abiotic environment V that fluctuates away from a biotic optimum state $|V - V_{opt}|$, made the likelihood of one symbiotic partner's contribution becoming obsolete lower. I further noted how the extra potential for differentiation in groups (discussed above) may result in extra tolerance α for fluctuation in the physical environment, and that this might overcome the cost C of being within the group. I showed that altruistic (mutualistic in this context of the lichen symbiosis) genotypes experiencing this cost could increase from rarity under the condition:

$$\alpha|V - V_{opt}| > C \tag{7.1}$$

I noted the more general evolutionary importance of taking account of the abiotic environment within the cost-benefit trade offs of multi-level selection. I suggested that given that the definition of kin relatedness can be relaxed to incorporate linked factors away from the focal locus (Axelrod et al, 2004), then perhaps kin selection is best viewed as a general form of positive feedback, made unique by the fact that it involves changing gene frequencies. I drew a parallel between relatedness r from Hamilton's rule $\frac{b}{C} > \frac{1}{r}$ (For relatedness r , benefit b and cost C , (Hamilton, 1964)), and the *probability of simultaneous occurrence* of a given genotype relative frequency $\frac{G}{G+P}$ (denoting altruists by G and cheaters by P), and a given environmental state $\frac{|V-V_{opt}|}{|V-V_{opt}|+|V_{abiotic}-V_{opt}|}$ relative to the abiotic background. I proposed that this relationship with the abiotic environment is a member of the set of relationships described by Hamilton's rule:

$$\frac{\alpha|V - V_{opt}|}{C} > \frac{1}{\frac{G}{G+P} \cdot \frac{|V-V_{opt}|}{|V-V_{opt}|+|V_{abiotic}-V_{opt}|}} \in \frac{b}{C} > \frac{1}{r} \tag{7.2}$$

I suggest that this idea should be tested by the empirical community by examining the relative abundance of costly co-operative traits within and away from deleterious and fluctuating abiotic environments. Specifically in the case of lichens, I would expect nutrient supply from the fungus to the photobiont to be relatively greater in environments that are deviating from optimal temperature/hydrologic conditions. More generally, I would expect any metric for the extent of transition to a group level division of labour in model systems such as *Volvox* (Michod, 1997) to be more prevalent in environments that deviate from the optimum for individual growth with a fluctuating direction and/or magnitude. The idea that groups can differentiate on an additional level to individuals is, I think, self-evident, (it is impossible to form organs in a single cell), but could be tested by a systematic com-

parison of the range of chemical microcosms that occur in any one individual bacterial cell (of different species) in comparison to that within a multicellular Eukaryote.

The cause of the Neoproterozoic glaciations

In chapter 3 I reached the somewhat unsatisfactory conclusion that it was ultimately not possible to confidently determine the cause of the Neoproterozoic “snowball Earth” glaciations without knowledge of various unconstrained model parameters:

1) T_f , the upper temperature threshold of the surface ice-albedo instability, below which the positive feedback between albedo, decreasing temperature and ice cover will eventually drive the Earth system to an equilibrium, high ice-cover state. The assumed range $0 < T_f < 15$ (North et al, 1981).

2) E_0 , the present day cumulative planetary biotic enhancement of silicate weathering rate, estimated at $E_0 \approx 100$ (Schwartzman, 1999). It is necessary to determine more precisely the nature of (present day) biological enhancement of silicate weathering rate, in particular how it relates to overall terrestrial biomass. Relevant to this is the fraction of global silicate weathering regimes that are limited by reaction kinetics rather than by substrate supply (West et al, 2005), and by implication the types of biome that are more relevant to the Urey reaction today.

3) D , the magnitude of the Neoproterozoic CO_2 degassing flux due to the combined effects of magmatic activity and subduction-decarbonation activity, in comparison to the present day flux of $D_0 = 6.65 \cdot 10^{12}$ moles per year (Bergman, 2003). The likely requirement for a Neoproterozoic degassing flux lower than the present value has been noted previously (Tajika, 2004) and is consistent with the results presented here.

Despite this inconclusiveness, I were able to derive a relationship between the biotic enhancement (Schwartzman, 1999) relative to present $\frac{E_{tr}}{E_0}$ that would be needed (at a given solar luminosity flux) to trigger planet-scale glaciation that would initiate at threshold temperature T_f , to the geochemical silicate weathering function (Walker et al, 1981) that this enhancement would correspond to (shown on the right hand side below):

$$\frac{E_{tr}}{E_0} = \frac{D_{tr}}{D} \frac{A}{A_{tr}} \left(\frac{CO_2}{CO_{2tr}} \right)^a e^{(b+c)(T-T_f)} \tag{7.3}$$

Higher resolution energy balance and radiative-convective climate modelling will likely eventually determine the value of the temperature threshold T_f , and isotopic data is already (slightly) constraining the tectonic parameters to $1.023 \leq \frac{D_{tr}}{D} \frac{A}{A_{tr}} \leq 312.5$ (Sheilds & Vezier, 1992, Berner, 1994, Franck & Bounama, 1997, Halverson et al, 2007, discussed in chapter 3). The letter exponents on the right hand side are empirically-constrained (Walker et al,

1981). Therefore the key uncertainties in this relationship are those listed above. A value of $\frac{E_{tr}}{E_0} > 1$ (Neoproterozoic silicate weathering enhancement greater than present) may not be as implausible as it first sounds, given that the kinetically-limited fraction of silicate weathering regimes may have been qualitatively higher than at present.

I noted in conclusion that tectonic forcings (i.e. lower degassing or concentrated equatorial land area) (Kirschvink 1992, Hoffman & Schrag, 2002, Tajika, 2004) could only serve to provide a negative forcing on atmospheric CO_2 , rather than to provide a single answer to the question of the cause of the snowball Earth glaciations. Lower CO_2 caused by lower degassing rate would cause a lower silicate weathering flux, hence a compensating positive CO_2 forcing, buffering the dynamics of the overall atmospheric partial pressure, preventing temperature reaching the required threshold T_f (Walker et al, 1981, Tajika, 2004). In order to trigger a snowball Earth, it is necessary to create a sustained negative degassing-weathering $\frac{dCO_2}{dt} = D - W$ balance, *despite the fact that progressively decreasing CO_2 would be continuously reducing the background rate of weathering W* . Abiotic kinetic weathering dependencies clearly cannot achieve this because they all increase with both CO_2 and temperature, but the biosphere may be able to, *particularly if the evolutionary incentive to extract nutrients from rocks increases with declining temperature*. The favoured scenario for the cause of the Neoproterozoic glaciations was therefore a tectonic “driver” with reduced degassing and/or increased continental area decreasing the greenhouse CO_2 forcing, but a biological “amplifier” being needed to tip the system over the edge $T < T_f$ by compensating for the kinetic decline in baseline silicate weathering rate. This is consistent with the available data on tectonic constraints (Tajika, 2003, Rino et al, 2006) and with increased pre-glacial, silicate-specific Sr isotope runoff data (Sheilds, 2007).

The “snowball” versus “slushball” debate

The impact on duration of the glacial interval, of the presence or absence of chemical equilibrium between atmosphere and ocean components of the CO_2 reservoir, was assessed in chapter 3. The species $CO_{2(aq)}$ makes up a very small fraction of the total marine CO_2 reservoir, due to the relative values of the various equilibrium constants, which cause most CO_2 to be partitioned into HCO_3^- and CO_3^{2-} (Lewis & Wallace, 1998). This means that as the ocean approaches saturation with respect to total CO_2 , the first species of which no more can be absorbed is the one that is in direct equilibrium with the atmosphere, $CO_{2(aq)}$, giving rise to an S-shaped relationship between the atmospheric fraction of the CO_2 reservoir and the total reservoir size. In turn, this means that the atmospheric CO_2 fraction in a Neoproterozoic slushball scenario in which silicate weathering is shut off, will rapidly increase, *even relative to the increase in reservoir size*. In contrast, the atmospheric fraction in a hard snowball scenario will change only in proportion to the fraction c of the degassing flux that enters the atmosphere directly, which was assumed to be a constant

dictated by the position of the continents relative to tectonic hotspots. The results of a simple 3-box model showed that the duration of a slushball solution Δt_{slush} can reasonably be expected to be qualitatively shorter than that of a hard snowball Δt_{hsb} in a manner roughly in proportion with the extra fraction that enters the atmosphere:

$$c \Delta t_{HSB} \simeq \Delta t_{SLUSH} \tag{7.4}$$

The intuitive reason for this is that any change in total reservoir size is equivalent for both cases, but in the case of a slushball there is a given (increasing) fraction of this reservoir, $\propto \frac{1}{c}$, that is ejected from the ocean by equilibration with the rest of the system. Current estimates of the atmospheric degassing fraction are limited to the assumption of linearity with the relative surface area covered by the ocean and the atmosphere, giving $c = \frac{1}{3}$, (Higgins & Schrag, 2003). More precise estimates of the position of tectonic hotspots, relative to various estimates of continental configuration (e.g. Kirschvink, 1992b) will be essential to distinguish between hard snowball and slushball arguments on the basis of duration, as will estimates of the magnitude of the degassing flux. Nevertheless, the assertion that only a hard snowball could span a time interval toward the upper end of the 3 – 30Myr estimated duration (Hoffman & Schrag, 2002) is supported to an extent by this study.

A second part of the work on glacial duration emphasized that a slushball scenario may not necessarily be the pragmatic synthesis that it appears to have been assumed to be. In order for the atmospheric component of the CO_2 reservoir to increase, the ocean must stabilise at a tangible level of carbonate alkalinity - which in turn requires that the carbonate weathering influx remains greater than the carbonate burial efflux:

$$R = W_{carb} : B_{carb} > 1 \tag{7.5}$$

Assuming that carbonate weathering W_{carb} is unaltered by glacial severity and planetary-scale temperature reduction amounts to assuming a slushball scenario in the first place, so the most objective assessment of whether a slushball scenario is recoverable will come from measurements of the upper temperature limit, below which carbonate burial B_{carb} declines to zero. The warmer the planetary temperature at which this happens, the more reasonable becomes a carbonate Carbon-dominated slushball scenario, of the form described by Ridgwell & Kennedy, (2004). This is likely to amount to the strength of the negative feedback between cold temperatures and growth that describes the marine biosphere, with bacterial activity being most relevant before the evolution of calcifiers, and coccolithophores and foraminifera more relevant afterward (Riding, 2000).

Climate stability and changes in the CO_2 -weathering buffer over Earth history

The vulnerability that the Earth system exhibits to global-scale glaciation boils down to the probability that temperature will decline to the appropriate threshold $T \rightarrow T_f$, a threshold that will change only mildly with differences in luminosity over the planet's history (Tajika, 2003). The fact that CO_2 experiences dynamics over a qualitatively longer timescale than the dynamics of the ice-albedo feedback creates a disposition to oscillation between icehouse and greenhouse states. I noted in chapter 5 the separation between what prevented the Neoproterozoic climate, already susceptible to global-scale glaciation, from re-entering the ice-covered state, and what caused the more long-term reduction in susceptibility from the Proterozoic to the Phanerozoic. The idea that there was not a single shared cause implicitly invokes a time lag between the end of the final Neoproterozoic glacial event, and the origin of a buffered system resistant to glaciation. During this time lag (presumably the first 50 – 100 million years of the Phanerozoic, prior to the planetary-scale spread of vascular plants) the system may have been more vulnerable to repeated “snowball” events than at present, and an element of chance must therefore be invoked to explain why the Neoproterozoic glaciations stopped at the precise time that they did. Combining a discretized ice-albedo formulation with a normalised function describing silicate weathering, I proposed the following qualitative hypotheses. Both ideas work from the starting assumption that non-zero biological enhancement of silicate weathering (or of $CaCO_{3(s)}$ precipitation) was a prerequisite for Neoproterozoic glaciation, in line with the results of chapter 3.

(1) The terrestrial biosphere required a tangible amount of evolutionary time between the end of its decimation by extreme glaciation events and it becoming able to enhance silicate weathering sufficiently to trigger a subsequent glaciation. This “succession time” explains the fact that the time required to simply draw down the necessary amount of CO_2 (once biotic weathering enhancement is sufficiently high), 2 – 3Myrs is qualitatively shorter than the 40 – 50Myrs that separate distinct Neoproterozoic glacial events. The proposed lack of silicate weathering in the immediate glacial aftermath is supported by the Si depletion of cap carbonates (Fairchild, 2007). The evolutionary succession time constitutes the time necessary for a lichen symbiosis sufficiently physiologically versatile to maintain weathering enhancement right up to the bifurcation point to glaciation. Implicitly, this includes the ability to tolerate global, geological scale fluctuations in the water cycle. This may conceivably take a timespan of the same order as that separating the glaciations.

(2) Changes in the preferred growth conditions of the terrestrial and/or marine biosphere lead to a reduced susceptibility to global-scale glaciation from the Cambrian onwards. This may have occurred by:

(a) Increased sensitivity to suboptimal temperatures of biological silicate weathering enhancement, associated with the narrower ecological temperature range of large biomass, vascular plant ecosystems in comparison to lower-biomass, lichen-based ecosystems. The basic idea is that plants replaced lichens as the primary biological weathering driver, causing a corresponding narrowing of the boundary conditions for this weathering. This idea is supported by the relative ecological distribution of plants and lichens today (Nash, 1996).

(b) A cap on biotic silicate weathering enhancement activity was imposed via a cap on total terrestrial biomass - due to increased photorespiration associated with the rise in oxygen (Lenton & Watson, 2004). This idea is supported by the close correspondance between a representation of the relationship between oxygen and global terrestrial productivity (Bergman, 2003) and a representation of biotic silicate weathering enhancement (Schwartzman, 1999). However, an empirical constraint on ε , the global silicate weathering enhancement factor per unit terrestrial biomass, is needed before any negative feedback based on net land production can be assessed.

The origin of animals

I showed in chapter 6 that the Neoproterozoic glaciations may well have significantly increased the probability of the evolution of macroscopic heterotrophs with terminal cellular differentiation - i.e. to have triggered the evolution of animals as I understand them today. I showed that the vague notion of “bottleneck and flush” (whereby snowball Earth “pumped” the evolution of unspecified species in an unspecified direction) (Hoffman & Schrag, 2002), has a solid mechanistic basis in accepted concepts in evolutionary theory, and likely resulted in the proliferation of costly co-operative traits - exactly as was observed paleontologically in the proliferation of the Ediacaran macrobiota. A key assumption was that the timing of emergence of such costly traits was not limited by internal developmental constraints rules on the cost-benefit trade-off $rb - c$ dictating how it is possible to build an organism with terminal cellular differentiation, but by the abiotic context E in which this very costly trait may become adaptive:

$$\frac{d}{dt}(rb - c) = \frac{\partial}{\partial E}(rb - c) \frac{\partial E}{\partial t} \tag{7.6}$$

Dense, refugia populations experienced repeated and extreme founder effects, driving up local relatedness and increasingly the fitness of altruistic traits by kin selection - on a global spatial scale, over a millennial timescale. In some cases, altruism reached fixation and subsequently became sufficiently co-ordinated as to be necessary for collective survival. In the latter circumstance, any patch in which cheats reached local fixation would, by definition, be killed. But in the context of a snowball Earth, the opportunity for cheat migration

to a neighbouring patch was negligible, meaning that in reaching fixation cheaters drove themselves extinct - again on a global spatial scale and over a millennial timescale. It is important to reiterate that the comparison between cheaters and altruists is a metaphor for different eukaryotic genotypes, which either avoid or incur the fitness cost of terminal cellular differentiation. The comparison emphasised by this work is *not* between prokaryotes (which, of course, contain many extremophilic taxa) and eukaryotes. It is also important to note the difference between buffering against variable abiotic extremes occurring in different directions (which is made more efficient by organ-grade physiologies) versus extremophilic tolerance of a directional abiotic extreme (of which there are abundant prokaryotic examples). I contend that the effect of snowball Earth on the hydrological cycle would be to make the availability of any nutrient obtained in solution much more variable - and that this selected for an organ-scale physiology involving compensating buffer functions. These mechanisms of local kin selection and global group viability selection, either separately or in combination, explain, I think, the proliferation of the Ediacara, and ultimately therefore of the Metazoa, in the aftermath of snowball Earth. It is arguable that the severity of extreme founder effects and between-deme isolation would be greater in a hard snowball scenario - in which the planetary hydrologic cycle had all but shut down, and habitable conditions persisted in land-locked geothermal lakes or transient leads in the ice. By contrast, a slushball scenario with a relatively “temperate” equatorial region would drive the biosphere towards low latitudes, but have a mild demographic effect likely insufficient for the extreme changes in life-history trade offs that I have posited here. Put simply, a hard snowball may well have been more likely to trigger the evolution of macroscopic form than a slushball, than to drive all complex terrestrial life extinct. At any rate, the prevailing assumption that complex eukaryotes could not be present today if Earth had undergone a hard snowball, and a slushball is therefore a more realistic synthesis of climate, is not a valid one.

Falsification and future work

Kinetic versus supply limitation of silicate weathering rate and its biotic enhancement

I have shown that a biological trigger for Neoproterozoic glaciation probably required a biological silicate weathering rate enhancement factor significantly greater than the present day. The most realistic explanation for this, in my view, is that contemporary estimates of biotic silicate weathering enhancement are made unrealistically high through inappropriate comparison between rate-limited and supply-limited silicate weathering regimes, only the former of which are directly relevant to the CO_2 -weathering buffer (West et al, 2005). If more silicate weathering was directly coupled to climate during the Neoproterozoic, as a result of increased kinetic limitation of silicate weathering, then the idea that a biotic

“amplifier” of the Urey reaction could drive CO_2 drawdown to a sufficient extent to compensate for a reduced abiotic weathering rate at lower temperatures (chapters 3 & 5), hence tip the system in a snowball, becomes more important. Supply limited regimes are characterised by slow erosion, and rate limited regimes by rapid erosion and lower biomass (West et al, 2005). Distinguishing between the two types will better constrain the collective biotic enhancement factor (Schwartzman, 1999, West et al, 2005) and will also allow the derivation of a meaningful relationship between terrestrial biomass and silicate weathering enhancement. The latter relationship is crucial for a meaningful assessment of my ideas on glacial susceptibility.

Founder effects, restricted dispersal, variable environments and altruism

Neither the idea that high local relatedness promotes altruism by kin selection (Hamilton, 1972, Van Baalen & Rand, 1998), nor the idea that restricted migration between demes promotes altruism by group viability selection (Sober & Sloan-Wilson, 1998, Nowak, 2007) are original aspects of this work, and both largely accepted within evolutionary theory. The proposition here is the idea that these conditions applied during the Neoproterozoic glaciations, on a global scale, over a multi-million year time interval, and that a context this extreme was needed to overcome the fitness cost associated with heterotrophic terminal differentiation. Theoretical approaches relating to this idea should quantify the strength of the founder effect required for a given level of kin relatedness, and the number of generations over which regular founder effects need to be repeated to make a given cost-benefit trade off adaptive, in a way equivalent to previous suggested links (Cohen & Eshel, 1972). In particular, the different results obtained from local (spatial) methods of weighting relatedness should be compared with strict definitions based only on shared ancestry at the focal locus. Empirical approaches should attempt to quantify the change in cellular potency associated with differentiation in animals and in plants, and in so doing assess the difference in cellular fitness penalty between the Metazoa and other macroscopic eukaryotes. The impact of extreme osmotic and oxidative gradients on collective behaviour in bacterial biofilms and glacial ice-mat and soil communities would also provide an important, more tangible falsification of the proposed links between co-operative phenotypes and snowball Earth.

***Si*-depletion in cap carbonates?**

I proposed that decimation of the biosphere during the glacial interval made biotic silicate weathering enhancement negligible after deglaciation, and that this prevented the system from rapidly entering a subsequent snowball interval, until terrestrial evolution had permitted the land biosphere to recover. I cited the silicate-depletion of post glacial cap carbonates (Fairchild & Kennedy, 2007) as evidence supporting a tangible reduction of the silicate weathering flux in the immediate glacial aftermath. A systematic survey of the *Si*

content of cap carbonates, as well as equivalent proxies for silicate weathering such as those in Shields, (2007) will determine whether this idea stands up to rigorous criticism.

The Paleoproterozoic glaciations and eukaryogenesis?

The Earth probably experienced extreme glaciations during the Paleoproterozoic at around 2.3 – 2.2Ga (Kirschvink, 1992b, Kopp et al, 2005). It follows from the ideas in chapter 6 that one would expect the Paleoproterozoic glaciations to have had an equivalent impact on the evolution of life history strategies to that of the Neoproterozoic events. The origin of eukaryotes is a transition in the level of selection that lacks a coherent causal explanation, and may exhibit a loose temporal correspondance to the Paleoproterozoic glaciations. In particular, the idea that it took four times as long for the evolution of eukaryotes from prokaryotes, than for the origin of life from primordial soup, is highly problematic (Maynard-Smith & Szathmary, 1995), perhaps lending support for an extra-terrestrial origin of life. As discussed in chapter 1, the earliest prokaryotic fossils date from at least 3.5Ga (Maynard-Smith & Szathmary, 1995), whereas the first eukaryotes are present implicitly (but ambiguously, (Cavalier-Smith, 2006)) at around 2.5Ga or earlier (Brocks et al, 1999, Dutkiewicz et al, 2006), and then unambiguously from ~ 1500 Ma (Javaux et al, 2001). The definitive feature that marks the eukaryotic origin is as problematic as the timing of the group's emergence - eukaryotes are distinguished from prokaryotes by a suite of characters (larger cell size, membrane-bound organelles - in particular mitochondria and a nucleus, a cytoskeleton co-ordinated at division by microtubules, etc). But the theme within this work has been that transitions in the level of selection are rooted most directly in a pooling of ancestrally autonomous genetic information; which subsequently allows more elaborate phenotypic differentiation. The trait proposed here to correspond to the definitive origin of eukaryotes is therefore the increase in genome size - derived (I suggest) from the symbiotic pooling, and/or costly duplication, of smaller, ancestrally autonomous genomes. The suite of phenotypic elaborations associated with eukaryotic origin was linked to genome size by Maynard-Smith & Szathmary (1995), who noted that “special circumstances - in fact, a series of them - must have been needed for these innovations to become fixed, despite the existence of potentially winning competitors” (Maynard-Smith & Szathmary, with communication with F.Karolyhazy, 1995). The assertion that follows from this work is that larger genome size resulted from symbiotic pooling events of smaller genomes, and that this pooling event required that the genomes were locally related. Once this happened, two key occurrences are predictable. First, an inherent shared interest associated with the reproductive bottleneck of a shared replication origin, mediating intragenomic conflict in an identical way to that thought to occur between cells (Michod, 1997). Second, the emergence of potential for phenotypic differentiation at the level of the secondary structure of DNA; i.e. for epigenetic inheritance and more facultative control of gene expression. I concluded in a general sense in chapter 2 that group formation provides

a new, between-individual level, on which differentiation may occur. Consistent with this idea therefore, the pooling of “groups” of genomes of ancestrally autonomous prokaryotes, gave rise to a potential for inter-genome differentiation (i.e. DNA/histone secondary structure between different loci), and subsequently permitted coherent acquisition evolution of the other phenotypic traits that characterise contemporary eukaryotes. Increased genome size, as a derived trait, requires that replication time is no longer critical to fitness. Active selection for increased genome size, and the associated changes in division of labour, require (I think) that survival becomes a more important component of fitness than fecundity (removing the pressure for cheaters) - and that increased genome size in some way aids survival (selecting for co-operation). I propose that this selection pressure may have been imposed by the Paleoproterozoic glaciations, by a combination of local kin selection, and/or group viability selection, on autonomously replicating neighbouring cells capable of some form of facultative genetic pooling. The likely mechanisms are identical to those proposed to have occurred between cells during the Neoproterozoic - local kin selection will be higher (between genomes) if extreme osmotic/temperature conditions impose repeated founder effects, and cheater strategies will be maladaptive under conditions of restricted dispersal. Increased genome size is the driver of every subsequent derived eukaryotic trait. This scenario is, of course, very speculative. However, I make one simple prediction amenable to paleontological tests, if appropriate cellular proxies can be found. Genome size in stem group eukaryotes will exhibit a dramatic increase immediately after the Paleoproterozoic glaciations.

Geophysiological relevance

Extreme environments, “complex” life and extra-terrestrial systems

Earth system science is vulnerable to ideas that are rooted in some anthropocentric search for underlying purpose - which was never the motivation of Lovelock’s original Gaia hypothesis (Lovelock, 1988). Extreme caution is therefore needed in extrapolating hypotheses concerning deep time climatic evolution of the Earth to what I might expect from future observations of life elsewhere. In terms of enhancing understanding of life elsewhere in the universe, no theoretical breakthrough will ever be a substitute for empirical exploration of other planets (Schulze-Makuch & Irwin, 2006). With these provisos in mind, the conclusions reached in this thesis may nevertheless be of relevance to the search for “complex” life away from planet Earth. The word “complex” is ambiguous, but is generally used to mean macroscopic life with a division of labour equivalent to that observed in multicellular eukaryotes on Earth. The levels of selection issue teaches us that fast-reproducing replicators will always outcompete their less fecund peers over short timescales, and that any social order derived from the co-operation of these replicators will always be vulnerable to disruption by cheaters. Therefore, if extraterrestrial life is cellular, complex extraterrestrial

life, by definition, requires altruism. The work in this thesis has proposed that altruism is promoted by extreme and fluctuating environments, and the most costly terrestrial altruism, heterotrophic terminal differentiation, required the extreme ecological context of snowball Earth. The idea that the evolution of biological complexity requires a novel and extreme disruption to the fitness landscape goes hand in hand with the assumption that the evolution of complex life is improbable, and very rare in the universe. There is no progress or inevitability from any anthropocentric perspective. A general diagnostic for extraterrestrial life has been shown to be atmospheric disequilibrium (Lovelock, 1979). But the implication of this work is that an additional, more-specific diagnostic for complex life may be a planetary climate system that has undergone an evolution through an equivalently catastrophic event with a discrete end, then subsequently to more mild abiotic conditions. The idea that climatic catastrophies promote the evolution of co-operative, macroscopic life, may be of some general use. The major problem is that my conception of “mild” and “catastrophic” climate is entirely constrained to the predictable impacts upon life on Earth, in the same way as any other diagnostic for alien biospheres.

The origin of Gaia?

A climate system that exhibits periodic switches between global glaciation and extreme greenhouse states is not homeostatically-maintaining itself within the habitable range. Assuming that the susceptibility exists to such oscillations, then the existence of a homeostatic climate system, causally linked to the presence of life (i.e. a “Gaia”, (Lovelock, 1979)), requires a mechanism to maintain temperature outside the unstable ice-albedo feedback temperature region $T > T_f$. In short, if a “Gaia” system exists, the point in Earth history in which climate ceased to be *susceptible* to snowball-greenhouse oscillations, must surely constitute the first time from which it functioned effectively. Schwartzman (1999) coined the term “geomembrane” for the biological soil/rock weathering interface, and its effect on climate and greenhouse gas concentration via the Urey reaction. The mechanisms I have suggested in this chapter for the removal of susceptibility to snowball-greenhouse oscillations may therefore constitute the origin of this geomembrane, and, perhaps, the origin of stable temperature regulation.

Schwartzman noted the relevance of the entropy flux across the Earth’s surface to estimates of the degree of planetary self organisation. Entropy is defined as the “unavailability of energy within a system to do work” (Ben-Naim, 2007), and can be thought of as the granularity of a system (A collection of molecules spread randomly across a space in a granular way, with much of the energy contained amongst them lost as heat, is a high entropy state. The same collection of molecules arranged together in an elaborate, improbable configuration, the bonds across which contain energy, is a low entropy state). Because the same amount of energy contains fewer photons in solar radiation than in terrestrial radiation

(crudely speaking, because solar radiation is more organised), entropy is produced when radiation interacts with the Earth’s surface (Peixoto, 1991). Life accentuates this interaction by capturing photons during photosynthesis, by altering the surface composition of the planet, and (to a much lesser extent) by metabolic entropy production (Schwartzman, 1999, Kleidon & Lorenz, 2005). A net result of the presence of life on Earth is therefore an increase in the entropy S produced over time t , $\frac{dS}{dt} > 0$ between solar radiation reaching the Earth and being emitted from its surface.

Schwartzman proposed that the entropy flux across the planet’s surface, in relation to the flux expected of a blackbody planet of equivalent size, $\frac{\frac{dS}{dt} \text{ surface}}{\frac{dS}{dt} \text{ blackbody}}$, would be expected to increase over Earth’s history, and might be a useful metric for the organisation of the biosphere (Schwartzman, 1999). The ideas concerning temperature preferences of the terrestrial biosphere that I have developed here make sense if a given level of normalised entropy production $\frac{\frac{dS}{dt} \text{ surface}}{\frac{dS}{dt} \text{ blackbody}}$, can only be maintained within a given planetary temperature range. The Neoproterozoic-Phanerozoic transition might have involved an increase in both the size of the terrestrial biosphere $\frac{B}{B_0}$ and in the total entropy flux across the Earth’s surface $\frac{\frac{dS}{dt} \text{ surface}}{\frac{dS}{dt} \text{ blackbody}}$. Although there is no discernable relationship between biomass and entropy production, at the planetary scale higher net biomass will often result in higher metabolic entropy production (Kleidon & Lorenz, 2005). I noted that metabolic/physiological constraints (specifically that different lichen species can grow across a far greater range of temperature conditions than can different vascular plant species) meant that this corresponds to an increase in the sensitivity c that this entropy flux has to deviation of temperature from the range within which maximum enhancement occurs $|T - T_{max}|$. In short, all of the changes I have suggested as possible explanations for the reduced susceptibility to global scale glaciation over Earth history, would, if they occurred, have resulted in an increase in the normalised entropy flux across the Earth’s surface. This temporal evolution could be interpreted in a “Gaian” context as a progressive increase in the geochemical sensitivity of the silicate weathering buffer. The cessation of the Paleoproterozoic glaciations would correspond to the origin of a geochemical CO_2 -weathering buffer (Walker et al, 1981), with a positive feedback later occurring between lichen evolution and Neoproterozoic glacial initiation, after which evolution within the terrestrial biosphere narrowed the temperature boundary conditions for silicate weathering, hence stabilizing climate. However, the extremely poor resolution on biotic silicate weathering enhancement means that it is just as likely that the terrestrial biosphere is irrelevant to glacial initiation, and that 500Myrs of climatic stability over the Phanerozoic are not strong evidence of a buffered “geomembrane” (Schwartzman, 1999), given the ~ 1 Byrs separating the Paleoproterozoic and Neoproterozoic glacial events. Empirical constraints on biotic silicate weathering enhancement by different species will resolve this issue.

It is interesting that my ideas on stability (in terms of vulnerability to greenhouse-icehouse oscillation) tie in with Schwartzman's entropy flux metric for organisation of the biosphere, $\frac{\frac{dS}{dt} \text{ surface}}{\frac{dS}{dt} \text{ blackbody}}$. I therefore end the thesis by proposing that biological silicate weathering enhancement $\frac{E}{E_0}$, in terms of its maximum impact ε_{max} , the required biomass $\frac{B}{B_0}$, and its sensitivity c , all tie in with this metric:

$$\frac{E}{E_0} = \frac{B}{B_0} \varepsilon_{max} (1 - c(T - T_{max})) \propto \frac{\frac{dS}{dt} \text{ surface}}{\frac{dS}{dt} \text{ blackbody}} \tag{7.7}$$

Relation (7.7) amounts to saying that the increase in surface entropy flux that would be expected to characterise Earth history (Schwartzman, 1999), was correlated with an increase in the biomass and temperature sensitivity of biological enhancement of the Urey reaction. This could be a tangible means of testing the link between organisation of the biosphere and the surface entropy flux (if future extrapolation of the temperature preferences of land life from fossils can provide a coherent picture across Earth history). I note that this is only a correlation - the physiological changes resulted from natural selection within individual populations, rather than being caused by any "top-down" forcing. Yet each variable in the biotic weathering enhancement function that I have developed does exhibit a positive relationship with entropy production by the biosphere. The homeostasis introduced as a result of evolutionary dynamics during the Neoproterozoic made it significantly less likely that climate would leave the habitable zone.

References

- [1] Agassiz, L. 1842. "The ice period: a period of history of my globe". Sel. Per. Litrs. Foreign ctries. 3 307-326.
- [2] Aggarwal, J.K. & Palmer, M.R. 1995. "Boron isotope analysis". Analyst 120. 1301-1307.
- [3] Aghamiri, R, & Schwartzman, D.W. 2002. "Weathering rates of bedrock by lichens: A mini-watershed study". Chem Geol. 188(3). 249-259.
- [4] Ahmadjian, V. 1993. "The lichen symbiosis." Wiley.
- [5] Aitken, J.D. 1991. "The ice brook formation and post Rapitan Late Proterozoic glaciation, Mackenzie mountains, Northwest territories". Geological Survey of Canada Bulletin, 404.
- [6] Albarede, F, et al, 1981. " $^{87}\text{Sr}/^{86}\text{Sr}$ ratios in hydrothermal waters and deposits from the East Pacific Rise at 21 deg North." Earth Plan. Sci. Lett. 55:229-236.
- [7] Allen, P.A., Hoffman, P.F. 2005. "Extreme winds and waves in the aftermath of a Neoproterozoic glaciation". Nature 433. 123-127
- [8] Amend, J.P., Rogers, K.L. & Meyer-Dombard, D.R. 2004. "Microbially mediated sulphur redox: Energetics in marine hydrothermal vent systems". Geol. Soc. Amer. Special paper 379.
- [9] Anbar, A.D. & Knoll, A.H. 2002. "Proterzoic ocean chemistry and evolution: a bioinorganic bridge". Science 297, 1137-1142.
- [10] Aris-Brosou, S. & Yang, Z. 2003. "Bayesian models of episodic evolution support a late Precambrian explosive diversification of the Metazoa". Mol. Biol. Evol. 20. 1947-1954.
- [11] Arrigo, K.R. 2005. "Marine micro-organisms and global nutrient cycles". Nature 437. 349-355.
- [12] Axelrod, R. & Hamilton, W.D. 1981. "The evolution of co-operation". Science 211, 1390-1396.
- [13] Axelrod,R., Grafen,A., Hammond,R., 2004. Altruism via kin selection strategies that rely on arbitrary tags with which they co-evolve. Evolution 58, 1833.
- [14] Ayala, F.Jose, Rzhetsky, A., and Ayala, F.J. 1998. "Origin of the metazoan phyla: Molecular clocks confirm paleontological estimates". PNAS 95(2). 606-611.

- [15] Baker, M.E. 2006. "The genetic response to Snowball Earth: role of HSP90 in the Cambrian explosion.". *Geobiology* 4. 11-14.
- [16] Banfield, J.F., Barker, W.W., Welch, S.A. & Taunton, A. 1999. "Biological impact on mineral dissolution: Application of the lichen model to understanding mineral weathering in the rhizosphere". *PNAS* 96(7). 3404-3411.
- [17] Barker, S.B., Higgins, J.A. & Elderfield, H. 2003. "The future of the Carbon cycle: review, calcification response, ballast and feedback on atmospheric CO_2 ". *Phil. Trans. Roy. Soc. Lond. A.* 361. 1977-1999.
- [18] Battistuzzi, F.U., Feijao, A, & Hedges, S.B. 2004. "A molecular timescale of eukaryotic evolution". *BMC Evol. biol.* 4(44). 1471-2148.
- [19] Baum, S.K., Crowley, T.J., 2001. "GCM Response to Late Precambrian Ice-covered continents". *Geophys. Res. Lett.* 28. pp 583-586.
- [20] Baum, S.K., Crowley, T.J. 2003. "The snow/ice instability as a mechanism for rapid climate change: A Neoproterozoic Snowball Earth model example.". *Geophys. Res. Lett.* 30. GL017333.
- [21] Beerling, D.J. & Berner, R.A. 2005. "Feedbacks and the coevolution of Plants and atmospheric CO_2 ". *Proc. Natl. Acad. Sci. USA.* 102(5). 1302-1305.
- [22] Bergman, N.M. 2003. "COPSE: A new biogeochemical Earth system model for the Phanerozoic". Phd thesis, UEA.
- [23] Ben-Naim, A. 2007. "Entropy demystified". World Scientific.
- [24] Bendtsen, J. & Bjerrum, C.J. 2002. "Vulnerability of climate on Earth to sudden changes in insolation". *Geophys. Res. Lett.* 29(15) DOI: 10.1029/2002GL014829.
- [25] Bennett. P.C, Rogers, J.R. & Choi, W.J. 2001. "Silicates, silicate weathering, and microbial ecology". *Geomicrobiol.* 18. 3-19.
- [26] Berner, R.A., Lasaga, A.C. & Garrels, R.M. 1983. "The carbonate-silicate geochemical cycle and its effect on atmospheric CO_2 over the past 100 million years". *Am J. Sci.* 283. 641-683.
- [27] Berner, R.A. 1990. "Atmospheric Carbon Dioxide levels over Phanerozoic time". *Science* 249, 1382-1386.
- [28] Berner, R.A. 1991. " A model for atmospheric CO_2 over Phanerozoic time". *Am. Journ. Sci.* 291. 339-376.
- [29] Berner, R.A. 1992. "Weathering, plants, and the long-term Carbon cycle". *Geochim. Cosmochim. Acta.* 56. 3225-3332.

- [30] Berner, R.A., 1994. "Geocarb II: A revised model of atmospheric CO_2 over phanerozoic time". American. Journ. Sci. 294, 56-91.
- [31] Berner, R.A. & Berner, E.K. 1997. "Silicate weathering and climate". "Tectonic Uplift and Climate change" pp353-365.
- [32] Berner, R.A. 2001. Modelling atmospheric O_2 over Phanerozoic time. *Geochimica et Cosmochimica Acta* 65, 685-694
- [33] Bertrand-Sarfarti, J. et al. 1995. "First Ediacaran fauna found in West Africa and evidence for an early Cambrian glaciation". *Geology* 23. 133-136.
- [34] Bickle, M.J. 1994. "The role of metamorphic deCarbonation reactions in returning strontium to the silicate sediment mass." *Nature* 367. 699-704.
- [35] Blum, A.E. & Stillings, L.L. 1995. "Feldspar dissolution rates". In *Chemical weathering rates of silicate minerals*. pp 291-351. Washington.
- [36] Bodieselitsch, B, Koeberl, C., Master, S. & Reimold, W.U., 2005. "Estimating duration and intensity of Neoproterozoic snowball glaciations from *Ir* anomalies". *Science* 308. 239-242.
- [37] Bosak, T & Newman, D.K. 2003. "Microbial nucleation of calcium carbonate in the Precambrian". *Geol. Soc. Am.* 31(7). 577-580.
- [38] Boucher, D.H., 1982. "The ecology of mutualism" *Ann. Rev. Ecol. Syst.* 13. 315-347.
- [39] Boulton, G.S. 1996. "Theory of glacial erosion, transport and deposition as a consequence of subglacial sediment deformation". *J. Glaciol* 42. 43-62.
- [40] Boyle, R.A. & Lenton, T.M., 2006. "Fluctuation in the physical environment as a mechanism for reinforcing evolutionary transitions.". *Journal of Theoretical Biology* 242. 832-843.
- [41] Brantley, S.L. & Chen, Y. 1995. "Chemical weathering rates of pyroxenes and amphiboles". In *Chemical weathering rates of silicate minerals: Reviews in Mineralogy* 31. 119-172.
- [42] Brasier, M., McCarron, G., Tucker, R., Leather, J., Allen, P., Shields, G. 2000. "New *U - Pb* zircon dates for the Neoproterozoic Ghubrah glaciation and for the top of the Huqf supergroup, Oman". *Geology*, 28(2), 173-178.
- [43] Bresch, C. et al, 1980. Hypercycles, parasites and packages. *J. Evo. Biol*, 85, 399-405.
- [44] Brocks, J.J., et al 1999. "Archean molecular fossils and the early rise of eukaryotes". *Science*, 285, 1033-1036,

- [45] Broecker, W.S. 1997. "Thermohaline circulation, the achilles heel of our climate system: Will man-made CO_2 upset the current balance?". *Science* 278. 1582-1589.
- [46] Brookfield, M.E. 1994. "Problems in applying preservation, facies and sequence models to Sinian (Neoproterozoic) glacial sequences in Australia and Asia". *Precambrian Res.* 78. 113-143.
- [47] Brown, J.K.M. 1999. "The evolution of sex and recombination in fungi" In Worrall, J.J. 1999 "Structure and dynamics of fungal populations" pp73-97. Springer.
- [48] Brown, R.H. et al. 1972. "The amino acid sequence of cytochrome c from *Helix aspera* (garden snail)". *Biochemical Journal* 128. 971-974.
- [49] Budyko, M.I.. 1969. "The effect of solar radiation variations on the climate of the Earth". *Tellus* 21. 611-619.
- [50] Butterfield, N.J., Knoll, A.H. & Swett, K, 1994. "Paleobiology of the Neoproterozoic Svanbergfjellet formation, Spitzbergen." *Fossils and Strata.* 34, pp84.
- [51] Butterfield, N.J. 2000. "Bangiomorpha pubescens n.gen., n. sp.: implications for the evolution of sex, multicellularity, and the Mesoproterozoic/Neoproterozoic radiation of eukaryotes. *Paleobiology* 26(3), 386-404.
- [52] Butterfield, N.J. 2004. "A vaucherian alga from the middle Neoproterozoic of Spitzbergen: implications for the evolution of Proterozoic eukaryotes and the Cambrian explosion". *Paleobiology* 30. 231-252.
- [53] Butterfield, N.J. 2005. "Probable Proterozoic Fungi". *Paleobiology* 31(1). 165-182.
- [54] Butterfield, N.J. 2005. "Reconstructing a complex early Neoproterozoic eukaryote, Wynniatt formation, Arctic Canada". *Lethaia* 38. 155-169.
- [55] Butterfield, N.J. 2007. "Macroevolution and Macroecology through deep time". *Paleontology* 50(1). 41-55.
- [56] Caldeira, K. & Kasting, J.F. 1992. "The life span of the biosphere revisited". *Nature* 360, 721-723.
- [57] Caldeira, K. & Rampino, M.R., 1993. "Aftermath of the end Cretaceous Mass Extinction - possible biogeochemical stabilization of the Carbon cycle and climate." *Paleoceanography* 8. 515-525.
- [58] Canfield, D.E. & Teske, A. 1996. "Late Proterozoic rise in atmospheric oxygen concentration inferred from phylogenetic and Sulphur isotope studies". *Nature* 382, 127-132.
- [59] Canfield, D.E. 1998. "A new model for Proterozoic ocean chemistry" *Nature* 396. 450-453.

- [60] Canfield, D.E. & Raiswell, R. 1999. "The evolution of the sulphur cycle". *Am. J. Sci.* 299. 697-723.
- [61] Canfield, D.E. 2004. "The evolution of the Earth surface Sulphur reservoir" *Am. J. Sci.* 304. 839-861,
- [62] Canfield, D.E. et al. 2007. "Late Neoproterozoic Deep-Ocean Oxygenation and the Rise of animal Life". *Science* 315, 92-95.
- [63] Cavalier-Smith, T. 2006. "Cell evolution and Earth history: stasis and revolution". *Phil. Trans. R. Soc. B.* 361, 969-1006.
- [64] Catling, D.C., Glein, C.R., Zahnle, K.J. & McKay, C.P. 2005. "Why O_2 is required by complex life on habitable planets and the concept of planetary "oxygenation time"". *Astrobiology* 5. 415-438.
- [65] Cawley, J.L. Burrus, R.C & Holland, H.D. 1969. "Chemical weathering in central Iceland: An analog of pre-Silurian weathering." *Science* 165. 391-392.
- [66] Celler, C.K. & Wood, B.D. 1993. "Possibility of chemical weathering before the advent of vascular land plants". *Nature* 364, 223-225.
- [67] Chamberlain, J.W. 1980. "Changes in the planetary heat balance with chemical changes in air". *Planetary & Space Science* 28. 1011-1018.
- [68] Charleson, R.J., Anderson, T.L. & McDuff, R.E. 2000. In "Earth system science: From biogeochemical cycles to global change" Chapter 13 "The sulphur cycle". pp343-359.
- [69] Chen, J., Blume, H.P. & Beyer, L. 2000. "Weathering of rocks induced by lichen colonization - a review". *Catena* 39. 121-146.
- [70] Clark, B.M., St-Clair, L.L., Mangelson, N.F., Rees, L.B., Grant, P.G., & Bench, G.S., 2001. "Characterisation of mycobiont adaptations in the foliose lichen *Xanthoparmelia chlorochroa* (Parmeliaceae)" *Am. Journ. Bot.* 88. 1742-1749.
- [71] Cloud, P. Wright, L.A., Williams, E.G., Diehl, P. & Walter, M.R., 1974. "Giant stromatolites and associated vertical tubes from Upper Proterozoic Noonday Dolomite, Death valley region, eastern California" *Geological Society of America Bulletin*, 85, 1869-1882.
- [72] Cochran, Mf. & Schwartzman, D.W. 1995. "Chemical weathering rates on lichen-colonized silicate rocks". Abstracts 27(6), A-185. Annual Meeting. Geological Society of America.

- [73] Cockell, C.S. & Raven, J.A. 2007. "Ozone and life on the early Earth". *Phil. trans. Roy. Soc. B.* 1889-1901.
- [74] Cohen, D, Eshel, I. 1976. "On the founder effect and the evolution of altruistic traits". *Theoretical Population Biology* 10(3). 276-302.
- [75] Conway Morris, S. 2006. "Darwin's dilemma: the realities of the Cambrian explosion". *Phil. Trans. R. Soc. B.* 361. 1069-1083.
- [76] Corsetti, F.A. Lorentz, N.J. , Pruss, S.B. 2004. "Formerly-aragonite seafloor fans from neoproterozoic strata, Death Vally, Southwestern Idaho, United States: Implications for "Cap carbonate" formation and Snowball Earth". *The extreme Proterozoic: Geology, Geochemistry and Climate. Geophysical Monograph Series 146. AGU.* pp 33-44.
- [77] Corsetti, et al, 2006. "The biotic response to Snowball Earth". *Paleogeography, Paleoclimatology & Paleoceanography* 232. 114-130.
- [78] Coxson, D.S., Harris, G.P. & Kershaw, K.A. 1982. "Contrasting gas exchange patterns between a lichenised and non-lichenised terrestrial nostoc cyanophyte". *New Phytol.* 92. 561-572.
- [79] Craig, H. 1957. "Isotopic standards for Carbon and Oxygen correction factors for mass spectromic analysis of Carbon dioxide". *Geochim Cosmochim. Acta.* 12. 133-149.
- [80] Crowell, J.C. 1983. "Ice ages recorded on Gondwanan continents". *Transactions Geol. Soc. South Africa.* 86. 237-262.
- [81] Day, T. 2003. "Virulence evolution and the timing of disease life history events." *Trends. Ecol. Evol.* 18(3). 113-118
- [82] de los Rios, A. Wierzschos, J, Sancho. L.G. & Ascaso, C. 2003. "Acid microenvironments in microbial biofilms of antarctic, endolithic, microecosystems". *Environ. Microbiol.* 5(4) 231-237.
- [83] de Villiers, S. 1999. "Seawater *Sr* and *Ca* variability in the Atlantic and Pacific oceans". *Earth Plan. Sci. Lett.* 171(4).
- [84] Deming, J.W., Huston, A.L., 2000. "An oceanographic perspective on microbial life at low temperatures with implications for polar ecology, biotechnology and astrobiology". *Journey to diverse microbial worlds: adaptation to exotic environments.* Kluwer, pp149-160.
- [85] Dempster, T.J. , Rogers, G., Tanner, P.W.G, Bluck, B.J., Muir, R.J., Redwood, S.D., Ireland, T.R., & Patterson, B.A., 2002. "Timing of deposition, orogenesis & glaciation within the Dalradian rocks of Scotland: Constraints on *U - Pb* zircon ages". *J. Geol. Soc. Lond.* 159. 83-94.

- [86] DePriest, P.T. 2004. "Early molecular investigations of lichen-forming symbionts". *Ann. rev. Microbiol* 58. 273-301.
- [87] Dessert, C., Dupre, B., Gaillardet, J., Francois, L.M. & Allegre, C.J. 2003. "Basalt weathering laws and the impact of basalt weathering on the global Carbon cycle". *Chem. Geol.* 202. 257-273.
- [88] De Vargas, C., Aubry, M., Probert, I. & Young, J. 2004. "Origin and evolution of Coccolithophores: from coastal hunters to oceanic farmers". pp251-285 In "Coccolithophores: From Molecular processes to global impact". Lavoisier.
- [89] Deynoux, M. & Trompette, R. 1976. "Late precambrian mixtite: glacial and/or non-glacial? Dealing especially with the mixtite of West Africa". *Am. Journ. Sci.* 276. 117-125.
- [90] Deynoux, M. 1980. "Les formations glaciares du Precambrian terminal et de la fin d'Ordovician en Afrique de l'ouest". *Travaux des laboratoires des sciences de la terre St. Jerome. Marseille*
- [91] Deynoux, M. 1982. "Periglacial polygonal structures and sand wedges in the late Precambrian glacial formations of the Taoudeni Basin in Adrar of Mauretania (West Africa)". *Paleoeco. Paleoclim. Paleoecol.* 39. 55-70.
- [92] Dickson, A.G. & Millero, F.J. 1987. "A comparison of the equilibrium constants for the dissociation of Carbonic acid in seawater media". *Deep Sea Res.* 34. 1733-1743.
- [93] Dobrzinski, N. et al. 2004. "Geochemical climate proxies applied to the Neoproterozoic glacial succession on the Yangtze platform, South China". *The extreme Proterozoic: Geology, Geochemistry and Climate. Geophysical Monograph Series 146. AGU.* pp13-32.
- [94] Donnadieu, Y., Ramstein, G., Fluteau, F., Roche, D., & Ganopolski, A. 2002. "The impact of atmospheric and oceanic heat transports on the sea ice-albedo instability during the Neoproterozoic". *Climate Dynamics* 22. 293-306.
- [95] Donnadieu, Y., Godderis, Y., Ramstein, G., Nedelec, A., & Meert, J. 2004. "A 'snowball Earth' climate triggered by continental break-up through changes in runoff". *Nature* 428. 303-306.
- [96] Douzery, E.J.P., Snell, E.A., Babtiste, E., Delsuc, F. & Phillippe, H. 2004. "The timing of Eukaryotic evolution: does a relaxed molecular clock reconcile proteins and fossils?" *Proc. Natl. Acad. Sci. USA.* 101. 15386-15391.
- [97] Drever, J.I. 1974. "Geochemical model for the origin of Precambrian banded iron formations". *Geol. Soc. Amer. Bull.* 85. 1099-1106.

- [98] Dutkiewicz, A., Volk, H, George, S.C., Ridley, J & Buick, R. 2006. "Biomarkers from Huronian oil-bearing fluid incursions: An uncontaminated record of life before the Great Oxidation event." *Geology*, 34, 437-440.
- [99] Dyson, I.A. & von der Borch, C.C. 1994. "Sequence stratigraphy of an incised valley fill: The Neoproterozoic seacliffe sandstone, Adelaide, Australia". In "Incised valley systems: Origin and sedimentary sequences" 51. 209-222.
- [100] Eichorn, S.E., Evert, R.F., & Raven, P.H. 2005. "Biology of plants" Freeman.
- [101] Eigen, M. 1971. Self organisation of matter and the evolution of biological macromolecules. *Naturwissenschaften* 65, 465-523
- [102] Eshel, I. 1977. "On the founder effect and the evolution of altruistic traits: an ecological approach". *Theoretical population biology* 11(3), 410-424.
- [103] Evans, D.A.D, et al, 1997. "Low latitude glaciation in the Paleoproterozoic era.". *Nature* 386, 262-266.
- [104] Evans, D.A.D., 2000. "Stratigraphic, geochronological, and paleomagnetic constraints on the Neoproterozoic climatic paradox." *American Journal of Science* 300. 347-433.
- [105] Evans, D.A.D., 2003. "True polar wander and supercontinents". *Tectonophysics* 362. 303-320.
- [106] Evans, D.A.D, 2005. "Proterozoic low orbital obliquity and axial-dipolar geomagnetic field from evaporite paleolatitudes." *Nature* 444. 51-55.
- [107] Ertl, L. 1951. "Uber die Lichverhaltnisse in Laubflechten" *Planta* 39. 245-270.
- [108] Eyles, C.H. & Eyles, N. 1983. "Sedimentation in a large lake: A reinterpretation of the late pleistocene stratigraphy at Scarborough bluffs, Ontario, Canada." *Geology* 11. 146-152.
- [109] Eyles, N. & Eyles, C.H. 1992. "Glacial depositional systems". In Walker, R.G., James, N.P.(Eds). *Facies models: Response to sea level change*. Geol. Assoc. Canada. pp73-100.
- [110] Eyles, N. 1993. "Earth's glacial record and its tectonic setting." *Earth Science Reviews* 35. 1-248.
- [111] Eyles, N & Januszczak, N. 2004. "Zipper rift: a tectonic model for Neoproterozoic glaciations during the breakup of Rodinia after 750 MA." *Earth. Sci. Rev.* 65, 1-73.
- [112] Fairchild, I.J. 1993. "Balmy shores and icy wastes: the paradox of carbonates associated with glacial deposits in Neoproterozoic times". *Sedimentology review*, Blackwell. pp 1-16.

- [113] Fairchild, I.J. & Kennedy, M.J. 2007. "Neoproterozoic glaciation in the Earth system". *Journ. Geol. Soc. London.* 164. 895-921.
- [114] Fanning, C.M., Link, P.K., 2004. "U-Pb SHRIMP age of Neoproterozoic (Sturtian) glaciogenic Pocatello formation, southeastern Idaho." *Geology* 10., 881-884.
- [115] Feng, D.F., 1997. "Determining divergence times with a protein clock: update and re-evaluation." *PNAS.* 94. 13028-13033.
- [116] Ferris, F.G. & Lowson, E.A. 1997. "Ultrastructure and geochemistry of microorganisms in limestone of the Niagara escarpment". *Can. Journ. Microbiol.* 43. 211-219.
- [117] Fix, A.G., 1985. "Evolution of altruism in kin-structured and random subdivided populations" *Evolution* 39, 928-939.
- [118] Franck, S.A. & Bounama, C. 1997. "Continental growth and volatile exchange during Earth's evolution". *Phys. Earth. Plan. Int.* 100. 189-196.
- [119] Franck, S.A., Kossacki, K. & Bounama, C. 1999. "Modelling the global Carbon cycle for past and future evolution of the Earth system". *Chem. Geol.* 159. 305-317.
- [120] Frank, S.A. 1998. "Foundations of social evolution". Princeton University press
- [121] Fricke, H.C. & O'Neill, J.R. 1999. "The correlation between $^{18}O/^{16}O$ ratios of meteoric water and surface temperature: its use in investigating terrestrial climate change over geologic time". *Earth Plan. Sci. Lett.* 170(3). 181-196.
- [122] Gislason, S.R., Arnorsson, S. & Armannsson, H. 1996. "Chemical weathering of basalt in southwest iceland: Effects of runoff, age of rocks and vegetative/glacial cover". *Am. J. Sci.* 296. 837-907
- [123] Godderis, Y., Donnadieu, Y., Nedelec, A., Dupre, B., Dessert, C., Grard., A., Ramstein, G. & Francois, L.M. 2003. "The Sturtian 'snowball' glaciation: fire and ice". *Earth. Plan. Sci. Lett.* 211. 1-12.
- [124] Gorjan, P., Walter, M.R., Swart, R. 2003. "Global Neoproterozoic (Sturtian) post glacial sulphide sulphur isotope anomaly recognised in Namibia". *J. Afr. Earth. Sci.* 36(1). 89-98.
- [125] Gough, D.O. 1981. "Solar interior structure and luminosity variations" *Solar Phys.* 74, 21-34.
- [126] Gow, N.A.R & Gadd, G.M. 1995. "The growing fungus". Chapman Hall.
- [127] Green, J.S.A., 2002. "Reflections on the Earth's albedo: A collection of scattered thoughts". *Weather* 57. 431-439.

- [128] Grey, K., et al. 2003. "Neoproterozoic biotic diversification: Snowball Earth or aftermath of the Acraman impact?" *Geology* 31, 459-462.
- [129] Griffin, A.S., West, S.A., 2002. "Kin selection: fact and fiction". *TREE* 17, 15-21.
- [130] Griffiths, D.J., 1998. "Introduction to electrodynamics" Prentice Hall
- [131] Grotzinger, J.P. & Knoll, A.H. 1995. "Anomalous carbonate precipitates: is the Precambrian the key to the Permian?". *Palaios*. 10. 578-596.
- [132] Grotzinger, J.P. et al, 2000. "Calcareous metazoans in thrombolithic bioherms of the terminal Proterozoic Nama group, Namibia". *Paleobiology* 26. 334-359.
- [133] Grube, M. & Kroken, S. 2000. "Molecular approaches and the concept of species and species complexes in lichenized fungi". *Mycological Research*. 104. 1284-1294.
- [134] Haeberli, W., et al. 1989. "World glacier Inventory: Status 1988". Teufeo, Switzerland, Kunz Druck & Co. AG.
- [135] Hall, A. 2004. "The role of surface albedo feedback in climate". *J. of Climate* 17, 1550-1568.
- [136] Halverson, G.P., Hoffman, P.F., Schragg, D.P. & Kaufman, A.J. 2002. "A major perturbation of the Carbon cycle before the Ghaub glaciation (Neoproterozoic) in Namibia: Prelude to snowball Earth?" *Geochem. Geophys. Geosystems*. 3(6). 1035.
- [137] Halverson, G.P., Maloof, A.C. & Hoffman, P.F., 2004. "The Marinoan (Neoproterozoic) Glaciation in North East Svalbard". *Basin Research* 16. 297-324.
- [138] Halverson, G.P. 2006. "A Neoproterozoic chronology". In "Neoproterozoic Geobiology and Paleobiology" pp231-271. Springer.
- [139] Halverson, G.P., Dudas, F.O., Maloof, A.C., & Bowring, S.A., 2007. "Evolution of the $^{87}\text{Sr}/^{86}\text{Sr}$ composition of Neoproterozoic seawater." *Paleogeo. Paleoclim. Paleoecol.* doi: 10.1016/j.paleo.2007.02.028.
- [140] Hambrey, M.J. & Harland, W.B. 1981. "Earth's Pre-Pleistocene Glacial Record. Cambridge University Press.
- [141] Hamilton, W.D. 1964 "The genetical evolution of social behaviour, II". *Journ. Theor. Biol.* 7. 17-52.
- [142] Hamilton, W.D., 1972. "Altruism and related phenomena, mainly in social insects". *Ann. Rev. Ecol. Syst.* 3. 193-232.
- [143] Harland, W.B., Bidgood, D.E.T., 1959. "Paleomagnetism in some Norwegian sparagmites and the late Precambrian ice age" *Nature* 184, 1860-1862, 1959.

- [144] Harland, W.B., Rudwick, M.J.S., 1964. "The Infra-Cambrian ice Age." *Scientific American* 211, 28-36.
- [145] Hawes, I. et al. 1993. "Environmental control of microbial biomass of the McMurdo Ice shelf, Antarctica." *Archiv fur Hydrobiologie* 127. 27-287.
- [146] Higgins, J.A. & Schrag, D.P. 2003. "Aftermath of a snowball Earth". *Geochem. Geophys. Geosyst.* 4(3). 1028-1048.
- [147] Hall, A. 2004. "The role of surface albedo feedback in climate". *Journal of Climate* 17. 1550-1568.
- [148] Haqq-Misra, J.D. 2007. "A revised Hazy Methane greenhouse for the Archaen Earth". Phd thesis, Penn State.
- [149] Hayes, J.M., Strauss, H. & Kaufman, A.J. 1999. "The abundance of $\delta^{13}C$ in marine organic matter and isotopic fractionation in the global biogeochemical cycle during the past 800MA". *Chem. Geol.* 161. 103-125.
- [150] Heckman, D.S. et al. 2001. "Molecular evidence for the early colonisation of land by fungi and plants." *Science* 293. 1129-1133.
- [151] Hedges, S.B. et al. 2001. "A genomic timescale for the origin of Eukaryotes." *BMC, Evol. Biol.* 1:4.
- [152] Hedges, S.B., 2004a. "Molecular clocks and a biological trigger for snowball earth and the Cambrian explosion". In "Telling the evolutionary time: Molecular clocks and the fossil record". pp27-40. CRC.
- [153] Hedges, S.B., Blair, J.E., Venturi, M.L. & Shoe, J.L. 2004b. "A molecular timescale of eukaryotic evolution and the rise of complex multicellular life". *BMC evol. biol.* 4(2), 1471.
- [154] Herrera, J.R. 1992. "Fungal cell wall: Structure, synthesis and assembly". CRC press.
- [155] Hochanka, P.W., Fields, J. & Mustafa, T. 1973. "Animal life without oxygen: basic biochemical mechanisms". *Integrative and comparative biology* 13. 543-555.
- [156] Hoffman, K.H., Condon, D.J. Bowring, S.A. & Crowley, J.L. 2004. "*U - Pb* zircon date from the Neoproterozoic Ghaub formation: Constraints on Marinoan glaciation". *32(9)*. 817-820.
- [157] Hoffmann, P.F., et al. 1998. "A Neoproterozoic Snowball Earth". *Science* 281. 1342-1346.
- [158] Hoffman, P.F. & Maloof, A.C., 1999. "Glaciation: The snowball theory still holds water". *Nature* 397, 384.

- [159] Hoffman, P.F., 1999. Response to Christie-Blick, N. & Sohl, L.E., 1999. "Considering a Neoproterozoic Snowball Earth". *Science* 284. 1087.
- [160] Hoffman, P.F, Schrag, D.P., 2002. "The Snowball Earth hypothesis: testing the limits of global change". *Terra Nova* 14. 129-155.
- [161] Hofmann, H.J. 1990. "Ediacaran remains from intertillite beds in northwestern Canada". *Geology* 18. 1199-1202.
- [162] Holser, W.T., Schidlowski, M., Mackenzie, F.T. & Maynard, J.B. 1988. "Chemical cycles in the evolution of the Earth". pp 105-173. New York.
- [163] Holland, H.D. 1984. "The chemical evolution of the atmosphere and oceans". Princeton University press.
- [164] Holland, H.D., 2002. "Volcanic gases, black smokers, and the great oxidation event". *Geochimica et Cosmochimica acta*. 66(21). 3811-3826.
- [165] Hollenbach, D.F. & Herson, J.M. 2001. "Deep Earth reactor: Nuclear fission, helium, and the geomagnetic field". *PNAS*. 98(20) 11085-11090.
- [166] Horita, J. Wesolowski, D.J. 1994. "Liquid vapour fractionation of Oxygen and Hydrogen isotopes of water from freezing to the critical temperature". *Geochim. Cosmochim. Acta*. 58(16). 3425-3437.
- [167] Huntly, J.W. et al 2006. "1.3 Billion years of acritarch history: An empirical morphospace approach". *Precambrian. Res.* 144. 52-68.
- [168] Hurtgen, M.T. 2002. "The sulphur isotopic composition of Neoproterozoic seawater sulphate: implications for a snowball Earth?". *Earth. Plan. Sci. Lett.* 203. 413-429.
- [169] Hurtgen, M.T., Arthur, M.A.& Prave, A.R. 2004. "The sulphur isotope composition of carbonate-associated sulphate in Mesoproterozoic to Neoproterozoic carbonates from Death valley, California". *Geol. Soc. Amer. Special Paper* 379.
- [170] Hurtgen, M.T. 2005. "Neoproterozoic sulfur isotopes, the evolution of microbial sulphur species, and the burial efficiency of sulphide as sedimentary pyrite." *Geology* 33(1). 41-44.
- [171] Hyde, W.T. et al. 2000. "Neoproterozoic 'snowball Earth' simulations with a coupled climate/ice-sheet model". *Nature* 405, 425-429.
- [172] Hyvarinen, M. Hardling, R & Tuomi, J. 2002. "Cyanobacterial lichen symbiosis: The fungal partner as an optimal harvester". *Oikos* 98(3). 498-504.

- [173] Ikeda, T & Tajika, E., 1999. "A study of the energy balance climate model with CO_2 dependent outgoing radiation: Implication for the glaciation during the Cenozoic" *Geophys. Res. Lett.* 26. 349-352.
- [174] Isley, A.E. & Abbott, D.H., 1999."Plume related mafic volcanism and the deposition of banded iron formations". *J. Geophys. Res.* 104(15). 461-477.
- [175] Jaanusson, V. 1976. "Faunal dynamics in the middle Ordovician (Viruan) of Baltoscandia". In "The Ordovician System: Proceedings of a Paleontological Association Symposium", pp 301-326. University of Wales Press.
- [176] Jackson, T.A. & Keller, W.D. 1970a. "A comparative study of the role of lichens and inorganic processes in the chemical weathering of recent Hawaiian lava flows". *Am. J. Sci.* 269. 446-466.
- [177] Jacobsen S.B. & Kaufman, A.J. 1999. "The *Sr*, *C* and *O* isotopic evolution of Neoproterozoic seawater". *Chem. Geol.* 161. 37-57.
- [178] James, N.P. , Narbonne, G.M. & Kyser, T.K. 2001. "Late Neoproterozoic cap carbonates: Mackenzie mountains, northwestern Canada: precipitation and global glacial meltdown". *Can. J. Earth. Sci.* 38. 1229-1262.
- [179] Javaux, E., Knoll, A.H. & Walter, A.R. 2001. "Morphological and ecological complexity in early Eukaryotic ecosystems" *Nature* 412. 66-69.
- [180] Javaux, E. 2003. "Recognizing and interpreting the fossils of early Eukaryotes". *Origins of life and Evolution of the Biosphere* 33. 75-94.
- [181] Jenkins, G.S. 2004. "High orbital obliquity as an alternative hypothesis to early and late Proterozoic extreme climate conditions". *The Extreme Proterozoic: Geology, Geochemistry and Climate. Geophysical monograph series 146*, pp183-192.
- [182] Jenkyns, HC. 1980. "Cretaceous Anoxic events: from continents to oceans". *J. Geol. Soc.* 137(2). 171-188.
- [183] Jensen, M.L. & Nakai, N. 1962. "Sulphur isotope meteorite standards: results and recommendations". "Biogeochemistry of Sulphur isotopes", pp 30-35. Yale University Press.
- [184] Jiang, G, Kennedy, M.J. & Christie-Blick, N. 2003. "Stable isotopic evidence for methane seeps in post-glacial cap carbonates". *Nature* 426. 822-826.
- [185] Johnson, C.G. & Vestal, J.R. 1991."Photosynthetic Carbon incorporation and turnover in Antarctic cryptoendolith communities.". *App. Env. Microbiol.* 57. 2308-2311.

- [186] Kakihana, H., Kotaka, M., Satoh, S., Nomura, M. & Okomoto, M. 1977. "Fundamental studies on the ion exchange separation of boron isotopes". *Bull. Chem. Soc. J.* 50. 158-163.
- [187] Kappne, L. 2000. "Some aspects of the great success of lichens in Antarctica". *Antarctic Science* 12(3). 314-324.
- [188] Kappen, I., Sommerkorn, M., & Schroeter, B. 1995. "Carbon acquisitions and water relations of lichens in polar regions-potentials and limitations". *Lichenologist* 27(6). 531-545.
- [189] Kasemann, S.A., Hawkesworth, C.J., Prave, A.R., Fallick, A.E. & Pearson, P.N. 2005. "Boron and Calcium isotopic composition in Neoproterozoic carbonate rocks from Namibia: Evidence for extreme environmental change". *Earth. Plan. Sci. Lett.* 231. 73-86.
- [190] Kasting, J.F. 1988. "Runaway and moist greenhouse atmospheres and the evolution of Earth and Venus". *Icarus* 74. 472-494.
- [191] Kasting, J.F., Whitmore, D.P. & Reynolds, R.T 1993. "Habitable zones around main sequence stars". *Icarus* 101. 108-128.
- [192] Kasting, J.F. 2005. "Methane and climate during the Precambrian Era". *Precambrian. Res.* 137. 119-129.
- [193] Kaufman, A.J. & Knoll, A.H. 1995. "Neoproterozoic variations in the *C*-isotopic composition of seawater: stratigraphic and biogeochemical implications". *Precambrian. Res.* 73. 27-49.
- [194] Keller, C.K. & Wood, B.D. 1993. "Possibility of chemical weathering before the advent of vascular plants". *Nature* 364. 223-225.
- [195] Kennedy, M.J., 1996. "Stratigraphy, sedimentology and isotope geochemistry of Australian Neoproterozoic postglacial cap dolostones: deglaciation $\delta^{13}C$ excursions, and carbonate precipitation." *J. Sed. Res.*, 66. 1050-1064.
- [196] Kennedy, M.J., Runnegar, B., Prave, A.R., Hoffman, K.H., & Arthur, M.A., 1998. "Two or four Neoproterozoic glaciations?" *Geology* 26. 1059-1063.
- [197] Kennedy, M.J., Christie-Blick, N. & Prave, A.R. 2001a. "Carbon isotopic composition of Neoproterozoic glacial carbonates as a test of paleoceanographic models for snowball Earth phenomena." *Geology* 29. 1135-1138
- [198] Kennedy, M.J., Christie-Blick, N. & Sohl, L.E. 2001b. "Are Proterozoic cap carbonates and isotopic excursions a record of gas hydrate destabilisation?". *Geology* 29. 443-446.

- [199] Kennedy, M.J., Droser, M., Mayer, L.M., Pevear, D. & Mrofka, D. 2006. "Late Precambrian Oxygenation: Inception of the clay mineral factory". *Science* 311. 1446-1449.
- [200] Kenny, R. & Knauth, L.P. 2001. "Stable isotope variations in the Beck Spring Dolomite and Mesoproterozoic Mescal limestone Paleokarst: Implications for life on land in the Precambrian". *Geol. Soc. Am. Bull.* 113. 650-658.
- [201] Kent, D.V., Smethurst, M.A. 1998. "A Shallow bias of paleomagnetic inclinations in the Paleozoic and Precambrian". *Earth. Planet. Sci. Lett* 160. 391-402.
- [202] Kershaw, K.A. 1985. "Physiological Ecology of lichens". C.U.P.
- [203] Kerzberg, M. & Wolpert, L. 1998. "The origin of Metazoa and the egg: a Role for Cell Death". *J. theor. Biol.* 193, 535-537.
- [204] Kieft, T.L. 1988. "Ice nucleation activity in lichens". *Appl. Environ. Microbiol* 54:1678-1681.
- [205] King, A.C., Billingham, J. & Otto, S.R. 2003 "Differential Equations: Linear, Non-linear, Ordinary, Partial". Cambridge University Press.
- [206] Kirschvink, J.L., 1992a. "Late Proterozoic Low-Latitude Global Glaciation: the Snowball Earth". *The Proterozoic Biosphere: A Multidisciplinary Study.* J.W. Schopf & C.Klein. Cambridge University Press. pp 51-52.
- [207] Kirschvink, J.L. 1992b. "A paleogeographic model for Vendian and Cambrian time" *The Proterozoic Biosphere: A Multidisciplinary Study.* J.W. Schopf & C.Klein. Cambridge University Press. pp 569-583.
- [208] Kleidon, A., Lorenz, R.D., 2004. "Entropy Production by Earth System Processes". In "Non-equilibrium thermodynamics and the production of entropy: Life, Earth and Beyond", pp1-20. Springer Verlag.
- [209] Knoll, A.H. & Walter, M.R. 1992. "Latest Proterozoic stratigraphy and Earth history". *Nature* 356. 673-678.
- [210] Knoll, A.H. 1994. "Proterozoic and Early Cambrian protists: Evidence for accelerating evolutionary tempo." *Proc. Natl. Acad. Sci. USA* 91. 6743-6750.
- [211] Knoll, A.H., Walter, M.R., Narbonne, G.M & Christie-Blick, N. 2004. "A new period for the Geologic time scale". *Science* 305. 621-622.
- [212] Knoll et al, 2006 "Eukaryotic organisms in Proterozoic Oceans." *Phil. Trans. Roy. Soc Lond. B.* 361, 1023-1038.

- [213] Kopp, R.E., Kirschvink, J.L, Hilburn, I.A & Nash, C.Z. 2005. "The Paleoproterozoic snowball Earth: A climate disaster triggered by the evolution of oxygenic photosynthesis". Proc. Natl. Acad. Sci. USA. 102 (32). 11131-11136.
- [214] Kreft, J, 2004. "Biofilms promote altruism". Microbiol. 150. 2751-2760.
- [215] Kroopnick, P.M., 1985. "The distribution of $\delta^{13}C$ and ΣCO_2 in the world's oceans". Deep sea Res. 32. 57-84.
- [216] Kump, L.R. 2008. "The rise of atmospheric oxygen". Nature 451. 277-278.
- [217] Kyte, F.T. & Wasson, J.T. 1986 "Accretion rate of extra - terrestrial matter: Iriridium deposited 33 to 67 million years ago". Science 232. 1125.
- [218] Landeweert,R. et al. 2001. Linking plants to rocks: ectomycorhizal fungi mobilize nutrients from minerals. TREE 16, 248-254.
- [219] Lamontagne, S. 1998. "Nitrogen mineralization in upland Precambrian Shield catchments: Contrasting the role of lichen-covered bedrock and forested areas". Biogeochemistry 41. 53-69.
- [220] Larson, D.W. 1983. "Environmental stress and *Umbilicaria* lichens: Oecologica 55. 268-278.
- [221] Leeming, M & Leeming, D, 1994. "A dictionary of creation myths". OUP.
- [222] Lehmann & Keller, 2006. "The evolution of co-operation and altruism - a general framework and a classification of models". J. Evol. Biol. 19. 1365-1376.
- [223] Lenton,T.M., 1998. "Gaia and Natural Selection". Nature 394. 437-447.
- [224] Lenton, T.M. 2000. "Land and ocean Carbon cycle feedback effects on global warming in a simple Earth system model". Tellus 52b. 1159-1188.
- [225] Lenton, T.M. & Watson, A.J. 2000a. "Redfield revisited 1: Regulation of phosphate, nitrate and oxygen in the ocean". Global Biogeochemical Cycles 14(1) 225-248.
- [226] Lenton, T.M & Watson, A.J. 2000b. "Redfield revisited 2: What regulates the oxygen content of the atmosphere?".
- [227] Lenton,T.M., 2001. "The role of land plants, phosphorous weathering and fire in the rise and regulation of atmospheric oxygen", Global Change Biology 7, 613-629.
- [228] Lenton,T.M., Watson, A.J., 2004, "Biotic enhancement of weathering, atmospheric oxygen and Carbon dioxide in the Neoproterozoic", Geophys. Res. Lett. 31, 1-5.

- [229] Lenton, T.M. , Schellnhuber, H.J. & Szathmary, E. 2004. "Climbing the coevolutionary ladder". *Nature* 431. 913.
- [230] Lenton, T.M. & Klausmeier, C.A. 2006. "Coevolution of Phytoplankton C:N:P stoichiometry and the deep ocean N:P ratio". *Biogeosciences Discuss.* 3. 1023-1047.
- [231] Levrard, B & Laskar, J. 2003. "Climate friction and the Earth's obliquity" *Geophys. Journ. Internatl.* 154. 970-990.
- [232] Lesins, G.B. 1991. "Radiative entropy as a measure of complexity". *Scientists on Gaia*, 1991. pp121-127. MIT press.
- [233] Lewis, E. & Wallace, D. 1998. "Program developed for CO_2 system calculations". Environmental Sciences division, publication No. 4735. Oak Ridge National Laboratory, USA.
- [234] Lewis, J.P., Weaver, A.J. & Eby, M. 2007. "Snowball versus slushball Earth: Dynamic versus nondynamic sea ice?" *Journ. Geophys. Res.* 112. DOI: 0148-0227/07/2006JC004037.
- [235] Li, C,W, et al, 1998. "Precambrian Sponges with cellular structures". *Science* 279. 879-883.
- [236] Li, Z.X., Li, X.H., Kinny, P.D., Wang, J., Zhang, S., & Zhou, H. 2003. "Geochronology of Neoproterozoic syn-rift magmatism in the Yangtze Craton, South China and correlations with other continents: evidence for a mantle superplume that broke up Rodinia". *Precamb. Res.* 122. 85-109.
- [237] Lian, M.S. & Cess, R.D. 1977. "Energy balance climate models: A reappraisal of ice-albedo feedback". *Journ. Atmos. Sci.* 34(7). 1058-1062.
- [238] Libby, S.M. 1992. "An introduction to marine biogeochemistry". Wiley.
- [239] Lottermoser, B.G. & Ashley, P.M. 2000. "Geochemistry, petrology and origin of Neoproterozoic Ironstones in the eastern part of the Adelaide geosyncline, South Australia." *Precambrian Res.*101. 49-67.
- [240] Lovelock, J.E., 1979. "Gaia: A new look at life on Earth". OUP.
- [241] Lovelock, J.E. 1988. "The ages of Gaia: A biography of my living Earth". Norton.
- [242] Madigan, M., & Martinko, J. 2005. "Brock biology of Microorganisms: 11th Edition". Prentice Hall.
- [243] Maguas, C, Griffiths, H. & Broadmeadow, S. 1995. "Gas exchange and Carbon isotope discrimination in lichens: Evidence for interactions between CO_2 concentrating mechanisms and diffusion limitation". *Planta* 196, 95-102.

- [244] Manabe, S & Stouffer, R.J. 1980. "Sensitivity of a global climate model to an increase of CO_2 concentration in the atmosphere". *J. Geophys. Res.* 85. 5529-5554.
- [245] Manabe, S. & Wetherald, R.T. 1980. "On the distribution of climate change resulting from an increase in the CO_2 content of the atmosphere". *J. Atmos. Sci.* 37. 99-118.
- [246] Margulis, L, Rambler, M. & Walker, J.C.G. 1976. "Reassessment of the Roles of oxygen and ultraviolet light in Precambrian evolution". *Nature* 264. 620-624.
- [247] Marshall, H.G., Walker, J.C.G. & Kuhn, W.R. 1988. "Long term climatic change and the geochemical cycle of Carbon". *J. Geophys. Res.* 93. 791-801.
- [248] Mawson, D. 1949. "The late Precambrian ice-age and the glacial record of the biandando dome". *J. Proc. Roy. Soc. New South Wales* 82. 150 - 174.
- [249] Maynard-Smith, J.M. 1983. "Hypercycles and the origin of life". *Nature* 280, 445-446.
- [250] Maynard-Smith, J.M., Szathmary, E. 1995. "The major transitions in evolution", pp40-58,99-121. OUP.
- [251] McCarroll, D & Viles, H. 1995. "Rock weathering by the lichen *Lecidea auriculata* in an arctic alpine environment". *Earth surface processes and landforms* 20. 199-206
- [252] McGuffie, K. & Henderson-Sellers, A. 1997. "A climate modelling primer". Wiley.
- [253] McKay, Cp, Lorenz, R.D. & Lunine J.I. 1999. "Analytic solutions for the anti-greenhouse effect: Titan and the early earth" *Icarus* 137, 56-61.
- [254] McKay, C.P. 2000. "Thickness of tropical ice and photosynthesis on a snowball Earth". *Geophys Res. Lett.* 27. 2153-2156.
- [255] McMenamin, M.A.S. 2004. "Climate, Paleoecology and abrupt changes during the late Proterozoic: A consideration of causes and effects". *Geophysical Monograph Series* 146. pp215-229.
- [256] Meert, J.G., Torsvik, T.H. 2004. "Paleomagnetic Constraints on Neoproterozoic 'Snowball Earth' continental reconstructions". *The Extreme Proterozoic: Geology, Geochemistry and Climate. Geophysical Monograph Series* 146. pp 5-11.
- [257] Mehrbach, C., Culberson, C.H., Hawley, J.E. & Pytkowicz, R.M. 1973. "Measurement of the apparent dissociation constants of Carbonic acid in seawater at atmospheric pressure.". *Limnol. Oceanogr.* 18. 897-907.
- [258] Michod, R., 1997. "Darwinian Dynamics: Evolutionary transitions in fitness and individuality". Princeton University Press.
- [259] Millero, F.J. & Sohn, M.L. 1992. "Chemical Oceanography". pp267-319. Boca Ratin.

- [260] Millero, F.J. 1995. "Thermodynamics of the Carbon dioxide system in the oceans". *Geochim. Cosmochim. Acta.* 54(4). 661-677.
- [261] Misi, A., Veizer, J., 1998. "Neoproterozoic carbonate sequences of the Una group, Irece Basin, Brazil; chemostratigraphy, age and correlations." *Precambrian Research* 89. 87-100.
- [262] Mook, W.G. 1986. " $\delta^{13}C$ in atmospheric CO_2 ". *Netherlands Journal of Deep Sea Research.* 20. 211-223.
- [263] Moulton, K.L, & Berner, R.A. 1998. "Quantification of the effect of plants on weathering: studies in Iceland". *Geology* 26: 895-898.
- [264] Mucci. A. 1983. "The solubility of calcite and aragonite in seawater at various salinities, temperatures and one atmosphere total pressure". *Am. J. Sci.* 283, 780-799.
- [265] Mulitza, S., Wolff, T., Patzold, J., Hale, W. & Weffer, G. 1998. "Temperature sensitivity of planktic Foraminifera and its influence on the Oxygen isotopic record". *Marine Micropaleontol.* 33(3). 223-240.
- [266] Munhoven, G. & Francois, L.M. 1996. "Glacial-interglacial variability of atmospheric CO_2 due to changing continental silicate rock weathering: A model study" *J. Geophys. Res.* 101. 21423-21437.
- [267] Nakajima, S., Hayashi, Y. & Abe, Y. 1992. "A study on the "runaway greenhouse effect" with a one dimensional radiative convective equilibrium model" *J. Atmos. Sci.* 49. 2256-2266.
- [268] Narbonne, G.M., Gehling, J.G. 2003. "Life after snowball: The oldest complex Ediacaran fossils". *Geology* 31, 27-30.
- [269] Narbonne, G.M., 2005. "The Ediacara biota: Neoproterozoic Origin of Animals and Their Ecosystems". *Ann. Rev. Earth Planet Sci.* 421-442.
- [270] Nash, T.H., Moser, T.J., Link, S.O., Ross, L.J., Olafsen, A., & Matthes, U. 1983. "Lichen photosynthesis in relation to CO_2 concentration". *Oecologia* 58. 52-56.
- [271] Nash, T.H. 1996. "Lichen Biology". C.U.P.
- [272] Nisbet, E.G., Fowler, C.M.R., 1999. "Archaean metabolic evolution of microbial mats". *Proc. Roy. Soc. Lond B.* 266. 2375-2382.
- [273] North. G.R. 1975. "Analytical solution to a simple climate model with diffusive heat transport". *J. Atmos. Sci.* 32. 1301-1307.

- [274] North, G.R. & Coakley, J.A. 1979. "Differences between seasonal and mean annual energy balance model calculations of climate and climate sensitivity". *J. atmos. Sci.* 36. 1189-1204.
- [275] North, G.R. Cahalan, R.F., Coakley, J.A., 1981. "Energy balance climate models". *Rev. Geophys. Space. Phys.* 19(1). 91-121.
- [276] Nowak, M.A. & May, R.M., 1992. "Evolutionary games and spatial chaos". *Nature* 359, 826-829.
- [277] Nowak, M.A. & Sigmund, K. 1998. "Evolution of indirect reciprocity by image scoring". *Nature* 593, 573-577.
- [278] Nowak, M.A., 2006. "Five rules for the evolution of co-operation". *Science* 314. 1560-1563.
- [279] Nursall, J.R. 1959. "Oxygen as a pre-requisite to the origin of Metazoa". *Nature* 183, 1170-1172.
- [280] Oberbeck, V.R. 1993. "Impacts, tillites, and the breakup of Gondwanaland". *J. Geol.* 101, 1-19.
- [281] Ogawa, T. & Kaplan, A. 1987. "The stoichiometry between CO_2 and H^+ fluxes involved in the transport of inorganic Carbon in cyanobacteria". *Plant Physiol.* 83. 888-891.
- [282] Oglby, R.J., & Saltzman, B, 1990. "Sensitivity of the equilibrium surface temperature of a GCM to systematic changes in atmospheric Carbon dioxide". *Geophys. Res. Lett.* 17. 1089-1092.
- [283] Okada, M. & Niitsuma, N. 1989. "Detailed paleomagnetic records during the Brunhes-Matuyama geomagnetic reversal, and a direct determination of depth-lag for magnetisation in marine sediments". *Physics of the Earth and Planetary interiors* 56(1). 133-150.
- [284] Pagani, M., Lemerchand, D., Spivack, A, & Gaillardet, J. 2005. "A critical evaluation of the Boron isotope-pH proxy: The accuracy of ancient ocean pH estimates". *Geochim. Cosmochim. Acta.* 69(4). 953-961.
- [285] Page, R.D.M, Holmes, E.C. 1996. "Molecular evolution: A phylogenetic approach". Blackwell Science.
- [286] Parrish, R. , Noble, S. 2003. "Zircon $U - Th - Pb$ Geochronology by isotope dilution: Thermal ionisation mass spectroscopy". *Reviews in Mineralogy & Geochemistry.* Mineralogical Society of America. pp183-213.

- [287] Pavlov, A.A., Hurtgen, M.T., Kasting, J.F. & Arthur, M.A. 2003. "Methane-rich Proterozoic atmosphere?" *Geology*, 31. 87-90.
- [288] Peixoto, J.P. Oort, A.H., de Almeida, M & Tome, A. 1991. "Entropy budget of the atmosphere" . *J. Geophys. Res.* 96 (10), 981-988.
- [289] Peterman, Z.E., Hedge, C.E. & Tourtelot, H.A. 1970. "Isotopic composition of Strontium in seawater through Phanerozoic time". *Geochim. Cosmochim. Acta.* 34. 105-120.
- [290] Pfeiffer, T., Bonhoeffer, S. 2003. "An evolutionary scenario for the transition to undifferentiated multicellularity". *PNAS* 100(3). 1095-1098.
- [291] Peltier, W.R. et al, 2004. "Climate dynamics in deep time: Modeling the "Snowball Bifurcation" and assessing the plausibility of its occurrence" *The Extreme Proterozoic: Geology, Geochemistry and Climate. Geophysical Monograph Series 146.* pp107-124.
- [292] Peltier, W.R., Liu, Y. & Crowley, J.W. 2007. "Snowball Earth prevention by dissolved organic Carbon remineralisation". *Nature* 450, 813-819.
- [293] Peterson et al, 2005. "Tempo and mode of early animal evolution: inferences from rocks, Hox, and molecular clocks." *Paleobiology* 31(2). 36-55.
- [294] Peterson & Butterfield, 2005. "Origin of the Eumetazoa: Testing predictions from molecular clocks against the Eukaryotic fossil record". *PNAS* 102 (27). 9547-9552.
- [295] Piercey-Normore M.D. & DePreist, P.T. 2001. "Algal switching among lichen symbioses" . *Am. Journ. Bot.* 88. 1490-1498.
- [296] Pierrehumbert, R.T. 2002. "The hydrologic cycle in deep-time climate problems". *Nature* 419. 191-198
- [297] Pierrehumbert, R.T. 2005. "Climate Dynamics of a hard snowball Earth". *Journ. Geophys. Res.* 110, D01111.
- [298] Pollard, D.P., Kasting, J.F., 2005. "Snowball Earth: A thin-ice solution with flowing sea glaciers." *Journ. Geophys. Res.* 110, C07010.
- [299] Poulsen, C.J. 2003. "Absence of a runaway ice-albedo feedback in the Neoproterozoic." *Geology* 31. 473-476.
- [300] Poulsen, C.J., Pierrehumbert, R.T. & Jacob, R.L.. 2001. "Impact of ocean dynamics on the simulation of the Neoproterozoic "snowball Earth"". *Geophys. Res. Lett.* 28. DOI: 10.1029/2000GL012058.

- [301] Poulsen, C.J., Jacob, R.L., Pierrehumbert, R.T. & Huynh, T.T. 2002. "Testing Paleogeographic controls on a Neoproterozoic snowball Earth". *Geophys. Res. Lett.* 29. DOI: 10.1029/2001GL014352.
- [302] Prave, A.R. 1999. "Two diamictites, two cap carbonates, two $^{13}\delta C$ excursions, two rifts: the Neoproterozoic Kingston peak formation, Death Valley, California". *Geology* 27. 339-342.
- [303] Prave, A.R., 2002. "Life on land in the Proterozoic; evidence from the Torridian rocks of Northwest Scotland". *Geology* 30. 811-814.
- [304] Preiss, W.V. 1987. "The Adelaide Geosyncline". *Geol. Surv. South Australia. Bulletin* 53.
- [305] Purvis, W., 2000. "Lichens". Natural History Museum Life Sciences.
- [306] Rafai, H.S., Newell, C.J., Gonzales, J.R. Dendrou, S & Dendrou, B. 1998. "Bioplume 3: Natural attenuation decision support system: User's Manual". United States Environmental Protection Agency.
- [307] Rainey, P., Travisano, M, 1998. Adaptive radiation in a heterogeneous environment. *Nature* 394, 68-72.
- [308] Rainey, P.B. & Rainey, K. 2003. "Evolution of co-operation and conflict in experimental bacterial populations". *Nature* 425. 72-74.
- [309] Rampino, M.R. 1994. "Tillites, diamictites, and ballistic ejecta of large impacts". *Journal of Geology*. 102, 439-456.
- [310] Raven, J.A. & Edwards, D. 2001. "Roots: Evolutionary origins and biogeochemical significance" *J. Exp. Bot.* 52. 381-401.
- [311] Raven, J.A., 2002. "Evolution of cyanobacterial symbioses" In "Cyanobacteria in symbioses". Springer. pp329-346.
- [312] Raven, J.A., Ball, L.A., Beardhall, J, Giordano, M & Maberly, S.C. 2005. "Algae lacking Carbon concentrations". *Canadian J. Bot.* 83. 879-890.
- [313] Redfield, A.C. 1958. "The biological control of chemical factors in the environment" in "American Scientist", 1958 ed.
- [314] Redfield, A.C., Ketchum, B.H. & Richards, F.A. 1963. "The Sea".
- [315] Rees, W.G. 1990. "Physical principles of remote sensing". C.U.P.
- [316] Retallack, G.J. 1994. "Were the Ediacaran fossils lichens?" *Paleobiology* 20(4). 523-544.

- [317] Retallack, G.J., 2001. "Soils of the past: An introduction to paleopedology". Blackwell.
- [318] Rice, A.H.N. & Hofmann, C.C., 2000. "Evidence for a glacial origin of Neoproterozoic III striations at Oaibaccannjar'ga, Finnmark, northern Norway." *Geol. MAg* 137. 355-366.
- [319] Ridgwell, A.J., Kennedy, M.J. & Caldeira, K. 2003. "carbonate deposition, climate stability and Neoproterozoic ice ages". *Science* 302. 859-862.
- [320] Ridgwell, A.J. & Kennedy, M. 2004. "Secular changes in the importance of Neritic carbonate Deposition as a control on the magnitude and stability of Neoproterozoic ice ages" in "The Extreme Proterozoic: Geology, Geochemistry & Climate". *Geophys. Monograph Series* 146. pp 55-71.
- [321] Rieu, R. Allen, P.A., Plotze, M. & Petke, T. 2007. "Climatic cycles during a Neoproterozoic "snowball" Glacial epoch". *Geology* 35(5). 299-302.
- [322] Riding, R. 2000. "Microbial carbonates: The geological record of calcified bacterial-algal mats and biofilms". *Sedimentology* 47, 179-214.
- [323] Ridley, M. 2004. "Evolution: 3rd Edition" Blackwell.
- [324] Riggs, D.S. 1976. "Control theory and physiological feedback mechanisms". Krieger
- [325] Rino, S, Komiya, T., Windley, B.F., Katayama, I, Motoki, A & Hirata, T. 2004. "Major episodic increases of continental crust growth from zircon ages of river sands: implications for mantle overturns of the early Precambrian." *Phys. Eath. Plan. Int.* 146. 369-394.
- [326] Roberts, J.D. 1971. "Late precambrian glaciation: An anti-greenhouse effect?". *Nature* 234. 216-217.
- [327] Roger, A.J. & Hug, L.A. 2006. "The origin and diversification of eukaryotes: problems with molecular phylogenetics and molecular clock estimation". *Phil. Trans. Roy. Soc. B.* 361, 1039-1054.
- [328] Rodgers, C.D. & Walshaw, C.D.. 1966. "The computation of infra-red cooling rates in planetary atmospheres". *Q.J. Roy. Metereol. Soc.* 92. 67-92.
- [329] Rogers, J.R. 1998. "Feldspars as a source of minerals for microorganisms". *Am. Mineral.* 83. 1532-1540
- [330] Ronov, A.B, 1976. Global Carbon geochemistry, volcanism, carbonate accumulation and life. *Geochemistry international* 13, 172-195.

- [331] Rothman, D.H., Hayes, J.M. & Summons, R.E. 2003. "Dynamics of the Neoproterozoic Carbon cycle". *PNAS* 100. 8124-8129.
- [332] Rothschild, L.J., Mancinelli, R.L., 2001. "Life in Extreme Environments". *Nature* 409, 1092-1101.
- [333] Rumble, D., Giorgis, D. Ireland, T, Zhang, Z., Xu, H, Yiu, T, Yang, J., Xu, Z & Liu, J.G. 2002. "Low $^{18}\delta$ zircons, $U - Pb$ dating, and the age of the Qinglongshan Oxygen and Hydrogen isotope anomaly near Donghai, in Jiangsu province, China". *Geochim. Cosmochim. Acta.* 66(12). 2299-2306.
- [334] Saltzman, B. 2002. "Dynamical paleoclimatology: A generalised theory of global climate change". Academic press.
- [335] Sancho, L.G., de la Torre, R., Horneck, G, Ascaso, C., de los Rios, A., Pintado, A & Wierzschos, J. 2005. "Lichens survive in space: Results from the 2005 LICHENS experiment". *Astrobiology* 7(3). 443-454.
- [336] Schermerhorn, J.G. 1974. "Late Precambrian mixtites: Glacial and/or non-glacial?" *Amer. J. Sci.* 274. 673-824.
- [337] Schmitz. B. Peuker-Ehrenbrink, M., Lindstrom, M. & Tassinari, M. 1997. "Accretion rates of meteorites and cosmic dust in the early Ordovician". *Science* 278. 88.
- [338] Schrag, D.P., Hoffman, P.F., Halverson, G.P., Bowring, S.A. & Abbasi, K. 1999. "Strontium isotopes in Neoproterozoic Cap carbonates from Namibia: Evidence for intense chemical weathering in the aftermath of a snowball Earth". VM Goldschmidt conference, 1999, abstract 7653.
- [339] Schrag, D.P., Berner, R.A., Hoffman, P.F. & Halverson, G.P. 2002. "On the initiation of a snowball Earth". *Geochem. Geophys. Geosyst.* doi 10.1029/2001GC000219
- [340] Schulze-Makuch, D. & Irwin, L.N. 2006. "Life in the universe: Expectations and constraints". Springer.
- [341] Schwartzman, D., 1999. "Life, Temperature and the Earth". Columbia University Press
- [342] Seaward, M.R.D., 1997. "Major impacts made by lichens in biodeterioration processes". *International biodeterioration and biodegradation*, 40. 269-273.
- [343] Sharp, M. Parks, J., Cragg, B., Fairchild, I.J., Lamb, H. & Tranter, M. 1999. "Widespread bacterial populations at glacial beds and their relationship to rock weathering and Carbon cycling". *Geology* 27(2). 107-110.

- [344] Sheilds, G., Stille, P., Brasier, M.D. & Atudorei, N.V. 1997. "Stratified oceans and oxygenation of the later Precambrian environment: A post-glacial geochemical record from the Neoproterozoic of W. Mongolia" *Terra Nova*, 9. 218-222.
- [345] Sheilds, G.A. & Veizer, J. 2002. "Precambrian marine carbonate isotope database: Version 1.1." *Geochem. Geophys. Geosyst.* 3. doi:10.1029/2001GC000266.
- [346] Sheilds, G.A. 2005. "Neoproterozoic cap carbonates: A critical appraisal of existing models and the plume world hypothesis" *Terra Nova* 17. 299-310.
- [347] Sheilds, G.A. 2007. "A normalised seawater strontium isotope curve: Implications for Neoproterozoic-Cambrian weathering rates and the further oxygenation of the Earth". *eEarth* 2. 35-42.
- [348] Sheldon, R.P. 1984. "Ice ring origin of the Earth's atmosphere and hydrosphere and Late Proterozoic-Cambrian phosphogenesis". *Geol. Surv. India. Spec. Publ.* 17. 17-21.
- [349] Sherwood-Pike
- [350] Skidmore, M, Anderson, S.P., Sharp, M., Foght, J. & Lanoil, B.D. 2005. "Comparison of microbial community compositions of two subglacial environments reveals a possible role for microbes in Chemical weathering process". *App. Env. Microbiol.* 71(11). 6986-6997.
- [351] Smith, A.G. 1997. "Estimates of the Earth's spin (geographic) axis relative to gondwana from glacial sediments and paleomagnetism" *Earth. Sci. Rev.* 42. 161-179.
- [352] Smith, E.C. & Griffiths, H. 1998. "Intraspecific variation in the photosynthetic responses of trebouxioid lichens with reference to the activity of a Carbon concentrating mechanism" *Oecologia* 113 (3). 360-369.
- [353] Snelgar, W.P. & Green, T.G.A., 1980. "Carbon dioxide exchange in Lichens: Apparent photorespiration and possible role for CO_2 re-fixation in some members of the *Stictaceae* (Lichenes)". *J. Exp. Bot.* 32(129). 661-668.
- [354] Snelgar, W.P. & Green, T.G.A., 1981. "Carbon dioxide exchange in lichens: Low Carbon dioxide compensation levels and lack of apparent photorespiratory activity in some lichens" *The Bryologist* 83(4). 505-507.
- [355] Snider, C.S., Hsiang, T., Zhao, G. & Griffith, M. 2000. "Role of ice nucleation and antifreeze activities in growth and Pathogenesis of snow molds". *Phytopathology* 90(4). 354-361.
- [356] Sober, E. & Sloan-Wilson, D.S., 1998. "Unto others: The evolution and psychology of unselfish behaviour". Harvard University press

- [357] Sohl, L.E., Christie-Blick, N. & Kent, D.V. 1999. "Paleomagnetic polarity reversals in the Marinoan (ca 600 MA glacial deposits of Australia: implications for the duration of low-latitude glaciation in Neoproterozoic time". *Geol. Soc. Am. Bull.* 111. 1120-1139.
- [358] Spencer, A.M., 1971. "Late Precambrian Glaciation in Scotland". *Memoirs of the geological society, London*, 6.
- [359] Spencer, A.M. & Spencer, M.O. 1972. "The late Precambrian/Lower Cambrian Bonahaven Dolomite of Ishay and its stromatolites". *Scott. J. Geol.* 8. 279-262.
- [360] Stanley, S.M. 1999. "Earth system history". Freeman
- [361] Stern, K.R., Jansky, S. & Bidlack, J.E. 2003. "Introductory plant biology". McGraw Hill.
- [362] Sterner, R., Elser, J., 2002. "Ecological Stoichiometry: The Biology of elements from molecules to the biosphere". Princeton University Press.
- [363] Stryer, L. 1995. "Biochemistry". Freeman.
- [364] Sundquist, E.T. 1993. "The global Carbon Dioxide Budget". *Science* 259. 934-941.
- [365] Sverdup, H. 1990. "The kinetics of base cation release due to chemical weathering.". Lund: Lund University Press.
- [366] Szathmary, E., 1989. "The emergence, maintenance and transitions of the earliest evolutionary units". *Oxf. Surv. Evo. Biol.* 6, 169-205.
- [367] Taiz, L & Zeiger, E. 1998. "Plant physiology". Sinauer.
- [368] Tajika, E. 2003. "Faint young Sun and the Carbon cycle: implications for the Proterozoic global glaciations". *Earth. Plan. Sci. Lett.* 214. 443-453.
- [369] Tajika, E. 2004. "Analysis of Carbon Cycle System During the Neoproterozoic: Implication fo Snowball Earth Events". *The Extreme Proterozoic: Geology, Geochemistry and Climate. Geophysical Monograph Series* 146. pp 45-54.
- [370] Taylor, J.W. & Berbee, M.L. 2006. "Dating divergences in the fungal tree of life: Review and new analyses". *Mycologica* 98(6). 838-849.
- [371] Taylor, T.N., Hass, H., Remy, W. & Kerp, H. 1995. "The oldest fossil lichen". *Nature* 378. 244.
- [372] Taylor, T.N. & Wilson, A. 2004. "SEM analysis of Spongiophyton interpreted as a fossil lichen" *Int. J. Plant Sci.* 165(5). 875-881.

- [373] Thierstein, H.R. & Young, J.R., 2004. "Coccolithophores: From molecular processes to global impact". Springer.
- [374] Thomas, D.N. Dieckmann, D.S., 2002. "Antarctic sea ice - a habitat for extremophiles". *Science* 295, 641-644.
- [375] Thomson, J.W. 1984. "American Arctic Lichens". *The Macrolichens: Volume 1*. Columbia University Press.
- [376] Thorseth, I.H, Furnes, H. & Heldal, M. 1992. "The importance of microbiological activity in the alteration of basaltic glass". *Geochim. Cosmochim. Acta.* 56. 845-850.
- [377] Torsvik et al, 1998. "Polar wander and the Cambrian: Comment". *Science.* 279, 9.
- [378] Traulsen, A, Nowak MA, 2006. "Evolution of co-operation by multi-level selection". *PNAS* 103, 10952-10955.
- [379] Trindade, R.I.F., Font, E. D'Agrella-Filho, A.S., Nogueirra, A.C.R., & Riccomini, C. 2003. "Low latitude and multiple geomagnetic reversals in the Neoproterozoic Puga cap carbonate, Amazon craton". *Terra Nova* 15, 441-446.
- [380] Trives, R. 1971. "The evolution of reciprocal altruism". *Q. Rev. Biol.* 46, 35-57.
- [381] Trompette, R., de Alvarenga, C.J.S. & Walde, D. 1998. "Geological evolution of the Neoproterozoic Corumba graben system (Brazil): depositional context of the stratified *Fe* and *Mn* ores of the Jacadigo group". *J.S.Am. Earth. Sci.* 11. 587-597.
- [382] Urey, H.C. 1947. "The thermodynamic properties of isotopic substances". *J. Chem. Soc.* 57. 562-581.
- [383] Valentine, J.W., et al, 1999. "Fossils, molecules and embryos: new perspectives on the Cambrian explosion". *Development* 126(5), 851-859.
- [384] Van Baalen, M., Rand, D.A. 1998. "The Unit of Selection in Viscous Populations and the evolution of altruism". *Journal of Theoretical Biology* 193, 631-648. pp191-192.
- [385] Van-Baalen, M., Jansen,V. 2001, Dangerous liasons: The ecology of private interest and common good. *OIKOS* 95, 2, 211-224.
- [386] Veizer, J., Ala, D., Azmy, K., Brucksehn, P., Buhl, D., Bruhn, P., Carden, G.A.P, Diener, A & Godderris, Y. 1999. " $^{87}Sr/^{86}Sr$, $\delta^{13}C$ and $\delta^{18}O$ evolution of Phanerozoic seawater". *Chem. Geol.* 161, 59-88.
- [387] Vernadsky, V.I. 1926. "The Biosphere". Biogeochemical Laboratory, USSR.
- [388] Vincent, W.F., 1988. "Microbial Ecosystems of Antarctica". Cambridge University Press

- [389] Vincent, W.F., et al, 2004. "Glacial periods on early Earth and implications for the evolution of life". *Origins: Genesis, Evolution and Diversity of Life*. Kluwer. pp 481-501.
- [390] Volkman, J.K, 2005. "Sterols and other triterpenoids: Source specificity and the evolution of biosynthetic pathways". *Organic Geochemistry* 36, 139-159.
- [391] Von Bloh, W., Franck, S., Bounama, C. & Schellnhuber, H.J. 2003. "Biogenic enhancement of weathering and the stability of the Ecosphere". *Geomicrbiol* 20. 501-511.
- [392] Wang D.Y.-C. et al. 1999. "Divergence time estimates for early history of animal phyla and the origin of plants, animals and fungi.". *Phil. Trans. Proc. Roy. Soc. Lond. B.* 266. 163-171.
- [393] Walker, J.G., Hayes, P.B. & Kasting, J.F. 1981. "Negative feedback mechanism for the long-term stabilisation of Earth's surface temperature". *Journ. Geophys. Res.* 86. 9776-9782.
- [394] Walter, M.R. , Veeves, J.J. Calver, C.R., Gorjan, P. & Hill, A.C., 2000. "Dating the 840 – 544 MA Neoproterozoic interval by isotopes of strontium, Carbon and sulphur in seawater, and some interpretive models". *Precambrian Res.* 100. 371-433.
- [395] Wasson, J.T. 1985. "Meteorites: Their record of solar system history" Freeman.
- [396] Watson, A.J., Nightingale, P.D. & Cooper, D.J. 1995. "Modelling atmosphere-ocean CO_2 transfer". *Phil. Trans. Roy. Soc: Biol. Sci.* 348 (1324). 125-132.
- [397] Watson, A.J. 2004. "Gaia and observer self-selection" *Scientists debate Gaia: The next century.* pp 201-208.
- [398] Waythomas, C.F. & Wallace, K.L., 2002. "Flank collapse at Mount Wrangell, Alaska recorded by volcanic mass flow deposits in the Copper river lowland". *Can. J. Earth. Sci.* 38, 1257-1279.
- [399] Weigel, D., Jurgens, G. 2002. "Stem cells that make stems". *Nature* 415. 751-754.
- [400] Weiss, R.F. 1974. "Carbon dioxide in water and seawater: The solubility of a non-ideal gas". *Marine Chem.* 2. 203-215.
- [401] West, S.A. et al, 2006. "Social evolutionary theory for micro-organisms". *Nature Rev. Microbiol.* 4, 597-607.
- [402] West, J.A., Galy, A. & Bickle, M. 2005. "Tectonic and climatic controls on silicate weathering". *Earth. Plan. Sci. Lett.* 235. 211-228.

- [403] Williams, G.E. 1972. "Geological evidence relating to the origin and secular rotation of the solar system". *Modern Geology* 3. 165-181.
- [404] Williams, G.E., 1975. "Late precambrian glacial climate and the Earth's orbital obliquity". *Geological magazine* 112. 441-465.
- [405] Williams, G.E., 1975. "Late precambrian glacial climate and the Earth's orbital obliquity". *Geological magazine* 112. 441-465.
- [406] Williams, G.E. 1979. "Sedimentology, stable isotope geochemistry and paleoenvironment of dolostones capping late precambrian glacial sequences in Australia". *J. Geol. Soc. Australia*. 26, 277-386.
- [407] Williams, G.E. & Tonkin, D.G. 1985. "Periglacial structures and paleoclimatic significance of a late Precambrian block field in the Cattle grid copper mine, Mount Gunson, South Australia". *Australian Journal of Earth Sciences* 32. 287-300.
- [408] Williams, G.E. 2000. "Geological constraints on the Precambrian history of Earth's rotation and the Moon's orbit". *Reviews of Geophysics*. 38. 37-59.
- [409] Williams, G.E. & Schmidt, P. 2000. "Proterozoic equatorial glaciation: Has snowball Earth a snowball's chance"? *The Austrian Geologist* 117. 21-25.
- [410] Williams, G.E. & Schmidt, P. 2004. "Neoproterozoic glaciation: reconciling low paleolatitudes and the geologic record.". In "The Extreme Proterozoic: Geology, Geochemistry and Climate" AGU Monographs 146. pp 145-159.
- [411] Wilkins, A.S. 2002. "The evolution of developmental pathways", pp 467-501. Sinaeur.
- [412] Wilkinson, D.M., 2001. Mycorrhizal evolution. *TREE* 16, 64-65.
- [413] Wolpert, L & Szathmary, E. 2002. "Evolution and the egg". *Nature* 420, 745.
- [414] Wolpert, L. 1994. "The evolutionary origin of development: cycle; patterning, privilege and continuity." *Development Suppl.* 79-84.
- [415] Wright, S. 1945. "Tempo and mode in Evolution - a critical review". *Ecology* 26, 415-419.
- [416] Wu, Y.B., Zheng, Y.F., Gong, B, Tang, J. Zhao, Z.F. & Zha, X.P. 2004. "Zircon $U - Pb$ ages and oxygen isotope compositions of the Luzhenguan complex in the Beihuaiyang zone". *Acta Petrologica Sinica*. 20(5). 1007-1024.
- [417] Xiao, S. 2004. "New multicellular algal fossils and acritarchs in Doushantuo Chert Nodules". *Journ. Paleontol.* 78 (2). 393-401.

- [418] Xiao, S. 2004. "Neoproterozoic glaciations and the fossil record". The Extreme Proterozoic: Geology, Geochemistry and Climate. Geophysical Monograph Series 146. pp 199-214.
- [419] Xue, Y. et al. 1992. "Discovery of the oldest skeletal forms from the Upper Sinian Doushantuo formation in Weg'an, Guizhou, and its significance." Acta Paleontologica Sinica 31. 530-539.
- [420] Yahr, R., Vilgalys, R., De Priest, P.T. 2004. "Strong fungal specificity and selectivity for algal symbionts in Florida Scrub Cladonia lichens". Molec. Ecol. 13(11). 3367-3378.
- [421] Yamasaki, H. et al, 1999. Role of Connexin (gap junction) genes in growth control and tumorigenesis. Comptes. Rend. Acad. Sci. Paris Serie 3. 322. 151-159.
- [422] Yeo, G.M. 1981. "The late proterozoic Rapitan glaciation in the northern cordillera." Geol. Surv. Can. Pap. 81-100.
- [423] Young, G.M., 1976. "Iron formation and glaciogenic rocks of the Rapitan group, Northwest territories, Canada". Precambrian. Res. 3. 137-158.
- [424] Young, G.M. & Gostin, V.A. 1990. "The evolution of a late Precambrian early paleozoic rift complex: The Adelaide geosyncline". pp 143-163. Geological Society of Australia.
- [425] Yuan, X. Xiao, S., Taylor, T.N., 2005. Lichen-like symbiosis 600 million years ago. Science 308, 1017-1020.
- [426] Zachariassen, K.E. & Kristiansen, E, 2000. "Ice nucleation and anti-nucleation in nature". Cryobiology 41. 257-279.
- [427] Zheng, Y.F., Wu, Y, Chen, F.K., Bing, G., Long, L, & Zhao, Z. 2004. "Zircon $U - Pb$ and oxygen isotope evidence for a large scale ^{18}O depletion event in igneous rocks during the Neoproterozoic". Geochim. Cosmochim. Acta. 68(20). 4145-4165.
- [428] Zhong, S.J. & Mucci, A. 1993. "Calcite precipitation in seawater using a constant addition technique - a new overall reaction kinetic expression." Geochim Cosmochim. Acta. 57. 1409-1417.